

INSTITUTE OF MOUNTAIN RISK ENGINEERING
UNIVERSITY OF NATURAL RESOURCES AND APPLIED LIFE SCIENCES
VIENNA

WOODY DEBRIS RECRUITMENT PREDICTION METHODS AND TRANSPORT ANALYSIS

PhD THESIS

Submitted by

Bruno Mazzorana

For the degree of

Doctor rerum naturalium technicarum

Vienna, July 2009

Supervisor:

Ao. Univ. Prof. Dipl.-Ing. Dr. Johannes Hübl

Contents

List of Figures and Tables	IV
1 Introduction	1
<i>References</i>	7
2 Hazard index maps for woody material recruitment and transport in alpine catchments	11
<i>Abstract</i>	11
2.1 <i>Introduction</i>	12
2.2 <i>Method</i>	13
2.2.1 <i>A hazard process oriented view of woody material dynamics</i>	14
2.2.2 <i>Classification of the woody material recruitment areas</i>	15
2.2.3 <i>Identification and spatial delimitation of the woody material recruitment areas</i>	20
2.2.4 <i>A woody material recruitment indicator</i>	24
2.2.5 <i>An indicator for woody material entrainment and transport</i>	25
2.3 <i>Results</i>	28
2.4 <i>Discussion</i>	29
2.5 <i>Conclusions</i>	31
2.6 <i>References</i>	32
3 Modelling woody material transport and deposition in alpine rivers	37
<i>Abstract</i>	37
3.1 <i>Introduction</i>	38
3.2 <i>Theoretical background</i>	40
3.2.1 <i>Woody material recruitment</i>	41
3.2.2 <i>Woody material entrainment and transport</i>	42
3.3 <i>Modelling approach</i>	44
3.3.1 <i>Identification, localization and classification of woody material recruitment areas</i>	45
3.3.2 <i>Assessment of the recruited woody material volume</i>	46
3.3.3 <i>Woody material transport dynamics</i>	53
3.3.4 <i>Potential hazard impacts at critical stream configurations</i>	56
3.4 <i>Study site and test application</i>	59
3.5 <i>Simulation results</i>	62
3.6 <i>Discussion and conclusions</i>	67
3.7 <i>References</i>	69
4 Improving risk assessment by defining consistent and reliable system scenarios	73
<i>Abstract</i>	73
4.1 <i>Introduction</i>	74
4.2 <i>Background – exploring alternative developments through scenarios</i>	76

4.3	<i>Method</i>	83
4.4	<i>Application and results</i>	85
4.4.1	<i>Case study one: Failure propensity case in an Alpine torrent and possible effects on sediment transport at the downstream outflow cross section</i>	86
4.4.2	<i>Case study two: Woody debris transport induced hazard scenarios at hydraulic weak points</i>	92
4.5	<i>Conclusions</i>	101
4.6	<i>References</i>	102
5	Determining natural hazard patterns at critical stream configurations by Formative Scenario Analysis	105
	<i>Abstract</i>	105
5.1	<i>Introduction</i>	106
5.2	<i>Methods</i>	111
5.2.1	<i>Formative Scenario Analysis</i>	111
5.2.2	<i>Model set-up</i>	116
5.3	<i>Model implementation</i>	120
5.3.1	<i>Initial set of key variables</i>	123
5.3.2	<i>Rating of key variables</i>	124
5.3.3	<i>Definition of the levels of each key variable</i>	130
5.3.4	<i>Consistency matrix, scenario construction and selection for the system loading shell</i>	135
5.3.5	<i>Consistency matrix, scenario construction and selection for the system response shell</i>	139
5.4	<i>Results</i>	142
5.5	<i>Conclusion</i>	144
5.6	<i>References</i>	146
6	Synopsis	150
	<i>References</i>	167
7	Zusammenfassung	169
	<i>Literatur</i>	186
	Acknowledgements	188

List of Figures and Tables

Figure 2-1:	<i>SIZ-zone: torrential processes with influence on entrainment and transport of woody material</i>	16
Figure 2-2:	<i>AWB-areas and RWB-areas: recruitment mechanisms on hillslopes</i>	17
Figure 2-3:	<i>PCA-areas: particularly active recruitment areas on hillslopes</i>	18
Figure 2-4:	<i>Schematic illustration of the types of woody debris recruitment areas</i>	19
Figure 2-5:	<i>Schematic illustration of the spatial delimitation of the different types of woody debris recruitment areas</i>	19
Figure 2-6:	<i>Classification of the torrent catchments by the woody debris recruitment and transport indicator WM</i>	29
Figure 2-7:	<i>Torrent catchments with observed woody material recruitment and transport during documented debris flow and overbank sedimentation processes</i>	31
Figure 3-1:	<i>Wood, sediment and fluxes and system dynamics</i>	41
Figure 3-2:	<i>Scheme for the assessment of the woody debris recruitment on regional scale</i>	46
Figure 3-3:	<i>Determination of the recruitment strips within the maximum extent buffer areas</i>	47
Figure 3-4:	<i>Decision matrix for the quantification of the woody debris availability on regional scale</i>	52
Figure 3-5:	<i>Determination of the following cells (A and B) and their particular portion of the woody material from the source cell to receive</i>	54
Figure 3-6:	<i>Example of a bridge as an obstacle consisting of two piers as in-stream-obstacles and the superstructure as a crossing obstacle</i>	57
Figure 3-7:	<i>Example of a collision with an in-stream-object</i>	58
Figure 3-8:	<i>Example of a woody material object floating between two piers of a bridge</i>	58
Figure 3.9:	<i>(a) Localization, (b) system description and (c) extent and delimitation of the study area</i>	59
Figure 3.10:	<i>An aerial image of the study area after the flood event in 1987</i>	60
Figure 3-11:	<i>Extract of the mapped vegetation structure</i>	63
Figure 3-12:	<i>Extract of the mapped morphology of the river influence zones</i>	63
Figure 3-13:	<i>Results of the cell-by-cell simulation of the woody material transportation and deposition volumes</i>	64
Figure 3-14:	<i>Results of the object-oriented simulation of the deposition of woody material</i>	66
Figure 3-15:	<i>Entrapment at a critical configuration</i>	66
Figure 3-16:	<i>Destroyed bridge across the Passerio river (flood event July 1987)</i>	67
Figure 4-1:	<i>Scenario Trumpet and possible outcomes of a system</i>	77
Figure 4-2:	<i>Toppling of a series of consolidation structures</i>	77
Figure 4-3:	<i>Ways to classify different scenarios</i>	79
Figure 4-4:	<i>The nine steps of Formative Scenario Analysis</i>	82
Figure 4-5:	<i>Pre-selection of possible impact factors or key variables (study 1)</i>	87
Figure 4-6:	<i>System grid of the activity and passivity scores for case study 1</i>	88
Figure 4-7:	<i>Pre-selection of possible impact factors or key variables (study 2)</i>	93
Figure 4-8:	<i>Relevant variables for the description of case study 2</i>	94
Figure 4-9:	<i>Selected key variables for case study 2 after a reconsideration step</i>	95
Figure 4-10:	<i>System grid of the selected key variables of case study 2</i>	96
Figure 5-1:	<i>Shell-structured risk scenario planning approach</i>	108
Figure 5-2:	<i>Possible hazard and risk scenarios along a stream configuration</i>	109

Figure 5-3:	<i>The nine steps of Formative Scenario Analysis</i>	113
Figure 5-4:	<i>Mental system map for the case study on woody material transport hazards</i>	121
Figure 5-5:	<i>Impact levels between variables</i>	127
Figure 5-6:	<i>Fuzzy intervals for consistency rating</i>	135
Figure 6-1:	<i>Examples of classified woody material recruitment areas</i>	152
Figure 6-2:	<i>Flow chart for the calculation of the woody material recruitment and transport indicator WM</i>	153
Figure 6-3:	<i>Classification of the stream catchments by the woody material recruitment and transport indicator WM</i>	154
Figure 6-4:	<i>Flow chart of the modelling steps for the evaluation of woody material transport hazard dynamics in alpine rivers</i>	156
Figure 6-5:	<i>Woody material transport simulation results</i>	157
Figure 6-6:	<i>Entrapment at a critical configuration (at the right side on a more detailed scale)</i>	158
Figure 6-7:	<i>The nine steps of Formative Scenario Analysis</i>	159
Figure 6-8:	<i>Pre-selection of possible impact factors or key variables</i>	160
Figure 6-9:	<i>System grid of the activity and passivity scores</i>	161
Figure 6-10:	<i>Mental system map: woody material transport hazards</i>	164
Figure 7-1:	<i>Beispiele klassifizierter Schwemmhölzeintragsflächen</i>	171
Figure 7-2:	<i>Flussdiagramm für die Berechnung des WM- Gefahrenindikators</i>	172
Figure 7-3:	<i>Klassifizierung der Einzugsgebiete gemäß dem WM- Indikator</i>	173
Figure 7-4:	<i>Ablaufschema der Modellierung der Schwemmholztransportdynamik in Gebirgsflüssen zur Ermittlung der potentiellen Gefahr</i>	175
Figure 7-5:	<i>Ergebnisse der Schwemmholztransportsimulationen</i>	176
Figure 7-6:	<i>Schwemmholzablagerungen im Bereich kritischer Konfigurationen. Detailansicht rechts</i>	177
Figure 7-7:	<i>Die neun Schritte der Formativen Szenario-Analyse</i>	178
Figure 7-8:	<i>Vorselektion der Einflussfaktoren für das Fallbeispiel</i>	179
Figure 7-9:	<i>System-Grid: „Activity“ und „Passivity“ Bewertungen für die Einflussfaktoren</i>	180
Figure 7-10:	<i>Mentale Systemkarte: Schwemmholztransportgefahren</i>	183
Table 3-1:	<i>Structural classification of forested areas within the river influence zone</i>	45
Table 3-2:	<i>Assumed values for the input of woody debris from the tributaries</i>	61
Table 4-1:	<i>The four main applications of scenarios</i>	80
Table 4-2:	<i>Impact matrix for case study 1</i>	87
Table 4-3:	<i>Definition of impact levels for each key variable for case study 1</i>	89
Table 4-4:	<i>Excerpt from the consistency matrix for case study 1</i>	90
Table 4-5:	<i>Set of all scenarios (and the most consistent ones) for case study 1</i>	92
Table 4-6:	<i>Impact matrix case study 2</i>	95
Table 4-7:	<i>Definition of impact levels for each key variable for case study 2</i>	97
Table 4-8:	<i>Excerpt from the consistency matrix for case study 2</i>	98
Table 4-9:	<i>Set of all scenarios (and the most consistent ones) for case study 2</i>	100
Table 5-1:	<i>Possible key variables for woody material transport hazards</i>	123
Table 5-2:	<i>Importance and uncertainty levels for each variable of the system loading shell in relation to the acceptance levels</i>	125
Table 5-3:	<i>Importance and uncertainty levels for each variable of the system response shell in relation to the acceptance levels</i>	126
Table 5-4:	<i>Impact matrix for the key variables belonging to the system loading shell</i>	128

<i>Table 5-5:</i>	<i>Impact matrix for the key variables belonging to the system response shell</i>	<i>129</i>
<i>Table 5-6:</i>	<i>Impact level definition for each key variable</i>	<i>130</i>
<i>Table 5-7:</i>	<i>Consistency matrix for the scenario shell $k=1$</i>	<i>136</i>
<i>Table 5-8:</i>	<i>Possible scenarios with corresponding additive consistency values</i>	<i>137</i>
<i>Table 5-9:</i>	<i>Scenario information system SIS_k with $k=1$ represented as a decision table</i>	<i>138</i>
<i>Table 5-10:</i>	<i>Consistency matrix for the scenario shell $k=2$</i>	<i>139</i>
<i>Table 5-11:</i>	<i>Possible scenarios with corresponding additive consistency values</i>	<i>140</i>
<i>Table 5-12:</i>	<i>Scenario information system SIS_k with $k=2$ represented as a decision table</i>	<i>141</i>
<i>Table 6-1:</i>	<i>Classification of woody material recruitment areas</i>	<i>152</i>
<i>Table 6-2:</i>	<i>Impact matrix: Woody material transport induced hazard scenarios at hydraulic weak points</i>	<i>160</i>
<i>Table 6-3:</i>	<i>Set of all scenarios (step 7 of FSA) and identification of the most consistent ones</i>	<i>162</i>
<i>Table 6-4:</i>	<i>Scenario information system SIS_k for the system loading scenario shell represented as a decision table</i>	<i>165</i>
<i>Table 6-5:</i>	<i>Scenario information system SIS_k for the system response scenario shell represented as a decision table</i>	<i>165</i>
<i>Table 7-1:</i>	<i>Klassifizierung der Schwemmholzeintragsflächen</i>	<i>171</i>
<i>Table 7-2:</i>	<i>Einflussmatrix: Schwemmholztransport Gefahrenszenarien im Bereich kritischer Konfigurationen</i>	<i>179</i>
<i>Table 7-3:</i>	<i>Mögliche Szenarien (Schritt 7 der FSA) und Auswahl der plausibelsten Szenarien</i>	<i>181</i>
<i>Table 7-4:</i>	<i>Szenario Informationssystem für die „Systembelastungshülle“</i>	<i>184</i>
<i>Table 7-5:</i>	<i>Szenario Informationssystem für die „Systemreaktionshülle“</i>	<i>184</i>

1. INTRODUCTION

Like all systems, the complex system is an interlocking structure of feedback loops ... This loop structure surrounds all decisions, public or private, conscious or unconscious. The process of man and nature, of psychology and physics, of medicine and engineering all fall within this structure.

Jay W. Forrester, Urban Dynamics (1969), p. 107

Extreme hydrological events that recently occurred in the Alpine region have clearly shown a variety of cause-effect interrelationships and tipping process patterns that accentuated the consequences in terms of damage and risk. Since the 1990s, considerable losses occurred all over the Alps due to torrential and fluvial processes (1987, 1999, 2002, 2005, 2006, and 2008). The causes of resulting consequences could regularly be traced back to the intense woody material transport that accompanied those processes. This development can be for a major part attributed to the following risk-influencing factors: (1) possible changes in the frequency and magnitude of natural processes due to the possible accentuation of precipitation and the increase in temperature, estimated to be approximately 0.8 °C in the northern hemisphere and 1.2 °C in Alpine regions (Wanner et al., 2000; Houghton et al., 2001; Foelsche, 2005; Solomon et al., 2007). The traditional approaches to risk assessment have shown to be partially unsuitable to thoroughly explain the different facets of systems complexity and the intricacy of possible changes within and between these systems; and (2) socioeconomic development in Alpine regions resulting in an increase of values at risk exposed (Fuchs et al., 2005; Fuchs and Keiler, 2006; Keiler et al., 2006). The spatial and temporal variability of risk can be attributed to the conjoint action of these two factors.

Furthermore, event documentation has shown that inherent design weaknesses of the mitigation measures and infrastructural systems, built over the last decades, contribute to increased systems vulnerability (Mazzorana, 2007; Mazzorana et al., 2008).

As pointed out by Sterman (2000), the behaviour of a system arises from its structure. That structure consists of feedback loops, stocks and flows, and nonlinearities created by the interaction of the physical and institutional structure of the system with the decision making process of the agents acting within it. Without doubt, feedback is one of the core concepts of system dynamics and our

mental models often fail to include the critical feedbacks determining unexpected system responses with severe consequences.

As a result robust risk mitigation approaches aiming to avoid some of the drawbacks experienced in the past have to include an extensive consideration of the different sources of uncertainty, both probabilistic and epistemic, that limit our ability to accurately predict frequency and magnitude of hazardous phenomena and to reliably assess their consequences (e.g., Paté-Cornell, 1996; Merz et al., 2008).

The ability to deal with the multiple facets of natural hazard risks can be enhanced by thinking in scenarios (Scholz and Tietje, 2002; Wiek and Binder, 2005) and by refining our coping mechanisms accordingly (O'Brien, 2007). Coping with natural hazard risks inevitably leads to the following list of fundamental questions: (1) What can happen? (2) What is acceptable to happen? (3) And what needs to be done? – represented by the concept of integral risk management (e.g., Fell et al. 2008).

From a hazard index level of analysis (Petraschek and Kienholz, 2003), the present dissertation contributes from a methodological point of view to a comprehensive understanding of hazard processes involving woody material transport phenomena, since these coupled processes had frequently been observed in recent years. From a conceptual perspective the developed analysis procedures provide important insights into natural hazard risk management and therefore might contribute to subordinated risk reduction strategies, such as targeted by the European Floods Directive (Commission of the European Communities, 2007).

Comiti et al. (2006) reviewed the effects of human impact on Alpine forests during the last century. The main impact on Alpine forests was related to timber and firewood harvesting practices before the 1940s. Regularly forests were clear-cut to create pastures and agricultural land. As a consequence, the sediment transport regime and the morphology of high-gradient streams were considerably altered. Furthermore, practices of splash-damming (i.e. artificially induced dam-break flows to allow for the transport of timber logs downstream), forest harvest and associated reduction of the dimensions of woody material, as well as the removal of in-stream woody material for fuel purposes affected the recruitment noticeably (Comiti et al., 2006). However, rural and forest economy declined in many Alpine regions during the last century, accentuated by the emigration waves at the beginning of the century and following World War II. The associated decline in land use pressure allowed wood to regenerate and to increase the stand volume; in parallel, succession of pioneer vegetation on abandoned crop and pasture land was observable. As a consequence, in-stream woody material volumes increased again. The above mentioned economical trends were particularly evident in the northern Italian regions, while in Southern Tyrol, Austria and Switzerland these consequences were less pronounced. Due to the development of mountain

tourism, initially originating from winter sports and thereafter progressively diversified, an unprecedented construction wave of new buildings and of a dense infrastructure network resulted. In parallel a patchwork of new commercial areas was created, often not associated with a comprehensive planning process based on a certain lack in land development planning. As a result, values at risk increased remarkably, in particular during the 1960s and 1970s (Bätzing, 1993; Fuchs and Bründl 2005), leading to a presumably increased risk emerging from torrential and fluvial processes in exposed stream sections such as riparian areas as well as on alluvial and debris fans.

To conclude, highly developed economic and social systems result in a large variety of natural threats for a postmodern society (Beck, 1992; Renn, 2008a, b) with a parallel increasing demand for safety in society. In mountain regions such as the Alps the complex tasks to achieve an optimal protection level against natural hazards on the one hand and to sustain a general economic development without excessive land use pressure on the other hand is a major challenge (Mazzorana, 2007; Rudolf-Miklau et al., 2008). During the last decades a considerable amount of protection systems had been realised, e.g. within the Autonomous Province of Bolzano, Italy, approximately 33,000 torrent control measures were erected, i.e. consolidation works and check dams (Autonome Provinz Bozen, 2008). For hazards other than torrent processes this development could also be proven: in Switzerland, 1 billion Euros have been spent for avalanche control protection measures since 1950 (Fuchs et al., 2004).

If risk mitigation efficacy of protection systems is proven, the demand for regular maintenance still remains considerably high; otherwise a reconfiguration of the protection systems is highly recommendable. With respect to the latter, recent events have shown that that additional cost-intensive risk mitigation strategies are needed in order to prevent inundation by floods, excessive bedload and woody material transport phenomena as well as to avoid destructive impacts from debris flows. Woody material is regularly regarded as a problem by the torrent control agencies (Rickly and Bucher, 2006; Lange et al., 2006; Hübl et al., 2008), (1) triggering severe flood flows due to outburst, (2) clogging of bridge openings and damaging hydraulic structures, (3) increasing the destructive power of debris flows, and (4) causing dambreaks by the formation of unstable in-stream debris dams. Therefore, woody material recruitment, entrainment and transport processes during extreme events exacerbate either the system loading or triggering conditions or the system response processes at critical stream configurations (e.g. bridge locations or stream constrictions). At these critical configurations tipping process patterns involve an immediate succession of backwater effects, flow diversions, erosion and scouring processes and frequently evolve in embankment failures and floodplain inundations (Diehl, 1997, Lyn et al., 2007). Severe damages are caused at the structural components at critical stream configurations (e.g. bridge elements, piers

and superstructures) and furthermore by subsequent inundation processes affecting objects at risk located in the flood prone areas or within the deposition zones of debris flows. Critical configurations are characterised by the fact that all risk-influencing factors exert a strong influence on the systems dynamics behaviour since currently used hazard assessment procedures only partially assure a complete identification of hazard scenarios and a quantification of hazard impacts attributable to woody material transport. In coherence with the requirements of systems thinking and the modelling of complex phenomena (Sterman, 2000) a structured analysis of the implications of woody material dynamics is needed. First an operational definition of critical configurations is given: critical configurations are here intended as spatial domains, where the torrential and fluvial processes involving woody material dynamics result in tipping process patterns inducing considerable consequences in terms of risk. This definition of critical configuration requires to meet some basic conditions in order to classify a certain spatial domain along the stream as critical:

- (1) Availability of recruited woody material in the upstream catchment: in this context particular attention has to be deserved to the identification and quantification of the recruitment processes.
- (2) Woody material entrainment and transport processes that deliver part of the recruited woody material volumes to the considered spatial domain supposed to be a critical configuration.
- (3) Interaction phenomena of the transported woody material with the geometrical features of the critical configuration: Woody material deposition and accumulation at specific geometrical elements and triggers tipping process patterns (e.g. cross-sectional obstructions with consequent floodplain inundations) or contributes to increase loadings on structural components (e.g. bridge piers, bridge superstructure).
- (4) Risk consequences: the above mentioned tipping process patterns influence the risk genesis process and result in an increase in risk exposure of vulnerable objects.

The analysis of natural hazard risk is embedded in the circle of integral risk management, including a risk assessment from the point of view of social sciences and economics, and strategies to cope with the adverse effects of hazards. The underlying objective for risk management is the planning and implementation of protective measures in an economically efficient and societal agreeable manner. Thus, risk assessment includes both, risk analysis and risk valuation within a defined system at the intersection between different disciplines (Renn 2008a, b). For this reason, the scales of valuation (temporal, spatial, degree of detail) have to be defined target-oriented for a sustainable risk minimisation. To be able to compare different types of hazards and their related risks, and to design and implement adequate risk reduction measures, a consistent and systematic approach has

to be established. While a hazard analysis focuses on natural processes such as debris flows and floods with related woody material transport, the method of risk analysis additionally includes the qualitative or quantitative valuation of elements at risk exposed to these hazards, i.e. their individual values and the associated vulnerability. Originating from technical risk analyses, the concept of risk with respect to natural hazards is defined as a quantifying function of the probability of occurrence of a process and the related extent of damage, the latter specified by the damage potential and the vulnerability (Varnes, 1984; Australian Geomechanics Society Sub-Committee on Landslide Risk Management, 2000; Fell et al., 2008):

$$R_{i,j} = f(p_{S_i}, A_{O_j}, p_{O_j,S_i}, v_{O_j,S_i}) \quad (1-1)$$

Hence, the following specifications are necessary for the ex-ante quantification of risk (Fuchs 2009):

$R_{i,j}$... risk, dependent on scenario i and object j

p_{S_i} ... probability of scenario i

A_{O_j} ... value of object j , which is derived through economic valuation techniques (Fuchs and McAlpin 2005)

p_{O_j,S_i} ... probability of exposure of object j to scenario i

v_{O_j,S_i} ... vulnerability of object j , depending on the intensity of scenario i

A closer look to equation (1-1) reveals the underlying difficulty of risk assessment if woody material dynamics is involved in the natural hazard process:

- (1) The diversity of possible scenarios is determined by the different modes of action of in-stream woody material exposed in the previous paragraphs. In Alpine regions, mainly in Switzerland, the Republic of Austria and the Autonomous Province of Southern Tyrol, significant improvements concerning the robustness of hazard assessment procedures have been achieved (Kienholz, 1977; Grunder, 1984; Bollinger et al., 1992; Kienholz and Krummenacher, 1995; Autonomous Province of Bolzano, 2008). Nevertheless the reliable determination of hazard potential and the related probability of occurrence of natural hazards involving woody material dynamics remains a major challenge. On a more basic

level even the identification of a consistent and reliable set of possible hazard scenarios is not completely satisfying. Therefore, the development of a technique to derive well defined sets of consistent hazard scenarios is an essential prerequisite for accurate hazard assessments (Mazzorana et al., 2009).

- (2) The difficulty of assessing the probability of exposure p_{O_j, S_i} of object j to scenario i is tightly linked to accuracy of the determination of the scenario itself.
- (3) Being the vulnerability v_{O_j, S_i} of the object j dependent on scenario i , again the identification of a reliable set of hazard scenarios and reasonable assumptions about the physical vulnerability of the objects at risk are necessary pre-requisites.

With respect to the presented constraints mainly related to critical configurations in mountain streams and the missing cause-effect relationship related to woody material transport the subsequent chapters address in particular the following issues:

- (1) The development of a procedure for the determination of the relative propensity of mountain torrents to the entrainment and delivery of recruited woody material on the basis of empirical indicators. Through the production of hazard index maps for woody material recruitment and transport processes in torrent catchments the identification of possible hazard scenarios is facilitated. As a consequence a substantial pre-requisite for a logically consistent hazard procedure, namely the knowledge about possible hazard scenarios, is provided.
- (2) The conceptualisation of a modelling approach for woody material transport in rivers. A modelling approach, allowing the estimation of woody material recruitment from wood covered bank slopes and floodplains is developed. Moreover this procedure is designed to support the analysis of woody material entrainment and transport to selected critical configurations. A further fundamental task on the way to a in-depth understanding of the risk genesis process is fulfilled.
- (3) The introduction of Formative Scenario Analysis (FSA, Scholz and Tietje, 2002) in the field of hazard assessment. The refinement of the level of analysis in order to meet the requirements specified in the different hazard mapping regulations is done by the introduction of FSA techniques in the field of natural hazard assessment, here with a special attention to hazardous processes involving woody material dynamics.
- (4) The extension of FSA to exploit its potential for defining natural hazard scenarios involving woody material dynamics. An enlarged FSA framework, incorporating computational

intelligence paradigms, is proposed. In this context fuzzy set theory has proven to be a powerful modelling framework for the necessary qualitative and quantitative knowledge integration and for coping with the underlying uncertainties, which were considered to be a key element in natural hazard risk assessment.

A synopsis, presented in the closing chapter, argues for a detailed study on interlocked natural hazard processes such as those involving woody material dynamics through a diversified research strategy. This research strategy includes multi-purpose modelling approaches, ranging from physical-mathematical models to computational intelligence based expert systems. Risk governance truly benefits from an enhanced capability to define consistent and reliable hazard scenarios and consequently reproducible and transparent risk assessments.

As a concluding comment in this introductory section it has to be stated that the investigation of the crucial ecological and morphological roles of wood in mountain streams (Gregory et al., 2003) is not covered in this dissertation.

References

- Australian Geomechanics Society Sub-Committee on Landslide Risk Management, 2000. Landslide risk management concepts and guidelines. *Australian Geomechanics* 35(1): 49-92.
- Autonome Provinz Bozen-Südtirol, 2008. Informationssystem zu hydrogeologischen Risiken, Methodischer Endbericht, Bozen: Autonome Provinz Bozen-Südtirol.
- Bätzing, W., 1993. *Der sozio-ökonomische Strukturwandel des Alpenraumes im 20. Jahrhundert*. Bern.
- Beck, U., 1992. *Risk Society: Towards a New Modernity*. Trans. M. Ritter. London: Sage.
- Bollinger, D., Noverraz, F. and Triplet, J.-P., 1992. Die kartographische Darstellung der Bodenbewegungsgefahren als Planungsgrundlage: Ein Beitrag zur Vereinheitlichung der Gefahrenaufnahmen in der Schweiz. *Internationales Symposium Interpraevent – Bern*. June 29 – July 3, Vol.3, 191-200.
- Comiti, F., Andreoli, A., Lenzi, M. A., and Mao, L., 2006. Spatial density and characteristics of woody debris in five mountain rivers of the Dolomites (Italian Alps), *Geomorphology*, 78, 44–63.
- Commission of the European Communities, 2007. Directive 2007/60/EC of the European Parliament and of the Council of 23 October 2007 on the assessment and management of flood risks, European Commission.

- Diehl, T. H., 1997. Potential Drift Accumulation at Bridges, US Department of Transportation, Federal Highway Administration Research and Development, Turner-Fairbank Highway Research Center, Virginia, Publication No. FHWA-RD-97-028.
- Fell, R., Corominas, J., Bonnard, C., Cascini, L., Leroi, E. and Savage, W., 2008. Guidelines for landslide susceptibility, hazard and risk zoning for land-use planning. *Engineering Geology* 102(3-4): 85-98.
- Foelsche, U., 2005. Regionale Entwicklung und Auswirkungen extreme Wetterereignisse am Beispiel Österreich. In: Steininger, K., Steinreiber, C., Ritz, C.: *Extreme Wetterereignisse und ihre wirtschaftlichen Folgen*. Berlin, Springer, 2005: 25-44.
- Fuchs, S., Bründl, M. and Stötter, J., 2004. Development of avalanche risk between 1950 and 2000 in the municipality of Davos, Switzerland. *Natural Hazards and earth System Sciences* 4 (2), 263-275.
- Fuchs, S. and Bründl, M., 2005. Damage potential and losses resulting from snow avalanches in settlements of the canton of Grisons, Switzerland. *Natural Hazards* 34 (1), 53-69
- Fuchs, S., Keiler, M., Zischg, A. and Bründl, M., 2005. The long-term development of avalanche risk in settlements considering the temporal variability of damage potential. *Natural Hazards and Earth System Sciences* 5 (6), 893-901.
- Fuchs, S. and McAlpin, M., 2005. The net benefit of public expenditures on avalanche defence structures in the municipality of Davos, Switzerland. *Natural Hazards and Earth System Sciences* 5 (3), 319-330.
- Fuchs, S. and Keiler, M., 2006. Natural hazard risk depending on the variability of damage potential. *WIT Transactions on Ecology and the Environment* 91, 13-22.
- Fuchs, S., 2009. Susceptibility versus resilience to mountain hazards in Austria – Paradigms of vulnerability revisited. *Natural Hazards and Earth System Sciences* 9 (2), 337-352.
- Gunder, 1984.
- Gregory, S.V., Boyer, K.L., Gurnell, A.M., 2003. *The Ecology and Management of Wood in World Rivers*. American Fisheries Society.
- Houghton, J., Yihui, D. and Griggs, D., 2001. *Climate Change 2001, The Scientific Basis: Contribution of Working Group I to the Third Assessment Report of the Intergovernmental Panel on Climate Change*. Cambridge: Cambridge University Press.
- Hübl, J., Anderschitz, M., Florineth, F., Gatterbauer, H., Habersack, H., Jäger, E., Kogelnig, A., Krepp, F., Rauch, J. P., Schulev-Steindl, E., 2008. *FLOODRISK II - Vertiefung und Vernetzung*

zukunftsweisender Umsetzungsstrategien zum integrierten Hochwasserschutz, Workpackage 2.3 - Präventive Strategien für das Wildholzrisiko in Wildbächen. Bundesministerium für Land- und Forstwirtschaft, Umwelt und Wasserwirtschaft, Abteilung IV/5, Wildbach und Lawinenverbauung, 43.

Keiler, M., Sailer, R., Jörg, P., Weber, C., Fuchs, S., Zischg, A. and Sauer Moser, S., 2006. Avalanche risk assessment – A multi-temporal approach, results from Galtür, Austria. *Natural Hazards and Earth System Sciences* 6 (4), 637-651.

Kienholz, H., 1977. Kombinierte geomorphologische Gefahrenkarte 1:10000 von Grindelwald. *Geographica Bernensia G4*. Bern.

Kienholz, H, and Krummenacher, B., 1995. Symbolbaukasten zur Kartierung der Phänomene. *BWW & BUWAL* (eds.): Mitteilungen des Bundesamtes für Wasserwirtschaft 6. Bern.

Lange, D. and Bezzola, G., 2006. Schwemmholz: Probleme und Lösungsansätze. Mitteilungen der Versuchsanstalt für Wasserbau, Hydrologie und Glaziologie (VAW) der ETH Zürich 188. Zürich: ETH.

Lyn, D., Cooper, T., Condon, D., Gan, L., 2007. Factors in debris accumulation at bridge piers, Washington, US Department of Transportation, Federal Highway Administration Research and Development, Turner-Fairbank Highway Research Center.

Mazzorana, B., 2007. Efficiency of protection systems in alpine torrents from a reliability, sustainability and maintainability perspective, Taiwan, Slope land Disaster Mitigation Conference.

Mazzorana, B., Scherer, C., and Marangoni, N., 2008. Additional torrent control strategies on debris flow alluvial fans with extremely high vulnerable settlements. Sánchez-Marrè, Béjar, M., J., Comas, J., Rizzoli A., and Guariso G. (eds.): *International Environmental Modelling and Software Society (iEMSs)*, 2008.

Mazzorana, B., and Scherer, C., 2009. Eine Methode zur Ermittlung von nachvollziehbaren Naturgefahrenszenarien. Verein der Diplomingenieure der Wildbach – und Lawinenverbauung Österreichs, Heft 160, Jänner 2009, 73. Jahrgang.

Merz, B., Kreibich, H. and Apel, H., 2008. Flood risk analysis: Uncertainties and validation. *Österreichische Wasser- und Abfallwirtschaft* 60 (5-6), 89-94.

O'Brien, F. and Dyson, R., 2007. Supporting strategy: Frameworks, methods and models. Chichester: Wiley.

- Paté-Cornell, E., 1996. Uncertainty in risk analysis: Six levels of treatment. *Reliability Engineering and System Safety* 54 (2-3), 95-111.
- Renn, O., 2008a. Concepts of risk: An interdisciplinary review. Part 1: Disciplinary risk concepts. *Gaia* 17 (1), 50-66.
- Renn, O., 2008b. Concepts of risk: An interdisciplinary review. Part 2: Integrative approaches. *Gaia* 17 (2), 196-204.
- Rickli, C. and Bucher, H.-U.: Schutzwald und Schwemmholz in Wildbacheinzugsgebieten, FAN-Agenda 1/06, 17–20, 2006.
- Rudolf-Miklau, F., and Mazzorana, B., 2008. Life-cycle oriented management of natural hazard protection measures providing sustainable safety: A strategic dimension. IDRC – International Disaster and Risk Conference, August 2008. Davos.
- Scholz, R. and Tietje, O., 2002. *Embedded case study methods*. London: Sage.
- Solomon, S., Qin, D., Manning, M., Chen, Z., Marquis, M., Averyt, K., Tignor, M. and Miller, H., 2007. *Climate change 2007. The scientific basis: Contribution of Working Group I to the Fourth Assessment Report of the Intergovernmental Panel on Climate Change*. Cambridge: Cambridge University Press.
- Sterman, J., 2000. *Business Dynamics: Systems thinking and Modeling for a Complex World*. Irwin/ McGraw-Hill, Homewood.
- Varnes, D., 1984. *Landslide hazard zonation*. Paris: UNESCO.
- Wanner, H., Gyalistras, D., Luterbacher, J., Rickli, R., Salvisberg, E. and Schmutz, C., 2000. *Klimawandel im Schweizer Alpenraum*. vdf Hochschulverlag AG an der ETH Zürich, Zürich.

2. HAZARD INDEX MAPS FOR WOODY MATERIAL RECRUITMENT AND TRANSPORT IN ALPINE CATCHMENTS

*"Begin at the beginning," the King said gravely, "and go on till
you come to the end: then stop."*

Lewis Carroll

B. Mazzorana, A. Zischg, A. Largiader, and J. Hübl (2009): Hazard index maps for woody material recruitment and transport in alpine catchments. Natural Hazards and Earth System Sciences 9. p. 197-209

Abstract

A robust and reliable risk assessment procedure for hydrologic hazards deserves particular attention to the role of transported woody material during flash floods or debris flows. At present, woody material transport phenomena are not systematically considered within the procedures for the elaboration of hazard maps. The consequence is a risk of losing prediction accuracy and of underestimating hazard impacts. Transported woody material frequently interferes with the sediment regulation capacity of open check dams and moreover, when obstruction phenomena at critical cross-sections of the stream occur, inundations can be triggered. The paper presents a procedure for the determination of the relative propensity of mountain streams to the entrainment and delivery of recruited woody material on the basis of empirical indicators. The procedure provided the basis for the elaboration of a hazard index map for all torrent catchments of the Autonomous Province of Bolzano/Bozen. The plausibility of the results has been thoroughly checked by a backward oriented analysis on natural hazard events, documented since 1998 at the

Department of Hydraulic Engineering of the aforementioned Alpine Province. The procedure provides hints for the consideration of the effects, induced by woody material transport, during the elaboration of hazard zone maps.

2.1 Introduction

In European mountain regions significant losses resulting from torrent processes occurred during the last decades (e.g., Oberndorfer et al., 2007; Autonome Provinz Bozen – Südtirol, 2008), in spite of considerable efforts undertaken for the protection of endangered areas (Fuchs and McAlpin, 2005). A retrospective analysis on hazard maps highlighted a series of shortcomings with respect to torrential processes (Berger et al., 2007). In particular the effects of changing channel morphology and associated woody material transport phenomena were found to remarkably amplify process intensities (e.g., Diehl, 1997; Lyn et al., 2007). Considering the effects of woody material transport specifically, clear indications emerged from the analysis of the debris flow and flood events which recently occurred in several alpine regions (e.g., Rickli and Bucher, 2006). At critical channel geometry configurations such as bridge cross sections the transported woody material can be easily entrapped and subsequently partially or totally block the cross-sectional area for conveyance. In addition to increasing the loading conditions on the structural components of the bridges (e.g. piers and superstructure), overflowing becomes more frequent and therefore flood hazard impacts increase (Bezzola et al., 2003). Transported woody material frequently interferes directly with the sediment regulating capacity of open check dams (Lange et al., 2006). Clogging of the check dam openings during the early stages of debris flow events induces deposition when the intensity of the events is rather low. As a consequence, if the retention capacity is limited, a hazard mitigation performance can be expected which is far from optimum. In the procedures and regulations currently being used in hazard mapping, the assessment of such potential impacts is left to expert discretion. Decisions made in this way involve subjective assumptions concerning certain impact variables (e.g. woody material transport) and this affects the transparency, comparability and ultimately the quality of the hazard mitigation. In order to avoid such shortcomings in mitigation planning, we propose a procedure, which, based on empirical indicators, determines the relative propensity of mountainous streams to the entrainment and delivery of woody material.

While the ecological and morphological role of woody debris in mountain streams have been extensively studied (Abbe et al., 1997; Hildebrand et al., 1997; Keim et al., 2002; Gurnell et al., 2002; Montgomery and Piegay, 2003; Comiti et al., 2006), hazard related topics of woody material transport have been less systematically investigated. Nevertheless, some literature exists concerning

in-stream structures. For example, Diehl (1997) studied the damage potential of transported woody material and Shields et al. (2001) analyzed the relation between flow resistance and increased inundation frequency due to the presence of large woody material. New insights into the dynamics of wood transport in streams have been achieved through flume experiments (Braudrick et al., 1997; Braudrick and Grant, 2000 and 2001; Curran et al., 2003; Degetto, 2000; Rickenmann, 1997; Haga et al., 2002). The interaction of woody debris transport with protection measures has been investigated with a special focus on check dams (Bezzola et al., 2004; Lange et al., 2006; Uchiogi et al., 1996) and on rope nets (Rimböck, 2004). Furthermore, advanced tools for modelling woody material recruitment storage and dynamics for small streams and their watersheds have been developed (Lancaster et al., 2001).

This work addresses the following questions from a hazard assessment perspective: (1) For which mountain torrents do woody material recruitment and transport phenomena have to be considered in hazard mapping? (2) Which mountain torrents are supposed to react in a sensitive way in terms of increasing hazard impacts if woody material transport occurs? (3) Which additional system loading and system response scenarios should be assumed, bearing in mind possible effects of woody material transport? (4) Can protection forest management policies be rationalized from a woody material transport hazard related perspective?

Based on these questions, the main objective of this study is to develop a procedure for generating hazard index maps (compare also Petraschek and Kienholz, 2003), in which the torrent catchments are classified according to their propensity to entrain and deliver woody material. Hazard index maps for debris flow and sediment transport and deposition processes already exist for the torrent catchments of the Autonomous Province of Bolzano/Bozen (Heinimann et al., 1998). These maps along with the newly created maps will constitute a reference on a hazard index level for the detection of the relevant hazard processes within each hazard assessment unit. In a successive analysis step the experts determine the hazard zones with more sophisticated procedures and can tailor the output maps to the requested level of detail.

2.2 Method

The proposed empirical method for the assessment of the hazard potential resulting from woody material recruitment and transport rests on the following outlined two step approach. In a first step the woody material recruitment areas are identified, localized and classified based on their capacity to increase the hazard potential of transport processes in alpine torrents. Woody material

recruitment areas are defined as both vegetated torrent bed as well as wood-covered areas on hill slopes in close proximity or with a high connectivity to the torrent. In a second step an indicator for woody debris recruitment and transport is calculated for each torrent catchment. The application of a GIS based procedure, in which both aforementioned steps have been implemented, allowed for the generation of comprehensive hazard index maps for all torrential catchments of the Autonomous Province of Bolzano/Bozen. The level of detail of the procedure is restricted to the level of detail defined for hazard index maps (Petraschek and Kienholz, 2003).

2.2.1 A hazard process oriented view of woody material dynamics

As outlined by Rickli and Bucher (2006), the volume of the transported woody material in a defined torrent reach is a product of: (1) the transport process in the considered reach (e.g. inflow and outflow of woody material), (2) the potentially recruitable woody material along the banks and the channel bed, if vegetated (e.g. vegetated bars), and (3) the recruitment processes taking place on hill slopes. Rickli and Bucher (2006) identify the following relevant recruitment processes:

- a) Bank erosion: Through the shear stress exerted on the wetted perimeter of the cross-section of the channel erosion processes occur along the banks altering the static equilibrium of the trees that can topple or slide into the channel. Hazard increasing conditions of synchronism between debris flow or flood events and the above mentioned woody material recruitment process is quite probable.
- b) Wind-throw: strong wind conditions can either destabilize the trees that consequently fall as a whole into the channel, or lead to the recruitment of the epigeous parts, if their stems break under the wind loading. May and Gresswell (2003) point out that falling trees with a horizontal distance to the channel that exceeds their height can exert a destabilizing action on other trees (e.g. knock-on effect).
- c) Snow loading: the pressure exerted by the snow, in particular wet snow in spring and autumn, can cause stability problems to broad-leaved trees increasing bending moments and shear forces. Through the concurring cleaving action of ice, crowns of trees are susceptible to break off.
- d) Landslides and other slope processes convey standing and lying woody material within the process perimeter towards the channel. Woody material temporarily stored in steep gullies on hill slope areas can also be conveyed toward the channel in connection with mass movements.

- e) Avalanches are likely to incorporate and convey large volumes of woody material within the process perimeter.

As a general rule, in the case of debris flows, a large part of the available woody material within the discharge cross-section is likely to be entrained and transported. In the case of flood processes above a threshold discharge value, entrainment of woody material starts due to the fact that the destabilizing forces (drag and buoyancy forces) exceed the resisting forces (friction and the gravity component normal to the channel bed). It has been evidenced by flume experiments (Braudrick and Grant, 2000; Bezzola et al., 2003) that in larger mountainous streams, characterized by channel widths greater than the wood element length, entrainment depends on the orientation of the wood element in relation to a series of parameters. These parameters are the flow direction, the roughness of the wood element, the roughness of the stream bed, the density of the wood and the ratio between wood element diameter and flow depth. In smaller streams transport phenomena are characterized by a certain intermittency involving pivoting and jamming of the wood elements.

In the following sections, a classification scheme of the woody material recruitment areas is proposed (section 2.2.2) and subsequently these areas are identified and spatially delimited (section 2.2.3).

2.2.2 Classification of the woody material recruitment areas

Referring to the description of the dynamics of woody material briefly outlined in the previous section, the recruitment areas are classified according to the following criteria: (1) wood stand productivity, (2) activity/intensity of the recruitment processes, and (3) activity/intensity of torrential processes:

- a) SIZ-areas (“stream influence zone”): The extent of these areas is determined by the wetted perimeter corresponding to the peak discharge of the considered extreme event of the debris flow or flood with intense bedload transport, depending on the dominant process (compare section 2.2.3 for details). Hazard index maps for debris flows and floods with intense sediment transport for the torrent catchments of the Autonomous Province of Bolzano/Bozen have been produced (Staffler et al., 2008). The SIZ-areas include either the areas exposed to debris flows, overbank sedimentation or the channel beds. Tree and shrub vegetation of the banks and the torrent bed which is directly exposed to the hydrodynamic forces is easily entrained. Vertical and lateral erosion can significantly reinforce the entrainment process (compare figure 2-1).



Figure 2-1: SIZ-zone: torrential processes with influence on entrainment and transport of woody material

b) AWB-areas (“active wood buffer”): These active recruitment areas border the SIZ-areas. Toppling trees can directly reach the stream and considerably influence geomorphologic processes (compare figure 2-2). Autochthonous jams are made of woody material that has not been entrained from the point where it first entered the channel, although it may have rotated or the channel may have moved (Abbe and Montgomery, 1996). Up to a certain intensity of the flood process, the formation of these jams has a stabilizing effect on the stream bed, but for higher intensities mobilization of the woody material starts to occur.



Figure 2-2: AWB-areas and RWB-areas: recruitment mechanisms on hillslopes

c) RWB-Areas (“recharging wood buffer”): This forested band is directly connected to the outside of the AWB. Toppling trees cannot reach the stream bed directly, but as evidence from documented events underpins, they can destabilize other trees from the AWB (compare figure 2-2) or in extremely steep and cliffy areas they can slide into the stream bed. The parameters determining the width of the AWB and the RWB are the fundamental parameters of the forest stands and geomorphologic parameters. For most areas in the Autonomous Province of Bolzano/Bozen a georeferenced map of the potential forest types is available (Klosterhuber et al., 2007). The parameter which correlates well with the wood stand productivity is the dominant height or top height, which is relatively independent from thinning measures. The dominant stand height h_r is the predicted height of the quadratic mean of diameters of the 20% largest trees per stand (Kramer and Akça, 1995). The geomorphologic influence is represented by the inclination of the hill slope.

- d) PRP (“preferential recruitment paths”): These are mainly steep stream channels in forested areas reaching the main channel. In these cases, transportation of woody material is possible even if the width of the AWB and the RWB is exceeded. The identification of these channels and areas is based on the hazard index map for debris flows and overbank sedimentation as well as on the event documentation of the Department of Hydraulic Engineering (Autonome Provinz Bozen – Südtirol – Abteilung Wasserschutzbauten, 2008).
- e) PCA (“preferential contributing areas”): These are areas of potential shallow landslides in forested areas close to the stream channel (compare figure 2-3). Using models such as SHALSTAB (Dietrich and Montgomery 1998) or SINMAP (Pack et al., 1998) to identify these areas enables the assessment of known and previously unknown areas of shallow landslides.



Figure 2-3: PCA-areas: particularly active recruitment areas on hillslopes

Regarding the fact that PRP and PCA provide particularly significant woody material recruitment, they are called “particularly active recruitment areas” (PARA). Figure 2-4 illustrates schematically the classification scheme adopted for the recruitment areas and the relevant processes involved. Figure 2-5 shows schematically the spatial distribution of the different recruitment areas.

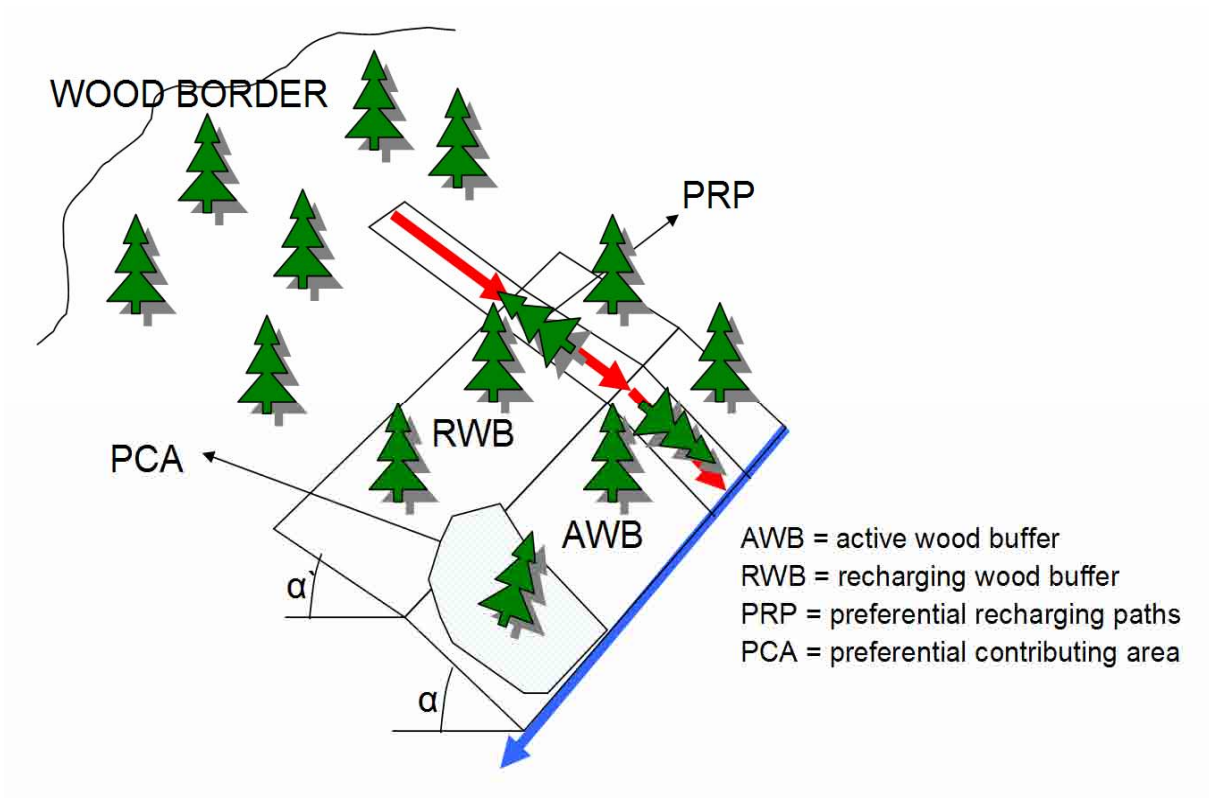


Figure 2-4: Schematic illustration of the types of woody debris recruitment areas

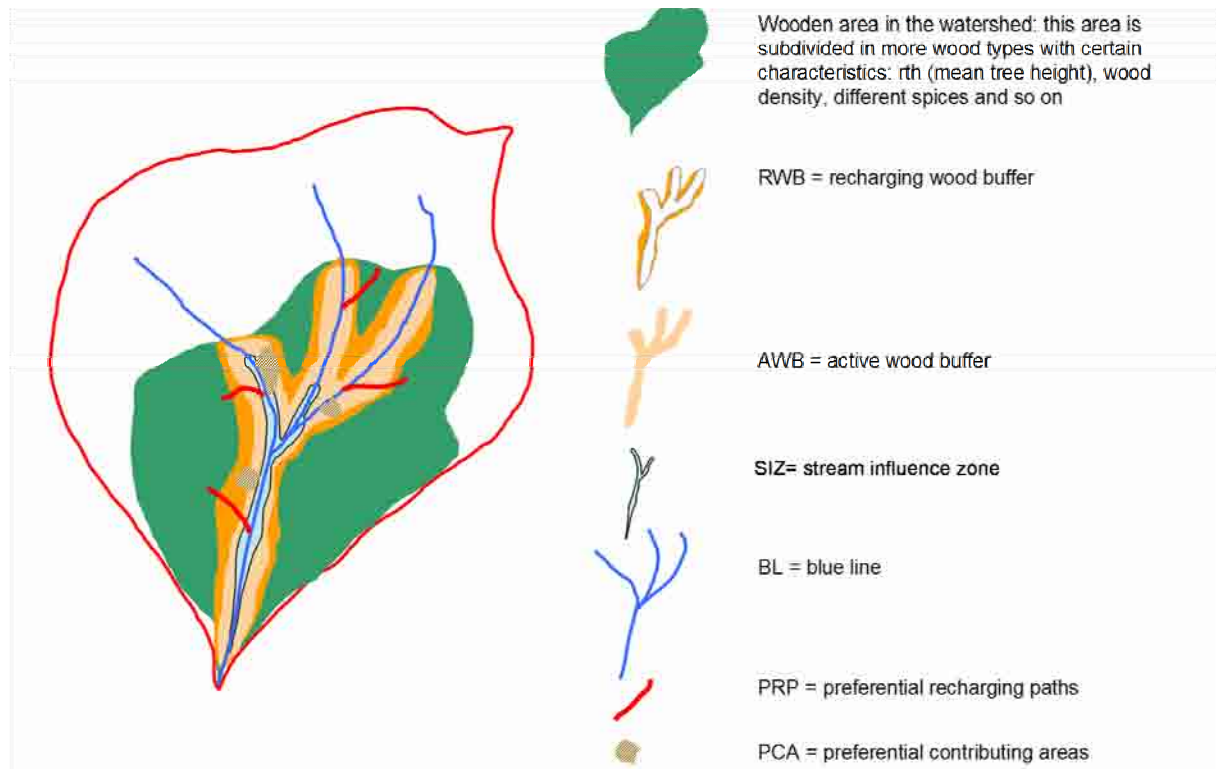


Figure 2-5: Schematic illustration of the spatial delimitation of the different types of woody debris recruitment areas.

2.2.3 Identification and spatial delimitation of the woody material recruitment areas

In this step, the woody debris recruitment areas were identified on the basis of existing datasets concerning forest cover, topography, hydrography and hydrology. The areas bordering the channel were selected. Furthermore, forested areas were identified which are prone to debris flows and shallow landslides and the connectivity of these areas to the stream bed was analysed. In a second step, the driftwood transport capacity of the stream is quantified using an indicator based on distinct topographic parameters. The combination of the delimited types of recruitment areas lead to the calculation of an index for the recruitment and transport capacity for woody debris of the torrent catchments.

The procedure used the following existing datasets:

- The digital terrain model of the Autonomous Province of Bolzano/Bozen with a resolution of 20 meters.
- The hazard index map for debris flow and overbank sedimentation processes (Staffler et al., 2008). This dataset identifies and localizes the potential debris flow hazard zones. The map was elaborated on the basis of the digital elevation model, the vegetation map and the geological map following the procedure of Zimmermann et al. (1992 and 1997) and Heinemann et al. (1998).
- The map of the classified land use of the Autonomous Province of Bolzano/Bozen (Autonome Provinz Bozen – Südtirol 2004). The forest cover was extracted from this map.
- The map of the modelled forest vegetation typologies (Klosterhuber et al., 2007). From this map, the potential tree heights were delineated.
- The map of the alpine torrent catchments. This dataset delimitates the alpine torrent catchments with debris flow and overbank sedimentation processes.

In the first step, the torrent channels were derived from the digital terrain model. According to the formulas (2-1), (2-2) and (2-3), the areas of the active wood buffer (AWB) and the recharging wood buffer (RWB) along the torrent channels were determined.

a) Calculation of the width of the active wood buffer (AWB) and the recharging wood buffer areas (RWB)

The probability of recruitment from a riparian forest on a plain surface is a function of a tree's height and distance from the stream, measured perpendicularly from the position of the tree to the

nearest channel boundary (Robison and Beschta, 1990). The probability space for a tree falling is a disk centred on the tree with radius equal to the tree's height. Van Sickle and Gregory (1990) quantified the probability of a tree entering the stream as follows:

$$P_s = \frac{\cos^{-1}\left(\frac{z}{h}\right)}{180} \quad (2-1)$$

P_s ... probability of entry

z perpendicular distance to the nearest channel boundary (in our model the border of the SIZ-area)

h effective tree height

The width of the AWB-areas on a plain surface w_{AWB} is obtained setting the probability of entry in equation (2-1) equal to zero and setting h equal to the top height of the forest type. Therefore, for hill slopes with slope inclination less than 40%, the width of the AWB-areas, is estimated as follows:

$$w_{AWB} = h_r \quad (2-2)$$

w_{AWB} ... width of the AWB

h_r ... top tree height

As pointed out by Sobota et al. (2006), individual trees exhibit a stronger tendency to fall towards the channel on steep hill slopes (>40%) than on moderately sloped landforms (<40%). Integration of field data into an established recruitment model indicated that 1.5 to 2.4 times more large wood (by number of tree boles) would be recruited to stream reaches with steep hill slopes than to reaches with moderate side slopes or flat banks, if riparian forest conditions are assumed to be constant. They conclude that stream valley topography should be considered in models that use tree fall directions in predictions of large wood recruitment to streams.

For wood stands on hill slopes (slope $\geq 40\%$), the width of the active wood buffer was determined as follows:

$$w_{AWB} = k \cdot h_r \quad (2-3)$$

k ... coefficient ($1.5 \leq k \leq 2.4$) for steep slopes (Sobota et al., 2006). On a hazard index level an average value of 1.95 has been chosen for the coefficient k .

Accounting for particular impact factors, such as wind throw or high forest dieback, the value of coefficient k in equation (2-3) should be increased, provided that experimental data is available.

As suggested by Harrington and DeBell (1996), in dense, spindly stands where the crowns support each other, trees can bend over and collapse entire sections of the stand (the domino effect).

After considering these impact factors, the additional buffer area (i.e. RWB) was identified. Due to falling trees within the RWB-area, destabilizing repercussions in the ABW-area can be expected. The width of the RWB-area was calculated analogously to the determination of the AWB-area as follows:

$$w_{RWB} = d \cdot h_r \quad (2-4)$$

d ... coefficient for the knock-on effect.

On a hazard index level a value of 1 has been chosen for the coefficient d . Accounting for particular impact factors, such as wind throw or high forest dieback, the value of coefficient d in equation (2-4) should be increased, provided that experimental data is available.

A higher accuracy level in the determination of extents of the AWB and RWB areas, as required for the production of hazard maps rather than on a hazard index level, can be achieved deserving particular attention to connectivity (Borselli et al., 2008), that could influence the recruitment to stream. Using a high resolution digital elevation model (e.g. cell size of $2.5m \cdot 2.5m$), all possible falling directions (max 8 directions) are determined for a tree (height equal to the top height), standing in the centre of the corresponding cell, that potentially permits recruitment (distance from SIZ-outward boundaries less than w_{AWB}). Connectivity is checked along each possible direction. The following connectivity criteria can be applied:

- 1) Connectivity is given along a possible tree fall direction, if the elevation profile along the tree fall direction does not exceed the linear elevation profile given by the straight line that connects the cell centre of the tree location with the cell centre of the cell identifying the SIZ- boundary.
- 2) If the elevation profile along the tree fall direction exceeds the linear elevation profile given by the straight line that connects the cell centre of the tree location with the cell centre of the SIZ-boundary cell the situation is different. It has to be checked whether or not the tree can tilt over the obstacles, which is defined here as the vertical props given by the cell centres with exceeding elevations with respect to the corresponding elevations of the straight connecting line.

In this way the tree fall directions which don't meet the connectivity criteria can be excluded.

It should be noted that the level of accuracy for hazard indexes uses a cell size of $20m \cdot 20m$ for computations. Moreover, if we consider that the top tree heights are not larger than 40 m (Klosterhuber et al., 2007), only the case of one intermediary cell between the tree location cell and the SIZ boundary cell is possible. In this case a simplified connectivity check is proposed. Connectivity is assumed to be given along a certain tree fall direction if the elevation of the intermediary cell does not exceeds the elevation of the tree location cell.

b) Identification of the preferential recruitment paths (PRP)

These areas were extracted from the hazard index maps for debris flows and overbank sedimentation processes. The preferential recruitment paths were identified and localized by geomorphic analyses of either the digital terrain model or the dataset of the superficial watercourses (after Zimmermann et al., 1992 and Heinimann et al., 1998). Steep and concave flowlines which are hydrologically connected with the SIZ areas were classified as PRP areas. Along these preferential recruitment paths woody material can be transported to the SIZ-areas from unstable forested areas despite that these recruitment areas are not topologically connected to the SIZ-areas themselves. If it is required, this information can be integrated with pre-existing maps from the event documentation database.

c) Identification of the preferential contributing areas (PCA)

In a first step, the potentially unstable areas were identified and localized using the GIS-based approach for calculating the slope stability (SHALSTAB, Dietrich and Montgomery, 1998). The unstable areas resulting from this procedure were intersected with the forest cover. In a further step, the active landslides were extracted from the landslide inventory of the Autonomous Province of Bolzano/Bozen (IFFI). Both the evident and the potentially unstable forested areas bordering or being hydrologically connected with SIZ areas through the PRP areas were considered as PCA.

d) Identification of the particularly active recruitment areas (PARA)

These areas result from the union of the PRP and the PCA.

e) Identification of the torrent influence zones (SIZ)

In this study, the SIZ-zone was determined based on the hazard index maps for debris flow and for overbank sedimentation processes, including their transit and deposition areas (Staffler et al., 2008). The analysis was made on a cell-by-cell basis for the whole territory of the Autonomous Province of Bolzano/Bozen – South Tyrol. The vector datasets were converted into raster datasets with the same resolution of the digital elevation model. Outputs of this step were the classified woody debris recruitment areas in the pre-defined torrent catchments.

2.2.4 A woody material recruitment indicator

After the identification of the potential woody debris recruitment areas, the indicator for the woody debris recruitment is calculated for each pixel and cumulated for each torrent catchment.

For every pixel in the stream channel the contributing woody debris recruitment areas are summarized using the following indicator:

$$RA_{hs,i} = a \cdot (AWB_{left,i} + AWB_{right,i}) + b \cdot (RWB_{left,i} + RWB_{right,i}) + c \cdot (PARA_{left,i} + PARA_{right,i}) \quad (2-5)$$

$RA_{hs,i} \dots$ recruitment areas on hill slopes connected to the i th stretch of the stream

The weighting coefficients a , b , c in equation (2-5) are calibration parameters which should be adapted according to the regional conditions. By means of an extensive analysis of the debris flow and overbank sedimentation events which occurred in the Autonomous Province of Bolzano/Bozen since 1998, the following procedure was used for the estimation of the parameter c . The process was based on visual inspection and image interpretation of adequately geo-referenced images. The active PARA-areas during the considered extreme events were localized and geo-referenced. On the basis of the high quality orthophoto-images from the year 2006, the ratio r_{V1} was estimated for wood volume V_{PARA}^t within the PARA-areas to the wood stand volume outside V_{WOOD}^t the PARA-areas (in the majority of the cases this involved the AWB- or RWB-areas). Additionally, pictures from the event documentation corresponding to the areas in the orthophotos were used to estimate the ratio r_{R1} of wood volume V_{PARA}^{t+1} still available after the event at time $t+1$ to the wood volume V_{PARA}^t present before the event at time t . The conditions of the wood in the PARA-areas before the event at time t were assumed to be comparable to those of the year 2006. The fact that V_{WOOD}^t can differ from the potential wood stand volume V_{POT}^t analyzed by Klosterhuber et al. (2007), the ratio r_{P1} of V_{WOOD}^t to V_{POT}^t should be recognized; however, assuming the requirements of the hazard index level $r_{P1} = 1$, the coefficient c can be expressed in terms of r_{V1} and r_{R1} as follows:

$$c = r_{V1} (1 - r_{R1}) \quad (2-6)$$

In practice, a set of representative PARA-area were analyzed in different catchments and the above defined ratios were estimated. An area-weighted average value $c_{\mu} = 0.48$ is used in the calculations.

A qualitative comparison between the recruitment processes occurring in PARA-areas and in AWB-areas of similar extent gave rise to the assumption that although recruitment from AWB-areas is an order of magnitude lower than recruitment from PARA-areas during extreme events, the recruitment from AWB-areas in the long term is a more continuous process. Taking into account the

effects of wood degradation in the long term, the weighting factor a for the recruitment contribution from the AWB-areas is chosen to be $a = 0.5 \cdot c$. The indirect influence on the recruitment process of the RWB-areas justified the assumption $a > b$ and subsequently a value of $b = 0.2 \cdot a$ was chosen.

Within the SIZ-areas more concurring processes take place: recruitment within the SIZ-area of tree and shrub vegetation of the banks and the torrent bed directly exposed to the hydrodynamic forces, entrainment, transport and deposition of the woody material. The recruitment process is modelled analogously to the above described processes occurring on the slopes as follows:

$$RA_{instream,i} = d \cdot (SIZ_i) \quad (2-7)$$

$RA_{instream,i} \dots$ in-stream recruitment areas corresponding to the i th stretch of the stream

The following ratios have been defined: a) ratio r_{V_2} of wood volume V_{TIZ}^t within the SIZ-areas to the wood stand volume outside V_{WOOD}^t and b) ratio r_{R_2} of wood volume V_{TIZ}^{t+1} still available after the event at time $t+1$ to the wood volume V_{TIZ}^t present before the event at time t . The coefficient d was qualitatively assessed as follows:

$$d = r_{V_2}(1 - r_{R_2}) \quad (2-8)$$

Due to the strong influence of the process type on in-stream recruitment, different coefficients for debris flows (d_1) and intense bedload transport processes with overbank sedimentation (d_2) have to be defined. A set of representative events were analyzed in different catchments and the above defined ratios were estimated. The area-weighted values of $d_{1,\mu} = 0.46$ and $d_{2,\mu} = 0.27$ were used in the calculations.

Subsequently the contributing in-stream recruitment areas were cumulated for each pixel in the stream channel as follows:

$$RA_{tot,i} = RA_{hs,i} + RA_{instream,i} \quad (2-9)$$

$RA_{tot,i} \dots$ total recruitment areas connected to the i th stretch of the stream.

2.2.5 An indicator for woody material entrainment and transport

Streams with a low longitudinal slope require a certain flow depth ($h \geq 2d_{BHD}$) and channel width ($b \geq L_{woody\ material}$) as well as an adequate radius of curvature in order to support woody material

transport over major distances (Braudrick et al., 1997). In torrents with intense bedload transport the entrainment and transport process are facilitated by the coupled action of hydrodynamics and mobile bed dynamics. In torrents with debris flow activity the driftwood is easily entrained and incorporated in the mixture of solid material and water. In this process, the driftwood can be partially broken up and, in the absence of obstacles, it can be transported to the depositional area. The following parameters are relevant to describe entrainment and transport of woody material on a hazard index level.

Q ... *Peak total discharge (liquid and solid) at the closure section of the catchment for a 100-years return period event.*

The liquid discharge Q for a 100-years return period event is given on a regionalized basis by the following expressions (Ferrari, 1996):

$$Q = 10.31 \cdot A^{0.593} \quad \text{in the Western Adige/Etsch basin} \quad (2-10a)$$

$$Q = 12.69 \cdot A^{0.606} \quad \text{in the Eastern Adige/Etsch basin} \quad (2-10b)$$

A ... *catchment area in [km²]*

Q_{tot} is derived specifically for either (1) floods with intense bedload transport and overbank sedimentation or (2) debris flows. For case (1), the solid discharge can be expressed according to Smart and Jaeggi's equation (1983):

$$q_s = 2.5qJ^{0.6} \left(J - \frac{d_m}{12.1h_m} \right) \quad (2-11)$$

q_s ... *solid discharge per unit width of the channel [m³/(m·s)]*

q ... *liquid discharge per unit width of the channel [m³/(m·s)]*

J ... *Channel slope [m/m]*

d_m ... *characteristic grain-size diameter [m]*

h_m ... *average flow depth [m]*

Assuming that $d_m \ll 12.1h_m$ and that b is the channel width, equation (2-11) can be simplified to:

$$Q_s = 2.5QJ^{1.6} \quad (2-12)$$

$Q_s = q_s \cdot b$... *solid discharge [m³/s]*

$Q = q \cdot b$... *liquid discharge [m³/s]*

Subsequently, in the bedload transport case, the total discharge Q_{tot} can be expressed by:

$$Q_{tot,bedload} = Q + 2.5QJ^{1.6} = (1 + 2.5J^{1.6})Q \quad (2-13)$$

For case 2), the debris flow peak discharge is estimated through Takahashi's volumetric criterion (1978, 1980, 1991):

$$Q_{tot,df} = Q \frac{C^*}{C^* - C_{df}} \quad (2-14)$$

C_{df} ... concentration of the granular mixture

$C^* = 0.65$... maximum possible concentration

C_{df} can be expressed as follows:

$$C_{df} = \frac{\tan \alpha}{\Delta(\tan \phi - \tan \alpha)} \quad (2-15)$$

Δ ... relative density of the submerged material, here assumed to be equal to 1.65

α ... slope angle of the channel

ϕ ... friction angle of the granular material, here assumed to be equal to 32°

The following two additional parameters need to be defined:

- The average downstream longitudinal slope from the i^{th} section to the basin outlet section, $J_{ds,i}$

The ratio $l_{Q,i}$ assigns a certain portion of the maximum discharge to every section of the channel depending on the location in the catchment, and is calculated as follows:

$$l_{Q,i} = \frac{Q_i}{Q} \quad (2-16)$$

Q_i ... 100 years return period liquid discharge at the i^{th} section

Q ... 100 years return period liquid discharge at the basin outlet section

For the estimation of the woody material entrainment and transport potential the following indicator is proposed:

Indicator WM for the bedload transport case:

$$WM = Q_{tot,bedload} \cdot \frac{1}{A_{tot}} \cdot \sum_{i=1}^k (l_{Q,i} \cdot RA_{tot,i}) \quad (2-17a)$$

Indicator WM for the debris flow case:

$$WM = Q_{tot,df} \cdot \frac{1}{A_{tot}} \cdot \sum_{i=1}^k (l_{Q,i} \cdot RA_{tot,i}) \quad (2-17b)$$

k ... number of control points, $i=1, \dots, k$

A_{tot} ... *catchment area*

WM ... *hazard potential indicator for wood material delivery*

The expression $\frac{1}{A_{tot}} \cdot \sum_{i=1}^k (l_{Q,i} \cdot RA_{tot,i})$ is an estimate of the relative availability of recruited woody material and is a synthetic indicator for the transport conditions along the channel. $Q_{tot,bedload}$ or $Q_{tot,df}$ estimate the relative propensity for entrainment and delivery of woody material under given transport conditions.

The WM indicator was calculated for each raster cell in the specified catchments. The value of the indicator at the basin outlet section of each torrent catchment was assigned to the particular catchment in the dataset.

2.3 Results

This procedure both delimited and classified woody material recruitment areas and computed recruitment and transport indicators for the pre-defined torrent catchments. The computed recruitment areas showed a high spatial variability within many of the catchments. Verifications in the field on control samples showed a significant correspondence of the modelled woody material recruitment areas with the mapped recruitment areas.

The computed indicator WM showed a high spatial variability (figure 2-6). For torrent catchments with a low percentage of forest cover, low values for the WM indicator resulted ($WM < 5m^3 / s$). For steep and abundantly forested torrent catchments involving frequent debris flow processes, high values for the WM indicator resulted ($WM > 15m^3 / s$). The relevance of the catchment area and therefore the relevance of the peak discharge is visible in the results of the procedure. In general, higher values of the WM indicator were calculated in larger catchments; however, figure 2-6 shows that the weight $l_{Q,i}$ has an influence on these results. Small and steep catchments as well as large catchments with high discharge were associated with high values for the WM indicator, whereas in torrent catchments with a relatively low activity of torrential processes (small process areas), low values for the WM indicator were computed. Figure 2-6 shows that torrent catchments with a relatively high proportion of recruitment areas close to the end section had higher values for the WM indicators compared to catchments with a high proportion of recruitment areas in the upper parts of the catchments.

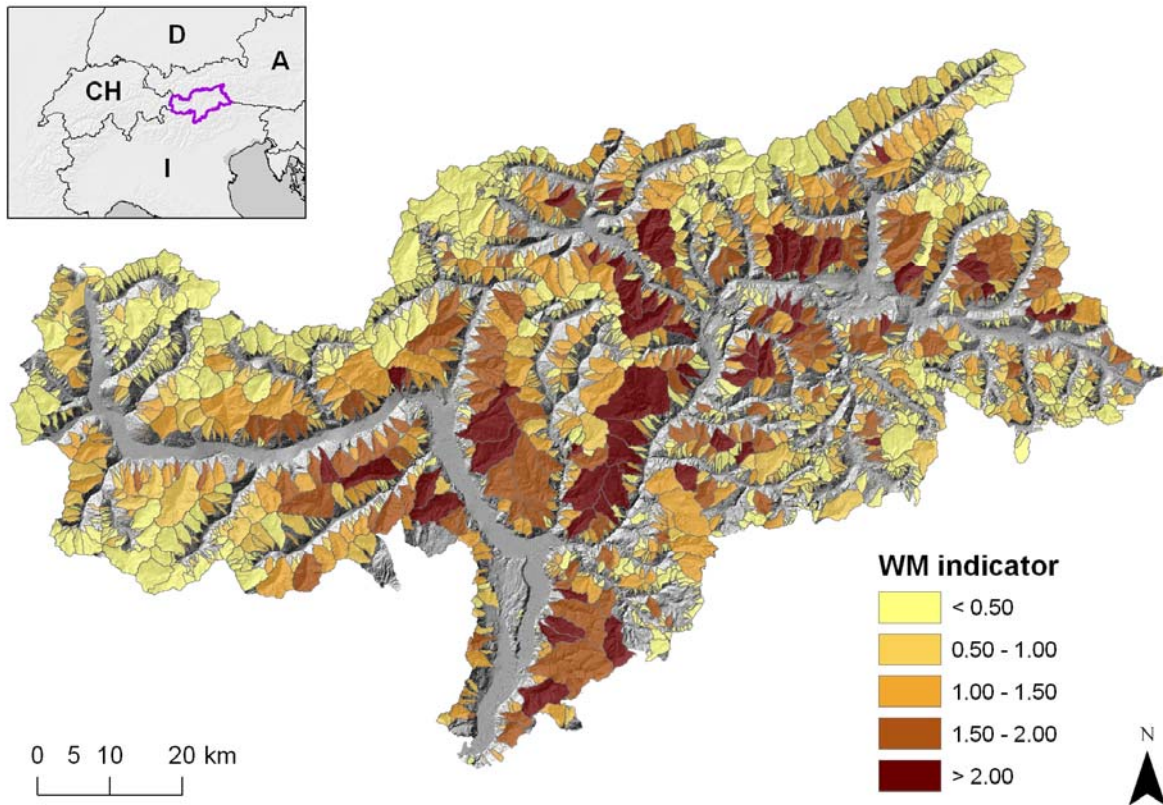


Figure 2-6: Classification of the torrent catchments by the woody debris recruitment and transport indicator WM. Legend classification in equal intervals.

2.4 Discussion

Verifications in the field on control samples showed a significant correspondence of the modelled woody debris recruitment areas with the mapped recruitment areas. The developed procedure was validated on the basis of the event documentation database of the Department of Hydraulic Engineering of the Autonomous Province of Bolzano/Bozen. Figure 2-7 shows the torrent catchments with observed woody material transport by torrential processes. In a further step, the computed results have been shown to the local mountain torrent control and hydraulic engineering experts. High values for the WM indicator were computed for those catchments which were also considered susceptible to woody material transport phenomena in the opinion of the local experts. The calculated WM indicator was verified qualitatively and semi-quantitatively as described below. Although no systematic event documentation procedure exists regarding specific details of woody material transport during torrential events, the necessary data was reconstructed from database photographs of events. Nearly 1800 images showing woody material transported by debris flow and flood processes were extracted from this database and further georeferenced and analysed. On the

basis of these images, the observed volume of transported material was estimated; however, these estimations were used for validation purposes in only a semi-quantitative way, since the analysed photographs show only a very small part of the torrent catchments. The validation procedure showed a reliable correspondence of the calculated woody debris recruitment and transport indicators with the analysed photographs. In general, catchments with high values of the WM indicator were found to be those catchments which, in reality, are documented as having events with significant transport and deposition of woody material (figures 2-5 and 2-6). In torrent catchments with values of the *WM* indicator $> 2 \text{ m}^3/\text{s}$, a minimum volume of 6 m^3 of woody material could be estimated from the photographs (range from 6 to 154 m^3 , mean 35 m^3 , $n = 11$). In torrent catchments with values of the *WM* indicator between 1 and $2 \text{ m}^3/\text{s}$, a minimum volume of 3 m^3 of woody material could be estimated from the photographs (range from 3 to 130 m^3 , mean 25 m^3 , $n = 51$). There was one exception in which a sizeable wood volume was observed ($\sim 3 \text{ m}^3$) despite a low calculated WM indicator ($0 \text{ m}^3/\text{s}$). This was due to the fact that the catchment was delimited at the upper end of the alluvial fan and the observed wood material was recruited in the area of the alluvial fan itself. Given that the outlined method delineates catchments by a lower boundary at the alluvial fan or debris flow cone, the recruitment of woody material downstream of these outlet points is overlooked. For such scenarios other approaches must be used (e.g. considering the hydrodynamic impacts on the wood stand).

A quantitative comparison between the computed values for the WM indicator and transported woody material volumes failed due to the following three reasons. Firstly, the photographs focused on deposited woody material in the areas where damages occurred and often neglected areas in the stream influence zones. Secondly, the frequency of torrential events in the considered catchments could not be estimated. Thus, the volume of debris in a given picture may not be an accurate indicator of volume if the frequency of events in the past decades is high (i.e. material has been transported downstream in previous events). Thirdly, the intensity/frequency relationship of the documented event is not known and therefore, the comparison of the documented events with the scenario of a return period of 100 years is difficult. Nevertheless, the comparison showed a noticeable spatial correlation between the WM indicator and observed transportation and deposition of woody material.

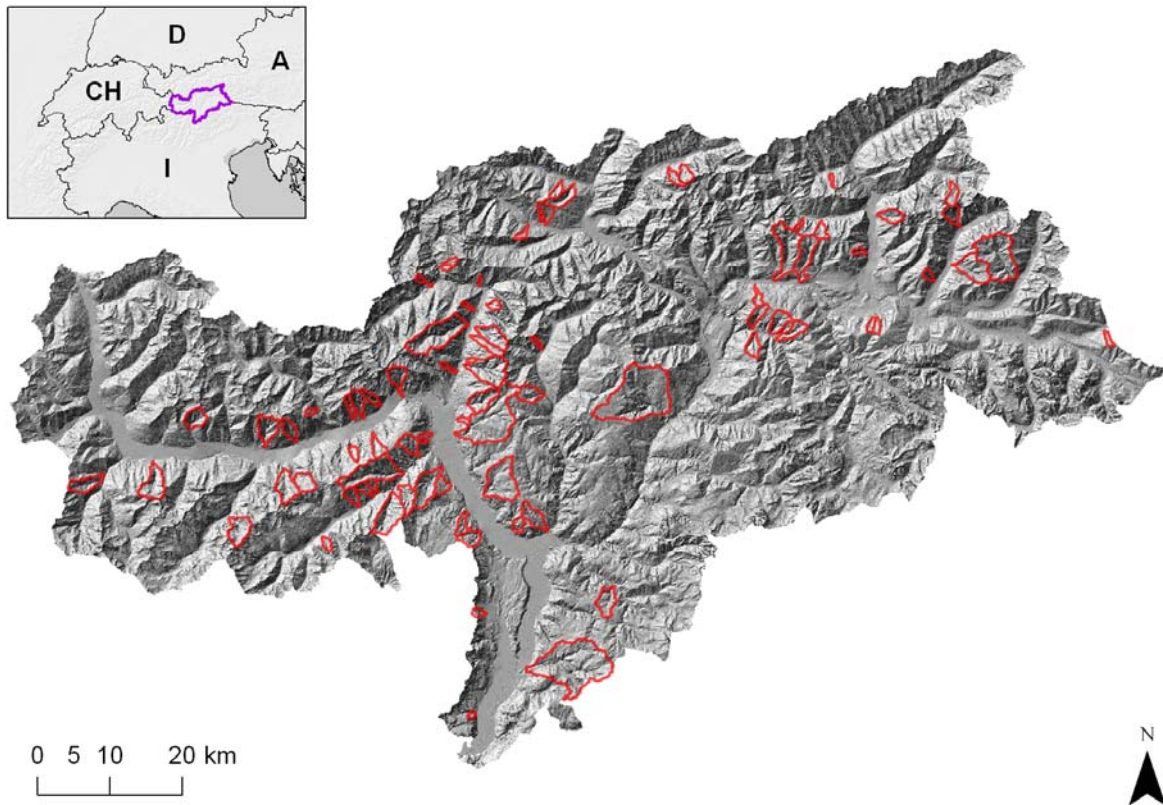


Figure 2-7: Torrent catchments with observed woody material recruitment and transport during documented debris flow and overbank sedimentation processes.

2.5 Conclusions

The questions stated in the introductory chapter were successfully answered. The procedure enables the identification of those torrent catchments susceptible to woody material recruitment and transport which must be considered in hazard mapping. The detection of hazards related to woody material transport is a fundamental prerequisite for a robust and reliable risk assessment procedure for hydrologic hazards. In catchments with high values of the woody material transport indicator (WM), a detailed analysis of torrential processes occurring at critical configurations (e.g. bridge locations) is highly recommended. The knowledge derived from the generated hazard index maps supports a hind- and foresighted conceptual planning process of functional and efficient protection systems. Due to the higher weight given to the recruitment areas close to the end section of a catchment, the procedure is able to identify those catchments for which forestry measures should be checked (e.g. thinning the wood stand within the relevant stream influence zone).

Detailed results on a catchment scale can be obtained using high resolution digital elevation and surface models, performing hydrological computations by means of distributed hydrological models

and retrieving detailed forest cover datasets (e.g. tree heights, areas with different canopy densities) and improving the parameter estimates for woody material recruitment and transport by ad hoc field surveys.

Regarding the young research stage of woody material transport processes, the possibility for further development of the application is a central aspect. In the authors' opinion, further improvements of the procedure could be attained by: a) introducing a probabilistic approach and connectivity indicators for the assessment of recruitment and b) using the results of 2D hydrodynamic computations for the description of the time-dependent entrainment and transport processes within the SIZ-areas.

2.6 References

Abbe, T.B. and Montgomery, D.R., 1996. Large woody debris jams, channel hydraulics and habitat formation in large rivers. *Reg. Rivers: Res. Mgmt.*, 12, 2001-221.

Abbe T.B., Montgomery D.R. and Petroff C., 1997. Design of stable in-channel wood debris structures for bank protection and habitat restoration: an example from the Cowlitz River, WA. In: S.S.Y. Wang, E.J. Langendoen and F.D. Shields, Editors, *Management of Landscapes Disturbed by Channel Incision: Stabilization, Rehabilitation, Restoration*, University of Mississippi, Mississippi (1997), pp. 809–815.

Autonome Provinz Bozen – Südtirol, 2004. *Forst- und Weidewirtschaftliche Realnutzungskarte*, Bozen.

Autonome Provinz Bozen – Südtirol – Abteilung Wasserschutzbauten, 2008. *IHR – Informationssystem zu Hydrogeologischen Risiken. Methodischer Endbericht*. Bozen.

Berger, E., Grisotto, S., Hübl, J., Kienholz, H., Kollarits, S., Leber, D., Loipersberger, A., Marchi, L., Mazzorana, B., Moser, M., Nössing, T., Riedler, S., Scheidl, C., Schmid, F., Schnetzer, I., Siegel, H. and Volk, G., 2007. *DIS-ALP. Disaster information system of alpine regions*, Final report, unpublished.

Bezzola G.R. and Lange D., 2003. Umgang mit Schwemmholz im Wasserbau, *Wasser Energie Luft* 95(11/12): 360-363.

Bezzola, G. R., Sigg, H. and Lange D., 2004. Driftwood retention works in Switzerland, *Internationales Symposium Interpraevent 2004 – Riva del Garda*.

Borselli L., Cassi P., Torri D., 2008. Prolegomena to sediment and flow connectivity in the landscape: A GIS and field numerical assessment. *CATENA* (Elsevier) doi:10.1016/j.catena.2008.07.006.

Braudrick, C.A., Grant, G.E., Ishikawa, Y., and Ikeda, H., 1997. Dynamics of wood transport in streams: a flume experiment. *Earth Surface Processes and Landforms*, 22, 669–683.

Braudrick C.A. and Grant G.E., 2000. When do logs move in rivers?, *Water Resources Research* 36 (2000), 571–583.

Braudrick C.A. and Grant G.E., 2001. Transport and deposition of large woody debris in streams: a flume experiment, *Geomorphology*, 41, 263–283.

Comiti F., Andreoli A., Lenzi M.A., and Mao L., 2006. Spatial density and characteristics of woody debris in five mountain rivers of the Dolomites (Italian Alps). *Geomorphology* 78, 44 – 63.

Curran J.H. and Wohl E.E., 2003. Large woody debris and flow resistance in step-pool channels, Cascade Range, Washington, *Geomorphology* 51, 141–157.

Degetto, M., 2000. Dinamica del legname in alveo e modellazione del suo comportamento in presenza di briglie filtranti. MS thesis, University of Padova.

Diehl, T.H., 1997. Potential Drift Accumulation at Bridges. Publication No. FHWA-RD-97-028. U.S. Department of Transportation, Federal Highway Administration Research and Development, Turner-Fairbank Highway Research Center, Virginia.

Dietrich, W. E., and Montgomery, D. R., 1998. SHALSTAB: a digital terrain model for mapping shallow landslide potential, NCASI (National Council of the Paper Industry for Air and Stream Improvement) Technical Report, February 1998, 29pp.

Ferrari; R., 1996. Censimento e sicurezza di piccoli invasi in provincia di bolzano - relazione esplicativa, report for the office 30.6 of the Autonomous Province of Bolzano/Bozen, unpublished.

Fuchs, S. and McAlpin, M., 2005. The net benefit of public expenditures on avalanche defence structures in the municipality of Davos, Switzerland, *Natural Hazards and Earth System Sciences*, 5 (3), 319-330.

Gurnell A.M., Piegay H., Gregory S.V. and Swanson F.J., 2002. Large wood and fluvial processes, *Freshwater Biology* 47, 601–619.

Haga H., Kumagai T., Otsuki K. and Ogawa S., 2002. Transport and retention of coarse woody debris in mountain streams: An in situ field experiment of log transport and a field survey of coarse woody debris distribution, *Water Resources Research*, 38, 8.

Harrington, C.A., DeBell D.S., 1996. Above- and below-ground characteristics associated with wind toppling in a young *Populus* plantation. *Trees*, 11: 109-118.

- Heinimann, H., Hollenstein, K., Kienholz, H., Krummenacher, B., and Mani, P., 1998. Methoden zur Analyse und Bewertung von Naturgefahren. Umweltmaterialien Bundesamt für Umwelt, Wald und Landschaft, Bern, 249 pp.
- Hildebrand R.H., Cemly A.D., Dolloff C.A. and Harpster K.L., 1997. Effects of large woody debris placement on stream channel and benthic macroinvertebrate, *Canadian Journal of Fisheries and Aquatic Sciences* **54**, 931–939.
- Keim R.F., Skaugset A.E. and Bateman D.S., 2002. Physical aquatic habitat: II. Pools and cover affected by large woody debris in three western Oregon streams, *North American Journal of Fisheries Management* **22**, 151–164.
- Klosterhuber R., Plettenbacher T., Hotter M., Schober T., Aschaber R., Vacik H., Pircher G., Gruber G., Ruprecht H., 2007. Ökologisches Handbuch zur Waldtypisierung und Waldstratifizierung Südtirol, Teil A, Zwischenbericht im Auftrag der Autonomen Provinz Bozen, Abteilung 32, Forstwirtschaft.
- Kramer, H., Akça, A.: Leitfaden zur Waldmesslehre. J.D. Sauerländers. Verlag, Frankfurt am Main, Germany. (In German), 1995
- Lancaster S.T. and Shannon K. H., 2001. Modelling Sediment and Wood Storage and Dynamics in Small Mountainous Watersheds, *Geomorphic Processes and Riverine Habitat Water Science and Application Volume 4*, 85-102.
- Lange, D., Bezzola G. R., 2006. Schwemmholz, Probleme und Lösungsansätze. Mittellungen der Versuchsanstalt für Wasserbau, Hydrologie und Glaziologie (VAW), Zurich.
- Lyn, D., Cooper, T., Condon, D. and Gan, L., 2007. Factors in debris accumulation at bridge piers. , Washington, U.S. Department of Transportation, Federal Highway Administration Research and Development, Turner-Fairbank Highway Research Center.
- May, C.L., Gresswell, R.E., 2003. Large wood recruitment and redistribution in headwater streams in the southern Oregon. Coast Range, U.S.A, *Can. J. For. Res.* **33**(8): 1352-1362, 2003.
- Montgomery D.R. and Piegay H.: Wood in rivers: interactions with channel morphology and processes, *Geomorphology* **51** (2003), 1–5.
- Oberndorfer, S.; Fuchs, S.; Rickenmann, D. and Andrecs, P., 2007. Vulnerabilitätsanalyse und monetäre Schadensbewertung von Wildbachereignissen in Österreich, BFW, Wien.
- Pack, R.T., Tarboton, D.G., Goodwin, C.N., 1998. The SINMAP approach to terrain stability mapping. Proceedings of the 8th Congress of the International Association of Engineering Geology, Vancouver, British Columbia, Canada 21-25 September 1998, Vancouver.

- Petraschek, A., Kienholz, H., 2003. Hazard assessment and mapping of mountain risks in Switzerland. In Rickenmann, D. und Chen, C. L. (eds.). Debris-flow hazard mitigation: mechanics, prediction and assessment. Millpress, Rotterdam.
- Rickenmann D., 1997. Schwemmholz und Hochwasser, Wasser, Energie, Luft **89**, 115–119.
- Rickli, C.; Bucher, H-U., 2006. Schutzwald und Schwemmholz in Wildbacheinzugsgebieten. FAN-Agenda 1/06: 17-20.
- Rimböck, A., 2004. Design of rope net barriers for woody debris entrapment, Introduction of a design concept. Proc. Int. Symp. Interpraevent 2004, Riva del Garda, Trento, Italy.
- Robison E.G., Beschta, R.L., 1990. Characteristics of coarse woody debris for several coastal streams of southeast Alaska, USA, Can. J. Fish. Aq. Sci. 47.
- Shields F.D., Morin N. and Kuhnle R.A., 2001. Effects of large woody debris structures on stream hydraulics, Proc. Wetlands Engineering and River Restoration Conference, ASCE, Reston, VA.
- Smart, G. and Jaeggi, M., 1983. Sediment transport on steep slopes, Mitteilungen der Versuchsanstalt für Wasserbau, Hydrologie und Glaziologie, Zürich Nr. 64.
- Sobota, D.J., Gregory, S.V., Van Sickle, J., 2006. Riparian tree fall directionality and modeling large wood recruitment to streams. Canadian Journal Forest Research 36(5): 1243–1254.
- Staffler, H.; Pollinger, R.; Zischg, A.; Mani, P., 2008. Spatial variability and potential impacts of climate change on flood and debris flow hazard zone mapping and implications for risk management, Natural Hazards and Earth System Sciences, 8, 539-558.
- Takahashi T., 1978. Mechanical characteristics of Debris Flow, Journal Hydraulic Division, ASCE, 104, HY8, 1153–1169.
- Takahashi T., 1980. Debris Flow on prismatic open channel, Journal Hydraulic Division, ASCE, 106, HY3, 381–396.
- Takahashi, T., 1991. Debris flows, Rotterdam, Balkema.
- Uchiogi, T., Shima, J., Tajima, H., and Ishikawa, Y., 1996. Design methods for wood-debris entrapment. Proc. Int. Simp. Interpraevent. Garmisch, Partenkirchen 5, 279–288.
- Van Sickle, J.; Gregory, S. V., 1990. Modeling inputs of large woody debris from falling trees. Canadian Journal Forest Research 20: 1593-1601.
- Zimmermann, M., Mani, P., and Gamma, P., 1997. Murganggefahr und Klimaänderung - ein GIS-basierter Ansatz. vdf, Zurich, 161 pp.

Zimmermann, M. and Haeberli, W., 1992. Climatic change and debris flow activity in high mountain areas: a case study in the Swiss Alps. *Catena Supplement*, 22, 59-72.

3. MODELLING WOODY MATERIAL TRANSPORT AND DEPOSITION IN ALPINE RIVERS

*As long as a branch of science offers an abundance of problems,
so long is it alive [...]
D. Hilbert*

B. Mazzorana, A. Zischg, A. Largiader, and J. Hübl (in press): Modelling woody material transport and deposition in alpine rivers. Natural Hazards.

Abstract

Recent flood events in Switzerland and in Western Austria in 2005 were characterized by an increase of hazards impacts and associated losses due to woody material transport phenomena. As a consequence, either protection measures or bridges suffered considerable damages. Furthermore, cross-sectional obstructions due to woody material entrapment caused unexpected floodplain inundations resulting in severe damage to elements at risk. Until now, these woody material transport phenomena are neither sufficiently taken into account nor systematically considered, leading to prediction inaccuracies during the procedure of hazard mapping. To close this gap, we propose a modelling approach that (1) allows the estimation of woody material recruitment from wood covered banks and floodplains; (2) allows the evaluation of the disposition for woody material entrainment and transport to selected critical configurations along the stream; and (3) enables the delineation of hazard process patterns at these critical configurations. Results from a case study suggested the general applicability of the concept. This primer on woody material transport analysis contributes to the refinement of flood hazard assessments due to the consideration of woody material transport scenarios.

Keywords: woody material transport, natural hazards, hazard mapping, risk assessment

3.1 Introduction

Socioeconomic developments in European mountain environments and related forelands are reflected in increasing settlement and economic activities in areas affected by natural hazards (Fuchs and Holub, 2007). Consequently, considerable economic losses have resulted in recent years (Mitchel, 2003; Autonome Provinz Bozen – Südtirol 2006; Oberndorfer et al., 2007) despite the efforts made towards the mitigation of flood hazards and the reduction of specific risks (Fuchs and McAlpin 2005). At critical stream geometry configurations (e.g. bridge cross sections) a remarkable increase of process intensities could be attributed to woody material transport phenomena in mountain streams (e.g., Diehl 1997; Lyn et al., 2007). Due to the general necessity of assessing natural hazard risk in a reproducible manner, guidelines for hazard mapping were defined in European countries (e.g., BUWAL 1998; Autonome Provinz Bozen – Südtirol, 2006), thereby providing milestones with respect to the quality of integral risk management. The major starting point for managing risk from an integral point of view is the deduction and systematic construction of consistent and reliable scenarios. However, subjective assumptions on relevant impact variables such as woody material transport intensities on the system loading side and response mechanisms at critical configurations often cause biases and inaccuracies in the results. Considering the hazardous effects of woody material transport, clear indications emerged from the analyses of the debris flow and flood events that occurred recently in several Alpine regions (e.g., Bänziger 1990; Rickli and Bucher 2006). At critical stream geometry configurations (e.g. bridge locations), the transported woody material is repeatedly entrapped. In addition to increasing the loading conditions on the structural components of the bridges (e.g. piers, abutments and superstructure), overflowing is likely to occur more frequently (Bezzola et al., 2002). In order to assess these phenomena, this paper aims at contributing to a systematic investigation of woody material recruitment processes, an evaluation of the propensity for woody material entrainment and transport to critical configurations, and a detection of hazard process patterns at these critical configurations during extreme floods. The analysis of such elements is indispensable for comprehensive flood hazard assessments and for optimizing forest management strategies. Moreover, knowledge about the quantity of woody material, the main woody material pathways in the stream channel, and the main places of deposition is fundamental for the design of resilient protection systems and for optimised emergency planning. In order to approach problems emerging from in-stream structures, a detailed study of the damage potential has been carried out by Diehl (1997). The relation between the flow resistance due to the presence of large woody debris (LWD) and increased inundation frequency has been analysed in detail by Shields et al. (2001). New insights into the dynamics of wood transport

in streams have been achieved by flume experiments (Rickenmann 1997; Braudrick et al. 1997, 2000 and 2001; Degetto 2000; Haga et al. 2002; Curran et al. 2003; Bocchiola et al. 2008). The interaction of woody material transport with protection measures has been investigated with a special focus on check dams (Uchiogi et al. 1996; Bezzola et al. 2004; Lange et al. 2006) and on rope nets (Rimböck 2005).

Acknowledging the fact that hazard impacts at critical configurations along the stream could be interpreted as effects of a complex process interaction field, the main objective of this paper is to propose a modelling concept for the analysis of the following key aspects in considering woody material transport in flood hazard mapping:

(1) Disposition: Wood stand productivity and deadwood production in the recruitment areas are important factors that determine the disposition for woody transport phenomena in mountain streams.

(2) Intensity of wood-flood interaction: Recruitment processes directly connected to the dynamics of wood-flood interaction become relevant. Recruitment processes due to wood-flood interaction can be attributed directly to hydrodynamic pressure loading and subsequent breakage of the stems. Moreover morphodynamics, such as streambed erosion and aggradation and side erosion play a relevant role (e.g., Abbe et al. 1997; Hildebrand et al. 1997; Gurnell et al. 2002; Keim et al. 2002; Montgomery et al. 2003; Comiti et al. 2006). In fact, the erosive action of the current is responsible for the scouring of root wads which in turn induces tree toppling.

(3) Entrainment and transport of the woody material: The intensity of the flood process, in terms of flow depths and flow velocities, has to be considered as a critical parameter.

(4) Interaction phenomena at critical channel geometry configurations: Significant in this context are woody material entrapment and the related consequences, e.g., bridge failures due to hydrostatic and hydrodynamic overloading. Because of the complexity of the involved process chains, magnitude-frequency related considerations deserve close attention.

Given the above, the developed conceptual structure comprises: (1) criteria for the localization and classification of woody material recruitment areas as well as the assessment of the woody material recruitment volumes; (2) a computational procedure for woody material entrainment processes; (3) a computational scheme for woody material transport and deposition and remobilization dynamics; and (4) an analysis procedure of the interaction phenomena involving transported woody material occurring at critical stream configurations.

The analyses were implemented into a GIS environment. Subsequently, we tested the GIS application for reconstructing woody material recruitment, transport and deposition patterns during

a design event with a reoccurrence period of 300 years and compared it with a flashflood event occurred in 1987 in the Passirio/Passer River in South Tyrol (Northern Italy).

3.2 Theoretical background

Throughout the paper, we will consider a wood-covered floodplain region as a system, Ω , as shown in Figure 3-1. The system is confined at the downstream side by the outflow boundaries, Γ_{out} , and at the upstream side by the inflow boundaries, Γ_{in} . To simplify matters, these boundaries are assumed to be invariant. Furthermore, it is supposed that the material flux exchanges (e.g. discharge, sediment rates and wood material amounts) within the environment are taking place at these boundaries. At the margins, the system is confined to lateral floodplain boundaries, namely the slopes of the mountains. The system consists of stocks or storage compartments and flows or fluxes. Three storage compartments, are defined as (1) sediment storage, $(X_{\Omega}^1)^Y$, (2) water storage, $(X_{\Omega}^2)^Y$, and (3) wood material storage, $(X_{\Omega}^3)^Y$. The corresponding fluxes within the system and at the inflow boundaries are: (1) sediment fluxes, $(\Delta_{\Omega}^1)^Y$ and $(\Delta_{\Gamma}^1)^Y$; (2) water fluxes, $(\Delta_{\Omega}^2)^Y$ and $(\Delta_{\Gamma}^2)^Y$, and (3) woody material fluxes, $(\Delta_{\Omega}^3)^Y$ and $(\Delta_{\Gamma}^3)^Y$.

Each flood can be intended as a disturbance of the system and the effects of a certain flood event depend also on the settings given by the previous floods. As a consequence at the beginning of each flood event, t_i^0 with $i = 1, \dots, N$, a specific set of initial conditions, $(X_{\Omega}^j)^Y_0$ and $(\Delta_{\Omega}^j)^Y_0$, with $j = 1, 2, 3$ and inflow boundary conditions, $(\Delta_{\Gamma}^j)^Y_i$, have to be considered.

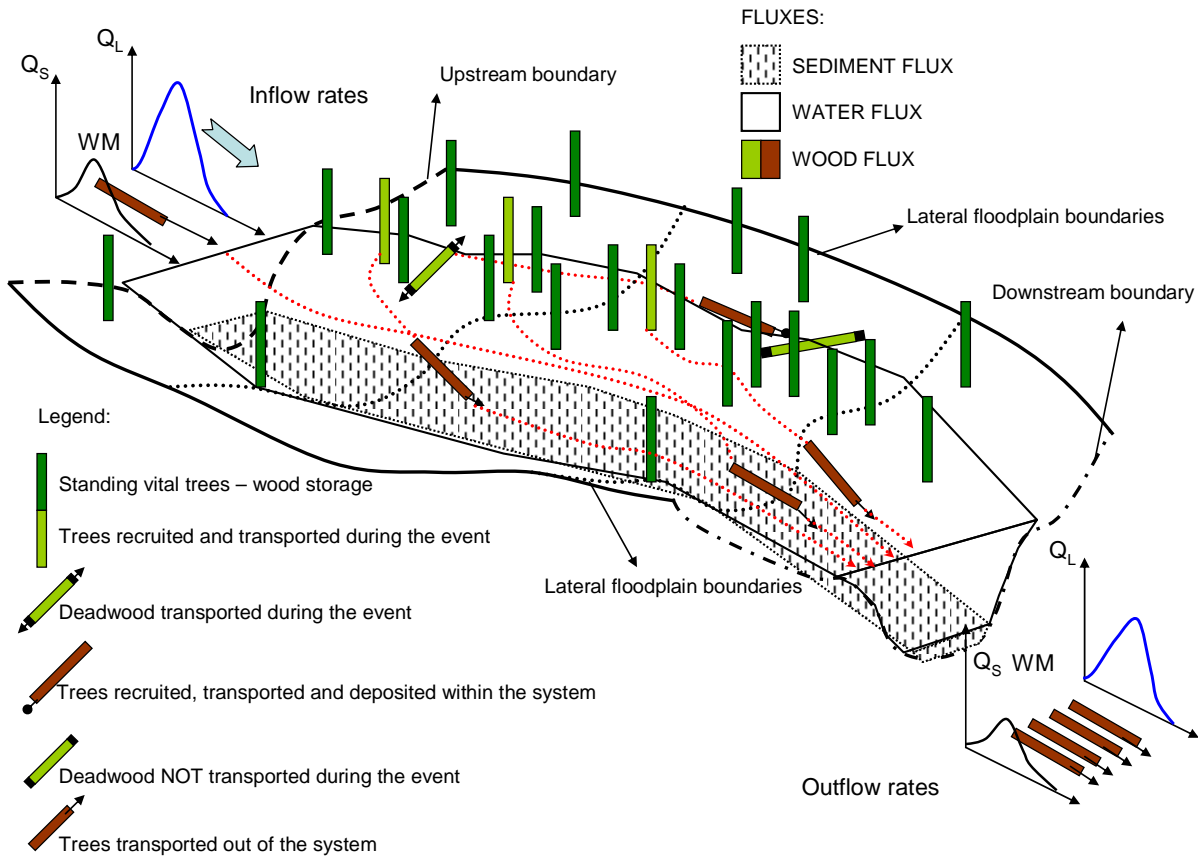


Figure 3-1: Wood, sediment and fluxes and system dynamics

The simulations of the material fluxes taking place within the considered system during successive extreme events would require the solution of distinct boundary conditions and initial value problems. Between successive extreme events the morphodynamical development as well as the growth of the wood stocks has to be monitored in order to correctly assess both the initial and boundary conditions. In the following subsections a concise summary of the main findings regarding woody material recruitment, entrainment and transport are given.

3.2.1 Woody material recruitment

Rickli and Bucher (2006) identify the following relevant recruitment processes from hill slopes:

1. Bank erosion: through the shear stress exerted on the wetted perimeter of the cross-section of the channel, erosion processes occur along the banks and alter the static equilibrium of the trees. Synchronisms between debris flows, flood events and the above mentioned woody material recruitment processes are quite probable.

2. Wind-throw: strong wind conditions can either destabilize the trees that consequently fall as a whole into the channel or lead to the recruitment of the epigeous parts if their stems break under the wind loading. May and Gresswell (2003) point out that falling trees with a horizontal distance to the channel that exceeds their height can exert a destabilizing action on other trees (e.g. knock-on effect).
3. Snow loading: the pressure exerted by the snow, in particular wet snow in spring and autumn, can cause stability problems to broad-leaved trees, increasing bending moments and shear forces. Through the cleaving action of ice, crowns of trees are susceptible to break off.
4. Landslides and other slope processes convey standing and lying woody material towards the channel.
5. Avalanches are likely to incorporate and convey large volumes of woody material within the process perimeter.

Only a few exhaustive experimental results currently exist regarding woody material production and recruitment from different wood structures which are exposed to hydrodynamic impacts. Extensive experimental investigations have been carried out in order to study the hydraulic impact on vegetated riverbanks, e.g. the experiments carried out in the soil bioengineering test flume of the Vienna river (Rauch 2005). Furthermore, a series of 3D numerical simulations of vegetated Compound Channel Flows has been performed (Wilson et al. 2004). A second impact factor influencing woody material production is the wood structure itself. An analysis of recent flood events documented in the Province of Bolzano showed that wood vegetation in the riverbed has a higher relative tendency to produce woody material (depending on wood stand volume) compared to wood vegetation on stream banks. In absolute terms, the amount of woody material recruited from the stream banks exceeded the volume recruited from the riverbank (Mazzorana et al; 2009). This fact can be attributed to the wood stand volume being on average larger on the bank slopes than in the riverbed. In relation to the wood stand volume, wood vegetation located on the stream banks delivers more woody material due to lateral erosion phenomena than wood vegetation of the floodplain.

3.2.2 Woody material entrainment and transport

Theoretical models for woody material entrainment based on the balance of hydrodynamic (F) and resistance forces (R) on individual large woody material pieces have been developed by Ishikawa et al. (1989), Braudrick et al. (1997), and Braudrick and Grant (2000). Assuming the shape of the

woody debris pieces being cylindrical, and neglecting the influence of buoyancy, the hydrodynamic force can be expressed as follows (Haga et al. 2002):

$$F = \frac{1}{2} C_d \rho (lh \sin \theta + A_{sub} \cos \theta) U^2 \quad (3-1)$$

where:

C_d drag coefficient for the woody material element in water

ρ density of the water

l length of the woody material element

h flow depth given by hydrodynamic simulations

A_{sub} submerged area of the log perpendicular to length

θ angle of the element axis relative to the main flow direction

U flow velocities given by hydrodynamic simulations as: $U = \sqrt{u^2 + v^2}$.

The resistance forces can be expressed as follows:

$$R = \left(g \sigma \frac{\pi d^2}{4} - g \rho A_{sub} l \right) (\mu \cos \alpha - \sin \alpha) \quad (3-2)$$

where:

d diameter of the woody material element

μ friction coefficient between the element and the channel bed

σ density of the woody material element

α channel bed slope

g gravity acceleration

Expressing the submerged area of the log perpendicular to its length can be defined as follows:

$$A_{sub} = d^2 \left\{ \frac{1}{4} \cos^{-1} \left(1 - \frac{2h}{d} \right) - \frac{1}{8} \sin \left[2 \cos^{-1} \left(1 - \frac{2h}{d} \right) \right] \right\} \quad (3-3)$$

Expressing the non-dimensional force $\Psi = \frac{F}{R}$ in terms of equations 3-1 and 3-2, the following expression can be obtained (modified from Haga et al. 2002):

$$\Psi = \frac{F}{R} = \frac{\frac{1}{2} C_d \rho (lh \sin \theta + A_{sub} \cos \theta) U^2}{\left(g \sigma \frac{\pi d^2}{4} - g \rho A_{sub} l \right) (\mu \cos \alpha - \sin \alpha)} \quad (3-4)$$

Analysing equation (3-4), the dynamics of a single woody material element with known dimensions can be described within a simplified scheme as follows (Haga et al. 2002):

1) Floating condition: $\frac{h}{d} \geq 1$ (3-5)

2) Resting condition: $\Psi = \frac{F}{R} \leq 1$ and $\frac{h}{d} < 1$ (3-6)

3) Sliding or rolling condition: $\Psi = \frac{F}{R} > 1$ and $\frac{h}{d} < 1$ (3-7)

Field observations (Bezzola et al., 2002) are in good agreement with the above outlined theory. According to those evidences the entrainment condition for smooth wood logs with an approximate cylindrical form is $1 \leq \frac{h}{d} \leq 1.2$. The ratio, $\frac{h}{d}$, increases for wood logs with branches up to 1.5 and for wood logs with root wads up to 1.7.

The above outlined theoretical model does not consider the effects of morphodynamics. After Lange and Bezzola (2006), the entrainment is facilitated in the case of sediment transport due to the fact that the movable stream bed layer acts like a roller-bearing. In these conditions the required flow depths, *ceteris paribus*, are 20% to 30% lower compared to the case without sediment transport.

The procedure for evaluating woody material dynamics from a hazard-related perspective relies on these theoretical principles and is described in the next section.

3.3 Modelling approach

This section provides a description of the developed modelling approach, which has been implemented into a GIS environment. The criteria for the identification, localization and classification of the woody material recruitment areas are explained, followed by the procedure for woody material volume assessment. Subsequently, the relevant aspects of woody material transport dynamics, namely the entrainment, transport and deposition and remobilization processes, are thoroughly discussed and a computational scheme is proposed. Finally, an analysis procedure of interactions at critical stream configurations is introduced.

3.3.1 Identification, localization and classification of woody material recruitment areas

Woody material recruitment areas are identified by the interpretation of aerial stereo images (photographs). According to the findings of Rauch (2005), an innovative *ad hoc* classification of the typologies of alluvial forests, lowland riparian forests and riverside woodland is proposed. The forested areas in the influence zone of the stream are classified into seven structural typologies according to their different behaviour when exposed to hydrodynamic loadings (Table 3-1).

ID	structure characteristics	assumed response characteristic	response in case of flooding	Stand volume [m ³ /ha] Example: Passirio river	Deadwood volume [m ³ /ha]
1	young-growth forest, dense	flexible	lie down, protect the soil	40	5
2	young-growth forest, fragmentary	flexible	lie down, increased turbulences, rough, protect the soil	20	3
3	multilayered structure, dense	flexible and inflexible	reduces flow velocity, rough, protect the soil	240	25
4	even aged population, dense	inflexible	reduces flow velocity, protect the soil	400	40.2
5	multilayered structure, fragmentary	flexible and inflexible	different velocities, turbulences, rough	120	18
6	even aged population, fragmentary	inflexible	different velocities, turbulences, unruffled	200	24
7	old growth, very patched	inflexible	elevated turbulences due to circulation around, leachate	150	20

Table 3-1: Structural classification of forested areas within the influence zone of the river (Blaschke, 2004)

The classification criteria take into account the response of different vegetation and forest typologies to the hydraulic forces and impacts of the flood processes. Figure 3-2 shows the interdependencies between woody material production (interpreted as “distance” from the point of origin in the coordinate system), the level of hydrodynamic impact forces (on the vertical axis), the position within the riparian zone (on the horizontal axis) and the vegetation structure (oblique axis).

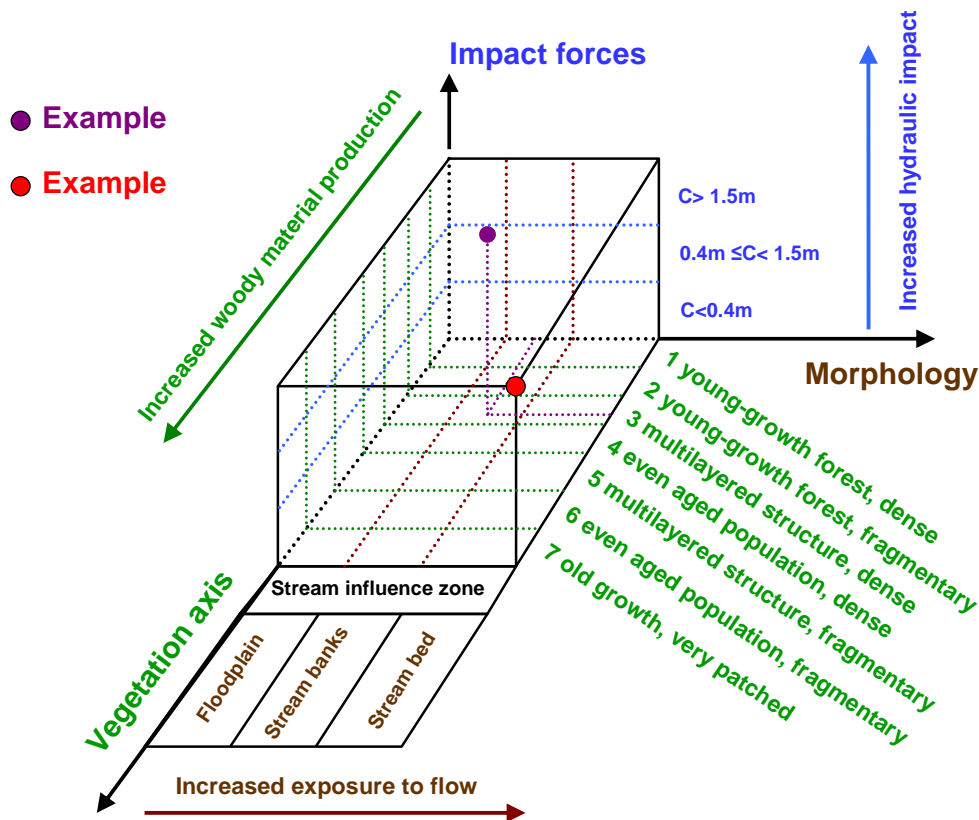


Figure 3-2: Scheme for the assessment of the woody debris recruitment on regional scale.

Table 3-1 shows the potentially available volumes of woody material for each vegetation structure typology.

In addition, Table 3-1 provides the description of the corresponding typical response mechanisms. The geomorphologic characteristics of the flood process areas have to be determined. These areas are classified as (1) stream bed, (2) stream bank, and (3) process area of an extreme flood event.

The classification is made on the basis of digital elevation models, aerial photographs and a Lidar-based digital terrain model with a high spatial resolution. An output dataset is obtained with the morphology of the stream influence zone.

3.3.2 Assessment of the recruited woody material volume

Three distinct computational procedures for the assessment of woody material recruitment volumes are presented for: (1) the recruitment from hill slopes, (2) the recruitment from tributaries, and (3) the recruitment within the maximum extent of the flooded area.

3.3.2.1 Assessment of the recruitment volumes from hill slopes

In this subsection a procedure to assess the recruited woody material volumes from hill slopes is outlined. This assessment involves the following steps:

Step 1: Determination of the perimeter of the flooded areas of the considered extreme event from flow depth or velocity raster data sets. The flow depth or velocity data sets corresponding to the different time steps are given as output files of the hydrodynamic simulations performed with 2D numerical model Sobek Rural (WL/Delft Hydraulics 2004). These raster data sets are overlaid in order to derive the perimeter identifying the maximum extent of the flood (compare figure 3-3 for details).

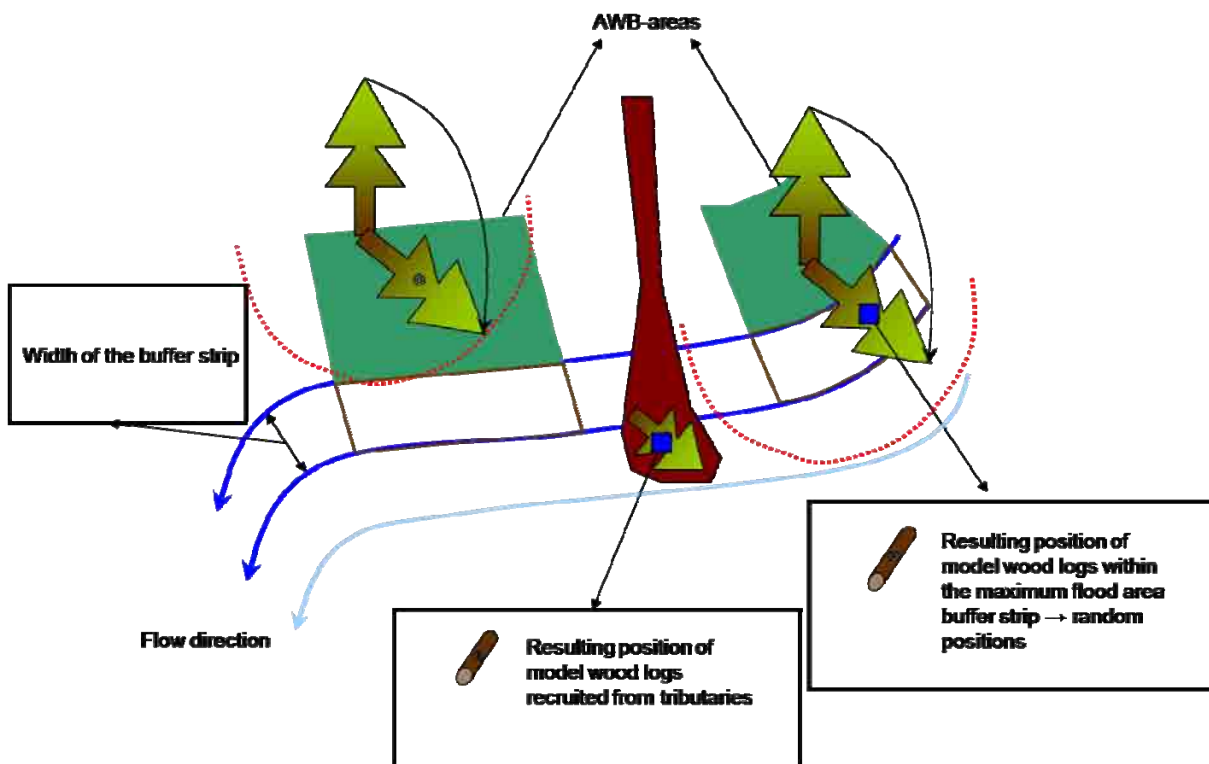


Figure 3-3: Determination of the recruitment strips within the maximum extent buffer areas

Step 2: A screening for the availability of wood covered areas outside of the maximum flood boundaries. These wood covered areas within a buffer width are categorized as AWB (active wood buffer) areas. This buffer width corresponds either to the potential tree height derived from the forest typology map of the Autonomous Province of Bolzano (Klosterhuber et al., 2007) or to the real tree height retrieved from the Lidar-based digital surface model and the digital terrain model (Mazzorana et al., 2009). The difference between the surface model and the terrain model can give hints about the reference tree height and therefore about the width of the active wood buffer.

Step 3: Identification of the recruitment wood buffer strips. Inside the delimitation polygon of the maximum extent flood area, buffer strips for the wood volumes, potentially recruited from the AWB areas, are identified in direct proximity to the AWB-areas (compare figure 3-3 for details). The width of these strips is half of the tree height of the adjacent AWB area and corresponds to the area of possible location of the centre of gravity of the recruited wood logs.

Step 4: Computation of the length of the contact boundary between the AWB areas and the buffer strips (identified in step 3). The user has to define the volume of recruited woody material per unit length of contact boundary for each AWB-area. An estimation of recruitment volume scenarios is made on the basis of experimental data provided by inventories (Rickli and Bucher, 2006). It should be noted that uncertainty is not negligible without detailed forest inventories and a precise estimation of dead wood volumes and forest stand stability conditions of the forest population. It is recommended to define a plurality of scenarios of recruitment volumes per unit length.

Step 5: Specification of the dimension and number of the model wood logs. In this step, the dimensions of the “model wood log” (diameter and log length) are specified and the determination of the recruited number of model wood logs for each strip is straightforward, once known the volumes from the recruitment scenarios defined in the previous step. The position of the centre of gravity of the “model wood logs” is either chosen at random (compare figure 3-3) or assessed by field investigations.

Step 6: Determination of the starting position of the “model wood logs”. The volume of each recruited “model wood log” is assigned to the corresponding flow cell depending on the position of its centre of gravity (compare figure 3-3).

3.3.2.2 Assessment of the recruitment volumes from tributaries:

This assessment involves the following two steps:

Step 1: The recruitment scenarios of wood material volumes from the tributaries can be reliably defined only if a detailed documentation for those events exists. If information is missing, possible scenarios of recruited woody material volumes can be defined on the basis of empirical formulas (Rickenmann, 1997) or with the procedure proposed by Rimböck (2003).

Step 2: The number of “model wood logs” is calculated. Again the problem arises of the positioning of the “model wood logs” within the maximum extent flood area. In the case of accurate event documentations, the “model wood logs” can be placed within the geo-referenced depositional areas (compare figure 3-3). Otherwise engineering judgement is required to position the “model wood logs”, e.g. choosing probable deposition sites.

3.3.2.3 Assessment of the recruitment volumes within the flooded area

Forests of different wood typologies produce determined amounts of deadwood ready for transport depending on the current stage in their “life cycle”. During the flood event itself additional deadwood is produced as a consequence of either direct hydrodynamic impact on trees or destabilization of the trees’ anchorage through erosion phenomena (root wad scouring).

The vegetation structures are mapped and the morphology of the riverbank is overlaid with the outputs of the respective flood simulation. A woody material recruitment indicator is computed based on an impact-response assessment approach, which considers either the morphological characteristics or the flood intensity. This impact-response assessment approach has been developed on the basis of the findings of Rauch (2005) and Hübl et al. (2009). Experimental studies should further investigate the interplay of the following key factors : (1) Hydrodynamic impact: The hydrodynamic impact acts, on the one hand, through static and dynamic pressure forces on wood vegetation and, on the other hand, by yielding stress on the soil, weakening the root-soil anchorages. (2) Wood stand volume: A positive correlation between the recruited woody material volume and the wood stand volume is postulated. Average wood stand volume estimations for different wood stand structures are reported in Table 1. (3) Wood vegetation resistance-resilience: The influence of the aforementioned key factors cannot be understood and quantitatively estimated without assessing wood vegetation resistance-resilience mechanisms. These depend on both wood structural and species-specific characteristics. For the necessary accuracy level, the analysis is limited to the first type of characteristics underlining that resistance-resilience against hydrodynamic impact depends significantly on the flexibility of the wood and on recovery capacity. In addition, a very flexible vegetation structure protects the soil from erosion, while inflexible – old growth – population structures are weakened by erosion mechanisms and are also unstable due to an unfavourable slenderness (h/d) ratio. These interaction phenomena are described in Table 3-1.

The assessment scheme is shown in Figure 3-2, where the energy indicator $C_{i,j}$ describes hydraulic impact on vegetation structures (see Equation 8). The energy indicator is composed of a hydrostatic and a hydrodynamic pressure term and it is calculated as follows (Egli 2008, Holub and Hübl 2008):

$$Q_{i,j} = \rho g h_{i,j} + \frac{c_d \rho U_{i,j}^2}{2} \quad (3-8a)$$

where:

$i,j \dots$ cell indices

$h_{i,j} \dots$ flow depth [m]

$U_{i,j} \dots$ flow velocity [m/s]

$Q_{i,j}$... pressure load

c_d ... drag coefficient

ρ ... density of the water

Dividing both terms on the right hand side of equation (3-8a) by ρg and assuming $c_d \approx 1$, we obtain the specific load:

$$C_{i,j} = \frac{Q_{i,j}}{\rho g} = h_{i,j} + \frac{U_{i,j}^2}{2g} \quad (3-8b)$$

The flow velocity is calculated from the velocities in direction x and y:

$$U_{i,j} = \sqrt{u_{x_{i,j}}^2 + u_{y_{i,j}}^2} \quad (3-9)$$

where:

$u_{x_{i,j}}$... flow velocity in x-direction [m/s]

$u_{y_{i,j}}$... flow velocity in y-direction [m/s]

By a qualitative analysis of documented flood events (Mazzorana et al., 2009) the following assessment procedure for woody material recruitment could be established (cf. Figure 3-4): (1) Identification and spatial delimitation of possible woody material recruitment areas, (2) assignment of these recruitment areas to the appropriate river morphology categories (e.g. streambed, river banks, floodplain), (3) determination of the wood structure characteristics and definition of the respective structure typologies (compare Table 3-1), 4) calculation of an indicator describing the hydraulic impact (Equation 3-8), (5) estimation of the recruitment volumes (recruited wood volume per hectare/stand volume per hectare), here referred to as woody material recruitment indicator (SVI) on the basis of the scheme shown in Figure 3-4, and (6) quantification (see Equation 3-10) of the absolute volume of recruited woody material (V_{SH}).

The parameter of the absolute volume of recruited woody material indicates the maximum volume of woody material that could be ripped at a given location by the flood process.

Finally, the recruited woody material volume for each cell is calculated as

$$V_{SH,i,j} = SVI_{i,j} \cdot V_{cell,i,j} \quad (3-10)$$

Since the wood stand volume is given as a parameter showing values per hectares, Equation (3-11) is used to calculate the woody material volume.

$$V_{SH,i,j} = SVI_{i,j} \cdot \left(\frac{A_{i,j}}{10000} \right) \cdot V_{ha} \quad (3-11)$$

where:

$V_{cell\ i,j}$... wood stand volume for the cell i,j

V_{ha} ... wood stand volume referred to an area of 1 ha

$A_{i,j}$... area of the cell i,j in m^2

The resulting output from this step is the calculated maximal volume of woody material that could be ripped out from each cell by the flood.

The estimations of the recruited wood volumes per hectare and the quantification of the absolute volume of recruited woody material (step 5 and 6 of the above outlined procedure, respectively) can be computed also following a slightly modified procedure, which explicitly accounts for the subdivision of the flood duration in time steps Δt . Two essential requirements are:

- a) Knowledge about the deadwood material available in each cell at time t^0 .
- b) Knowledge about the amount of greenwood, which, through either stem breakage or “uprooting” (and toppling) due to erosion, becomes deadwood ready for transport at the beginning of the successive time step.

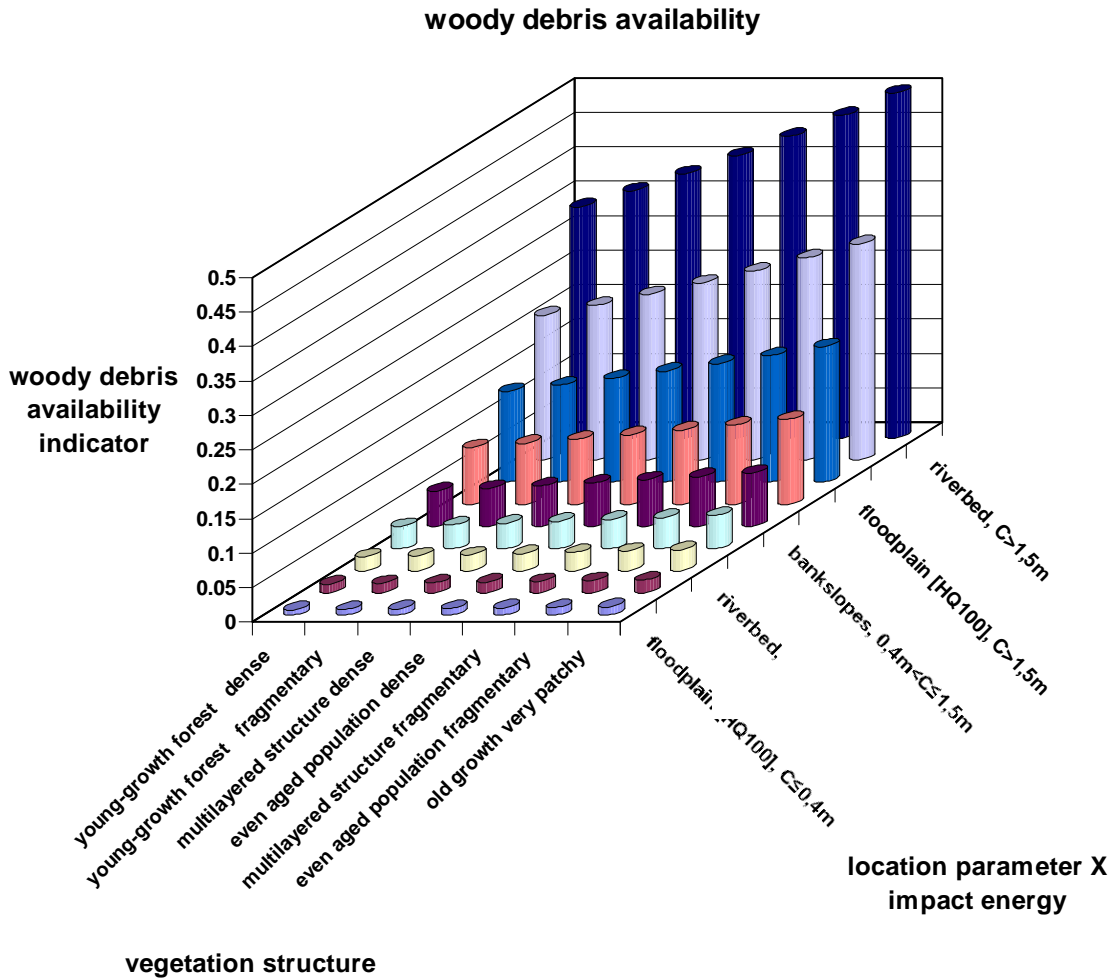


Figure 3-4: Decision matrix for the quantification of the woody debris availability on regional scale. Expert-based estimation of the woody material availability indicator

Consequently, maximum estimated deadwood amounts for different forest typologies and predictions of the deadwood amounts produced in a given time step are required.

Plausible values of deadwood volumes for different wood typologies range from 3 m³/ha to 40.2 m³/ha. In table 3-1 estimations of possible deadwood volumes for different wood typologies are reported.

The prediction of the deadwood volumes, which are produced in a given time step in a determined forest typology exposed to determined hydrodynamic impacts and to determined riverbed dynamics, is conducted with the following linear relationship:

$$V_{DW,i,j}^{\Delta t} = k \cdot SVI_{i,j}^t \cdot V_{GW,i,j}^t \cdot \Delta t \quad (3-12)$$

whereas:

$V_{DW,i,j}^{\Delta t}$... Deadwood produced within the time step Δt in the cell i,j

$SVI_{i,j}^t$ Response class [1/sec] (determined in full analogy to the first theory) for cell i,j

$V_{GW,i,j}^t$ Greenwood volume in the cell at time step t [m^3] in cell i,j

Δt Time step [sec]

k Empirical constant, to be assessed on the basis observed extreme floods.

The amount of greenwood at time Step $t+1$ is computed as follows:

$$V_{GW,i,j}^{t+1} = V_{GW,i,j}^t - V_{DW,i,j}^{\Delta t} \quad (3-13)$$

It should be noted that the influence of morphodynamics is not considered in its full complexity in this approach (e.g. no mobile bed or shear stress computations are performed). Morphodynamics are considered indirectly and in a simplified way in the estimation procedure of the woody material recruitment indicator ($SVI_{i,j}^t$) by assigning a location attribute (i.e. stream bed, stream bank or floodplain) to each cell (compare figures 3-2 and 3-4).

3.3.3 Woody material transport dynamics

Having defined and quantified the recruitment areas, the transport of material from these areas to the defined weak points or critical river locations and cross sections can be modelled. The modelling procedure is able to consider two different approaches for modelling the transport of woody material. If the main objective is the estimation of the pathways and the possible deposition zones, the transport of woody material is calculated on a cell-by-cell basis. This approach allows analysing the transportation and deposition dynamics either on a regional level or on a detail level. With this modelling approach, only one time step of the hydraulic modelling results can be considered. If the main objective is to study the interactions of transported woody material with obstacles such as bridges, the transport of woody material is calculated following an object-oriented approach. This approach allows the consideration of more time steps of the hydraulic modelling and the deposition of woody material on sand banks during the falling limb of a flood hydrograph. In such a way, it is possible to keep track of the positions of the woody material elements from time step to time step.

The basics for the calculation of the transport dynamics are the same in the two approaches and are based on the following simplified model. This model delineates the possible pathways for woody material transport and computes, for each of them the entrainment and transport conditions based on the theory outlined in section 3.2.2 and on the following method. The input data are the raster results from a hydrodynamic 2D simulation of the design event (1 in 300 years return period) for water depths $h_{i,j}$ and flow velocities in x and y direction, $u_{x_{i,j}}$ and $u_{y_{i,j}}$. These rasters represent the state of the hydraulic simulation of different timesteps. For each cell in the affected flood area, the flow direction is calculated according to the respective flow velocity in x- and y-direction and given this flow direction, the source cell is moved until it is fitted into the next two neighbouring cells. The amount of woody material arriving from the source cell is divided into two portions according to the overlapping area of the moved source cell with the two neighbouring cells (figure 3-5). The particular portion of each subsequent cell is added, giving the total amount in this cell. The volumes passed through each cell are cumulated and a grid dataset of the woody material volume passed through each cell of the river influence zone is produced.

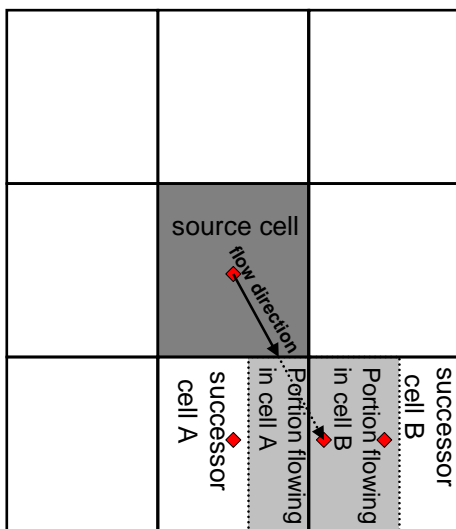


Figure 3-5: Determination of the following cells (A and B) and their particular portion of the woody material from the source cell to receive.

This approach is based on a further simplification of Equations (3-1) and (3-2) in order to precisely determine the woody material transport analysis conducted on a hazard index level (Petraschek and Kienholz 2003). Assuming that the woody material elements are positioned perpendicular to the flow direction ($\theta = 90^\circ$), and that the length of each element is expressed as a multiple of its diameter, $l = nd$, with $n \geq 1$; Equation (3-14) is obtained from Equation (3-1).

$$F = \frac{1}{2} C_d \cdot \rho \cdot k \cdot d \cdot h_{i,j} \cdot U_{i,j}^2 \quad (3-14)$$

Taking the hypothesis that the density of the wood element can be expressed as $\sigma = n \cdot \rho$ with $n \cong 1$ and that the local slope angle at the wood element locations is very small, $\alpha \cong 0^\circ$, Equation (3-2) can be rewritten as:

$$R = \mu \rho g l \left(\frac{\pi d^2}{4} - A_{sub} \right) = g \rho k d \mu \left(\frac{\pi d^2}{4} - A_{sub} \right) \quad (3-15)$$

Based on Equation (3-3), Equation (3-4) can be re-written as:

$$\Psi = \frac{F}{R} = \frac{\frac{1}{2} C_d \rho k d h_{i,j} U_{i,j}^2}{g \rho k d \mu \left(\frac{\pi d^2}{4} - A_{sub} \right)} = \frac{\frac{1}{2} C_d h_{i,j} U_{i,j}^2}{g \mu \left(\frac{\pi d^2}{4} - A_{sub} \right)} = \frac{2 C_d h_{i,j} U_{i,j}^2}{g \mu d^2 \left\{ \pi - \cos^{-1} \left(1 - \frac{2h_{i,j}}{d} \right) + \frac{1}{2} \sin \left[2 \cos^{-1} \left(1 - \frac{2h_{i,j}}{d} \right) \right] \right\}} \quad (3-16)$$

Subsequently the velocity corresponding to $\Psi = \frac{F}{R} = 1$, here named as threshold velocity, U_{lim} , for the movement of the wood element, is determined accordingly by

$$U_{lim,i,j} = \sqrt{\frac{2g\mu}{C_d h_{i,j}} \left(\frac{\pi d^2}{4} - A_{sub} \right)} = \sqrt{\frac{g\mu d^2}{2C_d h_{i,j}} \left\{ \pi - \cos^{-1} \left(1 - \frac{2h_{i,j}}{d} \right) + \frac{1}{2} \sin \left[2 \cos^{-1} \left(1 - \frac{2h_{i,j}}{d} \right) \right] \right\}} \quad (3-17)$$

Given these results and the conditions stated for expressions 3-5, 3-6 and 3-7, the cell- based transport inhibition parameter is defined as follows:

Case 1: If $h_{i,j} \geq d$ the wood material element is floating and the associated specific transport inhibition parameter is $c_{i,j}^* = 0$.

$$\text{Case 2: If } h_{i,j} < d \text{ and } 0 < U_{i,j} \leq \sqrt{\frac{g\mu_{i,j} d^2}{2C_d h_{i,j}} \left\{ \pi - \cos^{-1} \left(1 - \frac{2h_{i,j}}{d} \right) + \frac{1}{2} \sin \left[2 \cos^{-1} \left(1 - \frac{2h_{i,j}}{d} \right) \right] \right\}}$$

or $0 < U_{i,j} \leq U_{lim,i,j}$ a condition of resting is imposed to the wood material element. The associated specific transport inhibition parameters $c_{i,j}^* = 1$.

Case 3: If $h_{i,j} < d$ and $U_{i,j} > U_{lim,i,j}$ a condition of either sliding or rolling is imposed to the wood material element. The value of the associated transport inhibition parameter is expressed by:

$$c_{i,j}^* = 1 - \frac{F_{i,j}}{F_{i,j}^*} = 1 - \frac{\frac{1}{2}C_d\rho kd h_{i,j} U_{i,j}^2}{\frac{1}{2}C_d\rho kd^2 U_{i,j}^2} = 1 - \frac{h_{i,j}}{d} \quad (3-19)$$

where:

$c_{i,j}^*$... *transport inhibition parameter of the cell i,j (nondimensional)*

Observations noted by Diehl (1997) and Ng et al. (2001) indicate that woody material in ideal conditions is transported on the surface as individual pieces aligned with the flow and travelling at about the same velocity as the average water velocity at the surface.

Using the average velocity instead of the surface velocity as reference velocity for the moving woody material for a wide range of flow conditions, velocity along the transport trajectory for each moving woody material model log, is estimated as follows:

$$U_{wood_{i,j}} = (1 - c_{i,j}^*)U_{i,j} \quad (3-20)$$

whereas:

$U_{wood_{i,j}}$ *velocity of a wood log in the cell i,j.*

An analysis of the expression for the wood log velocity (equation 3-20) reveals that if the transport inhibition parameter tends to 1, coherently with resting or deposition conditions the velocity of the wood log tends to 0, whereas if the transport inhibition parameter tends to 0 the velocity of the wood log tends to $U_{i,j}$. Through this method, it is possible to describe woody material transport pathways under unsteady flow conditions. A deposited woody material log can be remobilized in a successive time step under changed flow depth and flow velocity conditions.

3.3.4 Potential hazard impacts at critical stream configurations

The object-oriented approach for modelling the woody material transport dynamics as outlined in chapter 3.3 allows the assessment of potential hazard impacts at critical stream configurations. This approach considers the model wood logs as points, representing the centre points of the model wood log. Each single object has information about log diameter, log length, diameter of root wads, and impact-resistance characteristics as outlined in figure 3-2. The flowing of the model wood logs is computed following the procedure as proposed in chapter 3.3.

A simplified assessment procedure for entrapment and deposition phenomena at special obstacles (e.g. bridges) is outlined. In figure 3-6, a stream section with a crossing bridge is shown. Along the

flow path, woody material can potentially interact with: (1) the superstructure of the bridge, (2) a single bridge pier, and/or (3) two or more bridge piers.

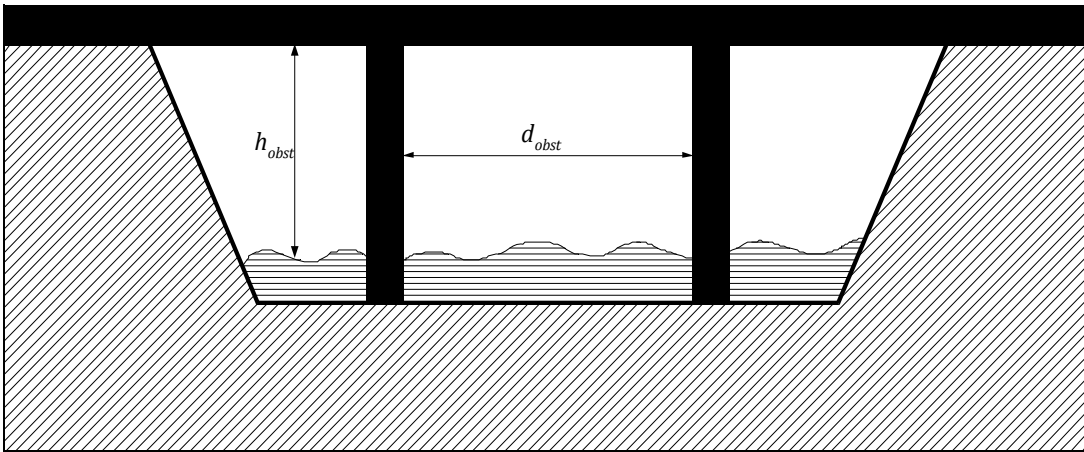


Figure 3-6: Example of a bridge as an obstacle consisting of two piers as in-stream-obstacles and the superstructure as a crossing obstacle d_{obst} indicates the minimum distance between the two piers and h_{obst} the height of the superstructure.

Two types of obstacles are defined in order to model the interaction between these obstacles and the floating woody material:

In-stream-obstacles: Obstacles standing in the water such as piers or abutments. On these obstacles transported logs can get entrapped upon collision at any stage of the flood.

Crossing obstacles: Obstacles crossing the stream at a given height on which the logs can get entrapped with their root plate when the flow depth approaches the object's height. (Lower chord of the superstructure of a bridge, see Figure 3-6.)

Within the computational procedure, these obstacles are represented by polygon objects. The following attributes are required to comprehensively describe these obstacles:

(1) Retention probability (p_{ret}): Probability for each colliding log to get entrapped at the considered obstacle. This gives the expert the possibility to consider the geometry (e.g. profile) of an obstacle (e.g. inappropriately shaped piers) and estimate a proper retention probability.

(2) Obstacle height (h_{obst}): Height of the lower chord of a crossing obstacle above the initial water level. The obstacle type is defined using the obstacle height (figure 3-6). In case the obstacle height equals zero an object is treated as in-stream-obstacle, otherwise the object is handled as a crossing obstacle.

A collision with an obstacle occurs when the flow path of a woody material log intersects an obstacle. If it is a crossing obstacle, the flow depth needs to reach a critical value. Above this value the root plate can contact the lower chord of the obstacle. Depending on the retention probability of

the obstacle, specified by expert judgement, the woody material logs may either be entrapped or flushed through (see figure 3-7).

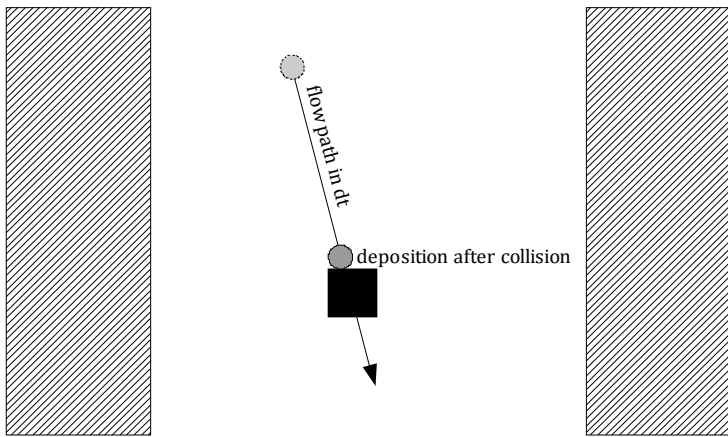


Figure 3-7: Example of a collision with an in-stream-object. The flowpath intersects the shape of a pier. In this case the floating log is entrapped at the first intersection point between the flow path and the shape of the pier.

If an object is floating between two in-stream-obstacles, e.g. two piers, it is checked whether the length of the log exceeds the shortest distance (d_{obst}) between the two piers. If so, a spanning blockage can occur, provided that the log is unfavourably oriented. The corresponding probability (p_{ent}) is estimated through expert judgement.

The entrapped wood logs occlude part of the available flow section and become a part of the obstacle for wood logs subsequently approaching the critical configuration (see Figure 3-8).

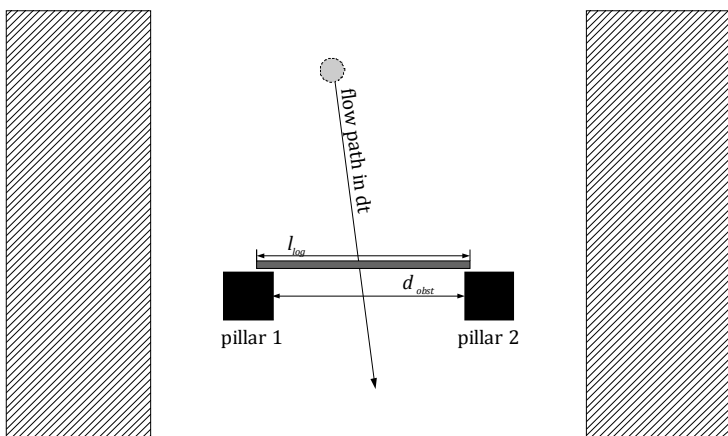


Figure 3-8: Example of a woody material object floating between two piers of a bridge. The flow path does not cross any of the piers; however, the length (l_{log}) exceeds the minimum distance between the two pillars (d_{obst}) and the possibility of entrapment occurs

3.4 Study site and test application

The Passer/Passirio River in the Autonomous Province of Bolzano – South Tyrol, Italy was chosen as test site for the application of the procedure described in the previous sections (figure 3-9). The Passer/Passirio River drains a catchment area of approximately 415 km² and opens to the receiving watercourse Etsch/Adige River nearby the city of Meran/Merano, Italy. The study area comprises the river-bed and the extent of the simulated flooded areas of the Passer/Passirio River during a flood event with a return period of 1 in 300 years. A relevant volume of woody material arriving from the upper parts of the catchment is entrapped at the open check dam located in the upstream river reach. The upstream boundary of the simulation area is located at this open check dam near the community of St. Leonhard in Passeier/S. Leonardo in Passiria. A high magnitude flash flood occurred in the Passer/Passirio River in 1987 (figure 3-10) resulting in severe damage to regionally important bridges and roads. The downstream boundaries were defined near the locality of Saltaus/Saltusio at a bridge location (figure 3-9b). The cumulative volume of the transported woody material was calculated here. Within the studied river reach, the channel bed is characterised by twelve tributaries with relevant input of woody material. The material supplied by the tributaries was considered in this study. Figure 3-9c summarizes the extent of the system.

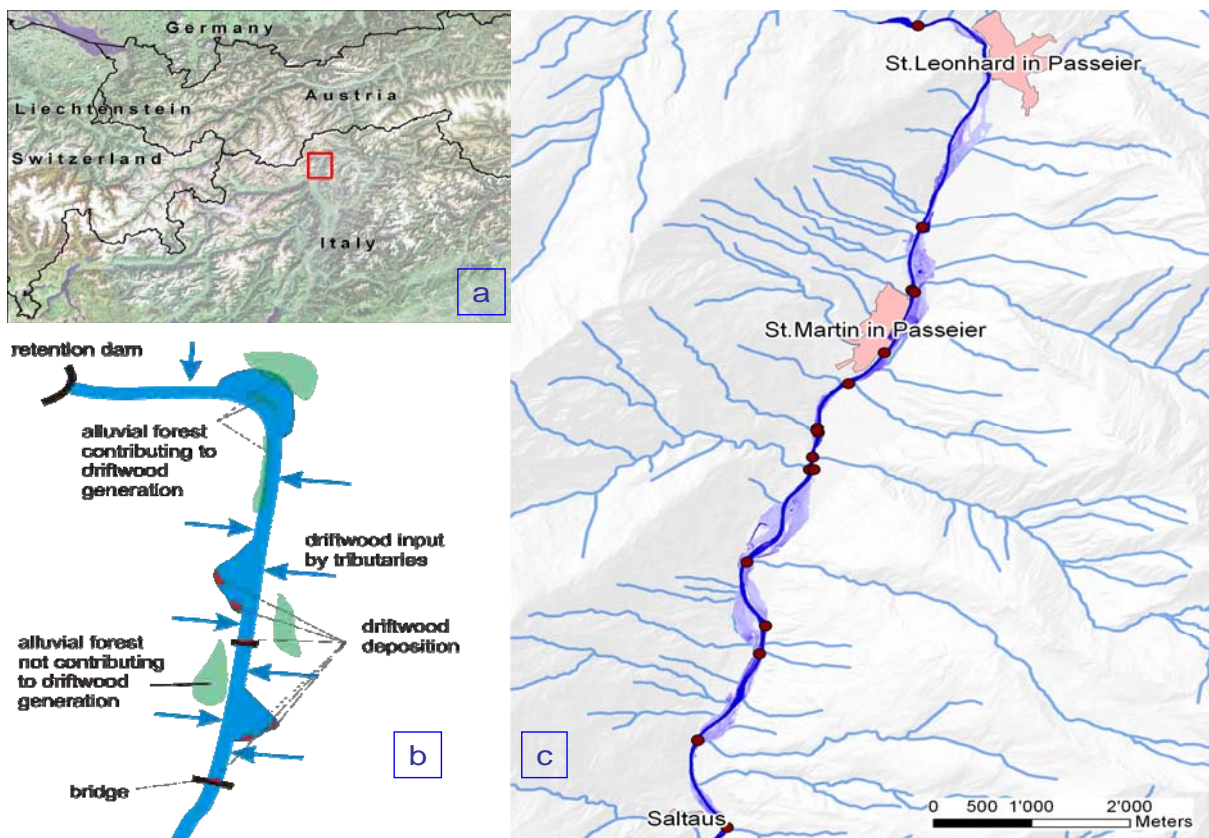


Figure 3-9: (a) Localization, (b) system description and (c) extent and delimitation of the study area.



Figure 3-10: An aerial image of the study area after the flood event in 1987.

The woody material volumes delivered by the tributaries were assessed and quantified by analysing recent debris flow events. Table 3-2 shows the assumed values for the available woody material inputs. The interceptors (e.g. bridges and check dams) within the river influence zones were geo-referenced. For each of these critical configurations, the geometrical characteristics were assessed and a retention probability was assumed. This retention factor accounted for the woody material volumes retained by the obstacle. The simulation procedure was repeated with and without consideration of these weak points.

torrent ID	name of torrent	woody debris volume [m³]	notes
G	Passer/Passira	10	initial condition: woody material passing through the retention dam
G.255	Keltalbach/Rio Lega	20	torrent with debris flow processes
G.235	Talbach/Rio di Valle	2	torrent with debris flow processes
G.230	Fartleisbach/ Rio dell'Avas	5	torrent with debris flow processes
G.220	Dorfbach/ Rio Dorf	5	torrent with debris flow processes
G.205	Schoenbichlbach (Kellerbach)/ Rio di Belcolle	5	torrent with debris flow processes
G.195	Heimatscheintal/ Rio del Masso dei Tovi	5	torrent with debris flow processes
		100	lumbryhood in the neighbourhood upstream of the confluence of the Heimatscheintal/ Rio del Masso dei Tovi torrent
		200	lumbryhood in the neighbourhood upstream of the confluence of the Heimatscheintal/ Rio del Masso dei Tovi torrent
G.190	Grafeisbach/ Rio Graves	20	torrent with debris flow processes
G.185	Kalbenbach/Rio della Clava	10	torrent with debris flow processes
		40	lumbryhood in the neighbourhood downstream of Grafeisbach/Rio Graves torrent
G.175	Prantlbach-Brandwaldbach/ Rio Prantola	30	torrent with debris flow processes
		20	lumbryhood in the neighbourhood upstream of the confluence of the G.155 torrent
G.145	Widnerbach/ Rio di Videna	2	torrent with debris flow processes
G.120	Badbach/ Rio di Bagno	4	torrent with debris flow processes
G.110	Mainlechnerbach/ Rio di Main	20	torrent with debris flow processes

Table 3-2: Assumed values for the input of woody debris from the tributaries

The inflow hydrograph (return period of 1 in 300 years) at the upstream boundaries of the study area was calculated with the GIS-based hydrologic modelling system BaSIn 30 (AIDI 2005). The flood propagation computations were carried out with the hydrodynamic simulation model SOBEK Rural (WL/Delft Hydraulics 2004), which is capable of computing the full numerical solution of the shallow water equations. For a hazard indication analysis level, a pure 2D overland flow simulation was performed. Outputs included the flow depths and the flow velocities in x and y direction for the different time steps (e.g. 30 min for computations at the hazard index level). The flood simulation was performed on the basis of a digital elevation model delineated by airborne laserscanning technique with an original resolution of 2.5 m, upsized to a resolution of 10 m.

For the calculation of the woody material transport dynamics, a reference diameter of the wood elements of $d = 0.3m$ was assumed. A drag coefficient of $C_d = 0.8$ and a friction coefficient of $\mu = 1.0$ were used during the sets of calculation. For an analysis conducted at a hazard index level, a value of $1.4 \cdot 10^{-4}$ was chosen for the parameter k_1 in equation 3-12.

A detailed analysis of transport dynamics at critical bridge locations has been carried out.

3.5 Simulation results

The application of the method outlined in Section 3.3.1 resulted in a map of the vegetation structures, a map of the morphological characteristics of the river influence zone and computed maximal volumes of recruited woody material within the considered system. Figure 3-11 shows an extract of the mapped vegetation structures within a channel section, indicating that a substantial part of the river influence zone in the study area is covered by vegetation. Thus, the recruitment of considerable amount of woody material is plausible.

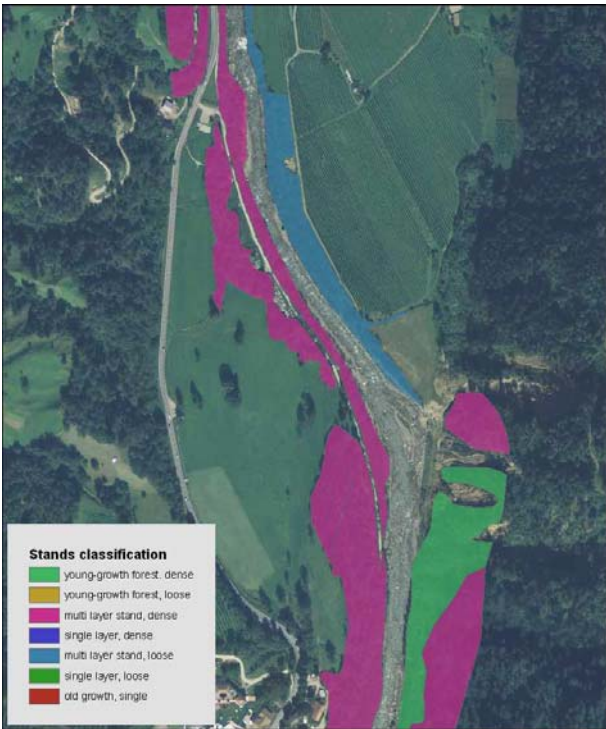


Figure 3-11: Extract of the mapped vegetation structure.

In figure 3-12, the mapped geomorphologic classification of the river influence zone is shown, and in figure 3-13 a detail of the cell-by-cell simulation results is provided.

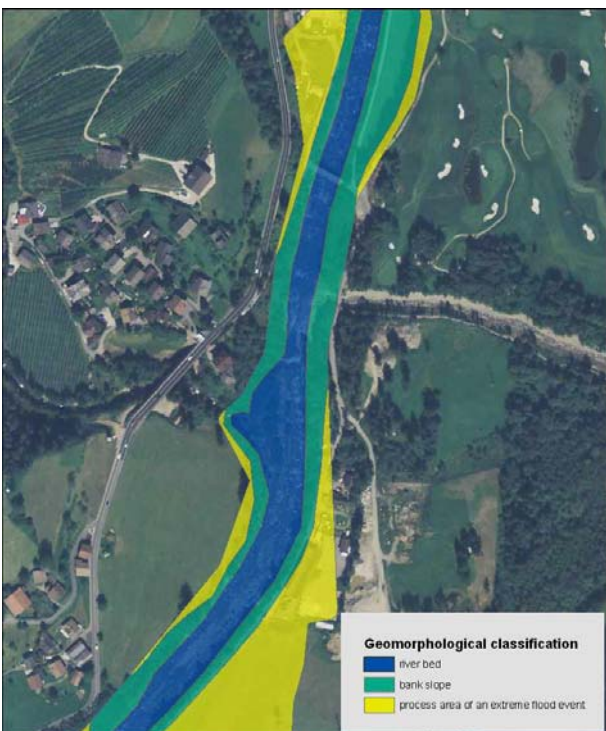


Figure 3-12: Extract of the mapped morphology of the river influence zones.

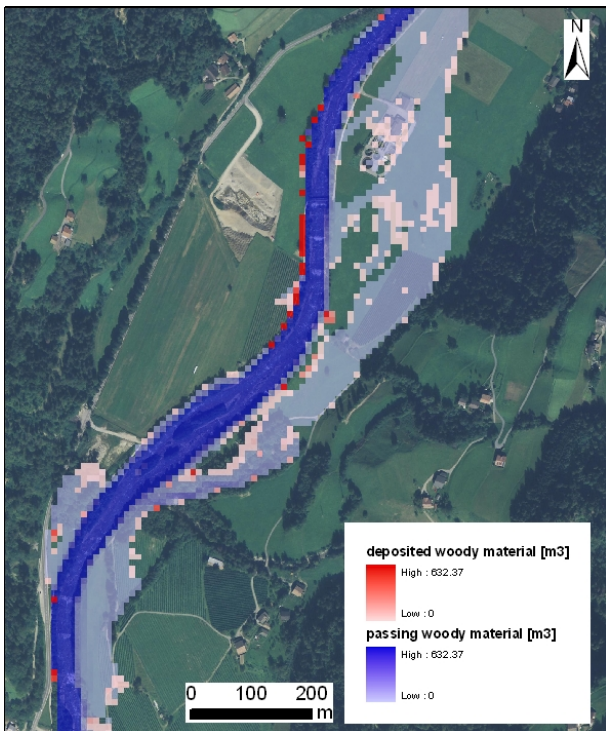


Figure 3-13: Results of the cell-by-cell simulation of the woody material transportation and deposition volumes. The red colours show the volume of deposited driftwood, the blue colours show the volume of passing driftwood at each cell. The maximum values are calculated at the outflow cell.

The results show an increased concentration of woody material transport in the centre of the streamline. Additionally, the potential deposition areas of woody material are given; deposition primarily took place in flooded areas with low flow depths or low flow velocities outside of the river channel. Within the river channel, deposition of woody material was modelled at the waterside slopes, at the waterside of river bends and at calm loops. The modelled woody material deposition areas corresponded accurately with the mapped potential deposition areas. The maximum of transported woody material was calculated as 632 m³ in the last flow cell. This value indicates the maximum amount of transported woody material during a flood event with a recurrence period of 300 years at the outflow cell of the studied river reach. It corresponds with the deadwood volumes of 35 flooded hectares of different forest classes as shown in table 3-1. This underlines that woody material transport and related phenomena are not negligible in the elaboration of the flood hazard zone map for the Passer/Passirio river. Additionally, the modelling results show the increase of transported driftwood along the river. At the upper reach of the river, small amounts of driftwood were computed; whereas downstream of each flooded wood stand with large deadwood volumes, the volume of transported driftwood increased. As expected, after a considerable deposition of driftwood, the volume of transported driftwood within the river channel decreased. Therefore, the modelling results lead to the identification of river reaches with significant driftwood transport.

Since time dependency was not considered, the modelled design event had virtually an infinite duration, meaning that the entire amount of potentially removable wood stand volume was removed and mobilised. Thus, the computed woody material volumes represent the upper threshold in terms of potentially maximum values.

The cell-by-cell based modelling procedure does not consider the rising and falling limb of the flood hydrograph as does the object-oriented modelling approach. Therefore, the results of the two approaches differ slightly. In general, the modelled deposition areas of both approaches are the same, but the computed deposition volumes differ slightly. Since the object-oriented approach considers different time steps of the flood process, it considers different process areas during the flood event. Therefore, the deposited volumes differ in situations where deadwood is re-mobilized after deposition due to the increase of the wetted perimeter or the increase in flow depth and/or velocities. The object-oriented approach outlines the track of each single model wood log and as such, the origin of the entrapped or deposited log could be assessed. Additionally, the consideration of more time steps of the flood simulation enables the tracking of the development of deadwood and the transport of the model wood logs in time. It was shown that most of the model wood logs flow repeatedly out from some of the flood forest areas. Only the flooding of a large area with the same wood stand characteristics and with high flood intensities led to a simultaneous burst of woody material into the river reach. The modelling procedure allows the observation of these situations and the assessment of the consequences of the evolvement of log jams due to a simultaneous overflooding. Figure 3-14 shows the woody material deposition areas computed by the object-oriented approach. Each red dot represents one model wood log. The results of the investigation of woody material dynamics at the selected weak point (i.e. bridge location) are shown in Figure 3-15. The computed interaction process of the model wood logs with the selected obstacles was plausible. The log jams at obstacles increased constantly during the modelled flood event. After the modelled flood process, the net volume of the log jam at the selected bridge between Oberpsairer and Mörre was around 3 m³. Figure 3-15 shows the computed log jam at the bridge and figure 3-16 show the bridge destroyed by the flood event in 1987.

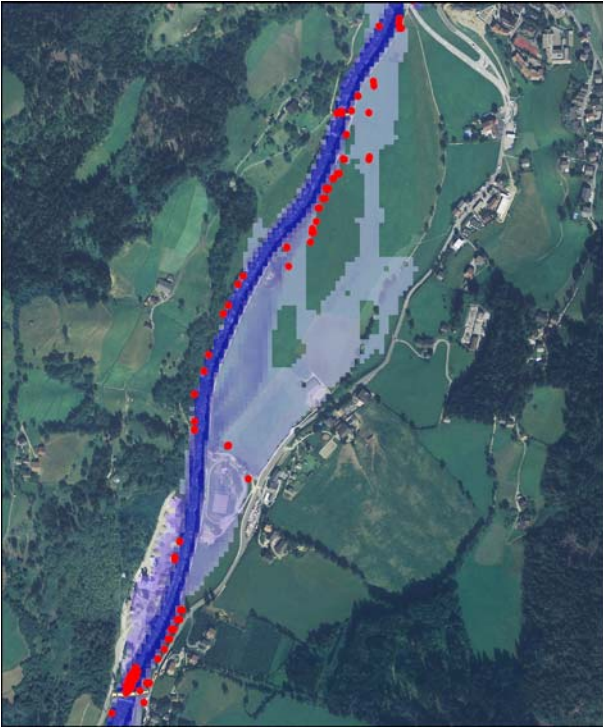


Figure 3-14: Results of the object-oriented simulation of the deposition of woody material. The red dots show the center of gravity of the deposited model wood logs.

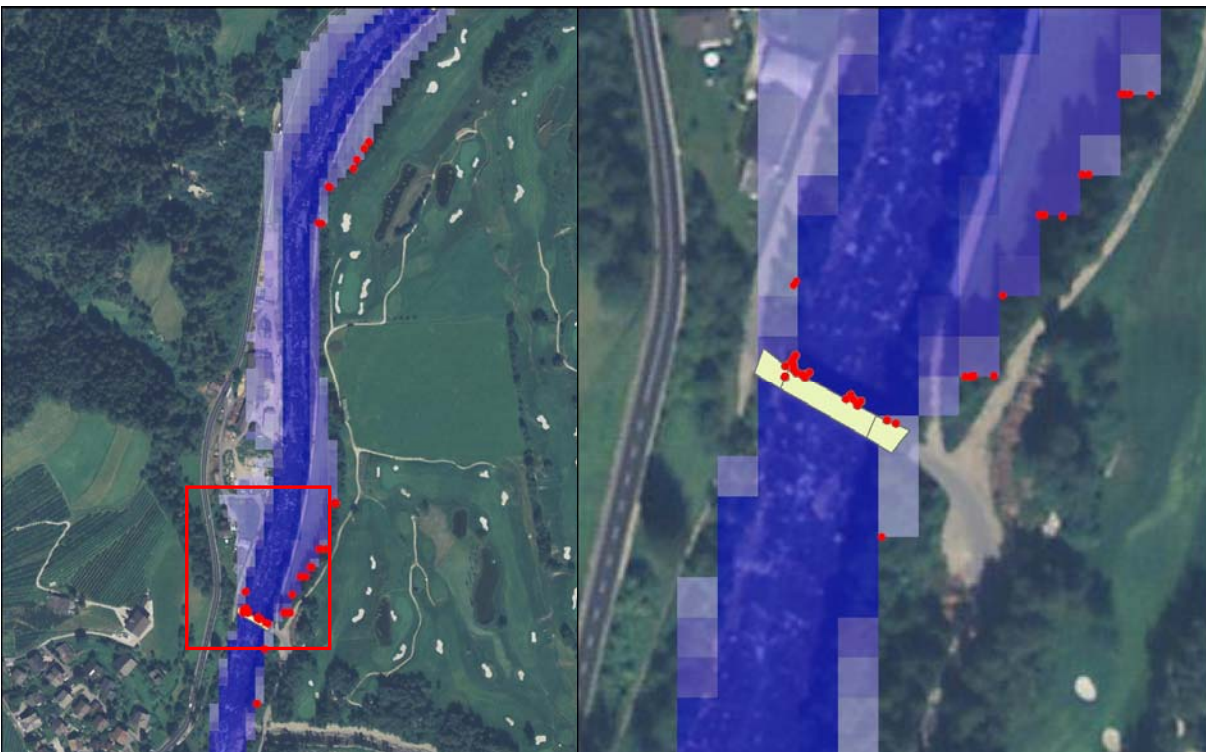


Figure 3-15: entrapment at a critical configuration. The graphic at the right side shows the entrapped driftwood on a more detailed scale.



Figure 3-16: The figure shows the destroyed bridge across the Passer/Passiria river soon after the flood event in July 18th, 1987. The bridge was occluded with woody material and was destroyed after the outbreak of the river on the left side. The figure shows only the driftwood at the bridge that remained after the event.

The picture does not allow reconstructing the total amount of driftwood entrapped at the bridge, as the bridge was over-flooded after the break of the left pillar and the entrapped woody material was transported away. However, figure 3-15 confirms the entrapment of driftwood with this obstacle. The procedure for modelling the interaction of the model wood logs with critical stream configurations calculates the volume of retained driftwood at every obstacle. The retention volume depends on the characteristics of the obstacle itself and trapped driftwood necessarily reduces the volume which is transported downstream of the obstacle. This method allows for the identification of the systematically most relevant weak points in the system.

3.6 Discussion and conclusions

By the application of the developed method, valuable insights were provided regarding woody material recruitment processes and the propensity for entrainment and transport to critical configurations during extreme flood events. In particular, an overview of the maximal amount of transported and deposited woody material in a defined river reach was given. Moreover, the main

pathways of the woody material in the river channel were traced and subsequently the potential depositional areas were identified. Furthermore, the procedure provided the order of dimension of the woody material volume expected to pass through bridges during a flood event. Such quantified knowledge on woody material volume approaching a weak point location is crucial for a reliable scenario definition during hazard assessment, in particular with respect to a possible log jam formation, clogging or similar obstruction phenomena. Consequently, the transparency of hazard mapping procedure and the quality of the results are increased and the supervision of the entire hazard mapping procedure by the respective public authorities is facilitated. The outcomes can also be used in order to support the definition of policies in riparian forest management and for defining particular measures such as thinning and other forest management actions. Nevertheless, the procedure presented above might still have certain limitations. The spatial resolution of the flood simulation has to be adapted and refined if the goal is a more detailed scale. With a grid size of 10 m, the river channel morphology is approximated with limited accuracy, resulting in a less precise calculation of the woody material flow paths. The procedure was found to be sensitive to the assumed wood stand volumes of different vegetation structures studied; however, a very detailed investigation on the wood structure might improve the procedure significantly. Additionally, the exposure time of the different vegetation structures to the flood event might be another relevant factor. During flood events with a relatively short duration, significantly smaller volumes are expected compared to long-duration flood events.

Despite these limitations, the developed method is of particular relevance to mitigate flood risk. The results of mapped recruitment areas with the respective forest structure typologies and identified transport paths with the transport dynamics for a determined critical configuration are essential indicators for hazard assessment.

The time-dependent modelling of woody material dynamics indicates whether or not the formation of log jams due to a simultaneous flooding of a large forested area with high flood intensities is plausible in the studied river reach. The assessment of the interaction processes induced at the considered critical configuration refines the hazard analysis and provides significantly more detailed input for the subsequent risk assessment. As shown during previous events, the critical configuration was repeatedly located at bridges; hence, the hypothetical debris accumulation for the entire bridge and the resulting consequences can be calculated according to the indications provided by Diehl (1997). This is fundamental information for effective risk mitigation strategies. Key elements of these strategies include: (1) the removal of those parts of the critical configuration that induce woody material accumulation, (2) the reconfiguration of the weak point to improve flow

conditions, and (3) the adherence to silvicultural measures in the respective recruitment areas in order to reduce the hazard source.

An application of the proposed model would allow enhanced emergency planning and preparations (e.g. excavating identified places in order to diminish accumulations at bridges; installation of temporary protection measures; implementation of local structural protection). These activities would introduce redundancies and buffer capacities into the system, thereby achieving an increased resilience of elements at risk.

3.7 References

- Abbe, T. B., Montgomery, D. R., Petroff, C., 1997. Design of stable in-channel wood debris structures for bank protection and habitat restoration: an example from the Cowlitz River, WA, In: Wang S S.Y, Langendoen E J, and Shields F D (ed) Management of Landscapes Disturbed by Channel Incision: Stabilization, Rehabilitation, Restoration, University of Mississippi, Mississippi, pp 809–815.
- Abbe, B., Montgomery, D., 2002. Patterns and processes of wood debris accumulation in the Queets river basin. Washington, *Geomorphology*, 51, pp 81-107.
- AIDI (Associazione Italiana di Idronomia), 2005. Procedura di calcolo dell'Idrogramma di piena a frequenza di superamento assegnata per il territorio della provincia Autonoma di Bolzano. Relazione tecnica.
- Autonome Provinz Bozen – Südtirol, 2006. Richtlinien für die Erstellung von Gefahrenzonenplänen und zur Klassifizierung des spezifischen Risikos. Bozen.
- Bänziger, R., 1990. Schwemmholz im Unwettersommer 1987. Schweiz. Ingenieur und Architekt, 47, pp 1354-1358.
- Bezzola, G. R., 2001. Schwemmholz – Rückhalt oder Weiterleitung? *Wasser, Energie, Luft* 93 (9/10), pp 247-252.
- Bezzola, G., Sigg, H., Lange, D., 2004. Schwemmholzurückhalt in der Schweiz. Internationales Symposium „Interpraevent 2004“, Riva, Trient; Tagungspublikation, Band 3, pp 29-40.
- Blaschke, T., Tiede, D., Heurich, M., 2004. 3D landscape metrics to modelling forest structure and diversity based on laser scanning data. In: *The International Archives of Photogrammetry, Remote Sensing and Spatial Information Sciences*, vol. XXXVI-8/W2, Freiburg, pp 129-132.
- Bocchiola, D., Rulli, M. C., Rosso, R., 2006. Transport of large woody debris in the presence of obstacles, *Geomorphology* 76, pp 166-178.

- Braudrick, C. A., Grant, G. E., Ishikawa, Y., Ikeda, H., 1997. Dynamics of wood transport in streams: a flume experiment. *Earth surf. process. landforms*, 22, pp 669–683.
- Braudrick, C. A., Grant, G. E., 2000. When do logs move in rivers?. *Water Resources Research* **36** (2000), pp 571–583.
- Braudrick, C. A., Grant, G. E., 2001. Transport and deposition of large woody debris in streams: a flume experiment, *Geomorphology*, 41, pp 263–283.
- BUWAL - Amt für Raumplanung Graubünden - Ufficio Cantonale di Pianificazione, 1998. Grundlage zur FAN-Tagung vom 13-16 October 1998 in Ittingen. 15 pp.
- Comiti, F., Andreoli, A., Lenzi, M. A., Mao, L. 2006, Spatial density and characteristics of woody debris in five mountain rivers of the Dolomites (Italian Alps). *Geomorphology* 78, pp 44 – 63.
- Curran, J. H., Wohl, E. E., 2003. Large woody debris and flow resistance in step-pool channels, Cascade Range, Washington. *Geomorphology* 51, pp 141–157.
- Degetto, M., 2000. Dinamica del legname in alveo e modellazione del suo comportamento in presenza di briglie filtranti, M.S. Thesis, University of Padova.
- Diehl, T. H. 1997. Potential Drift Accumulation at Bridges. Publication No. FHWA-RD-97-028 U.S. Department of Transportation, Federal Highway Administration Research and Development, Turner-Fairbank Highway Research Center, Virginia.
- Egli, T., 2008. Wegleitung Objektschutz gegen meteorologische Naturgefahren. Vereinigung Kantonalen Feuerversicherungen VKF, Bern.
- Fuchs, S., Holub, M., 2007. Risk management strategies for landslides in European mountain regions - current practice in Austria and future needs. *Geographical Phorum*, 6, pp 5-21
- Fuchs, S., McAlpin, M., 2005. The net benefit of public expenditures on avalanche defence structures in the municipality of Davos, Switzerland. *Nat. Hazards Earth Syst. Sci*, 5 (3), pp 319-330.
- Gurnell, A. M., Petts, G. E., Hannah, D. M., Smith, B. P. G., Edwards, P. J., Kollmann, J., Ward, J. V., and Tockner, K., 2000. Wood storage within the active zone of a large European gravel-bed river. *Geomorphology*, 34, pp 55-72.
- Haga, H., Kumagai, T., Otsuki, K., Ogawa, S., 2002. Transport and retention of coarse woody debris in mountain streams: An in situ experiment of log transport and a field survey of coarse woody debris distribution. *Water Resources Research*, 38, 8.
- Hildebrand, R. H., Cemly, A. D., Dolloff, C. A., Harpster, K. L., 1997. Effects of large woody debris placement on stream channel and benthic macroinvertebrate. *Can. J. Fish. Aquat. Sci.* 54, pp 931–939.

- Holub, M., Hübl, J., 2008. Local protection against mountain hazards - state of the art and future needs. *Nat. Hazards Earth Syst. Sci.*, 8, pp 81-99.
- Hübl, J., Anderschitz, M., Florineth, F., Gatterbauer, H., Habersack, H., Jäger, E., Kogelnig, A., Krepp, F., Rauch, J. P., Schulev-Steindl, E., 2008. FLOODRISK II - Vertiefung und Vernetzung zukunftsweisender Umsetzungsstrategien zum integrierten Hochwasserschutz, Workpackage 2.3 - Präventive Strategien für das Wildholzrisiko in Wildbächen. Bundesministerium für Land- und Forstwirtschaft, Umwelt und Wasserwirtschaft, Abteilung IV/5, Wildbach und Lawinenverbauung, 43.
- Keim, R. F., Skaugset, A. E., and Bateman, D. S., 2002. Physical aquatic habitat: II. Pools and cover affected by large woody debris in three western Oregon streams. *North American Journal of Fisheries Management* 22, pp 151–164.
- Klosterhuber, R., Plettenbacher, T., Hotter, M., Schober, T., Aschaber, R., Vacik, H., Pircher, G., Gruber, G., Ruprecht, H., 2007. Ökologisches Handbuch zur Waldtypisierung und Waldstratifizierung Südtirol, Teil A, Zwischenbericht im Auftrag der Autonomen Provinz Bozen, Abteilung 32, Forstwirtschaft.
- Lancaster, S. T. and Shannon, K. H., 2001. Modelling Sediment and Wood Storage and Dynamics in Small Mountainous Watersheds. *Geomorphic Processes and Riverine Habitat Water Science and Application Volume 4*, pp 85-102.
- Lange, D., Bezzola, G. R., 2006. Schwemmholz, Probleme und Lösungsansätze, Mittelungen der Versuchsanstalt für Wasserbau, Hydrologie und Glaziologie (VAW), Zurich.
- Lyn, D., Cooper, T., Condon, D., Gan, L., 2007. Factors in debris accumulation at bridge piers, Washington, US Department of Transportation, Federal Highway Administration Research and Development, Turner-Fairbank Highway Research Center.
- May, C. L., Gresswell, R. E., 2003. Large wood recruitment and Redistribution in headwater streams in the southern Oregon. Coast Range, USA, *Can. J. Forest Res.*, 33(6), pp 1352–1362.
- Mazzorana, B., Zischg, A., Largiader, A., Hübl, J., 2009. Hazard index maps for woody material recruitment and transport in alpine catchments, *Nat. Hazards Earth Syst. Sci.*, 9, pp 197–209.
- Mitchell, J. K., 2003. European River Floods in a Changing World, *Risk Anal.*, 23, pp 567–574.
- Montgomery, D. R. and Piegay, H., 2003. Wood in rivers: interactions with channel morphology and processes. *Geomorphology* 51 (2003), pp 1–5.
- Ng, Y. L. A., Richardson, J. R., 2001. “Transport Mechanics of Floating Woody Debris”, Thesis, Faculty of the Graduate School, University of Missouri-Columbia.
- Oberndorfer, S., Fuchs, S., Rickenmann, D. and Andrecs, P., 2007. Vulnerabilitätsanalyse und monetäre Schadensbewertung von Wildbachereignissen in Österreich. BFW, Wien.

- Petraschek, A., Kienholz, H., 2003. Hazard assessment and mapping of mountain risks in Switzerland. In: Rickenmann, D. und Chen, C. L. (ed) Debris-flow hazard mitigation: mechanics, prediction and assessment. Millpress, Rotterdam.
- Raetzo, H., Lateltin, O., Bollinger, D., Tripet, J. P., 2002. Hazard assessment in Switzerland – Codes of Practice for mass movements. Bull. Eng. Geol. Env., 61, pp 263-268.
- Rauch, H. P., 2005. Hydraulischer Einfluss von Gehölzstrukturen am Beispiel der ingenieurbiologischen Versuchsstrecke am Wienfluss. Dissertation, University of Life Sciences Vienna, Vienna.
- Rickenmann, D., 1997. Schwemmholz und Hochwasser. Wasser, Energie, Luft. Schweizer Wasserwirtschaftsverband, Baden. 89. Jahrgang, 5/6, pp 115-119.
- Rickli, C., Bucher, H-U., 2006. Schutzwald und Schwemmholz in Wildbacheinzugsgebieten. FAN-Agenda 1/06: pp 17-20.
- Rimböck, A., Strobl, T., 2002. Loads on rope net constructions for woody debris entrapment in torrents. International Congress „Interpraevent 2002 in the Pacific Rim“, Matsumoto, Japan; Congress publication, volume 2, pp 797-807.
- Shields, F. D., Morin, N., Kuhnle, R. A., 2001. Effects of large woody debris structures on stream hydraulics, Proc. Wetlands Engineering and River Restoration Conference, ASCE, Reston, VA, 2001.
- Wilson, C. A. M. E., Yagci, O., Olsen, N. B. R., Rauch, H. P., 2004. 3D Numerical Modelling of Vegetated Compound Channel Flows. IAHR/IWA 6th International Conference on Hydroinformatics, Singapore.
- WL | Delft Hydraulics, 2004. Release Notes, SOBEK version v2.09.001. Delft.

4. IMPROVING RISK ASSESSMENT BY DEFINING CONSISTENT AND RELIABLE SYSTEM SCENARIOS

*We need to expand our sense of the possible and contract our
sense of the probable
Kevin Langdon*

B. Mazzorana, and S. Fuchs (2009): Improving risk assessment by defining consistent and reliable system scenarios. Natural Hazards and Earth System Sciences 9. p. 145-159.

Abstract

During the entire procedure of risk assessment for hydrologic hazards, the selection of consistent and reliable scenarios, constructed in a strictly systematic way, is fundamental for the quality and reproducibility of the results. However, subjective assumptions on relevant impact variables such as sediment transport intensity on the system loading side and weak point response mechanisms repeatedly cause biases in the results, and consequently affect transparency and required quality standards. Furthermore, the system response of mitigation measures to extreme event loadings represents another key variable in hazard assessment, as well as the integral risk management including intervention planning. Formative Scenario Analysis, as a supplement to conventional risk assessment methods, is a technique to construct well-defined sets of assumptions to gain insight into a specific case and the potential system behaviour. By two case studies, carried out (1) to analyse sediment transport dynamics in a torrent section equipped with control measures, and (2) to identify hazards induced by woody debris transport at hydraulic weak points, the applicability of the Formative Scenario Analysis technique is presented. It is argued that during scenario planning in general and with respect to integral risk management in particular, Formative Scenario Analysis allows for the development of reliable and reproducible scenarios in order to design more

specifically an application framework for the sustainable assessment of natural hazards impact. The overall aim is to optimise the hazard mapping and zoning procedure by methodologically integrating quantitative and qualitative knowledge.

Keywords: Formative Scenario Analysis, hazard mapping, integral risk management, flood risk, debris flow

4.1 Introduction

In European mountain regions considerable losses resulting from torrent processes occurred during the last decades (e.g., Oberndorfer et al., 2007; Autonome Provinz Bozen-Südtirol, 2008) in spite of considerable efforts undertaken for the protection of endangered areas (Fuchs and McAlpin, 2005; Oberndorfer et al., 2007). It is not only an economic challenge and a political mission to define an optimal protection level against natural hazards, but also a societal desire to guarantee rural development in alpine regions. Therefore, decision makers have to deal with issues of excessive land-use pressure and ecological and economic viability, which is an often complex and interlinked task. One major contribution towards this direction is the attempt to control land-use by reducing vulnerability on the basis of hazard and risk maps (Fuchs et al., 2007, 2009), as recently laid down in the European Floods Directive (Commission of the European Communities, 2007). Hazard maps indicate, for defined return periods of the underlying design events, the spatial distribution of classes of maximum process intensities. Risk maps result by intersecting these hazard maps with values at risk exposed. Despite the long tradition of hazard mapping in several European mountain regions, a retrospective analysis on hazard maps highlighted a series of shortcomings, above all with respect to the magnitude (and frequency) of torrent processes (Berger et al., 2007; Autonome Provinz Bozen-Südtirol, 2008).

At the watershed scale, the magnitude of channel-based hazard processes is often expressed by the measured geomorphic features, such as potential debris volume, mean flow velocity, peak discharge, and runout distance (Fuchs et al., 2008). For this purpose, empirical and semi-empirical equations may be used. As an alternative dynamic (often numerical) simulation models might be considered to assess the flow properties and the depositional behaviour. However, in particular the effects of changing channel morphology and associated woody debris transport phenomena were found to amplify process intensities considerably (e.g., Diehl, 1997; Lyn et al., 2007), which is not taken into account sufficiently by the respective models. Furthermore, facing recent events existing hazard maps turned out to be not as reliable as expected (e.g., Bezzola and Hegg, 2007).

Consequently, subsequent risk reduction measures did not necessarily provide the most efficient management strategy and therefore the implemented solutions were only suboptimal. In order to improve risk analyses and to support decision making, above all underlying scenarios have to be re-defined based on these issues, in particular with respect to sources of uncertainty affecting the predictability of hazardous phenomena (e.g., Paté-Cornell, 1996; Merz et al., 2008). As outlined by Fuchs et al. (2008) and Mazzorana and Fuchs (in press), such uncertainties include with respect to hydrological hazards and torrent processes

- (1) uncertainties about the possible range of rheological behaviour and about the liquid-solid mixture concentration of debris flows;
- (2) uncertainties in system loading assumptions (e.g., duration-intensity related uncertainties, uncertainties related to sediment transport rates, uncertainties emerging from woody debris transport);
- (3) uncertainties in system response mechanisms (e.g., localised obstructions that divert the flow patterns, influence of small-scale topological features);
- (4) uncertainties concerning the protection system functionality and mitigation reliability (e.g., failure propensities of key components within the protection system, sediment dosing behaviour of retention basins, dike failures); and
- (5) uncertainties concerning morphological changes that induce hazard processes or amplify their disposition (e.g., erosion phenomena in alluvial channels or on alluvial fans, and flow path changes in steep mountain rivers).

Commonly used 2D-simulation models with limited computation capabilities for movable bed (e.g., only deposition processes are simulated) are only partially capable to take into account hazards induced by morphological changes. Situations when the torrent diverges through lateral erosion processes from the originally incised channel forms are not fully detected and the consequent propagation patterns are therefore not identified (for a comparison, see e.g. ETAlp Consortium, 2003; Rickenmann et al., 2006).

In the procedures and regulations actually being used in hazard mapping it is discretionary to the experts to subjectively set limits to some of the above-mentioned uncertainties, interestingly and fittingly through expertise and by expert knowledge. This methodological gap represents a possible source of controversies during the process of mandatory audit of the preliminary hazard maps by administrative bodies and affected stakeholders with legal standing, which might result in additional work and consequently increased expenditures.

A reliable and efficient procedure that allows for the above-mentioned factors of uncertainty is to conduct a participative scenario analysis. This analysis allows for a multi-disciplinary approach merging results derived by different analysis tools such as estimates, empirical and numerical simulation models, and event documentation. By participative scenario analyses, a set of consistent scenarios is identified by a team of specialists. The identified scenarios contribute to the robustness of the entire hazard zoning procedure as a basis for risk assessment. As a result, subordinated derived products, such as intervention plans, benefit from this fully coherent derivation procedure. In order to meet these aims, a Formative Scenario Analysis approach (Scholz and Tietje, 2002) was chosen to identify sources of uncertainty resulting from the assessment of hydrologic hazards. Following Scholz and Tietje (2002), Formative Scenario Analysis is a technique to construct well-defined sets of assumptions to gain insight into a system and its potential development.

4.2 Background – Exploring alternative developments through scenarios

Scenarios are constructed for the purpose of focusing attention on causal processes and decisive points. A scenario is a plausible image of a possible future system state, hence a fundamental premise on which scenario planning is based is the uncertain predictability of the future. Figure 4-1 shows the scenario trumpet metaphor, where the starting point of scenario analysis is t_0 and all possible future states of the system are represented within the trumpet. While the upper margin identifies the most optimistic case (XE1), the lower margin represents the most pessimistic one (XE2). This representation of possible multiple futures takes into account either deviations from an undisturbed evolution (midline of the trumpet) or other disturbances at t_1 that would change a hypothetical trajectory to XB to the future state XC or a failure event at t_2 that would lead to the final state XD.

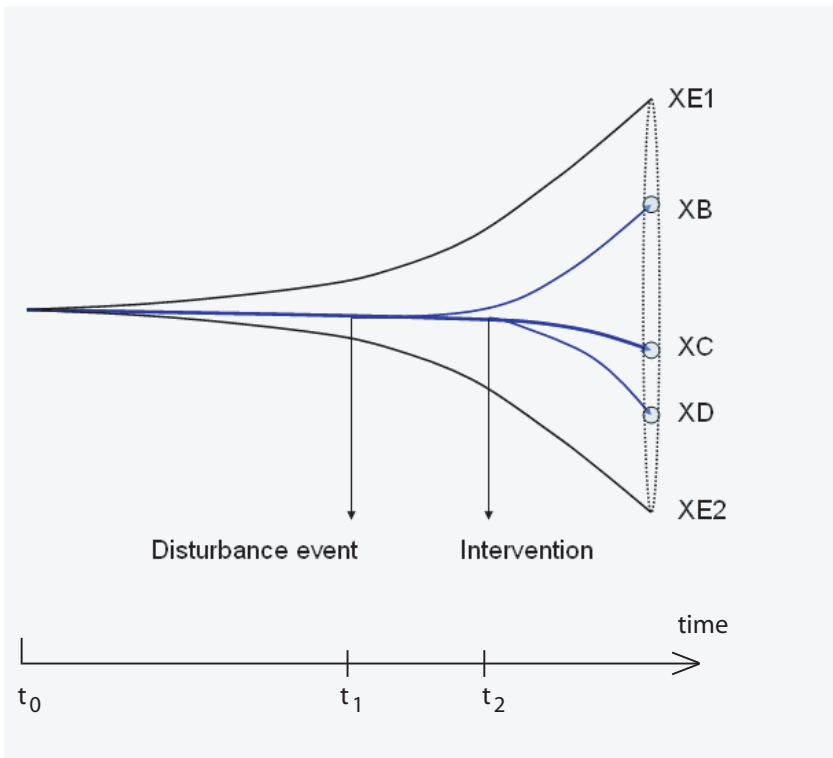


Figure 4-1. Scenario Trumpet indicating five identified possible outcomes of a system to be analysed



Figure 4-2. Toppling of a series of consolidation structures

As shown in Figure 4-2 (toppling of a series of consolidation dams), the consideration of disturbances is an indispensable requirement if debris flow phenomena are analysed. However, as O'Brien and Dyson (2007) pointed out, one single scenario provides only one possible view of the future state of a system and takes therefore uncertainty not sufficiently into account.

Conversely, scenario planning is an approach to develop sets of scenarios that therefore provide a number of possible future states of a system. Scenarios can be classified following the topology proposed by Ducot and Lubben (1980) according to three different axes (see Figure 4-3):

- (1) The causal nature of the scenario (vertical axis). At one pole exploratory scenarios are situated, where effects are projected given an initial set of causes. At the opposite pole anticipatory scenarios are located which offer explanations of possible causes given an initial set of effects. With respect to torrent processes, an example of an exploratory scenario is the determination of the liquid and solid discharge at the downstream end of a reach with consolidation control structures gives the liquid and solid discharges at the upstream boundary. Key variables determining the output of the considered system are, among others, the performance of the protection system, potential landslides adding a certain volume of solids to the system, and the stability of the torrent bed and bank slopes. Without very detailed information about these key variables, only a scenario set projection gives insight into the system dynamics. Typical anticipatory scenarios include analyses of particular damage configurations in consequence of extreme events. During scenario identification, specialists integrate the available quantitative knowledge (e.g. rainfall data and precipitation distribution) and qualitative knowledge (e.g. silent witnesses, interviews with affected citizens) in order to plausibly reconstruct the dynamics of the event.
- (2) The existing normative and descriptive relationships between scenarios are represented by the horizontal axis. The descriptive scenario states an ordered set of possible occurrences regardless of the desirability of the outcomes. Normative scenarios conversely are those which incorporate values, concerns and interests of the developer or consumer of the scenario. In natural hazard risk management the focus is either on descriptive scenarios, namely on the determination of an ordered set of possible incidences given a particular situation, or on normative scenarios when the performance of a planned protection system is defined.
- (3) The temporal dimension is represented by the inclined axis, and a distinction is made between trends and peripheral scenarios. Trends or timeline scenarios represent hazardous events in a causally related manner to provide explanations of how relevant factors evolve in

time (e.g. the temperature evolution within the next 20 years). Conversely, a peripheral or a cross-sectional scenario represents a description of a particular future point in time.

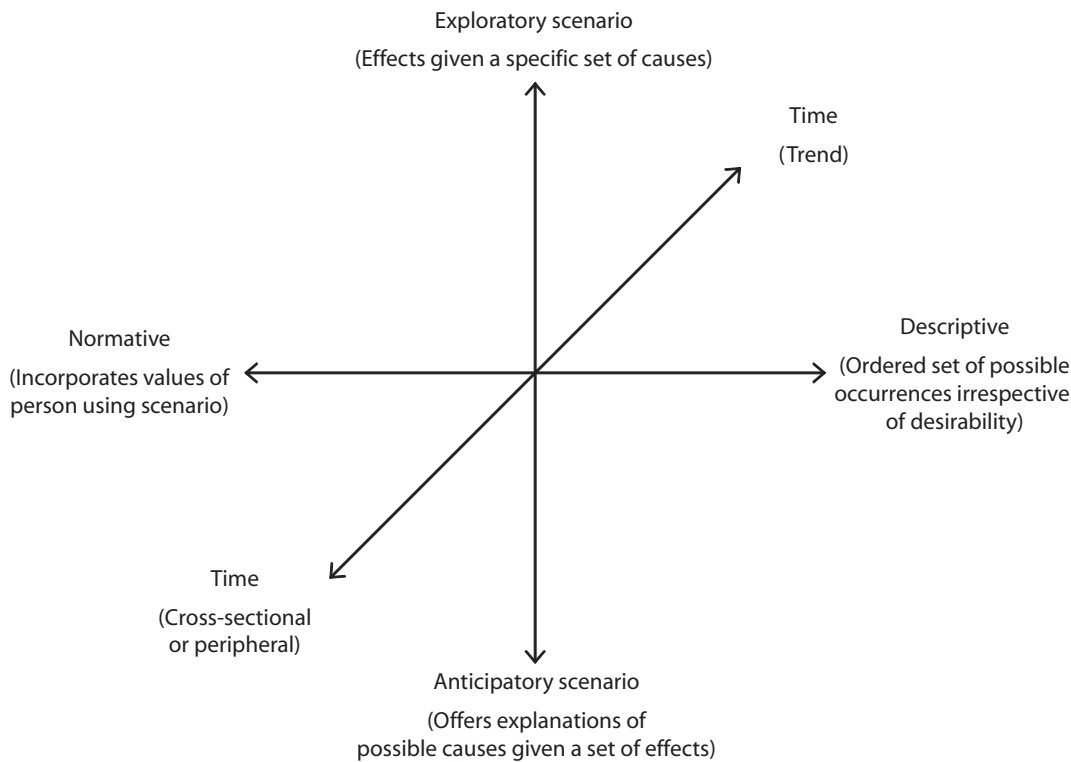


Figure 4-3. Ways to classify different scenarios

Scenario analysis started to become a major tool particularly in the field of management, economics and environmental decision making after the publication of the works of Kahn and Wiener (1967). Determinant reasons for the growing attention paid to scenario analyses were the drawbacks and pitfalls of a relevant number of deterministic environmental, economic or ecological forecasting models. Yielding only individual predictions and not adequately including qualitative system changes (disruptions, Godet, 2000), deterministic models were found to be only partially useful when trying to predict future states of complex systems. If a sediment dosing system, typically composed of an approaching reach, a deposition basin, an open check dam and an outlet reach is considered, the evolution of the channel bed level in the retention basin during either the increasing or the decreasing part of the hydrograph can be accurately and precisely predicted by deterministic models (Armanini and Larcher, 2001; Miyazawa et al., 2003; Remaître et al., 2008). However, the simultaneous presence of woody debris transport phenomena obstructing the openings (e.g. slits) of the check dam interfere significantly with the evolution of the torrent bed, leading to an – at least partially – invalidation of the prediction resulting from the deterministic model. To overcome these restrictions in predictability, the identification of small numbers of scenarios which represent

different future states of a system is needed. It is possible, through a reliable scenario analysis, to re-perceive an image of reality, and to enhance individual engagement, commitment and mental flexibility in order to develop best reply strategies (Scholz and Tietje, 2002; Tietje, 2005). In Table 4-1, the four main applications of scenarios with respect to natural hazard risk management are shown. Apart from the overall goal to assess risk, the development and evaluation of strategies as well as adaptive organisational learning became increasingly important for public bodies involved in dealing with natural hazards in Europe.

	Unique problem solving	Multiple problem solving
Open up exploration	Making sense (risk assessments)	Anticipation (strategy evaluation)
Closure – decisions	Developing strategy (strategy development)	Adaptive organisational learning (skills)

Table 4-1. The 4 four main uses applications of scenarios

From a formal perspective scenario analysis can be classified into three different types, (1) holistic scenario analysis, (2) model scenario analysis, and (3) Formative Scenario Analysis. A holistic scenario analysis (which is analogue to the elicitation of responses from expert hearings) includes the construction of scenarios based on the opinion of specialists from the individual disciplines involved. A subjective mental integration of interdisciplinary qualitative and quantitative knowledge takes place, and intuitions and formal analyses of experts are combined (see e.g. Kahn and Wiener, 1967; van der Heijden, 2005). In doing so, mathematical methods, experimental results and individual local knowledge are used to refine certain aspects of these scenarios. Model scenario analyses are mainly based on (not always dynamical) systems modelling. By systematically varying the unknowns and assuming different values for uncertain parameters, the model is forced to create a number of trajectories, some of which are subsequently selected as scenarios by the expert pool. Following Scholz and Tietje (2002), Formative Scenario Analysis is a method to construct well-defined sets of assumptions to gain insight into a system and its potential development. With this procedure the study team is guided towards a differentiated and structured understanding of the current state and dynamics of a system. It is usually performed by small groups with specialised expertise about different aspects of the system, which they share with one another. Hence, Formative Scenario Analysis is based on qualitatively assessed impact factors. Experts determine by a rating procedure quantitative relations between these factors. Basically a Formative Scenario Analysis consists of two steps, (1) analytic modelling and decomposition of the initial state of the case studied, and (2) formative synthesis. In the first step an expert team identifies a set of key

impact factors or variables that serve as preceptors. In the second step of formative synthesis, various operations are carried out on these impact variables in order to generate all possible scenarios. Subsequently, a consistency analysis is performed in order to identify a number of different but internally consistent scenarios. A scenario interpretation phase refines this procedure to iteratively identify relevant settings. This methodology was proposed by Scholz and Tietje (2002) by application of a nine-step Formative Scenario Analysis (see Figure 4-4). First, the specialised team of experts precisely defines the case study to be investigated, resulting in a conceptual sketch and a concise description of the problem to be assessed (steps 1 and 2). Second, the expert team identifies the broad set of impact variables or impact factors that possibly determine the actual state of the studied system and the expected future developments (step 3). Third, the relative importance of the key variables is estimated; based on this rating the case study is structured by an impact matrix (step 4). This impact matrix provides activity, passivity, impact strengths and involvement measures for each variable (Scholz and Tietje, 2002). Activity quantifies the effectiveness of the impact of a variable on other variables. Passivity (or sensitivity) is correlated with the medium dependency of a variable on other variables. Impact strength is a summarising indicator of the medium impact strength of a variable on the entire case studied. Involvement indicates how strongly a certain variable is interlinked with the system. Fourth, a grid of activity and passivity scores supports the expert team in selecting the core set of relevant key variables that are supposed to be most important within the studied system (step 5). The classical Formative Scenario Analysis subsequently applies the MICMAC Analysis (Cross Impact Matrix-Multiplication Applied to Classification, step 6). The scenario construction phase (step 7) is of crucial importance for the subsequent consistency analysis (step 8). Scenario interpretation completes the Formative Scenario Analysis (step 9).

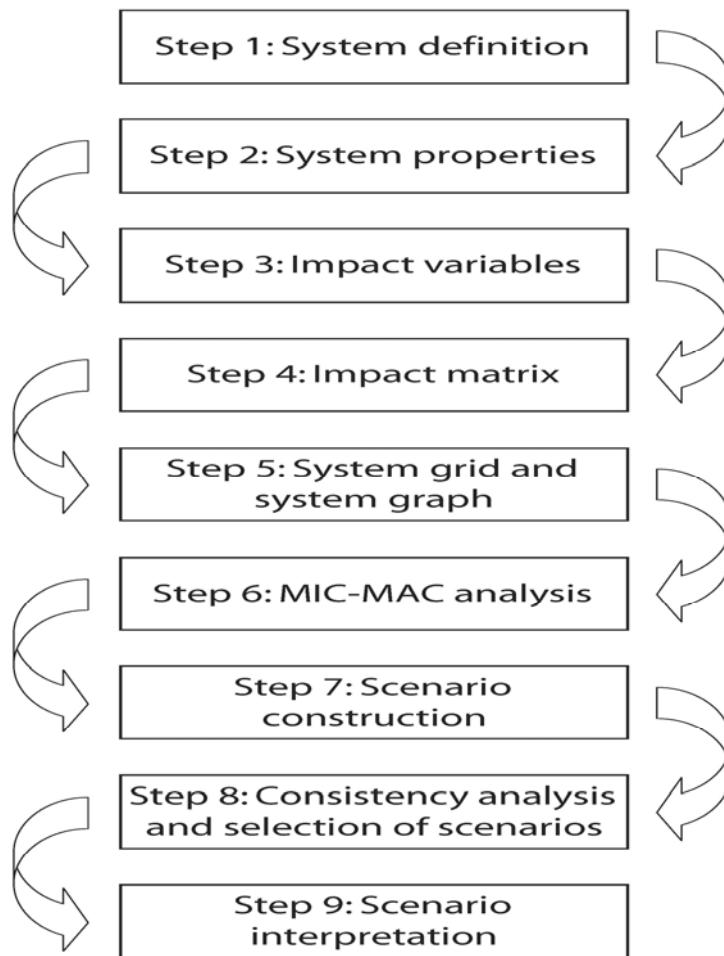


Figure 4-4. The nine steps of Formative Scenario Analysis

With respect to hydraulic risk management, two essential criteria for scenario selection were identified, (1) consistency, since inconsistent scenarios draw no realistic image of the system development, (2) difference between scenarios, since decision makers focus on a set of principally possible system developments, while small differences between similar scenarios are of minor importance. With respect to common hazard zoning procedures, Formative Scenario Analysis provides input data for modelling, contributing for example to a retraceable and reproducible explanation of the assumed system loading conditions (e.g., definition of process types and corresponding solid and liquid discharge hydrographs). Moreover, possible systems behaviour at weak points (e.g., log jam at bridge cross sections) can be qualitatively assessed and subsequently considered in the simulations. Furthermore, scenarios provide an integrated framing approach (backward planning) ensuring the adjustment of scenario data and modelling results and facilitate their validation.

4.3 Method

As a reference the nine steps Formative Scenario Analysis procedure described above is followed. Outlining succinctly the method it is referred to (1) a failure propensity case in an alpine torrent reach with a relevant number of consolidation protection measures (compare also with Figure 4-2) and to (2) woody debris transport hazard scenarios at hydraulic weak points. The key steps of Formative Scenario Analysis applied were the following:

- (1) The expert team listed $d_i, i = 1, \dots, N$ impact variables, also referred to as system variables, impact factors or case descriptors.
- (2) For each individual impact variable the expert team assessed the mutual impacts between the variables d_i and d_j ($i, j = 1, \dots, N; i \neq j$). To account for the relative importance of each individual impact variable on the entire system studied, qualitative and quantitative knowledge integration is essential. Only the identified key variables were included in the final set of selected impact factors. Since, with respect to hydrologic hazards, considerable scientific evidence exists for such variables, the specific information content was directly taken into consideration.
- (3) The expert team subsequently constructed the impact matrix, in which mutual impacts, $a_{i,j}$, between the variables d_i and d_j were rated on the basis of three levels: 0 = no or very little impact; 1 = medium impact; 2 = high impact. The impact matrix can be formally written as $A = (a_{i,j}), i, j = 1, \dots, N$ and is shown in extended form as follows:

$d_i \downarrow / d_i \rightarrow$	1 .. N	$a_{i,}$	$a_{i,} / a_{,j}$
1	$a_{1,1}$.. $a_{1,N}$	<div style="background-color: #f8d7da; padding: 5px; display: inline-block;"> Activity $\sum_{j=1}^N a_{1,j}$.. $\sum_{j=1}^N a_{N,j}$ </div>	<div style="background-color: #fff3cd; padding: 5px; display: inline-block;"> Impact strength $a_{1,} / a_{,1}$.. $a_{N,} / a_{,N}$ </div>
..		
N	$a_{N,1}$.. $a_{N,N}$		
$a_{,j}$	$\sum_{i=1}^N a_{i,1}$.. $\sum_{i=1}^N a_{i,N}$ <div style="background-color: #d4edda; padding: 5px; display: inline-block; color: green;"> Passivity </div>	$a_{,j} = \sum_{i=1}^N \sum_{j=1}^N a_{i,j}$	
$a_{,j} * a_{j,}$	$a_{,1} * a_{1,}$.. $a_{,N} * a_{N,}$ <div style="background-color: #d1ecf1; padding: 5px; display: inline-block; color: blue;"> Involvement </div>		

Activity $\sum_{j=1}^N a_{1,j}$ and passivity $\sum_{i=1}^N a_{i,1}$ for each variable were calculated, and mean activity and mean passivity was obtained by the arithmetic mean of the activity and passivity of each key variable. The comparison of the activity of a variable with mean activity, and of the passivity of a variable with mean passivity allowed for categorising the variables into active, passive, ambivalent and buffer variables making use of the system grid representation (compare case studies presented in Sections 4.4.1 and 4.4.2). A variable is considered to be active if its activity is above the average activity of all variables and its passivity is smaller than the average passivity of all variables. A variable is considered to be passive if the activity is below the average activity and its passivity is larger than the average passivity of all variables. A variable is considered to be ambivalent if its activity is above the average activity of all variables and its passivity is larger than the average passivity of all variables. A variable is considered to be a buffer variable if its activity is below the average activity of all variables and its passivity is smaller than the average passivity of all variables.

- (4) In a next step, the group of experts defined the levels of impact variables for each individual key variable. Since the combinatorial number of scenarios is considerably influenced by the number of levels defined for each impact variable, impact factors and their levels should be

defined parsimoniously (Scholz and Tietje 2002). Each impact variable d_i required the definition of at least two discrete levels ($N_i \geq 2$) which were denoted by $d_i^1, d_i^2, \dots, d_i^{N_i}$.

(5) Formally a scenario was a vector $S_k = (d_i^{n_i}, \dots, d_i^{n_i}, \dots, d_N^{n_N})$ with $k = 1, \dots, k_0$; the number of

scenarios was $k_0 = \prod_{i=1}^N N_i$.

(6) The next step included the construction of the consistency matrix $C = [c(d_i^{n_i}, d_j^{n_j})]$ which

contained the consistency ratings, $c(\cdot, \cdot)$, for all pairs of impact variables at all levels $c, (i, j = 1, \dots, N, i \neq j, n_i = 1, \dots, N_i, n_j = 1, \dots, N_j)$ (for an application of criteria for consistency ratings see Sections 4.1 and 4.2).

(7) For each scenario a consistency value was calculated as additive measure as

$$c^*(S_k) = \sum c(d_i^{n_i}, d_j^{n_j}) \text{ with } i, j = 1, \dots, N, i \neq j, d_i^{n_i}, d_j^{n_j} \in S_k.$$

(8) The scenario selection was based conjointly on the consistency value of the scenarios and the difference between them. As proposed by Tietje (2005) the distance measure Δ corresponded to the number of differences between the scenarios

$$\Delta(S_k, S_l) = \sum_{i=1}^n \begin{cases} 1 & \text{if } d_i(S_k) \neq d_i(S_l) \\ 0 & \text{otherwise} \end{cases}. \text{ The scenarios were ranked decreasingly according to}$$

consistency in an array. The scenario with the highest consistency value S_k was selected from the array and compared with the second scenario S_l . If $\Delta(S_k, S_l)$ was sufficiently high, e.g. $\Delta(S_k, S_l) \geq \Delta^*$, where Δ^* was a chosen threshold value, then scenario S_l was also selected and become the new comparison reference for scenario three, otherwise the third scenario was compared with the first scenario, etc.

(9) Scenario interpretation completed the Formative Scenario Analysis.

4.4 Applications and results

In this Section two case studies, (1) the analysis of sediment transport dynamics in a torrent reach with a series of consolidation works and (2) the identification of hazards induced by wood debris transport at hydraulic weak points, are presented. Characteristics of both case studies include the need to combine knowledge from well-defined research sectors in order to determine the factors that could significantly influence the current state of each system and the underlying dynamics. In

the first application (4.4.1), a synopsis of the main findings about issues related to sediment transport and a qualitative understanding of protection system responses in terms of reliability and feedback loop effects on sediment transport intensity is required. In the second case study (4.4.2), a knowledge integration of woody debris recruitment and transport phenomena and the caused interactions (e.g. obstruction) at hydraulic weak points (e.g. bridge locations) is indispensable. Therefore, an interdisciplinary study team with experts of the required knowledge domains (e.g. hydraulics, sediment and woody debris transport, structural reliability, system dynamics) had been formed.

4.4.1 Case study one: Failure propensity case in an Alpine torrent and possible effects on sediment transport at the downstream outflow cross section

The study team, familiar with the test site, defined the system to be analysed (steps 1 and 2 of FSA) and assessed in an exploratory investigation step the set of impact variables that presumably could have a significant influence on the current state of the dynamics of the system. The case was first decomposed by the study team and analysed by means of different preceptors, e.g. condition monitoring of the protection system, event documentation and topographic surveys, available hydrodynamic simulations, as well as geological and geotechnical expertises. The following synthesis step (step 3 of FSA) lead to a new conception of the case with the identification of relevant impact factors and their interaction. A pre-selection of possible impact factors is shown in Figure 4-5. It was assumed that at the upstream boundary of the analysed liquid discharge of the torrent reach and the inflow rate of sediment had to be taken into consideration. As a consequence, two impact factors, hydro inflow [HI] and sediment inflow [SI] were defined. Reliability of the protection system components was judged to play an essential role in releasing significant amounts of sediment in case of a protection system failure. Consequently, an additional impact factor, the reliability of the protection system [PSR] was identified. The study team pointed out that the forest cover [FC] could have a regulating effect on sediment availability in the system [SSA]. The ratio between deposition and erosion [ED] on the one hand and the retention capacity of the system [SRC] completed the picture of impact factors that influence the solid transport intensity at the downstream boundary, considered within the model by the impact factor variation of solid outflow [VSO].

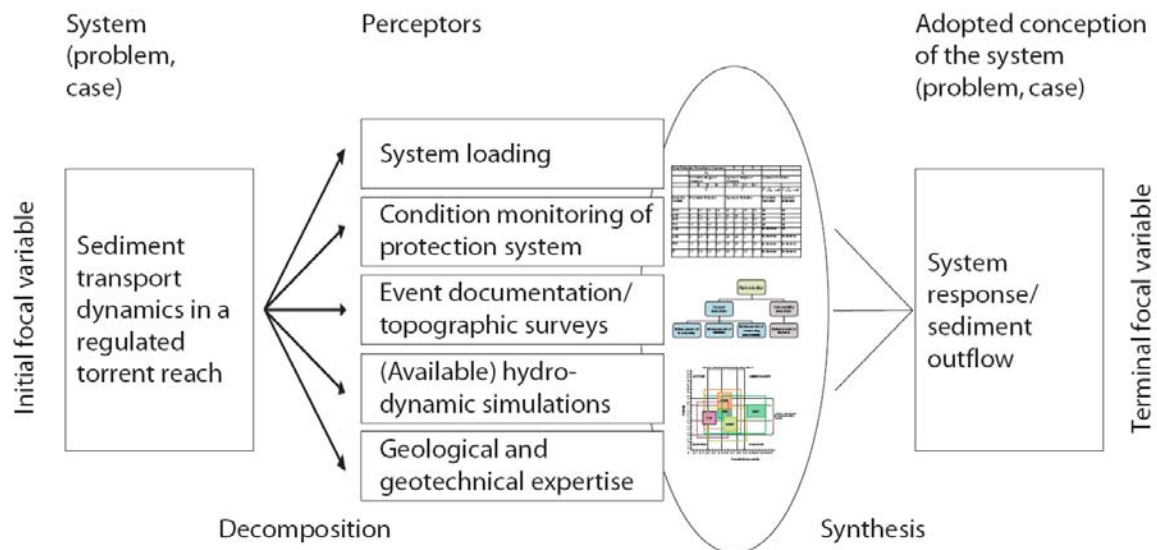


Figure 4-5. Pre-selection of possible impact factors or key variables relevant for case study 1

In a second consultation, after having judged that (1) hydro inflow [HI] and solid inflow [SI] could be considered together as a new key variable solid/liquid input [SLIT], (2) the forest cover [FC] is not considered to be essential and (3) the availability of sediment in the system [SSA] incorporates to a certain extent the retention capacity of the system [SRC], the study team reduced the impact factors to a core set which was taken as basis for the impact analysis (Table 4-2).

	SLIT	ED	PSR	SSA	VSO	Activity	Impact strength	Mean activity	5
SLIT	0	2	1	1	2	6	6.00		
ED	1	0	1	2	2	6	0.86		
PSR	0	1	0	1	2	4	1.00		
SSA	0	2	1	0	2	5	1.00		
VSO	0	2	1	1	0	4	0.50		
Passivity	1	7	4	5	8				
Involvement	6	42	16	25	32				
Mean passivity									
5									

Table 4-2. Impact Matrix for case study 1: Failure propensity case in an Alpine torrent and possible effects on sediment transport at the downstream outflow cross section

For the further steps of Formative Scenario Analysis, the study team decided to retain all the key variables selected during the second consultation and assessed impact levels for the key factors (for

an overview, see Table 4-3). On the basis of the impact matrix (step 4 of FSA) an additional analysis step consisted in producing the system grid (see Figure 4-6), where, as a consequence of the activity and passivity scores determined for each key factor, SLIT turned out to play an active role and VSO a passive role. While PSR had a rather ambivalent character, and ED was a buffer variable. SSA could not be assigned to any of the quadrants in the system grid (step 5 of FSA). A MIC-MAC analysis (step 6 of FSA) was judged to be not necessary.

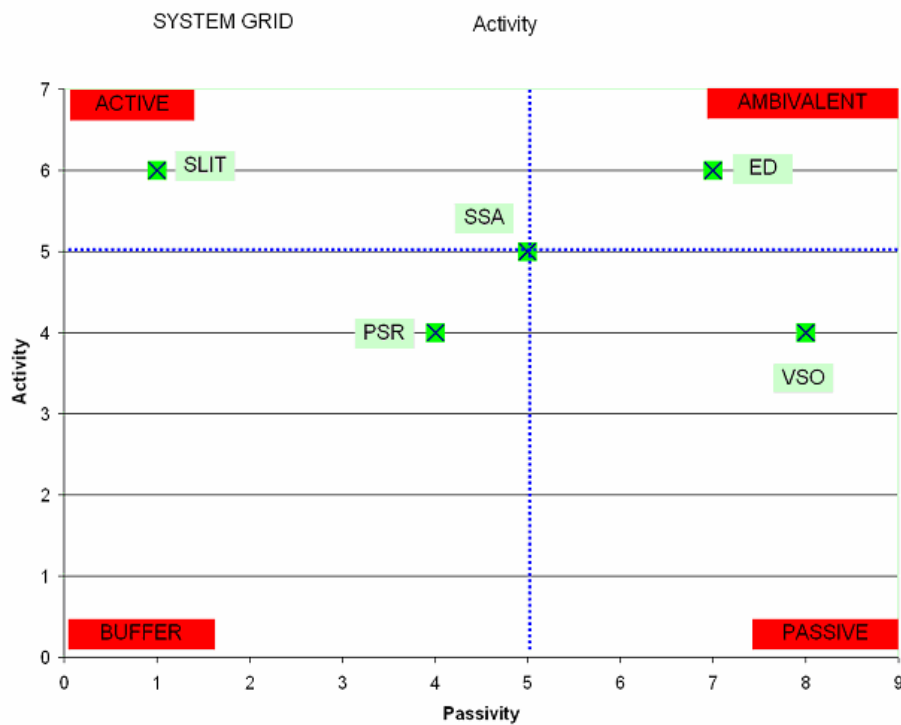


Figure 4-6. System grid of the activity and passivity scores for case study 1

As a successive step the impact levels for each impact factor were defined.

Impact variable	Short description	Impact levels defined	
SLIT	Incoming solid transport and liquid discharge	d_1^1	Hypo-concentrated sediment transport – SLIT.HYPO
		d_1^2	Average sediment transport – SLIT.ORD
		d_1^3	Debris flow – SLIT.DF
ED	Erosion/deposition behaviour	d_2^1	Erosion propensity- ED↓
		d_2^2	Equilibrium propensity - ED→
		d_2^3	Deposition propensity - ED↑
PSR	Protection system reliability	d_3^1	Failures likely - FL
		d_3^2	Failures unlikely - FU
SSA	Sediment availability in the system	d_4^1	Availability high – SSA.H
		d_4^2	Availability low – SSA.L
VSO	Variation of solid outflow (sedimentogram)	d_5^1	Positive variation - VSO↑
		d_5^2	No variation - VSO→
		d_5^3	Negative variation - VSO↓

Table 4-3. Definition of impact levels for each key variable for case study 1: Failure propensity case in an Alpine torrent and possible effects on sediment transport at the downstream outflow cross section

Concerning incoming solid transport and liquid discharge [SLIT], three impact levels capturing the relevant flow processes were defined: low sediment transport rate (below the local transport capacity) [SLIT.HYPO, d_1^1], average sediment transport rate (equals the local transport capacity) [SLIT.ORD, d_1^2], and debris flow [SLIT.DF, d_1^3]. The study team also identified three impact levels for the ratio between deposition and erosion [ED]: Low erosion propensity [ED↓, d_2^1], Average propensity [ED→, d_2^2], and High deposition propensity [ED↑, d_2^3]. The description of the reliability of the protection system [PSR] was carried out by assigning one of the following two impact levels: Failures likely [FL, d_3^1], and failures unlikely [FU, d_3^2]. The sediment availability of the system [SSA] was described in terms of impact levels by either a high level of availability [SSA.H, d_4^1] or a low level of availability [SSA.L, d_4^2]. The variation of solid transport [VSO] was identified by three levels: Positive Variation [VSO↑, d_5^1], no variation [VSO→, d_5^2] and negative variation [VSO↓, d_5^3].

The scenario construction (step 7 of FSA) consisted in assigning the consistency rating for each individual pair of impact levels of different impact variables as follows:

$c(\cdot, \cdot) = 3 \rightarrow$ Complete consistency, the levels of the impact factors are coherent and support each other

$c(\cdot, \cdot) = 1 \rightarrow$ Partial or weak inconsistency

$c(\cdot, \cdot) = 0 \rightarrow$ Inconsistency

In Table 4-4, an excerpt of the consistency ratings assigned to each pair of impact levels of different impact variables is presented.

Impact variable	Impact levels defined	SLIT			ED		
		Hypo concentrated sediment transport – SLIT.HYPO	Average sediment transport – SLIT.ORD	Debris flow – SLIT.DF	Erosion propensity – ED↓	Equilibrium propensity – ED→	Deposition propensity – ED↑
ED	d_2^1 Erosion propensity – ED↓	0	1	3			
	d_2^2 Equilibrium propensity – ED→	1	1	1			
	d_2^3 Deposition propensity – ED↑	3	1	0			
PSR	d_3^1 Failures likely – FL	0	1	3	3	0	1
	d_3^2 Failures unlikely – FU	3	1	0	0	1	3

Table 4-4. Excerpt from the consistency matrix for case study 1: Failure propensity case in an Alpine torrent and possible effects on sediment transport at the downstream outflow cross section

Subsequently, all possible scenarios were derived (step 7 of FSA). For each possible scenario an additive consistency value was assigned. Table 4-5 reports the consistency values for all possible scenarios. While in the first two rows of the table all impact level combinations of the two impact factors SLIT and ED are reported, the last three columns report all possible impact level combinations of the remaining impact factors, VSO, PSR and SSA, respectively. In order to select the relevant hazard scenarios (step 8 of FSA), the additive consistency values of all complete scenarios consisting of determined impact levels for each impact factors were reported at the crossing cell positions of the corresponding rows and columns. The most consistent scenarios are highlighted. The highest consistency value was assigned to the following two different, and thus possible, scenarios: (1) VSO↑, PSR.FL, SSA.H, ED↓, SLIT.DF, indicating that a positive solid outflow variation was judged to be consistent with a high failure likelihood of the protection system, a large amount of available sediment in the considered torrent reach characterised by erosion propensity and debris flows; and (2) VSO↓, PSR.FU, SSA.L, ED↑, SLIT.HYPO, reflecting an opposite situation. As a result of scenario interpretation (step 9 of FSA) particular attention has to be paid in assessing the possible flow processes at the upstream boundary of the considered torrent reach. In Table 4-5 the possibility of different sediment transport related behaviours that could take place in the considered torrent reach depending on the inflow type (different levels of variable SLIT) and the response in terms of reliability of the protection system (different levels of variable PSR) are highlighted. The subsequent determination of hazard zones on the downstream located alluvial fan has to take into consideration these results of Formative Scenario Analysis by defining a sufficiently broad range of system loading conditions in terms of liquid and solid inflow in order to capture possible system responses.

Erosion/deposition behaviour – ED	ED ↓	ED ↓	ED ↓	ED →	ED →	ED →	ED ↑	ED ↑	ED ↑			
Incoming solid transport and liquid discharge – SLIT	SLIT.HYPO	SLIT.ORD	SLIT.DF	SLIT.HYPO	SLIT.ORD	SLIT.DF	SLIT.HYPO	SLIT.ORD	SLIT.DF			
	1	2	3	4	5	6	7	8	9	Variation of solid outflow – VSO	Protection system reliability – PSR	Sediment availability in the system – SSA
1	13	15	20	10	11	14	14	13	15	VSO ↑	FL	SSA.H
2	4	6	11	4	5	8	8	7	9	VSO →	FL	SSA.H
3	4	6	11	4	5	8	11	10	12	VSO ↓	FL	SSA.H
4	13	14	18	7	7	9	8	6	7	VSO ↑	FL	SSA.L
5	7	8	12	4	4	6	5	3	4	VSO →	FL	SSA.L
6	10	11	15	7	7	9	11	9	10	VSO ↓	FL	SSA.L
7	9	8	10	10	8	8	15	11	10	VSO ↑	FU	SSA.H
8	3	2	4	7	5	5	12	8	7	VSO →	FU	SSA.H
9	6	5	7	10	8	8	18	14	13	VSO ↓	FU	SSA.H
10	11	9	10	9	6	5	10	6	4	VSO ↑	FU	SSA.L
11	8	6	7	9	6	5	10	6	4	VSO →	FU	SSA.L
12	14	12	13	15	12	11	20	15	13	VSO ↓	FU	SSA.L

Table 4-5. Set of all scenarios (step 7 of FSA) and identification of the set of most consistent scenarios (step 8, highlighted) for case study 1: Failure propensity case in an Alpine torrent and possible effects on sediment transport at the downstream outflow cross section

4.4.2 Case study two: Woody debris transport induced hazard scenarios at hydraulic weak points

In full analogy to case investigated in Section 4.4.1 the scope of the study team, familiar with the test site, was to determine the factors that could significantly influence the current state of the case and the associated system dynamics. The experts identified five major preceptors explaining the interaction of woody debris transport at hydraulic weak points. First of all, available woody debris, disposed to be transported towards the considered weak point, was considered to be essential. A second condition to be met was the existence of the necessary flow conditions since the recruited woody debris can potentially reach the hydraulic weak point. The flow conditions at the weak point

(liquid and woody debris transport) determined the system loading. The resistance of the configuration of the weak point was defined to be influenced by the structural (also geometrical) properties. The preceptor that incorporates the possible system response mechanisms to the blocking within the flow section, e.g. the entrapment of woody debris at a bridge with a certain number of piers, was called interaction between woody debris and the configuration of the weak point. The subsequent synthesis steps lead to the identification of possible relevant impact variables that significantly influence the current state of the system and related dynamics (see Figure 4-7).

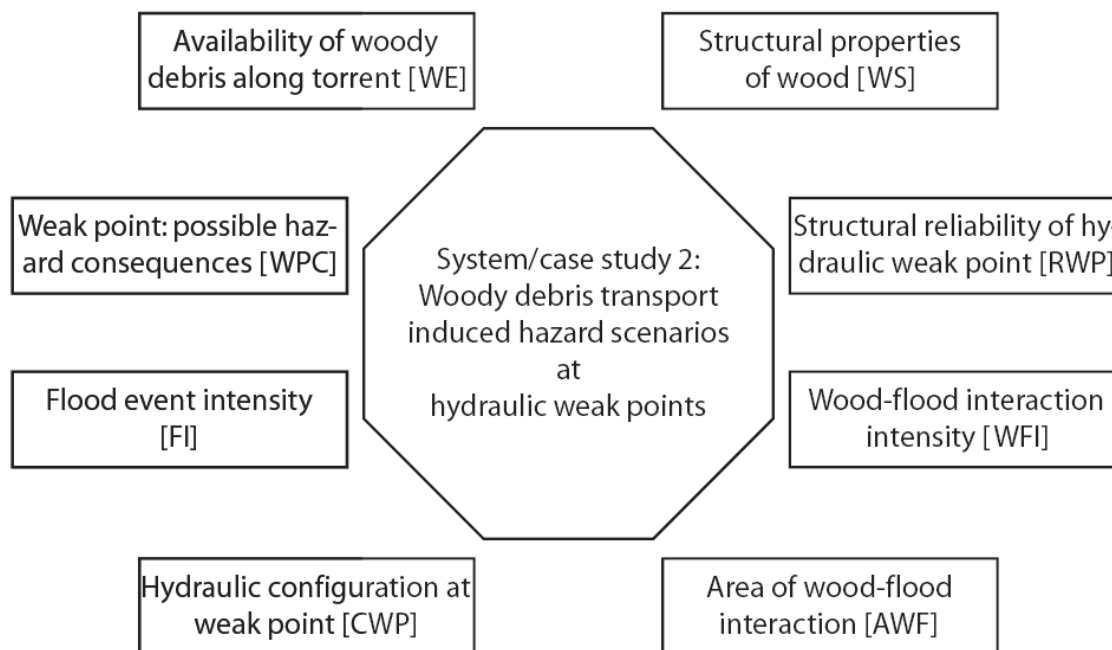


Figure 4-7. Pre-selection of possible impact factors or key variables for case study 2

The study team recognised that in case study 2, the selection of the relevant impact factors was affected by considerable additional criteria, i.e. uncertainty and importance, which consequently needed to be taken into account during the sets of calculation. O'Brien and Dyson (2007) pointed out criteria for selecting the key factors that will form the structure of the scenarios, i.e. the level of uncertainty in quantifying impact variables with respect to their future behaviour, and the associated level of importance of the variable for the system which reflects the significance of the individual factor within the dynamics of the analysed phenomenon. The expert team estimated the respective levels of uncertainty and of importance. In Figure 4-8 the levels of uncertainty are plotted versus the levels of importance. The study team defined the region of significance by (1) minimum level of

uncertainty, $U_{\min} \geq 2$, and (2) minimum level of importance $I_{\min} \geq 2$. As a result, the variables structural properties of wood [WS], reliability of hydraulic weak point [RWP], wood-flood interaction intensity [WFI], and possible hazard consequences at the location of the weak point [WPC] were judged by the study team to be significant variables for the description of the system.

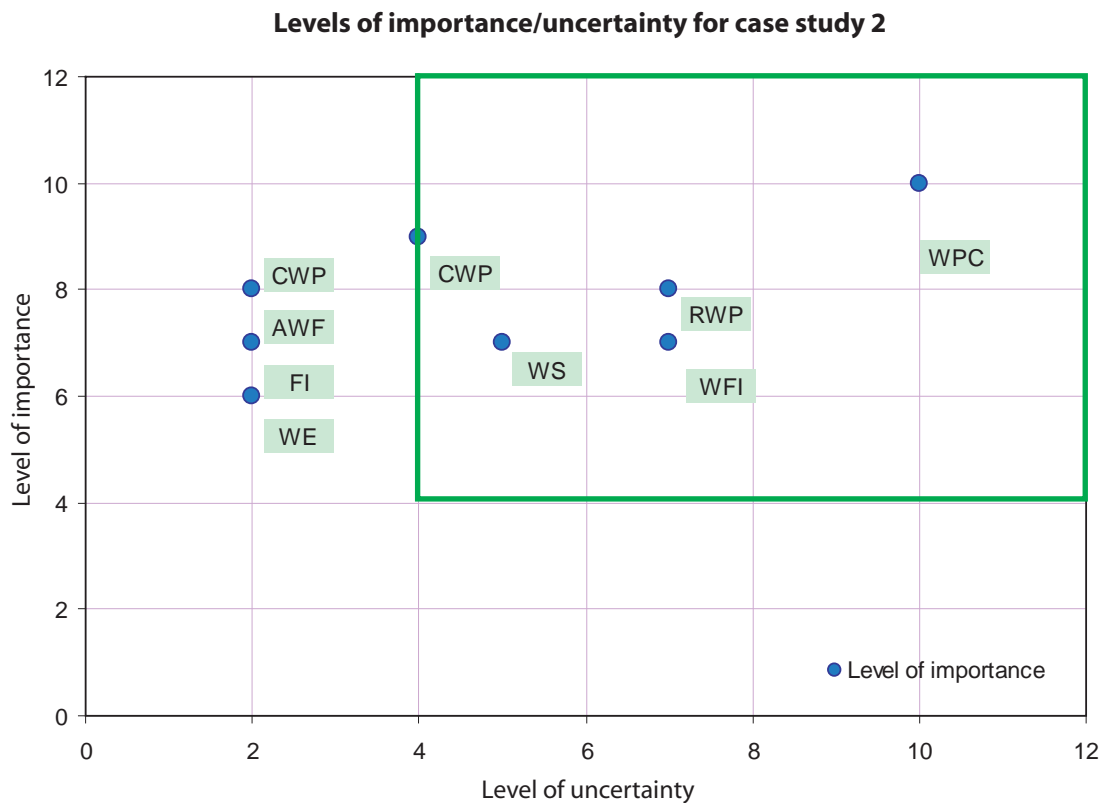


Figure 4-8. Relevant variables for the description of case study 2

The relevance of variable hydraulic configuration at the weak point [CWP] was reconsidered (the level of importance was very high), and the variables area of wood-flood interaction [AWF], flood event intensity [FI], and availability of woody debris along the torrent [WE] were partially included in the variable WFI, as shown in Figure 4-9.

Levels of importance/uncertainty for case study 2

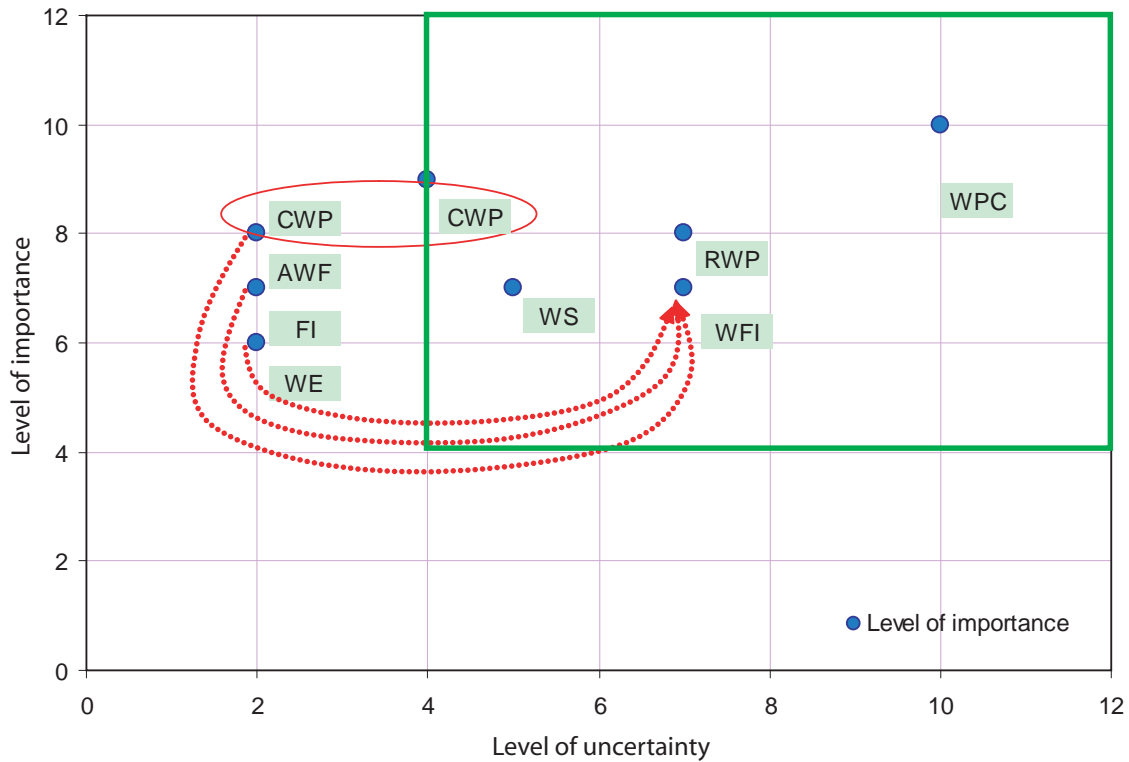


Figure 4-9. Selected key variables for case study 2 after a reconsideration step

In a subsequent step, the impact matrix for the selected variables was constructed for the variables CWP, WS, RWP, WFI, and WPC (see Table 4-6).

	WFI	CWP	WS	RWP	WPC	Activity	Impact strength	Mean activity	4.4
WFI	0	1	1	1	2	5	1.25		
CWP	2	0	0	2	2	6	1.50		
WS	1	0	0	1	2	4	4.00		
RWP	0	1	0	0	2	3	0.60		
WPC	1	2	0	1	0	4	0.50		
Passivity	4	4	1	5	8				
Involvement	20	24	4	15	32				
Mean passivity									
4.4									

Table 4-6. Impact Matrix case study 2: Woody debris transport induced hazard scenarios at hydraulic weak points

Plotting the levels of activity versus the levels of passivity/sensitivity of each key variable in a system grid (Figure 4-10), CWP and WFI resulted to be active key variables, therefore influencing the other variables, and RWP and WPC resulted to be sensitive on the influence of the above-mentioned variables. WS was found to be a buffer variable.

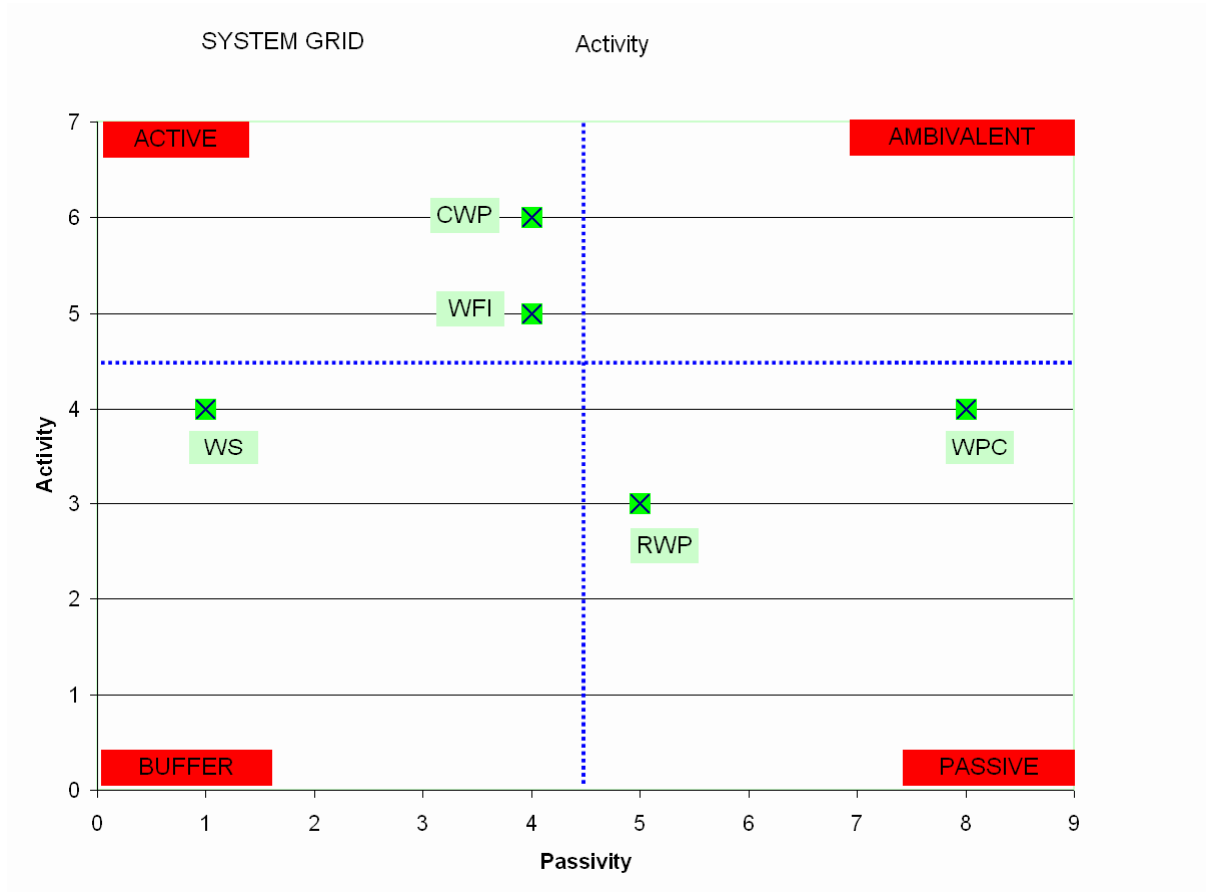


Figure 4-10. System grid of the selected key variables of case study 2

The impact levels were assigned to each impact factor as shown in Table 4-7. Concerning the interaction between the wood and the flooding process [WFI], two impact levels were used to describe the interaction intensity: Intense interaction [d_1^1], and moderate weak interaction [d_1^2]. The study team subsequently identified two impact levels for the hydraulic configuration at the weak point [CWP]: Entrapment propensity is likely [d_2^1], and entrapment propensity is unlikely [d_2^2]. The description of the structural properties of the wood [WS] was carried out by assigning one of the following two impact levels: Long pieces (defined as those pieces larger than the channel width available for flow-through) predominant [d_3^1], and short pieces (defined as those pieces smaller than the channel width available for flow-through) predominant [d_3^2]. The structural reliability of the hydraulic weak point [RWP] was described in terms of impact levels by either a high level of reliability [d_4^1] or a low level of reliability [d_4^2]. The possible hazard consequences at the weak

point [WPC] were identified by three levels: Catastrophic effect [d_5^1], hazard increase [d_5^2] and no variation [d_5^3].

Impact variable	Short description	Impact levels defined	
WFI	Wood-flood intensity interaction	d_1^1	Intense interaction
		d_1^2	Moderate interaction
CWP	Hydraulic configuration at the weak point	d_2^1	Entrapment propensity → likely
		d_2^2	Entrapment propensity → unlikely
WS	Structural properties of wood	d_3^1	Long pieces predominant
		d_3^2	Short pieces predominant
RWP	Structural reliability of hydraulic weak point	d_4^1	High reliability
		d_4^2	Low reliability
WPC	Possible hazard consequences at weak point	d_5^1	Catastrophic effect
		d_5^2	Hazard increase
		d_5^3	No variation

Table 4-7. Definition of the Impact levels for each key variable for case study 2: Woody debris transport induced hazard scenarios at hydraulic weak points

For the case study presented in Section 4.4.2, the expert team assigned the consistency rating for each pair of impact levels of different impact variables (see Table 4-8).

Impact variable	Impact levels defined		Intense interaction	Entrapment propensity → likely	Entrapment propensity → unlikely	Long pieces predominant	Short pieces predominant	High reliability	Low reliability
WFI	d ₁ ¹	Intense interaction							
	d ₁ ²	Moderate interaction							
CWP	d ₂ ¹	Entrapment propensity → likely	3						
	d ₂ ²	Entrapment propensity → unlikely	1						
WS	d ₃ ¹	Long pieces predominant	3	3	1				
	d ₃ ²	Short pieces predominant	1	1	3				
RWP	d ₄ ¹	High reliability	1	0	1	1	0		
	d ₄ ²	Low reliability	3	1	0	0	1		
WPC	d ₅ ¹	Catastrophic effect – ↑↑↑	1	3	0	1	0	0	1
	d ₅ ²	Hazard increase – ↑	3	3	0	3	1	1	3
	d ₅ ³	No variation – →	0	0	3	0	1	3	1

Table 4-8. Consistency Matrix for case 2: Woody debris transport induced hazard scenarios at hydraulic weak points

For each possible scenario an additive consistency value was assigned. Table 4-9 reports the consistency values for all possible scenarios, and the most consistent scenarios are highlighted. In Table 4-9, the additive consistency values for all possible scenarios are shown. While in the first two rows of the table all impact level combinations of the two impact factors CWP and WFI are presented, the last three columns describe all possible impact level combinations of the remaining impact factors WS, RWP and WPC, respectively. The additive consistency values of all complete scenarios consisting of determined impact levels for each impact factors are shown at the crossing cell positions of the corresponding rows and columns. The most consistent scenarios are highlighted. The highest consistency value was assigned to the following two different, and thus possible, scenarios, with an additive consistency value of 25 and 23, respectively:

1. CWP – likely, WFI – intense, WS – long pieces, RWP – low reliability, WPC – hazard increase, indicating that a hazard increase at the weak point was judged to be consistent with a weak point configuration where entrapment of woody debris is likely, given that an intense

wood-flood interaction takes place, the structural reliability (e.g. at a bridge location) is low and long pieces are involved in woody debris transport.

2. CWP – unlikely, WFI – weak, WS – short pieces, RWP – high reliability, WPC – no variation, reflecting an opposite situation. This is a clear indication that particular attention has to be paid either to the assessment of the structural properties of the wood (large or small pieces of woody debris) or to the structural and reliability characteristics of the weak point configuration (failures and likelihood of entrapment).

In Table 4-9 other possible and consistent future states for the case study are also highlighted, depending on the levels assumed for the impact variables. The scenario involving catastrophic effects at the weak point has also to be taken into consideration (relatively high additive consistency value). Within the hazard mapping procedure and in particular when performing the hydrodynamic simulations the set of model scenarios should correctly reflect the weak point system behaviour. The results of Formative Scenario Analysis are relevant in order to consider a sufficiently broad range of hydrodynamic simulations and capture possible system responses. By redesigning the weak point configuration, decreasing the likelihood of obstruction through woody debris and increasing the structural reliability, an important step towards efficient hazard mitigation could be achieved.

Entrapment propensity – CWP →	Likely	likely	Unlikely	Unlikely			
Wood-flood interaction – WFI →	Intense	Light	Intense	Light			
	1	2	3	4	Wood structure – WS	Structural reliability – RWP	WPC
1	16	13	10	11	Long pieces	High reliability	Catastrophic effect – ↑↑↑
2	21	17	15	15	Long pieces	High reliability	Hazard increase – ↑
3	14	15	14	19	Long pieces	High reliability	No variation – →
4	19	12	11	8	Long pieces	Low reliability	Catastrophic effect – ↑↑↑
5	25	17	17	13	Long pieces	Low reliability	Hazard increase – ↑
6	14	11	12	13	Long pieces	Low reliability	No variation – →
7	10	11	8	13	Short pieces	High reliability	Catastrophic effect – ↑↑↑
8	14	14	12	16	Short pieces	High reliability	Hazard increase – ↑
9	10	15	14	23	Short pieces	High reliability	No variation – →
10	15	12	11	12	Short pieces	Low reliability	Catastrophic effect – ↑↑↑
11	20	16	16	16	Short pieces	Low reliability	Hazard increase – ↑
12	12	13	14	19	Short pieces	Low reliability	No variation – →

Table 4-9. Set of all scenarios (step 7 of FSA) and identification of the set of most consistent scenarios (step 8, highlighted) for case study 2: Woody debris transport induced hazard scenarios at hydraulic weak points

4.5 Conclusions

By adopting the Formative Scenario Analysis framework the study team analysed relevant issues in hazard analysis essential for a comprehensive risk assessment procedure. The underlying case studies were presented in Sections 4.4.1 and 4.4.2 accordingly. The expert knowledge available in the different domains was successfully integrated by interaction and collaboration of the study team through a guided scenario building and a rigorous scenario selection procedure. Throughout the entire process of hazard assessment and mapping the identification of consistent assumptions either concerning system loading or system response mechanisms provided crucial insights into the systems behaviour. It had been shown that possible case developments can be described with a particular focus on feedback loops (reliability of the protection measures vs. sediment availability) and nonlinear cause-effect chains (transported woody debris vs. entrapment propensity at hydraulic weak point locations). As a consequence, it was possible to better describe the relative importance and uncertainty of each impact factor. The structured decomposition of the case by a series of preceptors, followed by a knowledge integrating synthesis efficiently supported the control of coherence and traceability of the results (as required during hazard mapping) and the informed decision making process (as required for an efficient prioritisation of mitigation strategies).

The two case studies performed in this work put into evidence that a small set of consistent and reliable exploratory scenarios to identify effects given a specific set of causes have to be taken into account. One of the crucial challenges of integral risk management is to be prepared for the unexpected. If weak signals of an unexpected future are not discerned by deterministic models, or probabilistic models neglect important facets of the case, the possibility-based approach of Formative Scenario Analysis offers apparent problem-solving advantages.

By meeting basic and operational principles (Shepard, 2005), Formative Scenario Analysis can provide remarkable insights in the entire process of hazard assessment, integrating, where necessary, consistent assumptions either concerning system loading or system response mechanisms or bounding uncertainties where possible. However, the method has to be used in combination with hydrological and hydraulic simulation models in order to produce consistent, fully intelligible and retraceable results. It is therefore also of considerable importance to capture at least qualitatively the different facets of multi-hazard situations and nonlinearity in cause-effect relationships in order to design resilient protection systems.

The interaction necessary for Formative Scenario Analysis requires participation within the study team; i.e. with respect to reveal tacit and mental assumptions of the team members or with respect to promote organisational learning aspects (e.g., the use of a common language).

In particular concerning the European Flood Risk Directive (Commission of the European Communities, 2007), but also with respect to the overall aim of building hazard-resilient communities, future studies should include the applicability of Formative Scenario Analysis within flood risk management plans. Since such plans are of certain relevance in order to deal pro-actively and from an ex-ante perspective with flooding hazards including torrent processes, the applicability in the framework of flood risk management plans is obvious. A particular focus should be placed on the combination between participative effects such as Formative Scenario Analyses and conventional modelling approaches in order to better achieve the overall aim of managing natural hazard risk in a sustainable manner.

4.6 References

Armanini, A., and Larcher, M., 2001. Rational criterion for designing opening of slit-check dam, *Hydraulic Engineering*, 127 (2), 94-104.

Autonome Provinz Bozen-Südtirol, 2008. Informationssystem zu hydrogeologischen Risiken, Methodischer Endbericht, Bozen: Autonome Provinz Bozen-Südtirol.

Berger, E., Grisotto, S., Hübl, J., Kienholz, H., Kollarits, S., Leber, D., Loipersberger, A., Marchi, L., Mazzorana, B., Moser, M., Nössing, T., Riedler, S., Scheidl, C., Schmid, F., Schnetzer, I., Siegel, H. and Volk, G., 2007. DIS-ALP. Disaster information system of alpine regions, Final report, unpublished.

Bezzola, G. and Hegg, C., 2007. Ereignisanalyse Hochwasser 2005, Teil 1 – Prozesse, Schäden und erste Einordnung, Bern und Birmensdorf, Bundesamt für Umwelt BAFU, Eidgenössische Forschungsanstalt WSL.

Commission of the European Communities, 2007. Directive 2007/60/EC of the European Parliament and of the Council of 23 October 2007 on the assessment and management of flood risks, European Commission.

Diehl, T., 1997. Potential drift accumulation at bridge, Washington, U.S. Department of Transportation, Federal Highway Administration Research and Development, Turner-Fairbank Highway Research Center.

Ducot, C. and Lubben, J., 1980. A typology of scenarios, *Futures*, 12, 49-57.

ETAlp Consortium, 2003. Kompendien: Erosion, Transport in alpinen Systemen, BFW, Wien.

- Fuchs, S. and McAlpin, M., 2005. The net benefit of public expenditures on avalanche defence structures in the municipality of Davos, Switzerland, *Natural Hazards and Earth System Sciences*, 5 (3), 319-330.
- Fuchs, S., Heiss, K., and Hübl, J., 2007. Towards an empirical vulnerability function for use in debris flow risk assessment, *Natural Hazards and Earth System Sciences*, 7 (5), 495-506.
- Fuchs, S., Kaitna, R., Scheidl, C., and Hübl, J., 2008. The application of the risk concept to debris flow hazards, *Geomechanics and Tunnelling*, 1 (2), 120-129.
- Fuchs, S., Dorner, W., Spachinger, K., Rochman, J., and Serrhini, K., 2009. Flood risk map perception through experimental graphic semiology, in: *Flood risk management. Research and practice*, edited by: Samuels, P., Huntington, S., Allsop, W., and Harrop, J., Taylor & Francis, London, 705-714.
- Godet, M., 2000. The art of scenarios and strategic planning: tools and pitfalls, *Technological Forecasting and Social Change*, 65, 3-22.
- Kahn, H. and Wiener, A., 1967. *The Year 2000: A framework for speculation on the next thirty-three years*, Macmillan, New York.
- Lyn, D., Cooper, T., Condon, D. and Gan, L., 2007.: *Factors in debris accumulation at bridge piers*, Washington, U.S. Department of Transportation, Federal Highway Administration Research and Development, Turner-Fairbank Highway Research Center.
- Mazzorana, B. and Fuchs, S.: *A Fuzzy Formative Scenario Analysis modelling framework for natural hazard management*, *Environmental Modelling & Software*, in press.
- Merz, B., Kreibich, H. and Apel, H., 2008. Flood risk analysis: Uncertainties and validation, *Österreichische Wasser- und Abfallwirtschaft*, 60 (5-6), 89-94.
- Miyazawa, N., Tanishima, T., Sunada, K., and Oishi, S., 2003. Debrisflow capturing effect of grid type steel-made sabo dam using 3D distinct element method, in: *Debris-flow hazards mitigation: Mechanics, prediction, and assessment*, edited by: Rickenmann, D., and Chen, L., Milpress, Rotterdam, 527-538.
- O'Brien, F. and Dyson, R., 2007. *Supporting strategy – Frameworks, methods and models*, John Wiley and Sons, Chichester.
- Oberndorfer, S.; Fuchs, S.; Rickenmann, D. and Andrecs, P., 2007. *Vulnerabilitätsanalyse und monetäre Schadensbewertung von Wildbachereignissen in Österreich*, BFW, Wien.

- Paté-Cornell, E., 1996. Uncertainty in risk analysis: Six levels of treatment, *Reliability Engineering and System Safety*, 54 (2-3), 95-111.
- Remaître, A., van Asch, T., Malet, J.-P., and Maquaire, O., 2008. Influence of check dams on debris-flow run-out intensity, *Natural Hazards and Earth System Sciences*, 8 (6), 1403-1416.
- Rickenmann, D., Laigle, D., McArdell, B., and Hübl, J., 2006. Comparison of 2D debris-flow simulation models with field events, *Computational Geosciences*, 10, 241-264.
- Scholz, R. and Tietje, O., 2002. Formative scenario analysis, edited by Scholz, R. and Tietje, O., *Embedded case study methods*, Sage, Thousand Oaks, 79-116.
- Tietje, O., 2005. Identification of a small reliable and efficient set of consistent scenarios, *European Journal of Operational Research*, 162, 418-432.

5. DETERMINING NATURAL HAZARD PATTERNS AT CRITICAL STREAM CONFIGURATIONS BY FORMATIVE SCENARIO ANALYSIS

*Two roads diverged in a wood and I –
I took the one less traveled by,
and that has made all the difference.
Robert Frost*

B. Mazzorana, and S. Fuchs: Determining natural hazard patterns at critical stream configurations by Formative Scenario Analysis. Journal of Environmental Modelling and Software (submitted)

Abstract

Extreme torrent events occurring in alpine regions during the last decades have clearly shown a variety of process patterns involving morphological changes due to increased local erosion and deposition phenomena, and clogging of critical flow sections due to woody material accumulations. Simulation models and design procedures currently used in hazard and risk assessment are only partially able to explain these hydrological cause-effect relationships since the selection of appropriate and reliable scenarios still remains unsolved. Here we propose a scenario development technique, based on a system loading shell and a system response shell. By Formative Scenario Analysis we derived well-defined sets of assumptions about possible system dynamics at selected critical stream configurations which allowed to reconstruct in a systematic manner the underlying system loading mechanisms and the induced system responses. The derived system scenarios are fundamental prerequisite to assure quality throughout the hazard assessment process and to provide a coherent problem setting for risk assessment. The proposed scenario development technique has proven to be a powerful modelling framework for the necessary qualitative and quantitative knowledge integration and for coping with the underlying uncertainties, which were considered to be a key element in natural hazards risk assessment.

Keywords: Formative Scenario Analysis; Fuzzy set theory; Reliability; Decision analysis; Integral risk management; Woody material transport

5.1 Introduction

Particularly since the 1990s, considerable damage occurred due to torrent processes (1999, 2002, 2005, and 2008) and inundation (2002, 2005, 2006) in the European Alps. This development has been attributed to both risk-influencing factors, changes in the intensity and magnitude of processes (Houghton et al. 2001; Solomon et al. 2007) and an increase in values at risk exposed (Fuchs et al. 2005; Fuchs and Keiler 2006; Keiler et al. 2006). As a result society increasingly realised – also on the political level – that despite of considerable amounts of public money spent for conventional technical mitigation and hazard mapping, a comprehensive protection of settlements and infrastructure against any loss resulting from hazard processes is not affordable and economically justifiable (Weck-Hannemann 2006; Fuchs et al. 2007). People and political decision makers are increasingly aware of this situation, thus, in some Alpine countries a paradigm shift took place from hazard reduction to a risk culture (PLANAT 2004) while dealing with natural hazard risk in other countries still remains conservative until now (Stötter and Fuchs 2006; Fuchs et al. 2008).

The analysis of natural hazard risk is embedded in the circle of integral risk management, including a risk assessment from the point of view of social sciences and economics, and strategies to cope with the adverse effects of hazards. The underlying objective for risk management is the planning and implementation of protective measures in an economically efficient and societal agreeable manner. Thus, risk assessment includes both, risk analysis and risk valuation within a defined system at the intersection between different disciplines (Renn 2008a, b). For this reason, the scales of valuation (temporal, spatial, degree of detail) have to be well defined for a sustainable risk minimisation. To be able to compare different types of hazards and their related risks, and to design and implement adequate risk reduction measures, a consistent and systematic approach has to be established. While a hazard analysis focuses on natural processes such as debris flows and floods with related woody material transport, the method of risk analysis additionally includes the qualitative or quantitative valuation of elements exposed to these hazards, i.e. their individual values and the associated vulnerability. Originating from technical risk analyses, the concept of risk with respect to natural hazards is defined as a quantifying function of the probability of occurrence of a process and the related extent of damage, the latter specified by the damage potential and the vulnerability:

$$R_{i,j} = f(p_{S_i}, A_{O_j}, p_{O_j,S_i}, v_{O_j,S_i})$$

Hence, the following specifications are necessary for the ex-ante quantification of risk (Varnes 1984; Fuchs 2009):

$R_{i,j}$... risk, dependent on scenario i and object j

p_{s_i} ... probability of scenario i

A_{o_j} ... value of object j , which is derived through economic valuation techniques (Fuchs and McAlpin 2005)

p_{o_j,s_i} ... probability of exposure of object j to scenario i

v_{o_j,s_i} ... vulnerability of object j , depending on the intensity of scenario i

The event documentation of recent alpine river floods and torrent processes, such as debris flows and excessive bed load transport in gravel bed streams, highlighted considerable shortcomings in the current procedures used for natural hazard and risk assessment (Berger et al. 2007; Autonome Provinz Bozen-Südtirol 2008). In particular the effects of changing channel morphology and cross-sectional clogging imputable to woody material transport phenomena were found to amplify process intensities significantly (e.g., Diehl 1997; Lyn et al. 2007). Furthermore, existing hazard maps turned out to be not as reliable as expected (e.g., Bezzola and Hegg 2007). In order to improve risk analyses and to support decision making, underlying scenarios have to be re-built based on such issues (Girod and Mieg 2008), in particular with respect to sources of uncertainty that affect the predictability of the hazard process paths (e.g., Paté-Cornell 1996; Merz et al. 2008).

To apply the risk equation and redesign the underlying scenarios, we propose a shell-structured scenario planning approach (Figure 5-1). According to the parameters of the risk equation, the shell structure is composed by (1) natural hazard scenarios, (2) exposure scenarios, (3) vulnerability scenarios, (4) analyses of values at risk, resulting in combination in (5) risk scenarios.

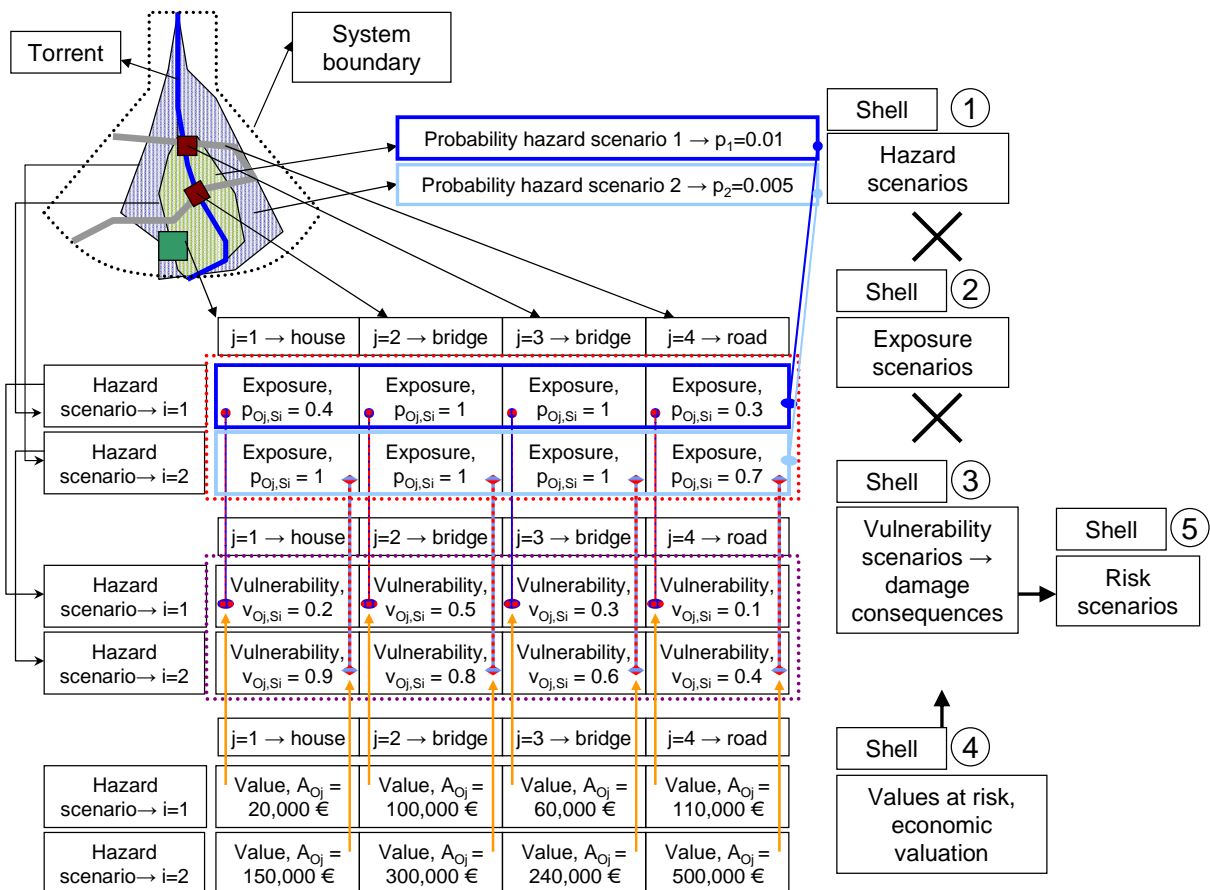


Figure 5-1: Shell-structured risk scenario planning approach

In this paper we put the focus on the hazard part of the risk equation, i.e. the investigation of woody material transport related risk scenarios in mountain torrents. Acknowledging the fact that the definition of robust woody material transport related risk scenarios necessarily is based on an accurate deduction of consistent and reliable hazard scenarios, the case study presented here addresses the following issues: (1) identification of an adequate natural hazard scenario shell structure, hereafter denominated as system loading scenario shell and (2) identification of an appropriate scenario shell for the description of possible system responses taking place at critical stream configurations (e.g. bridges), hereafter denominated as system response scenario shell. In Figure 5-2 possible hazard and risk scenarios along a stream configuration are shown. The importance of a robust definition of either consistent system loading scenarios (e.g. flood with high woody material transport rates) or system response scenarios (e.g. system changes such as possible bridge clogging) is indicated to reliably infer the main consequences for the exposed objects (e.g. roads and buildings) in terms of risk.

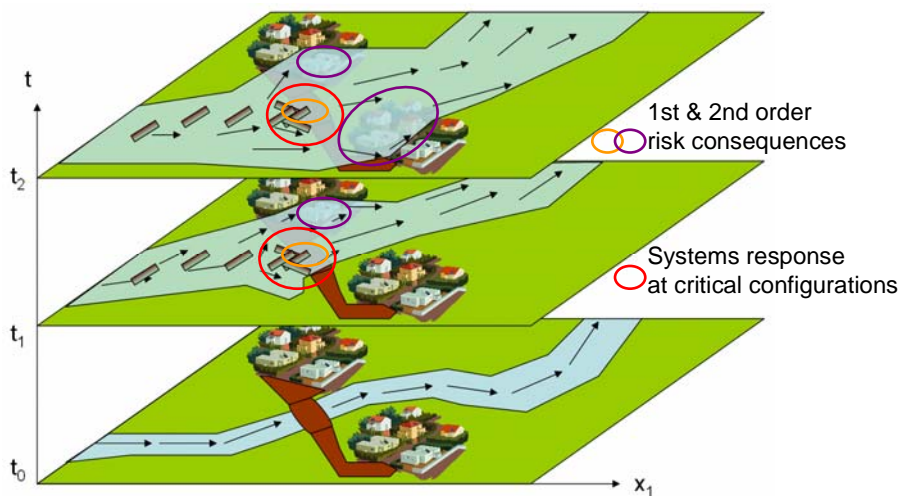


Figure 5-2: Possible hazard and risk scenarios along a stream configuration

With respect to the determination of hazard scenarios for debris flows and flood processes characterised by woody material transport, a series of uncertainty sources have to be considered. These uncertainties include

- (1) uncertainties about the possible range of rheological behaviour and about the liquid-solid mixture concentration of debris flows;
- (2) uncertainties in system loading assumptions (e.g., duration-intensity related uncertainties, uncertainties related to sediment transport rates, uncertainties emerging from woody material transport);
- (3) uncertainties in system response mechanisms (e.g., localised obstructions that divert the flow patterns, influence of small-scale topological features);
- (4) uncertainties concerning the protection system functionality and mitigation efficacy (e.g., failure propensities of key components within the protection system, sediment dosing behaviour of retention basins, dike failures); and
- (5) uncertainties concerning morphological changes inducing hazard processes (e.g., large erosion phenomena on alluvial fans, flow path changes in steep mountain rivers);

and cannot precisely be mirrored by common 2D-hydrodynamics simulation models so far. We postulate here on the basis of the comprehensive analysis of event documentations that uncertainties

regarding the statistical extrapolations of peak discharges for high return period flood events increase if the floods were accompanied by considerable sediment transport. This trend was found to be even more accentuated if woody debris transport takes place (for an overview, see Montgomery and Piégay 2003). It is a fact that the accuracy, precision and reliability of extrapolations for discharge time series with longer return periods significantly depends on the robustness of the underlying measured discharge time series. Such robust measurement series are comparatively scarce for sediment transport rates in alpine catchments and practically unavailable for woody debris transport rates. Moreover, compared to liquid discharge, currently used investigation methods and calculation procedures are less accurate if sediment dynamics and woody material transport characterise the hazard process.

In order to overcome these shortcomings related to measured data and uncertainties, we propose a concept to support a balanced strategy of investigation, integrating available and retrievable, qualitative and quantitative knowledge of uncertainties. The approach aims at an integration of relevant impact factors by determining possible system loading conditions and system response mechanisms at hydraulic weak points along mountain streams during extreme events which allows assessing the process-response system comprehensively. Therefore we extended and tested a Formative Scenario Analysis approach originally proposed by Scholz and Tietje (2002). Formative Scenario Analysis is based on qualitatively assessed impact factors and expert-rated quantitative relations between these factors, such as impact and consistency analysis. Within this framework, formative indicates a generic mathematical structure behind the scenarios that is combined with quantitative and qualitative expert assessments (Tietje 2005). Apart from the hazard assessment *sensu stricto*, all subsequently linked products, such as risk maps, intervention plans, and mitigation concepts benefit from this coherent derivation procedure for hydrological hazards involving woody material transport.

The requirement of a modelling framework that enables rational integration of qualitative and quantitative knowledge in order to analyse complex and often unstructured problems becomes essential if the elements of uncertainty are considerable on both sides, the system loading side and the system response (Funtowicz and Ravetz 1994; Kolkman et al. 2005; Refsgaard et al. 2007).

Similar arguments are valid from a system response perspective. If flooding processes were not characterised by considerable sediment load and woody debris transport, currently used hydraulic simulation tools provide reliable results. However, if sediment loads and woody debris transport phenomena occur, complex system responses can be expected in particular with respect to critical channel sections such as constrictions at bridge cross sections. Woody debris might be entrapped at bridge piers leading to debris accumulation at individual piers. Moreover, if the distance between

the bridge piers is smaller than the design log length of woody material (Diehl 1997), a spanning blockage debris accumulation might occur. Such spanning blockage accumulations can occlude relevant parts of the cross-section originally available for the flow discharge. As a consequence, a change in the flow pattern from open channel flow conditions to orifice flow conditions is detectable. Additionally, considerable scour depths will develop at the pier toes and abutments destabilising the entire structure of the bridge. On the upstream side of the construction lateral overflow becomes increasingly probable as a consequence of backwater effects.

Argumentations outlined above had shown that either from the system loading or from the system response perspective a practical and effective solution has to be developed in order to close the existing gaps and to increase the reliability and robustness of natural hazard risk management. Therefore, within a scenario development framework (Mahmoud et al. 2009), we applied a shell-based scenario approach for woody material transport in torrents and related mountain rivers. The major focus was on the explorative analysis of consequences emerging from hazards induced by woody material transport during extreme flood events at critical channel cross-sections. Therefore, we used (1) Formative Scenario Analysis in combination with (2) Fuzzy set theory to enhance knowledge representation. By applying Rough Set Data Analysis we validated the accuracy prediction of the selected set of consistent scenarios generated by Formative Scenario Analysis.

5.2 Methods

5.2.1 Formative Scenario Analysis

From a formal perspective scenario analysis can be classified into three different types (Tietje 2005), (1) holistic scenario analysis, (2) model scenario analysis, and (3) Formative Scenario Analysis. A holistic scenario analysis (which is analogue to the elicitation of responses from expert hearings) includes the construction of scenarios based on the opinion of specialists from the individual disciplines involved. A subjective mental integration of interdisciplinary qualitative and quantitative knowledge takes place, and intuitions and formal analyses of experts are combined (see e.g., Kahn and Wiener 1967; van der Heijden 2005). In doing so, mathematical methods and experimental results are commonly used to refine certain aspects of these scenarios, in particular with respect to a scale taking into account individual (local) knowledge. Model scenario analyses are mainly based on (not always dynamical) systems modelling. By systematically varying the unknowns and assuming different values for uncertain parameters, the model is forced to create a number of trajectories, some of which are subsequently selected as scenarios by the expert pool.

Following Scholz and Tietje (2002), Formative Scenario Analysis is a scientific technique to construct defined sets of assumptions to gain insight into a system and its potential development. With this procedure the study team is guided towards a differentiated and structured understanding of a system's current state and its dynamics. It is usually performed by small groups with specialised expertise about different aspects of the system, which they share with one another. Hence, Formative Scenario Analysis is based on qualitatively assessed key factors. Experts determine by a rating procedure quantitative relations between these factors. A Formative Scenario Analysis consists of two steps, (1) analytic modelling and decomposition of the initial state of the case studied, and (2) formative synthesis. In the first step an expert team identifies a set of key impact factors or variables that serve as perceptors. In the second step of formative synthesis, various operations are carried out on these key variables in order to generate all possible scenarios. Subsequently, a consistency analysis is performed in order to identify a number of different but internally consistent scenarios, and a scenario interpretation phase refines this procedure to iteratively identify relevant settings. This methodology was proposed by Scholz and Tietje (2002) by application of a nine-step Formative Scenario Analysis (see Figure 5-3) and it has been shown, that it could be successfully applied to natural hazard analysis (Mazzorana et al. 2009).

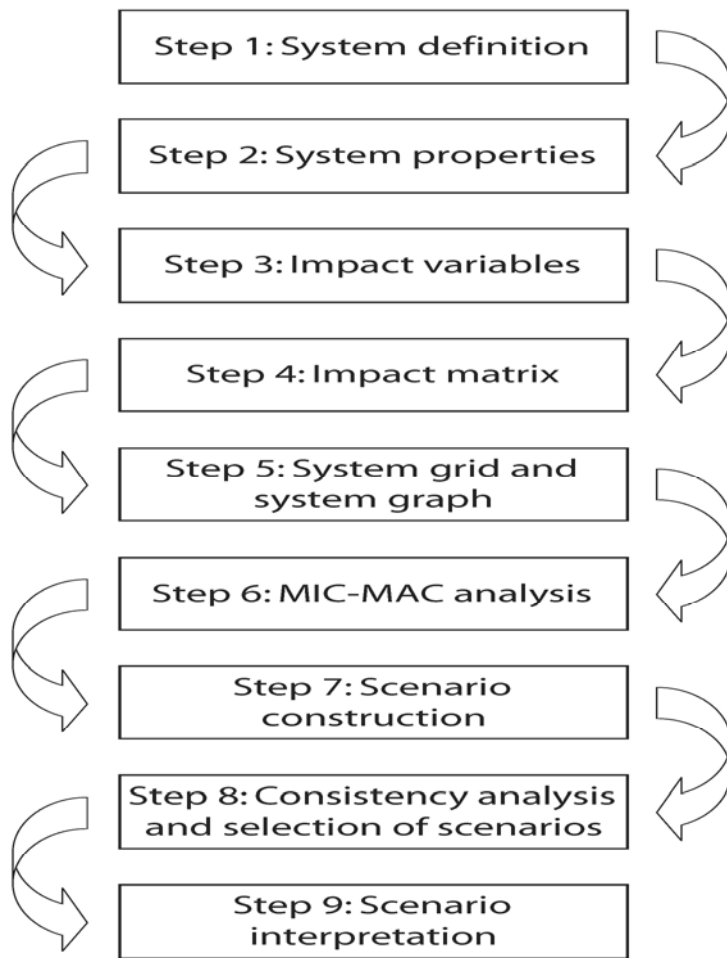


Figure 5-3. The nine steps of Formative Scenario Analysis proposed by Scholz and Tietje (2002).

Here the methodology of Formative Scenario Analysis was refined introducing methods of knowledge representation using type-1 fuzzy sets. In environmental modelling, we are dealing with imprecise and incomplete data (Brown et al. 2005; Mahmoud et al. 2009). In this context decisions made by experts are subjective and depend mainly on their individual concepts. Fuzzy set theory allows making decisions in a fuzzy environment, which is made of fuzzy objectives, fuzzy constraints and a fuzzy decision (Rommelfanger and Eickemeier 2001; Mouton et al. 2009). If a general system with multiple objectives and constraints is assumed, we result in $n > 1$ fuzzy objectives, G_1, \dots, G_n and $m > 1$ fuzzy constraints, C_1, \dots, C_m and defined as fuzzy sets in the set of options X_{op} . A fuzzy decision is determined as follows:

$$D = G_1 \cap G_2 \cap \dots \cap G_n \cap C_1 \cap C_2 \cap \dots \cap C_m$$

In order to reach agreement among different experts about their opinion on a certain event, the Fuzzy Delphi method was applied (Rutkowski 2008). This method, which is employed in every rating procedure within this extended version of Formative Scenario Analysis consists of the following steps: (1) the experts E_i express their opinion on a certain event in terms of triangular fuzzy numbers: $A_i = (a_s^{(i)}, a_M^{(i)}; a_l^{(i)})$, $i = 1, \dots, n$. (2) The average is computed as follows:

$$A_{aver} = \left(\frac{1}{n} \sum_{i=1}^n a_s^{(i)}, \frac{1}{n} \sum_{i=1}^n a_M^{(i)}; \frac{1}{n} \sum_{i=1}^n a_l^{(i)} \right). \quad (3)$$

Each expert E_i expresses his/her opinion again, taking into account the received averages from the previous round of inquiries and new fuzzy numbers and

$$averages \text{ are created: } B_i = (b_s^{(i)}, b_M^{(i)}; b_l^{(i)}), \quad i = 1, \dots, n. \quad \text{and} \quad B_{aver} = \left(\frac{1}{n} \sum_{i=1}^n b_s^{(i)}, \frac{1}{n} \sum_{i=1}^n b_M^{(i)}; \frac{1}{n} \sum_{i=1}^n b_l^{(i)} \right)$$

respectively. The process is repeated until two subsequent sufficiently close averages ($A_{aver}, B_{aver}, C_{aver}, \dots$) are obtained. (4) Subsequently, if new relevant information is obtained concerning a given problem, the procedures (1)-(3) may be repeated. In this way the effectiveness of a participative problem-solving approach is supported.

According to the Formative Scenario Approach, the specialised team of experts precisely defines the case study to be investigated (cf. Figure 5-3). A conceptual sketch of this study is drawn and a concise description is carried out. In a second step, the expert team identifies the broad set of key variables that possibly determine the actual state of the studied system and the expected future developments. Importance and uncertainty of the key variables are rated by fuzzy intervals that are able to represent the broad spectrum of the expert's case-specific knowledge better than crisp values do. Third, the relative importance of the key variables is estimated; based on this rating the case study is structured by an impact matrix. This step provides activity, passivity, impact strengths and involvement measures for each variable (Scholz and Tietje 2002). Activity quantifies the effectiveness of the impact of a variable on other variables. Passivity (or sensitivity) is correlated with the medium dependency of a variable on other variables. Impact strength is a summarising indicator of the medium impact strength of a variable on the entire case studied. Involvement indicates how strongly a certain variable is interlinked with the system. For these fundamental rating steps fuzzy intervals were used to model the knowledge of specialised experts in an appropriate way. The above-mentioned parameters were determined by fuzzy algebraic operations. A grid of activity and passivity scores supports the expert team in selecting the core set of relevant key variables that are supposed to be most important within the studied system. The classical Formative Scenario Analysis subsequently applies the MICMAC Analysis (Cross Impact Matrix-Multiplication Applied to Classification) that in the present version of Fuzzy Formative Scenario

Analysis is omitted because the results of the impact matrix alone enable the expert team to select the relevant key variables. Instead of the MICMAC Analysis step, the following classification scheme is applied to the selected key factors. The set of key factors Q can be separated into two disjointed subsets, namely a set of conditional factors Co and the set of evolutionary factors Ev , which are complementary to Q . Taking climate change as an example, conditional factors such as temperature and rainfall intensity changes influence evolutionary factors such as peak discharges and sediment transport rates. Hence, a classification of the key variables in different levels can be introduced. Global factors (e.g., changes in rainfall intensity) are attributed to an outer shell of influence and local factors (e.g., peak discharges) to an inner shell of influence. Dissecting the spatiotemporal continuum into p “spatiotemporal shells of influence”, indexed by k , we obtain the

following structure of the key factor set Q^* : $Q^* = \bigcup_{k=1}^p Q_k = \bigcup_{k=1}^p Co_k \cup Ev_k$. Here Q^* is used instead of Q , because some key factors can belong to more than one shell. An evolution factor of an outer shell can constitute a conditional factor of an inner shell. Q can be structured as

$$Q = Q_1 \cup \bigcup_{k=2}^p (Q_k \setminus (Q_k \cap Q_{k-1})).$$

The subsequent consistency analysis is of crucial importance for the scenario construction phase. The expert team first identifies the levels to be assigned to each key variable and then assigns consistency ratings (fuzzy intervals) to all combinations of key factor levels belonging to each shell k . Furthermore, a conjoint internal consistency measure for each scenario belonging to each shell k is computed by means of fuzzy algebra. Common key factors between different shells are named connectors. The external consistency between scenarios of different shells derives from the shearing of common key factors. The key factor levels assumed by the common key factors along the hierarchy of shell levels is the outcome of the internal consistency analysis performed in the hierarchically superior shell. In a nutshell the most consistent scenarios of a hierarchically superior shell, identified by a certain sequence of key factor levels determine automatically the levels assumed by the common key factors of the hierarchically inferior shell. Scenario selection is performed on the basis of an overall conjoined consistency measure covering all identified shells. With respect to natural hazard risk management, two essential criteria for scenario selection were identified, (1) consistency, since inconsistent scenarios draw no realistic image of the system development, (2) difference between scenarios, since decision makers focus on a set of principally possible system developments, while small differences between similar scenarios are of minor importance.

At the end of the procedure the result is a series of consistent all shell comprising scenarios that build up a case-specific scenario information system *SIS* .

Typically knowledge contained in the scenario information system *SIS* is represented in the form of p decision tables DT_k , which are defined as follows: A decision table DT_k is the ordered 5-tuple $DT_k = \langle U_k, Co_k, Ev_k, V_q, f_q \rangle_{q \in Co_k \cup Ev_k}$, where U_k denotes a set of scenarios with cardinality $|U| = h_{max, h_{max, k}}$, with $h_{max, k}$ indicating the number of consistent scenarios selected for the shell k , $Co_k \cup Ev_k$ is a finite set of key variables, V_q is the set of possible levels the key variables can assume, and f_q is the information function defined as $f_q : Co_k \times Ev_k \rightarrow V_q$. The information function defines unambiguously the set of rules included in the decision table, and is codified in the Formative Scenario Analysis procedure.

The resulting scenario information system is optimised by means of Rough Sets Data Analysis (Pawlak 1997; Greco et al. 2001, Tan 2005; Olson and Delen 2008; Rutkowski 2008). The elimination of redundant information to provide more compact rules is achieved by identifying reducts, or subsets of key variables that still manage to preserve all the information within the decision tables DT_k and directly within the scenario information system *SIS* . If the results of Rough Sets Data Analysis indicate that the information content of the information system *SIS* is not complete and therefore fails to provide an accurate description of the case and its developments, the study team has to refine iteratively the key variable structure and re-perform the Formative Scenario Analysis procedure.

5.2.2 Model set-up

The framework of Formative Scenario Analysis, as proposed by Scholz and Tietje (2002), was extended by means of Fuzzy set theory and Fuzzy algebra in order to meet the requirements in natural hazards and risk management, namely with respect to the problem data uncertainty and diverse experts' notion. Using fuzzy set theory (Kosko 1992; Kruse et al. 1994; Rutkowski 2008) is possible to formally define imprecise and ambiguous notions (e.g. "high temperature" or "average height").

The procedural steps for setting up the model are summarised in concise form as follows:

(A) Formative scenario construction steps:

(1) The expert team pre-selects $q_i, i = 1, \dots, N$ key variables, also referred to as system variables, impact factors or case descriptors.

(2) Next, the group of experts assigns each selected key variable to one of the following disjointed subsets of $Q : Co \vee Ev$.

(3) In a following step, the group of experts organises the selected key variables $q_i \in Q$ in an

adequate shell structure $Q^* = \bigcup_{k=0}^p Q_k = \bigcup_{k=1}^p Co_k \cup Ev_k$ with p shells. The apex r is introduced

to describe the membership of $\tilde{q}_{i,k}^r$ to one of the above identified subsets of Q^* as follows:

$r = 1$ if $q_{i,k}^r \in Co_k$; $r = 2$ if $q_{i,k}^r \in Ev_k$. In $q_{i,k}^r$ we have: $i = 1, \dots, N; k = 1, \dots, p; r = 1, 2$.

(4) For each individual key variable the expert team assesses the relative importance, \tilde{I}_i , for the

case, as well as the uncertainty associated with each key variable, \tilde{U}_i , in terms of fuzzy

intervals of the type $\tilde{X} = \left(\begin{matrix} \varepsilon & 1 & -1 & -\varepsilon \\ x & x & x & x \\ -i & -i & i & i \end{matrix} \right)^\varepsilon$ within the closed interval $[1, 10]$ for x . The lower

bounds for acceptance are defined with fuzzy intervals of the same type (e.g., for

uncertainty $\tilde{L}_U = \left(\begin{matrix} \varepsilon & 1 & -1 & -\varepsilon \\ l & l & l & l \\ -i & -i & i & i \end{matrix} \right)^\varepsilon$). The expert team pre-selects all key variables with a relative

importance \tilde{I}_i that exceeds \tilde{L}_i and for the associated uncertainty \tilde{U}_i . To account for the

relative importance of each individual key variable on the entire system studied, qualitative

and quantitative knowledge integration is essential. The major focus is on the detection of

key variables with high importance, while associated uncertainties are considered to be

small and information demand is low. These key variables are identified and included in the

final set of selected impact factors. With respect to hydrologic hazards, considerable

scientific evidence exists for such variables and the specific information content will directly

be taken into consideration. The interaction between key variables rated with lower and

higher uncertainties has to be discussed within the expert team.

(5) The expert team subsequently constructs the impact matrix, in which mutual impacts

(explain impacts) (exerted influences) between the variables $q_{i,k}$ and $q_{j,k}$ are rated. These

impacts are expressed in terms of fuzzy intervals. The impact matrix can be formally written

as $IM = \left(\tilde{A}_{i,j} \right), i, j = 1, \dots, N$. To analyze the systemic relations among the selected

indicators, an impact analysis is performed according to Formative Scenario Analysis by

Scholz and Tietje (2002) or the biocybernetic approach of Vester (1988). The group of

experts defines for each pair of indicators the strength of the one-directional impact or influence between them (Wiek and Binder 2005). Activity and passivity for each variable are calculated by means of fuzzy algebra as row and column sums of $\tilde{A}_{i,j}$, respectively. Mean activity and mean passivity is obtained by the (fuzzy) arithmetic mean of the activity and passivity of each key variable. The comparison of the activity of a variable with mean activity, and of the passivity of a variable with mean passivity allows for categorising the variables into active, passive, ambivalent and buffer variables. It is important for congruity to check if the key variables $q_{i,k} \in Ev$ are categorized as passive variables. Conversely for the same congruity reasons key variables $q_{i,k} \in Co$ should not be categorized as passive.

- (6) The group of experts selects on the basis of the results of steps d and e the relevant key variables for the description of the case, namely $\hat{q}_i \in \hat{Q} \subseteq Q, i = 1, \dots, \hat{N}$.
- (7) In a next step, the group of experts defines the levels of each individual key variable, namely $\hat{q}_{i,k}^{r,n_i}$, where $n_i = 1, \dots, \bar{N}_i$. Since the combinatorial number of scenarios is considerably influenced by the number of levels defined for each key variable, impact factors and their levels should be defined parsimoniously (Scholz and Tietje 2002). Each key variable $\hat{q}_{i,k}^r$ has at least two levels ($\bar{N}_i \geq 2$) which have to be discrete and denoted by $\hat{q}_{i,k}^{r,1}, \hat{q}_{i,k}^{r,2}, \dots, \hat{q}_{i,k}^{r,\bar{N}_i}$.
- (8) Formally for each shell a scenario $S_{h,k}$ can be written as a vector $S_{h,k} = (\hat{q}_{1,k}^{r,n_1} \dots \hat{q}_{i,k}^{r,n_i} \dots \hat{q}_{\hat{N}_k,k}^{r,\hat{N}_k})$, where \hat{N}_k is the number of key variables belonging to the considered shell k , and h is a scenario index.
- (9) At this stage a cascading consistency analysis procedure composed of the following steps is proposed: A consistency matrix for the outmost shell ($k=1$) is constructed $CM_k = \tilde{C}(\hat{q}_{i,k}^{r,n_i}, \hat{q}_{j,k}^{r,n_j})$ which contains the consistency ratings in terms of fuzzy intervals $\tilde{C}(\cdot, \cdot)$ for all pairs of levels of all pairs of key variables $\hat{q}_{i,k}^{r,n_i} \leftrightarrow \hat{q}_{j,k}^{r,n_j}$, where $(i, j = 1, \dots, \hat{N}_k, i \neq j, n_i = 1, \dots, \bar{N}_i, n_j = 1, \dots, \bar{N}_j)$.
- (10) For each scenario referring to the shell k a consistency value is calculated as additive measure by means of fuzzy algebra as $\tilde{C}^*(S_{h,k}) = \sum \tilde{C}(\hat{q}_{i,k}^{r,n_i}, \hat{q}_{j,k}^{r,n_j})$ with $i, j = 1, \dots, \hat{N}_k; i \neq j; \hat{q}_{i,k}^{r,n_i}, \hat{q}_{j,k}^{r,n_j} \in S_{h,k}$.
- (11) The scenario selection within the shell k is based conjointly on the consistency value of the scenarios and the difference between them. As proposed by Tietje (2005) the distance

measure is the number of differences between the scenarios

$$d(S_{h_1,k}, S_{h_2,k}) = \sum_{i=1}^{\tilde{N}_k} \begin{cases} 1 & \text{if the key variable level of } \tilde{q}_{i,k}^r(S_{h_1,k}) \neq \tilde{q}_{i,k}^r(S_{h_2,k}) \\ 0 & \text{otherwise} \end{cases}. \text{ The scenarios are}$$

ranked decreasingly according to consistency in an array. The scenario $S_{h_1,k}$ with the highest consistency value is selected from the array and is compared with the second scenario $S_{h_2,k}$.

If $d(S_{h_1,k}, S_{h_2,k})$ is sufficiently high, e.g. $d(S_{h_1,k}, S_{h_2,k}) \geq d^*$, where d^* is a chosen threshold value, then scenario $S_{h_2,k}$ is also selected and becomes the new comparison reference for scenario three, otherwise the third scenario is compared with the first scenario etc. The

selected scenarios with $\tilde{C}^*(S_{h,k}) \geq \tilde{K}(S_{h,k})$, where $\tilde{K}(S_{h,k})$ is a required minimum consistency

according to the expert team, are considered. The obtained scenario structure SIS_k is now refined according to the optimisation procedure outlined under point (2).

- (12) The set of the considered scenarios of the shell k fixes the levels of key variables shared with the shell $k+1$. This is a required robustness condition. The procedural steps from (9) to (12) are repeated for the successive shells.

(B) Optimisation procedure:

The scenarios identified for shell $k=1$ are organized in an updatable scenario information system SIS_k with $k=1, \dots, p$ according to the decision table structure

$$DT_k = \langle U_k, Co_k, Ev_k, V_q, f_q \rangle_{q \in Co_k \cup Ev_k} \text{ introduced in subsection 5.2.1.}$$

A set $Co_k^* \subseteq Co_k$ which is a minimal determining set for Ev_k is identified by means of Rough Sets Data Analysis. If no minimal determining set is found, either the key variables $\tilde{q}_{i,k}^r$ or the key variable level structure $\tilde{q}_{i,k}^{r,n_i}$ have to be adapted and the scenario construction procedure for this shell has to be repeated.

The following definitions are needed to derive the minimal determining set $Co_k^* \subseteq Co_k$:

Definition 1: Equivalence class: For each $Co_k \subseteq Q$ we associate an equivalence relation R_{Co_k} on U . The equivalence classes induced by R_{Co_k} are denoted by U/R_{Co_k} . If $x \in U$, $[x]_{R_{Co_k}}$ is the equivalence class of R_{Co_k} containing x . Suppose that

$U / R_{Co_k} = \{U_1, U_2, \dots, U_n\}$ and $\forall x, y \in U_i, 1 \leq i \leq n$, we have $f_{\bar{q}}(x) = f_{\bar{q}}(y)$ for all $\bar{q} \in Co_k$ or $[x]_{R_{Co_k}} = [y]_{R_{Co_k}}$.

Definition 2: Supposing that $Co_k, Ev_k \subset Q$ we say that Ev_k is dependent on Co_k , written as $Co_k^* \rightarrow Ev_k$, if every class of U / R_{Ev_k} is a union of classes U / R_{Co_k} . In this case $Co_k^* = Co_k$ and is called a minimal determining set for Ev_k .

Definition 3: A set Co_k^* is a minimal determining set for Ev_k , if $Co_k^* \rightarrow Ev_k$ and Ev_k is not dependent on R for all $R \subset Co_k^*$.

In order to measure the degree of dependence of $(Co_k \rightarrow Ev_k)$, a measure of the prediction or approximation quality has been introduced by Düntsch et al. (1997) as follows:

$$\gamma(Co_k \rightarrow Ev_k) = \frac{\sum_{X \in U / R_{Ev_k}} |R_{(Co_k)}X|}{|U|}$$

where $R_{(Co_k)}X$ is the lower approximation of X by Co_k ($R_{(Co_k)}$ -lower approximation), $0 \leq \gamma(Co_k \rightarrow Ev_k) \leq 1$, and $R_{(Co_k)}X = \{x \in U \mid [x]_{R_{Co_k}} \subseteq X\}$. $R_{(Co_k)}X$ is the set of all elements of X that are correctly classified with respect to the attributes in Co_k , and $\gamma(Co_k \rightarrow Ev_k)$ is the ratio of the number of all elements of U / R_{Ev_k} that can be correctly classified based on the variables in Co_k to the total number of elements of U . Larger values $\gamma(Co_k \rightarrow Ev_k)$ indicate enhanced prediction quality. Note that $Co_k \rightarrow Ev_k$ implies $\gamma(Co_k \rightarrow Ev_k) = 1$ and that $\gamma(Co_k \rightarrow Ev_k) \neq 1$ indicates that Ev_k is not dependent on Co_k .

5.3 Model implementation

In this section the model being set up is implemented, based on the case study on selected woody material transport induced hazard scenarios at hydraulic weak points.

Figure 5-4 shows the mental system map ideated by the expert team for the case study being analysed. The group of experts identified two shells suitable for describing the hazard mechanisms related to woody material transport phenomena: (1) the system loading scenario shell ($k=1$) and

(2) the system response scenario shell ($k = 2$). The group of specialised experts identified five perceptors that explain the hazard potential due to woody material transport to be considered in structuring the system loading scenario shell: (a) recruitment volumes from hill slopes, (b) in-stream recruitment volumes, (c) reachability of the considered critical stream configuration, (d) severity of woody material transport conditions at the considered configuration and (e) woody material system loading severity at the considered configuration.

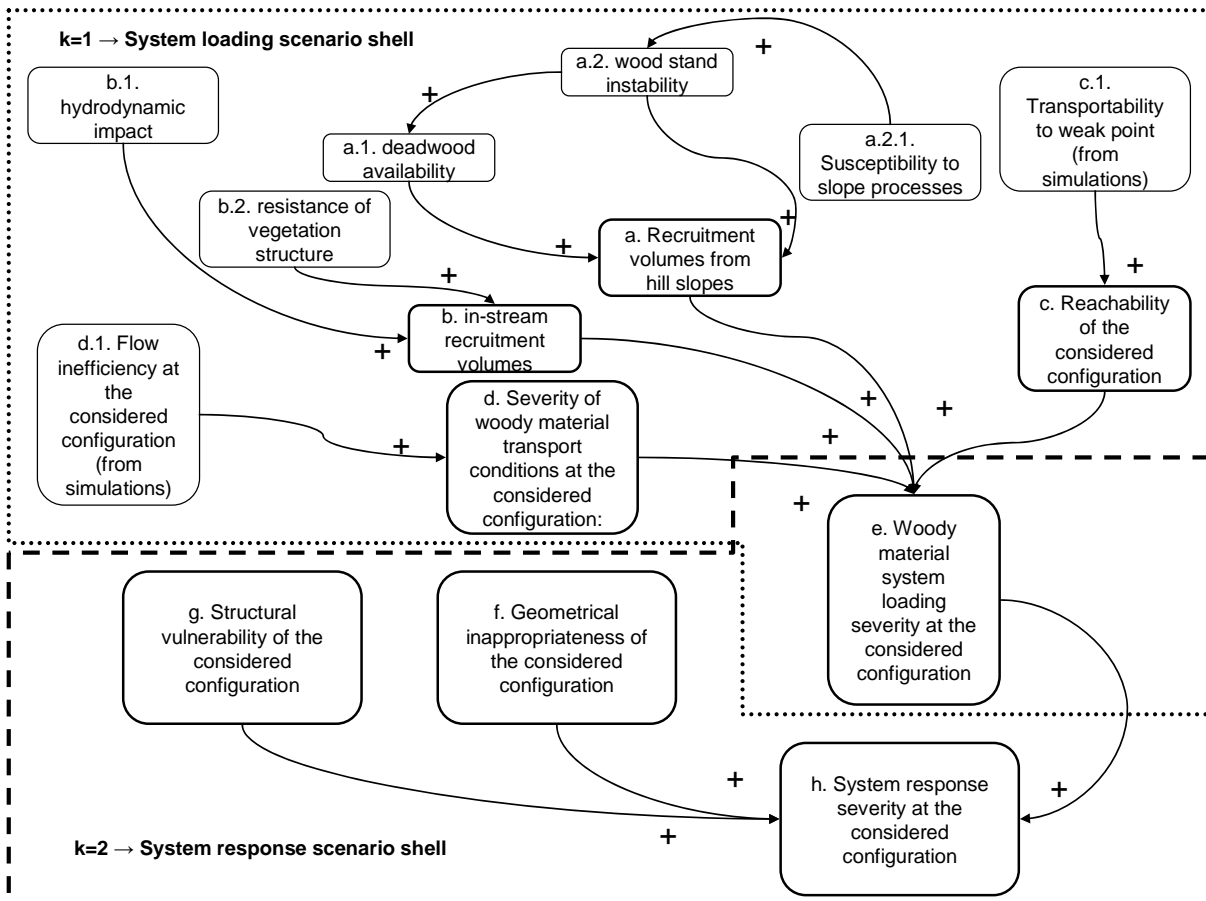


Figure 5-4. Mental system map for the case study on woody material transport hazards.

In a next step, in addition to (e) identified as a common perceptor, the group of experts identified three receptors necessary to describe the interaction of the transported woody material at hydraulic weak points and the possible consequences (system response scenario shell): (f) geometrical inappropriateness of the considered configuration, (g) structural vulnerability of the considered configuration and (h) system response severity at the considered configuration.

As can be seen from the following description of the system loading and the system response scenario shells, this woody material hazard assessment framework is at the same time multi-

instrumental and multi-expert based, involving computational modelling steps and expert knowledge elicitation phases.

In the following paragraph, a detailed description of the perceptors of the system loading scenario shell is given (upper part of Figure 5-4).

As shown by Figure 5-4 the experts subdivided the recruitment process in (a) recruitment from hill slopes and (b) in-stream recruitment. In accordance to the findings of Rickli and Bucher (2006) woody material recruitment volumes from hill slopes were judged to depend mainly on deadwood availability (a.1) and on wood stand stability (a.2). The susceptibility to slope processes (a.2.1) (e.g. landslides) was judged to exert an influence either on deadwood availability or on wood stand stability. In the expert opinion in-stream recruitment (b) could be estimated according to a conceptual framework proposed by Mazzorana et al. (in press). The in-stream recruitment volumes depend on the hydrodynamic impact forces (b.1) on in-stream vegetation and (b.2) on the resistance of vegetation exposed to those impacts. Flow conditions that assure a sufficient hydraulic connectivity between the woody material recruitment areas and the hydraulic weak point are required to satisfy the reachability condition (c). Calculations of the transportability (c.1) of woody material based on a computational procedure (Mazzorana et al. in press) were judged to be an important prerequisite. The flow conditions at the weak point (liquid and woody material transport) contribute substantially in determining the system loading at the considered configuration (hydraulic loading). The severity of these flow conditions (d) can be estimated by detecting flow inefficiencies (d.1). Woody material transport induced system loading severity (e) was identified as a suitable descriptor of possible consequences of woody material transport dynamics at the considered configuration.

In the following paragraph, a detailed description of the perceptors of the system response scenario shell is given (lower part of Figure 5-4).

The group of experts agreed on assigning to woody material transport induced system loading severity (e) a relevant role as perceptor also for the system response scenario shell. The geometrical inappropriateness (f) is another important perceptor identified by the pool of experts and indicates the propensity of woody material entrapment and subsequent decrease of the available flow section for conveyance and the closely related accentuation of hydrostatic and hydrodynamic pressures. These accentuated pressure loads are particularly severe if spanning blockage phenomena induced by cross-section wide woody material accumulations occur. Moreover the expert pool underlined the importance of assessing properly the structural vulnerability (g) of the in-stream structures at the critical configuration in order to draw a complete spectrum of conclusions about system response severity (h).

5.3.1 Initial set of key variables

According to the first procedural step of Formative Scenario Analysis and as a result of the mental system map for the case study, possible relevant key variables $q_{i,k}^r, i = 1, \dots, N, r = 1, 2, k = 1, 2$ significantly influencing the current state of the system and the system dynamics were identified (see Table 5-1).

Key variable	Shell	Perceptor	Name	Description
$\hat{q}_{1,1}^1$	System loading shell	(a) Recruitment volumes from hill slopes	RPH	Recruitment propensity from hill slopes. Estimates are externally provided through computational modelling (Mazzorana et al. 2009). The computational procedure takes into consideration the following parameters: wood stand instability, susceptibility to slope processes and deadwood availability
$q_{2,1}^1$	System loading shell	(b) In-stream recruitment volumes	IRP	In-stream recruitment propensity . Estimates are externally provided through computational modelling (Mazzorana et al. 2009). The computational procedure takes into the intensity of the flood processes and the resistance of the vegetation structures within the wetted perimeter of the flood
$q_{3,1}^1$	System loading shell	(c) Reachability of the critical configuration	WTC	Woody material transport cost (transportability) to reach the critical configuration. Estimates are externally provided through computational modelling (Mazzorana et al. in press). The transportability depends primarily on existing hydrodynamic conditions, given considered stream geometry, and on the woody material characteristics, which can be suitably described through the parameters design log length (Diehl 1997) and design log diameter.
$q_{4,1}^1$	System loading shell	(d) Severity of woody material transport conditions at the considered configuration	PWD	Potential woody material distribution at the considered configuration. Diehl (1997) proposes a structured expert based procedure to assess this parameter. Knowing the design log characteristics and characteristics of the flow the experts suggest hypotheses about the spatial distribution of the woody material volumes potentially approaching the critical configuration

Table 5-1. Possible key variables for the case study on woody debris transport hazards.

Key variable	Shell	Perceptor	Name	Description
$q_{5,1}^2 \vee q_{1,2}^1$	System loading shell and system response shell	(e) Woody material system loading severity	WSL	Woody material system loading severity. On the basis of the overall picture of the system loading conditions the level of the system loading severity is deduced
$q_{2,2}^1$	System response shell	(f) Geometrical inappropriateness of the considered configuration	WEP	Woody material entrapment propensity. Here the experts judge the propensity of woody material being entrapped as a consequence of the interaction with certain geometrical features and components of in-stream structures. Practical indications have been provided by Diehl (1997) and Lange et al. (2006)
$q_{3,2}^1$	System response shell	(f) Geometrical inappropriateness of the considered configuration	BR	Blockage ratio. Here the experts judge possible cross-sectional blockage configurations on the basis of its geometry and the woody material characteristics (i.e. design log length)
$q_{3,2}^1$	System response shell	(g) Structural vulnerability of the considered configuration	SCP	System change propensity. The experts assess this parameter on the basis of the vulnerability of the structural components of the in-stream structures and the possible erosion of the streambed and banks. Stable channel design computations (USACE 2008) are of great advantage.
$q_{4,2}^2$	System response shell	(h) System response severity at the considered configuration	SRS	System response severity. On the basis of the overall picture of the system loading and response conditions the level of the system response severity is deduced

Table 5-1. Possible key variables for the case study on woody debris transport hazards (continued).

5.3.2 Rating of key variables

O'Brien and Dyson (2007) pointed out criteria for selecting the key factors that will form the structure of the scenarios, i.e. the level of uncertainty in quantifying key variables, and the associated level of importance of the variable for the system. The group of specialised experts

assessed the relative importance \tilde{I} for each key variable on the system, the uncertainty associated with each key variable \tilde{U} and the lower bounds of acceptance \tilde{L}_I and \tilde{L}_U (cf. Table 5-2).

5.3.2.1 Uncertainty versus importance matrices

The experts constructed two distinct uncertainty versus importance matrices, one for the key variables of the system loading scenario shell (Table 5-2) and one for the key variables of the system response scenario shell (Table 5-3). While on the system loading side the relevance of the key variables RPH, IRP, WTC and WSL were fixed, the relevance of variable PWD has been acknowledged after a reconsideration step. On the system response side, the relevance of variable WEP has been extensively discussed. Some experts argued that the variable BR indirectly depends on WEP. The final decision was to not discard the variable WEP.

Fuzzy evaluation: Uncertainty vs. importance										
	\tilde{L}_U				\tilde{L}_I					
	Uncertainty margins of acceptance				Importance margin of acceptance				Acceptance evaluation	
	3	3.5	4.5	5	3	3.5	4.5	5		
	\tilde{U}				\tilde{I}				$\tilde{U} \geq \tilde{L}_U \rightarrow ok$	$\tilde{I} \geq \tilde{L}_I \rightarrow ok$
Key Variable	Uncertainty evaluation				Importance evaluation				Uncertainty constraints	Importance constraints
RPH	5	6	7	8	8.5	9	9.5	10	OK	OK
IRP	6	6.5	7	9	4	5	6	7	OK	OK
WTC	5	5.5	6	7	8	8.5	9	9.5	OK	OK
PWD	3	3.5	4.5	5	7	7.5	8	8.5	Re-discussion → OK	OK
WSL	8	9	9	9	6	7	8	9	OK	OK

Table 5-2. Importance and uncertainty levels for each variable of the system loading shell in relation to the acceptance levels.

Fuzzy evaluation: Uncertainty vs. importance										
	\tilde{L}_U				\tilde{L}_I					
	Uncertainty margins of acceptance				Importance margin of acceptance				Acceptance evaluation	
	3	3.5	4.5	5	3	3.5	4.5	5		
	\tilde{U}				\tilde{I}				$\tilde{U} \geq \tilde{L}_U \rightarrow ok$	$\tilde{I} \geq \tilde{L}_I \rightarrow ok$
Key Variable	Uncertainty evaluation				Importance evaluation				Uncertainty constraints	Importance constraints
WSL	5	6	7	8	8.5	9	9.5	10	OK	OK
WEP	6	6.5	7	9	3	4	4.5	5	OK	Re-discussion → OK
BR	5	5.5	6	7	8	8.5	9	9.5	OK	OK
SCP	3	3.5	4.5	5	7	7.5	8	8.5	OK	OK
SRS	8	9	9	9	6	7	8	9	OK	OK

Table 5-3. Importance and uncertainty levels for each variable of the system response shell in relation to the acceptance levels.

5.3.2.2 Construction of impact matrices

The next step consisted in the construction of the impact matrix for the pre-selected variables of the system loading and the system response shell in accordance to the following matrix structure:

	1	..	N	$\tilde{A}_{i,\cdot}$	$\tilde{A}_{i,\cdot} / \tilde{A}_{i,j}$
1	$\tilde{A}_{1,1}$..	$\tilde{A}_{1,N}$	$\sum_{j=1}^N \tilde{A}_{1,j}$	$\tilde{A}_{1,\cdot} / \tilde{A}_{1,1}$
..
N	$\tilde{A}_{N,1}$..	$\tilde{A}_{N,N}$	$\sum_{j=1}^N \tilde{A}_{N,j}$	$\tilde{A}_{N,\cdot} / \tilde{A}_{N,N}$
$\tilde{A}_{\cdot,j}$	$\sum_{i=1}^N \tilde{A}_{i,1}$..	$\sum_{i=1}^N \tilde{A}_{i,1}$	$\tilde{A}_{\cdot,\cdot} = \sum_{i=1}^N \sum_{j=1}^N \tilde{A}_{i,j}$	
$\tilde{A}_{\cdot,j} * \tilde{A}_{j,\cdot}$	$\tilde{A}_{\cdot,1} * \tilde{A}_{1,\cdot}$..	$\tilde{A}_{\cdot,N} * \tilde{A}_{N,\cdot}$		

where the symbols $\sum_{j=1}^N$ and $\sum_{i=1}^N$ represent the fuzzy algebraic sum operation \oplus of two or more fuzzy intervals, $\tilde{A}_{i,j} * \tilde{A}_{j,i}$ represent the fuzzy algebraic multiplication operation \otimes and $\frac{\tilde{A}_{i,j}}{\tilde{A}_{j,i}}$ represent the fuzzy division operation \div . The mutual impacts between the variables d_i and d_j were rated according to three fuzzy impact levels $(\tilde{L}_{IMPACT}; \tilde{M}_{IMPACT}; \tilde{H}_{IMPACT})$ as shown in Figure 5-5. Taking Medium impact as an example the fuzzy interval is written as $\tilde{M}_{IMPACT} = (0.5, 1.0, 1.5, 2.0)^e$. The underlying impact matrix of the system loading shell is shown in Table 5-4 and the impact matrix of the system response shell is shown in Table 5-5.

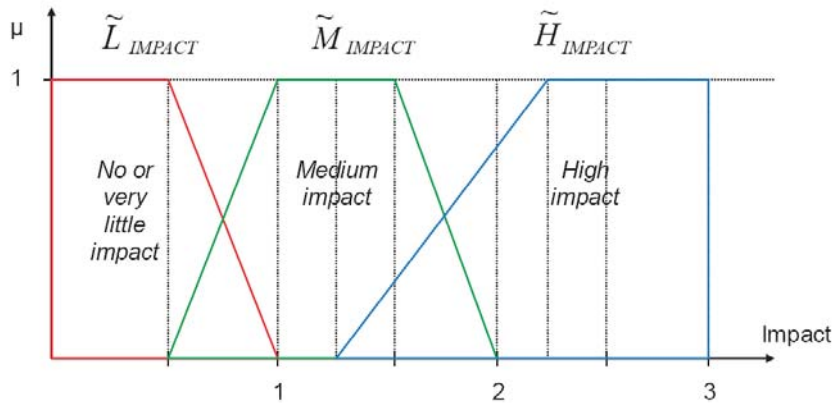


Figure 5-5: Impact levels between variables.

The results of the impact analyses led to the conclusion that the congruity of the choice of the key variables is satisfactory. As expected in the system loading cell RPH, IRP and WTC are clearly active variables, while WSL is passive. As supposed, the role of WSL in the system response shell turns out to be active. SRS logically is passive. A crucial role is expected to be played by the ambivalent key variables, namely WEP, BR and SCP. Hence, the expert team decided to retain both the current shell structure and the pre-selected key variables.

	RPH				IRP				WTC				PWD				WSL				Activity				Mean activity			
RPH	0.00	0.00	0.00	0.00	0.00	0.00	0.50	1.00	0.50	1.00	1.50	2.00	0.00	0.00	0.50	1.00	1.25	2.25	3.00	3.00	1.75	3.25	5.50	7.00	1.45	2.75	4.90	6.60
IRP	0.00	0.00	0.50	1.00	0.00	0.00	0.00	0.00	0.50	1.00	1.50	2.00	0.50	1.00	1.50	2.00	1.25	2.25	3.00	3.00	2.25	4.25	6.50	8.00				
WTC	0.00	0.00	0.50	1.00	0.50	1.00	1.50	2.00	0.00	0.00	0.00	0.00	0.50	1.00	1.50	2.00	1.25	2.25	3.00	3.00	2.25	4.25	6.50	8.00				
PWD	0.00	0.00	0.50	1.00	0.50	1.00	1.50	2.00	0.00	0.00	0.50	1.00	0.00	0.00	0.00	0.00	0.50	1.00	1.50	2.00	1.00	2.00	4.00	6.00				
WSL	0.00	0.00	0.50	1.00	0.00	0.00	0.50	1.00	0.00	0.00	0.50	1.00	0.00	0.00	0.50	1.00	0.00	0.00	0.00	0.00	0.00	0.00	2.00	4.00				
Passivity	0.00	0.00	2.00	4.00	1.00	2.00	4.00	6.00	1.00	2.00	4.00	6.00	1.00	2.00	4.00	6.00	4.25	7.75	10.50	11.00								
Mean passivity																												
	1.45	2.75	4.90	6.60																								

RPH	1.00	0.00	active
IRP	1.00	0.00	active
WTC	1.00	0.00	active
PWD	0.00	0.00	buffer
WSL	0.00	1.00	passive

Table 5-4. Impact matrix for the key variables belonging to the system loading shell and characterisation of the key variables either as active, passive, buffer or ambivalent variables

	WSL				WEP				BR				SCP				SRS				Activity				Mean activity			
WSL	0.00	0.00	0.00	0.00	0.50	1.00	1.50	2.00	0.50	1.00	1.50	2.00	0.50	1.00	1.50	2.00	0.50	1.00	1.50	2.00	2.00	4.00	6.00	8.00	2.00	3.88	6.00	7.60
WEP	0.00	0.10	0.50	1.00	0.00	0.00	0.00	0.00	1.25	2.25	3.00	3.00	0.50	1.00	1.50	2.00	1.25	2.25	3.00	3.00	3.00	5.60	8.00	9.00				
BR	0.00	0.10	0.50	1.00	0.50	1.00	1.50	2.00	0.00	0.00	0.00	0.00	1.25	2.25	3.00	3.00	0.50	1.00	1.50	2.00	2.25	4.35	6.50	8.00				
SCP	0.00	0.10	0.50	1.00	0.50	1.00	1.50	2.00	0.50	1.00	1.50	2.00	0.00	0.00	0.00	0.00	1.25	2.25	3.00	3.00	2.25	4.35	6.50	8.00				
SRS	0.00	0.10	0.50	1.00	0.50	1.00	1.50	2.00	0.00	0.00	0.50	1.00	0.00	0.00	0.50	1.00	0.00	0.00	0.00	0.00	0.50	1.10	3.00	5.00				
Passivity	0.00	0.40	2.00	4.00	2.00	4.00	6.00	8.00	2.25	4.25	6.50	8.00	2.25	4.25	6.50	8.00	3.50	6.50	9.00	10.00								
Mean passivity																												
	2.00	3.88	6.00	7.60																								

WSL	1.00	0.00	active
WEP	1.00	1.00	ambivalent
BR	1.00	1.00	ambivalent
SCP	1.00	1.00	ambivalent
SRS	0.00	1.00	passive

Table 5-5. Impact matrix for the key variables belonging to the system response shell and characterisation of the key variables either as active, passive, buffer or ambivalent variables.

5.3.3 Definition of the level of each key variable

The subsequent step consisted in defining the impact levels $\widehat{q}_{i,k}^{r,1}, \widehat{q}_{i,k}^{r,2}, \dots, \widehat{q}_{i,k}^{r,N_i}$ for each key variable $\widehat{q}_{i,k}^r$ (see Table 5-6).

Name	Description	Impact levels defined	
RPH	Recruitment propensity from hill slopes	$q_{1,1}^{1,1}$	Low or negligible recruitment propensity from hill slopes. Fragmentary wood buffer along the stream positioned far away from the critical configuration.
		$q_{1,1}^{1,2}$	Medium recruitment propensity from hill slopes. Continuous wood buffer along the stream, relatively stable wood structure.
		$q_{1,1}^{1,3}$	High recruitment propensity from hill slopes. Continuous wood buffer along the stream, relatively unstable due to lateral erosion processes; and isolated and rather infrequent hill slope processes.
		$q_{1,1}^{1,4}$	Very high recruitment propensity from hill slopes. Continuous wood buffer along the stream, unstable due to lateral erosion and extended and frequent hill slope processes.
IRP	In-stream recruitment propensity	$q_{2,1}^{1,1}$	Low in-stream recruitment propensity. Small in-stream woody vegetation volumes, rather flexible structure.
		$q_{2,1}^{1,2}$	Medium in-stream recruitment propensity. Larger in-stream woody vegetation volumes, structures rather inflexible; movable stream bed during high floods.
		$q_{2,1}^{1,3}$	High in-stream recruitment propensity. Large in-stream woody vegetation volumes; inflexible, movable stream bed and high erosion rates during high floods.

Table 5-6: Impact level definition for each key variable

Name	Description	Impact levels defined	
WTC	Woody material transport cost (transportability) to reach the critical configuration	$q_{3,1}^{1,1}$	Low transportability or high woody debris roughness. Highly curved stream, small water depths with respect to the design wood log diameters, narrow channel widths with respect to the design wood log lengths.
		$q_{3,1}^{1,2}$	Medium transportability or medium woody debris roughness. Rather straight-lined stream, occasionally narrow water depths with respect to the design wood log diameters, occasionally narrow channel widths with respect to the design wood log lengths.
		$q_{3,1}^{1,3}$	High transportability or low woody debris roughness. Straight lined stream. Large water depths with respect to the design wood log diameters, large channel widths with respect to the design wood log lengths.

Table 5-6: Impact level definition for each key variable (continued)

Name	Description	Impact levels defined	
PWD	Potential woody material distribution at the considered configuration	$q_{4,1}^{1,1}$	Rather favourable potential distribution. Woody material is presumed to be transported in a small part of the flow section and the orientations of the woody material logs is supposed parallel to the flow direction.
		$q_{4,1}^{1,2}$	Rather unfavourable potential distribution. Woody material is presumed not to be restricted to a small part of the flow section and the orientations of the woody material logs are randomly distributed with respect to the flow direction.
		$q_{4,1}^{1,3}$	Extremely unfavourable potential distribution. Woody material is presumed to be transported throughout the flow section and the orientations of the woody material logs are randomly distributed with respect to the flow direction.
WSL	Woody material system loading severity	$q_{5,1}^{2,1} \vee q_{1,2}^{1,1}$	Low or negligible woody material system loading severity. This is an impact level of a key variable classified as an evolutionary factor (shell $k = 1$).
		$q_{5,1}^{2,2} \vee q_{1,2}^{1,2}$	Medium woody material system loading severity. This is an impact level of a key variable classified as an evolutionary factor (shell $k = 1$).
		$q_{5,1}^{2,3} \vee q_{1,2}^{1,3}$	High woody material system loading severity. This is an impact level of a key variable classified as an evolutionary factor (shell $k = 1$).

Table 5-6: Impact level definition for each key variable (continued)

WEP	Woody material entrapment propensity	$q_{2,2}^{1,1}$	Low or negligible woody material entrapment propensity. Interference between the potentially transported woody material and the geometrical features is unlikely (no piers, no protruding abutments, sufficient flow section).
		$q_{2,2}^{1,2}$	Medium woody material entrapment propensity. Interference between the potentially transported woody material and the geometrical features is likely but large accumulations of woody material are unlikely (max. single pier accumulations, sufficient flow section).
		$q_{2,2}^{1,3}$	High woody material entrapment propensity. Interference between the potentially transported woody material and the geometrical features is likely. Large accumulations of woody material are possible (single pier and spanning blockage accumulations, insufficient flow section).
BR	Blockage ratio	$q_{3,2}^{1,1}$	Low or negligible blockage ratio.
		$q_{3,2}^{1,2}$	Medium blockage ratio.
		$q_{3,2}^{1,3}$	High blockage ratio.

Table 5-6: Impact level definition for each key variable (continued)

SCP	System change propensity	$q_{4,2}^{1,1}$	Low or negligible system change propensity. The vulnerability of the components of the critical configuration is low: Either the in-stream structures or the flow confining structures are structurally reliable.
		$q_{4,2}^{1,2}$	Medium system change propensity. The vulnerability of the components of the critical configuration is medium: The reliability of either the in-stream structures or the flow confining structures is medium. Increasing damage with increasing system loading conditions is likely.
		$q_{4,2}^{1,3}$	High system change propensity. The vulnerability of the components of the critical configuration is low: The reliability of either the in-stream structures or the flow confining structures is low. Sudden collapses cannot be excluded.
SRS	System response severity	$q_{5,2}^{2,1}$	Low or negligible system response severity. Low or negligible structural damage. Floodplain inundation processes not induced by system responses at the critical configuration.
		$q_{5,2}^{2,2}$	Medium system response severity. Increasing damages with increasing system loading conditions are likely.
		$q_{5,2}^{2,3}$	High system response severity either in terms of damage to the in-stream structures or to the flow confining structures. Significant damage with medium system loading severity is possible. Consequences also in terms of subsequent floodplain inundation processes.

Table 5-6: Impact level definition for each key variable (continued)

5.3.4 Consistency matrix, scenario construction and selection for the system loading shell

In order to construct the consistency matrix, the expert team started the cascading consistency analysis procedure for the outmost shell ($k = 1$). The consistency ratings $CM_k = \tilde{C}(\hat{q}_{i,k}^{r,n_i}, \hat{q}_{j,k}^{r,n_j})$ for each pair of impact levels (cf. Table 5-6) of different key variables $\hat{q}_{i,k}^{r,n_i} \leftrightarrow \hat{q}_{j,k}^{r,n_j}$ were assigned, with $(i, j = 1, \dots, \hat{N}_k, i \neq j, n_i = 1, \dots, \bar{N}_i, n_j = 1, \dots, \bar{N}_j)$, in terms of fuzzy intervals $\tilde{C}(\cdot, \cdot)$, see Figure 5-6.

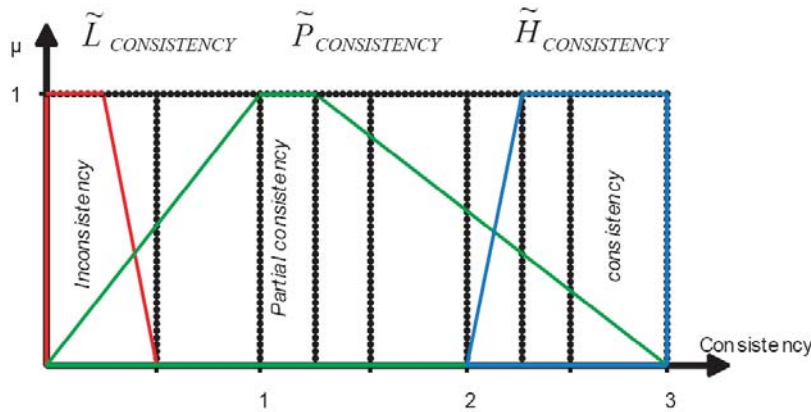


Figure 5-6: Fuzzy intervals for consistency rating

Taking $(\hat{q}_{1,1}^{1,3}, \hat{q}_{4,1}^{1,2})$ as an example, rated consistency between pairs of impact levels of different key variables $(\hat{q}_{i,1}^{r,n_i}, \hat{q}_{j,1}^{r,n_j})$ was identified by the fuzzy interval $\tilde{P}_{CONSISTENCY} = (0.0, 1.0, 1.25, 3.0)^{\mathcal{F}}$.

The result was the consistency matrix $CM_1 = \tilde{C}(\hat{q}_{i,1}^{r,n_i}, \hat{q}_{j,1}^{r,n_j})$ containing all consistency ratings between pairs of impact levels of different key variables, as shown in Table 5-7.

Name Description		Name	RPH				IRP			WTC			PWD		
		Impact levels	$q_{1,1}^{1,1}$	$q_{1,1}^{1,2}$	$q_{1,1}^{1,3}$	$q_{1,1}^{1,4}$	$q_{2,1}^{1,2}$	$q_{2,1}^{1,2}$	$q_{2,1}^{1,3}$	$q_{3,1}^{1,1}$	$q_{3,1}^{1,2}$	$q_{3,1}^{1,3}$	$q_{4,1}^{1,1}$	$q_{4,1}^{1,2}$	$q_{4,1}^{1,3}$
RPH	Recruitment propensity from hill slopes	$q_{1,1}^{1,1}$													
		$q_{1,1}^{1,2}$													
		$q_{1,1}^{1,3}$													
		$q_{1,1}^{1,4}$													
IRP	In-stream recruitment propensity	$q_{2,1}^{1,1}$	\tilde{P}	\tilde{P}	\tilde{P}	\tilde{L}									
		$q_{2,1}^{1,2}$	\tilde{P}	\tilde{L}	\tilde{L}	\tilde{P}									
		$q_{2,1}^{1,3}$	\tilde{L}	\tilde{P}	\tilde{P}	\tilde{P}									
WTC	Woody material transport cost to reach the critical configuration	$q_{3,1}^{1,1}$	\tilde{P}	\tilde{P}	\tilde{P}	\tilde{L}	\tilde{H}	\tilde{H}	\tilde{L}						
		$q_{3,1}^{1,2}$	\tilde{P}	\tilde{P}	\tilde{P}	\tilde{P}	\tilde{H}	\tilde{P}	\tilde{H}						
		$q_{3,1}^{1,3}$	\tilde{L}	\tilde{P}	\tilde{P}	\tilde{P}	\tilde{L}	\tilde{H}	\tilde{H}						
PWD	Potential woody material distribution at the considered configuration	$q_{4,1}^{1,1}$	\tilde{H}	\tilde{P}	\tilde{P}	\tilde{L}	\tilde{H}	\tilde{P}	\tilde{P}	\tilde{H}	\tilde{P}	\tilde{P}			
		$q_{4,1}^{1,2}$	\tilde{P}												
		$q_{4,1}^{1,3}$	\tilde{L}	\tilde{P}	\tilde{P}	\tilde{H}	\tilde{P}	\tilde{P}	\tilde{H}	\tilde{P}	\tilde{P}	\tilde{H}			
WSL	Woody material system loading severity	$q_{5,1}^{2,1} \vee q_{1,2}^{1,1}$	\tilde{H}	\tilde{P}	\tilde{L}	\tilde{L}	\tilde{H}	\tilde{P}	\tilde{L}	\tilde{H}	\tilde{P}	\tilde{L}	\tilde{H}	\tilde{P}	\tilde{L}
		$q_{5,1}^{2,2} \vee q_{1,2}^{1,2}$	\tilde{P}	\tilde{L}	\tilde{L}	\tilde{P}									
		$q_{5,1}^{2,3} \vee q_{1,2}^{1,3}$	\tilde{L}	\tilde{L}	\tilde{P}	\tilde{H}									

Table 5-7: Consistency matrix for the scenario shell $k = 1$: \tilde{L} = inconsistency; \tilde{P} = partial consistency; \tilde{H} = high consistency

At this stage for each scenario referring to the shell $k = 1$ a consistency value was calculated as

additive value by means of fuzzy algebra as $\tilde{C}^*(S_{h,1}) = \sum \tilde{C}(\tilde{q}_{i,1}^{r,n_i}, \tilde{q}_{j,1}^{r,n_j})$ with

$i, j = 1, \dots, \hat{N}_1$; $i \neq j$; $\tilde{q}_{i,1}^{r,n_i}, \tilde{q}_{j,1}^{r,n_j} \in S_{h,1}$. Taking as an example the scenario

$q_{1,1}^{1,1} \wedge q_{2,1}^{1,1} \wedge q_{3,1}^{1,1} \wedge q_{4,1}^{1,2} \wedge (q_{5,1}^{2,1} \vee q_{1,2}^{1,1})$ the additive consistency value is calculated as follows:

$$\begin{aligned} \tilde{C}^*(S_{1,1}) &= \tilde{C}(\tilde{q}_{1,1}^{1,1}, \tilde{q}_{2,1}^{1,1}) \oplus \tilde{C}(\tilde{q}_{2,1}^{1,1}, \tilde{q}_{3,1}^{1,1}) \oplus \tilde{C}(\tilde{q}_{3,1}^{1,1}, \tilde{q}_{4,1}^{1,1}) \oplus \tilde{C}(\tilde{q}_{4,1}^{1,1}, \tilde{q}_{5,1}^{1,1}) \oplus \tilde{C}(\tilde{q}_{1,1}^{1,1}, \tilde{q}_{3,1}^{1,1}) \oplus \tilde{C}(\tilde{q}_{1,1}^{1,1}, \tilde{q}_{4,1}^{1,1}) \oplus \tilde{C}(\tilde{q}_{1,1}^{1,1}, \tilde{q}_{5,1}^{1,1}) \oplus \\ &\tilde{C}(\tilde{q}_{2,1}^{1,1}, \tilde{q}_{4,1}^{1,1}) \oplus \tilde{C}(\tilde{q}_{2,1}^{1,1}, \tilde{q}_{5,1}^{1,1}) \oplus \tilde{C}(\tilde{q}_{3,1}^{1,1}, \tilde{q}_{5,1}^{1,1}) = \tilde{P} \oplus \tilde{H} \oplus \tilde{H} \oplus \tilde{H} \oplus \tilde{P} \oplus \tilde{H} = (16.0, 20.0, 26.5, 30.0)^{\epsilon} \end{aligned}$$

The respective summands are highlighted in yellow colours in Table 5-7.

The consistency of and distance criteria between scenarios allowed to select twelve scenarios,

with $\tilde{C}^*(S_{h,k}) \geq \tilde{K}(S_{h,k})$, as shown and highlighted in Table 5-8 by numbers.

		$q_{5,1}^{2,1}$	$q_{5,1}^{2,2}$	$q_{5,1}^{2,2}$	$q_{5,1}^{2,2}$	$q_{5,1}^{2,2}$											
		$q_{4,1}^{1,1}$	$q_{4,1}^{1,2}$	$q_{4,1}^{1,2}$	$q_{4,1}^{1,2}$	$q_{4,1}^{1,2}$	$q_{4,1}^{1,1}$	$q_{4,1}^{1,1}$	$q_{4,1}^{1,1}$	$q_{4,1}^{1,1}$							
		$q_{3,1}^{1,1}$	$q_{3,1}^{1,1}$	$q_{3,1}^{1,1}$	$q_{3,1}^{1,1}$	$q_{3,1}^{1,2}$	$q_{3,1}^{1,2}$	$q_{3,1}^{1,2}$	$q_{3,1}^{1,2}$	$q_{3,1}^{1,1}$	$q_{3,1}^{1,1}$	$q_{3,1}^{1,1}$	$q_{3,1}^{1,1}$	$q_{3,1}^{1,2}$	$q_{3,1}^{1,2}$	$q_{3,1}^{1,2}$	$q_{3,1}^{1,2}$
$q_{1,1}^{1,1}$	$q_{2,1}^{1,1}$	16.0	20.0	26.5	30.0					8.0	15.0	19.5	30.0	6.0	13.8	17.8	30.0
$q_{1,1}^{1,2}$	$q_{2,1}^{1,1}$	12.0	17.5	23.0	30.0	8.0	15.0	19.5	30.0								
$q_{1,1}^{1,1}$	$q_{2,1}^{1,2}$	12.0	17.5	23.0	30.0												
		$q_{5,1}^{2,3}$															
		$q_{4,1}^{1,3}$	$q_{4,1}^{1,3}$	$q_{4,1}^{1,3}$	$q_{4,1}^{1,3}$	$q_{4,1}^{1,2}$	$q_{4,1}^{1,2}$	$q_{4,1}^{1,2}$	$q_{4,1}^{1,2}$	$q_{4,1}^{1,3}$	$q_{4,1}^{1,3}$	$q_{4,1}^{1,3}$	$q_{4,1}^{1,3}$				
		$q_{3,1}^{1,2}$	$q_{3,1}^{1,2}$	$q_{3,1}^{1,2}$	$q_{3,1}^{1,2}$	$q_{3,1}^{1,3}$											
$q_{1,1}^{1,4}$	$q_{2,1}^{1,2}$									12.0	17.5	23.0	30.0				
$q_{1,1}^{1,3}$	$q_{2,1}^{1,3}$	8.0	15.0	19.5	30.0					12.0	17.5	23.0	30.0				
$q_{1,1}^{1,4}$	$q_{2,1}^{1,3}$	12.0	17.5	23.0	30.0	8.0	15.0	19.5	30.0	16	20	26.5	30				

Table 5-8: Possible scenarios with corresponding additive consistency values

In a subsequent step, the scenarios identified for shell $k = 1$ were organized in a scenario information

system SIS_k with $k = 1$ according to the decision table structure $DT_k = \langle U_k, Co_k, Ev_k, V_q, f_q \rangle_{q \in Co_k \cup Ev_k}$

(Table 5-9).

NR	RPH				IRP			WTC			PWD			WSL
	$q_{1,1}^{1,1}$	$q_{1,1}^{1,2}$	$q_{1,1}^{1,3}$	$q_{1,1}^{1,4}$	$q_{2,1}^{1,2}$	$q_{2,1}^{1,2}$	$q_{2,1}^{1,3}$	$q_{3,1}^{1,1}$	$q_{3,1}^{1,2}$	$q_{3,1}^{1,3}$	$q_{4,1}^{1,1}$	$q_{4,1}^{1,2}$	$q_{4,1}^{1,3}$	$q_{5,1}^{2,1} \vee q_{5,1}^{2,2} \vee q_{5,1}^{2,3}$
1	1	0	0	0	1	0	0	1	0	0	1	0	0	1
2	1	0	0	0	1	0	0	1	0	0	0	1	0	1
3	1	0	0	0	1	0	0	0	1	0	1	0	0	2
4	0	1	0	0	1	0	0	1	0	0	1	0	0	1
5	0	1	0	0	1	0	0	0	1	0	1	0	0	1
6	1	0	0	0	0	1	0	1	0	0	1	0	0	1
7	0	0	0	1	0	1	0	0	0	1	0	0	1	3
8	0	0	1	0	0	0	1	0	1	0	0	0	1	3
9	0	0	1	0	0	0	1	0	0	1	0	0	1	3
10	0	0	0	1	0	0	1	0	1	0	0	0	1	3
11	0	0	0	1	0	0	1	0	0	1	0	1	0	3
12	0	0	0	1	0	0	1	0	0	1	0	0	1	3

Table 5-9: Scenario information system SIS_k with $k = 1$ represented as a decision table.

Definition of equivalence classes $U / R_{C_{o_1}}$:

$$U / R_{RPH} = \{\{x_1, x_2, x_3, x_6\}, \{x_4, x_5\}, \{x_8, x_9\}, \{x_7, x_{10}, x_{11}, x_{12}\}\}$$

$$U / R_{IRP} = \{\{x_1, x_2, x_3, x_4, x_5\}, \{x_6, x_7\}, \{x_8, x_9, x_{10}, x_{11}, x_{12}\}\}$$

$$U / R_{WTC} = \{\{x_1, x_2, x_4, x_6\}, \{x_3, x_5, x_8, x_{10}\}, \{x_7, x_9, x_{11}, x_{12}\}\}$$

$$U / R_{PWD} = \{\{x_1, x_3, x_4, x_5, x_6\}, \{x_2, x_{11}\}, \{x_7, x_8, x_9, x_{10}, x_{12}\}\}$$

$$U / R_{WSL} = \{\{x_1, x_2, x_4, x_5, x_6\}, \{x_3\}, \{x_7, x_8, x_9, x_{10}, x_{11}, x_{12}\}\}$$

$$(C_{o_k} \rightarrow E_{v_k})$$

$$U / R_{C_{o_1}} = \{\{x_1\}, \{x_2\}, \{x_3\}, \{x_4\}, \{x_5\}, \{x_6\}, \{x_7\}, \{x_8\}, \{x_9\}, \{x_{10}\}, \{x_{11}\}, \{x_{12}\}\}$$

Definition of the lower approximations:

$$\underline{R}_{C_{o_1}} X_1 = \{x_1, x_2, x_4, x_5, x_6\}; \underline{R}_{C_{o_1}} X_2 = \{x_3\}; \underline{R}_{C_{o_1}} X_3 = \{x_7, x_8, x_9, x_{10}, x_{11}, x_{12}\}$$

Calculation of the approximation quality:

$$\gamma(C_{o_k} \rightarrow E_{v_k}) = \frac{\sum_{X \in U / R_{(E_{v_k})}} |R_{(C_{o_k})} X|}{|U|} = 1$$

5.3.5 Consistency matrix, scenario construction and selection for the system response shell

In analogy to the estimations and computations carried out for shell $k=1$, the expert team constructed a consistency matrix for the innermost shell ($k=2$) assigning the consistency ratings $CM_k = \tilde{C}(\hat{q}_{i,k}^{r,n_i}, \hat{q}_{j,k}^{r,n_j})$ for each pair of impact levels (Table 5-10) of different key variables $\hat{q}_{i,k}^{r,n_i} \leftrightarrow \hat{q}_{j,k}^{r,n_j}$, with $(i, j = 1, \dots, \bar{N}_k, i \neq j, n_i = 1, \dots, \bar{N}_i, n_j = 1, \dots, \bar{N}_j)$, in terms of fuzzy intervals $\tilde{C}(\cdot, \cdot)$ (see Figure 5-6).

		Name	WSL			WEP			BR			SCP		
		Impact levels	$q_{1,2}^{1,1}$	$q_{1,2}^{1,2}$	$q_{1,2}^{1,3}$	$q_{2,2}^{1,1}$	$q_{2,2}^{1,2}$	$q_{2,2}^{1,3}$	$q_{3,2}^{1,1}$	$q_{3,2}^{1,2}$	$q_{3,2}^{1,3}$	$q_{4,2}^{1,1}$	$q_{4,2}^{1,2}$	$q_{4,2}^{1,3}$
WSL	Woody material system loading severity	$q_{1,2}^{1,1}$												
		$q_{1,2}^{1,2}$												
		$q_{1,2}^{1,3}$												
WEP	Woody material entrapment propensity	$q_{2,2}^{1,1}$	\tilde{H}	\tilde{P}	\tilde{L}									
		$q_{2,2}^{1,2}$	\tilde{P}	\tilde{P}	\tilde{P}									
		$q_{2,2}^{1,3}$	\tilde{L}	\tilde{P}	\tilde{H}									
BR	Blockage ratio	$q_{3,2}^{1,1}$	\tilde{P}	\tilde{P}	\tilde{L}	\tilde{H}	\tilde{P}	\tilde{L}						
		$q_{3,2}^{1,2}$	\tilde{P}	\tilde{P}	\tilde{P}	\tilde{P}	\tilde{H}	\tilde{P}						
		$q_{3,2}^{1,3}$	\tilde{L}	\tilde{P}	\tilde{P}	\tilde{L}	\tilde{P}	\tilde{H}						
SCP	System change propensity	$q_{4,2}^{1,1}$	\tilde{H}	\tilde{P}	\tilde{L}	\tilde{H}	\tilde{L}	\tilde{L}	\tilde{H}	\tilde{P}	\tilde{L}			
		$q_{4,2}^{1,2}$	\tilde{P}	\tilde{P}	\tilde{P}	\tilde{L}	\tilde{P}	\tilde{L}	\tilde{P}	\tilde{H}	\tilde{P}			
		$q_{4,2}^{1,3}$	\tilde{L}	\tilde{P}	\tilde{H}	\tilde{L}	\tilde{L}	\tilde{H}	\tilde{L}	\tilde{P}	\tilde{H}			
SRS	System response severity	$q_{5,2}^{2,1}$	\tilde{P}	\tilde{L}	\tilde{L}	\tilde{H}	\tilde{L}	\tilde{L}	\tilde{H}	\tilde{P}	\tilde{L}	\tilde{H}	\tilde{P}	\tilde{L}
		$q_{5,2}^{2,2}$	\tilde{L}	\tilde{P}	\tilde{L}	\tilde{L}	\tilde{H}	\tilde{L}	\tilde{P}	\tilde{H}	\tilde{P}	\tilde{P}	\tilde{H}	\tilde{P}
		$q_{5,2}^{2,3}$	\tilde{L}	\tilde{P}	\tilde{P}	\tilde{L}	\tilde{L}	\tilde{H}	\tilde{L}	\tilde{P}	\tilde{H}	\tilde{L}	\tilde{P}	\tilde{H}

Table 5-10: Consistency matrix for the scenario shell $k=2$: \tilde{L} = inconsistency; \tilde{P} = partial consistency; \tilde{H} = high consistency

The respective consistency ratings in terms of additive consistency values are reported in Table 5-11. The consistency of and distance criteria between scenarios allowed to select nine scenarios, with $\tilde{C}^*(S_{h,k}) \geq \tilde{K}(S_{h,k})$, as shown and highlighted in Table 5-11 by numbers.

		$q_{5,2}^{2,1}$											
		$q_{4,2}^{1,1}$	$q_{4,2}^{1,2}$	$q_{4,2}^{1,2}$	$q_{4,2}^{1,2}$	$q_{4,2}^{1,2}$							
		$q_{3,2}^{1,1}$	$q_{3,2}^{1,1}$	$q_{3,2}^{1,1}$	$q_{3,2}^{1,1}$	$q_{3,2}^{1,2}$	$q_{3,2}^{1,2}$	$q_{3,2}^{1,2}$	$q_{3,2}^{1,2}$	$q_{3,2}^{1,1}$	$q_{3,2}^{1,1}$	$q_{3,2}^{1,1}$	$q_{3,2}^{1,1}$
$q_{1,2}^{1,1}$	$q_{2,2}^{1,1}$	16	20	26,5	30	10	16,3	21,3	30	8	14	18,5	27,5
$q_{1,2}^{1,2}$	$q_{2,2}^{1,1}$	12	16,5	22	27,5								
		$q_{5,2}^{2,2}$	$q_{5,2}^{2,2}$	$q_{5,2}^{2,2}$	$q_{5,2}^{2,2}$	$q_{5,2}^{2,3}$							
		$q_{4,2}^{1,2}$	$q_{4,2}^{1,2}$	$q_{4,2}^{1,2}$	$q_{4,2}^{1,2}$	$q_{4,2}^{1,3}$							
		$q_{3,2}^{1,2}$	$q_{3,2}^{1,3}$	$q_{3,2}^{1,3}$	$q_{3,2}^{1,3}$	$q_{3,2}^{1,3}$							
$q_{1,2}^{1,2}$	$q_{2,2}^{1,2}$	10	16,3	21,3	30								
$q_{1,2}^{1,3}$	$q_{2,2}^{1,2}$	10	15,3	20,3	27,5								
$q_{1,2}^{1,2}$	$q_{2,2}^{1,3}$									12	17,5	23	30
$q_{1,2}^{1,3}$	$q_{2,2}^{1,3}$					10	16,3	21,3	30	16	20	26,5	30

Table 5-11: Possible scenarios with corresponding additive consistency value

In a subsequent step, the scenarios identified for shell $k = 2$ were organised in an scenario information system SIS_k with $k = 2$ according to the decision table structure $DT_k = \langle U_k, Co_k, Ev_k, V_q, f_q \rangle_{q \in Co_k \cup Ev_k}$ (Table 5-12).

NR	WSL			WEP			BR			SCP			SRS
	$q_{1,2}^{1,1}$	$q_{1,2}^{1,2}$	$q_{1,2}^{1,3}$	$q_{2,2}^{1,1}$	$q_{2,2}^{1,2}$	$q_{2,2}^{1,3}$	$q_{3,2}^{1,1}$	$q_{3,2}^{1,2}$	$q_{3,2}^{1,3}$	$q_{4,2}^{1,1}$	$q_{4,2}^{1,2}$	$q_{4,2}^{1,3}$	$q_{5,2}^{2,1} \vee q_{5,2}^{2,2} \vee q_{5,2}^{2,3}$
1	1	0	0	1	0	0	1	0	0	1	0	0	1
2	1	0	0	1	0	0	0	1	0	1	0	0	1
3	1	0	0	1	0	0	1	0	0	0	1	0	1
4	0	1	0	1	0	0	1	0	0	1	0	0	1
5	0	1	0	0	1	0	0	1	0	0	1	0	2
6	0	0	1	0	1	0	0	1	0	0	1	0	2
7	0	1	0	0	0	1	0	0	1	0	0	1	3
8	0	0	1	0	0	1	0	1	0	0	0	1	3
9	0	0	1	0	0	1	0	0	1	0	0	1	3

Table 5-12: Scenario information system SIS_k with $k = 2$ represented as a decision table.

Definition of equivalence classes U/R_{Co_2} :

$$U/R_{WSL} = \{\{x_1, x_2, x_3\}, \{x_4, x_5, x_7\}, \{x_6, x_8, x_9\}\}$$

$$U/R_{WEP} = \{\{x_1, x_2, x_3, x_4\}, \{x_5, x_6\}, \{x_7, x_8, x_9\}\}$$

$$U/R_{BR} = \{\{x_1, x_3, x_4\}, \{x_2, x_5, x_6, x_8\}, \{x_7, x_9\}\}$$

$$U/R_{SCP} = \{\{x_1, x_2, x_4\}, \{x_3, x_5, x_6\}, \{x_7, x_8, x_9\}\}$$

$$U/R_{SRS} = \{\{x_1, x_2, x_3, x_4\}, \{x_5, x_6\}, \{x_7, x_8, x_9\}\}$$

$$(Co_k \rightarrow Ev_k)$$

$$U/R_{Co_2} = \{\{x_1\}, \{x_2\}, \{x_3\}, \{x_4\}, \{x_5\}, \{x_6\}, \{x_7\}, \{x_8\}, \{x_9\}\}$$

Definition of the lower approximations:

$$\underline{R}_{Co_2} X_1 = \{x_1, x_2, x_3, x_4\}; \underline{R}_{Co_2} X_2 = \{x_5, x_6\}; \underline{R}_{Co_2} X_3 = \{x_7, x_8, x_9\}$$

Calculation of the approximation quality:

$$\gamma(Co_k \rightarrow Ev_k) = \frac{\sum_{X \in U/R_{(Ev_k)}} |\underline{R}_{(Co_k)} X|}{|U|} = 1$$

Table 5-9 and Table 5-12 contain the knowledge structure and the specific contents about the case study on woody material transport, as elicited from the expert team. The conceptual validity of the mental system map shown in Figure 5-3 was supported by the results. Thus a coherent step-by-step

interpretation of the woody material transport related hazard processes and the severity of the induced consequences is provided.

5.4 Results

By the application of the Formative Scenario Analysis procedure it was possible (1) to assess and validate the expert knowledge contained in the mental system map (Figure 5-4) and (2) to specify and weight the relevant system components in the system loading and system response shell. Based on a reasonable identification and robust selection of the relevant key variables, followed by an accurate characterisation of each key variable in terms of activity and passivity ratings, the multiple facets of system dynamics induced by woody material transport related hazard processes were detected. As a result, specific key variables with major influence on the system were defined and rated. Subsequently, by the definition of appropriate impact levels for each specific key variable the description of possible changes in the system behaviour was possible. In a nutshell the most consistent and representative system loading and system response scenarios were systematically derived which added quality to the cause-effect relationships outlined in Figure 5-4.

The results of the application of the Formative Scenario Analysis are represented by the twelve system loading scenarios and nine system response scenarios, respectively, as shown in Tables 5-9 and 5-12 in terms of a Scenario Information System. These results were based on the selection of consistent scenarios derived from Tables 5-8 and 5-11.

For the scenarios given in Table 5-9 it is shown that the individual impact level of the key variable WLS results from a concisely defined combination of different levels for each conditional key variable belonging to the conditional factor subset.

The scenarios reported in Table 5-9 show that the different impact levels of the key variable WLS (evolution factor of the shell $k=1$) are a consequence of different system loading conditions, expressed in terms of specific level combinations of different key variables belonging to the conditional factor subset. Taking as an example the six consistent scenarios of $WLS = 3$, characterised by a high system loading severity, six different explanations in terms of different level combinations can be adduced. Among these six scenarios, the most consistent one can be deduced from Table 5-8 as follows:

Recruitment propensity from hill slopes – very high ($\hat{q}_{1,1}^{1,4}$), in-stream recruitment propensity – medium ($q_{2,1}^{1,3}$), woody material transport costs – low ($\hat{q}_{3,1}^{1,3}$), potential woody material transport

distribution extremely unfavourable ($\hat{q}_{4,1}^{1,3}$), and woody material system loading severity – high ($\hat{q}_{5,1}^{2,3}$).

The additive consistency value for this scenario is given by

$$\begin{aligned} \tilde{C}^*(S_{324,1}) &= \tilde{C}(\hat{q}_{1,1}^{1,4}, \hat{q}_{2,1}^{1,3}) \oplus \tilde{C}(\hat{q}_{2,1}^{1,3}, \hat{q}_{3,1}^{1,3}) \oplus \tilde{C}(\hat{q}_{3,1}^{1,3}, \hat{q}_{4,1}^{1,3}) \oplus \tilde{C}(\hat{q}_{4,1}^{1,3}, \hat{q}_{5,1}^{2,3}) \oplus \tilde{C}(\hat{q}_{1,1}^{1,4}, \hat{q}_{3,1}^{1,3}) \oplus \tilde{C}(\hat{q}_{1,1}^{1,4}, \hat{q}_{4,1}^{1,3}) \oplus \tilde{C}(\hat{q}_{1,1}^{1,4}, \hat{q}_{5,1}^{2,3}) \oplus \\ &\tilde{C}(\hat{q}_{2,1}^{1,3}, \hat{q}_{4,1}^{1,3}) \oplus \tilde{C}(\hat{q}_{2,1}^{1,3}, \hat{q}_{5,1}^{2,3}) \oplus \tilde{C}(\hat{q}_{3,1}^{1,3}, \hat{q}_{5,1}^{2,3}) = \tilde{P} \oplus \tilde{H} \oplus \tilde{H} \oplus \tilde{H} \oplus \tilde{P} \oplus \tilde{H} \oplus \tilde{H} \oplus \tilde{H} \oplus \tilde{H} \oplus \tilde{H} = (16.0, 20.0, 26.5, 30.0)^e \end{aligned}$$

A similar result can be drawn for the system response scenario shell. Taking a high system loading severity (WLS = high), the corresponding most consistent scenario of the system response scenario shell can be deduced from Table 5-11 as follows:

Woody material system loading severity – high ($\hat{q}_{1,2}^{1,3}$), woody material entrapment propensity – high ($\hat{q}_{2,2}^{1,3}$), blockage ratio – high ($\hat{q}_{3,2}^{1,3}$), system change propensity – high ($\hat{q}_{4,2}^{1,3}$), and system response severity – high ($\hat{q}_{5,2}^{2,3}$).

The additive consistency value for this scenario is given by

$$\begin{aligned} \tilde{C}^*(S_{243,2}) &= \tilde{C}(\hat{q}_{1,2}^{1,3}, \hat{q}_{2,2}^{1,3}) \oplus \tilde{C}(\hat{q}_{2,2}^{1,3}, \hat{q}_{3,2}^{1,3}) \oplus \tilde{C}(\hat{q}_{3,2}^{1,3}, \hat{q}_{4,2}^{1,3}) \oplus \tilde{C}(\hat{q}_{4,2}^{1,3}, \hat{q}_{5,2}^{2,3}) \oplus \tilde{C}(\hat{q}_{1,2}^{1,3}, \hat{q}_{3,2}^{1,3}) \oplus \tilde{C}(\hat{q}_{1,2}^{1,3}, \hat{q}_{4,2}^{1,3}) \oplus \tilde{C}(\hat{q}_{1,2}^{1,3}, \hat{q}_{5,2}^{2,3}) \oplus \\ &\tilde{C}(\hat{q}_{2,2}^{1,3}, \hat{q}_{4,2}^{1,3}) \oplus \tilde{C}(\hat{q}_{2,2}^{1,3}, \hat{q}_{5,2}^{2,3}) \oplus \tilde{C}(\hat{q}_{3,2}^{1,3}, \hat{q}_{5,2}^{2,3}) = \tilde{H} \oplus \tilde{H} \oplus \tilde{H} \oplus \tilde{H} \oplus \tilde{P} \oplus \tilde{H} \oplus \tilde{P} \oplus \tilde{H} \oplus \tilde{H} \oplus \tilde{H} = (16.0, 20.0, 26.5, 30.0)^e \end{aligned}$$

However, the same degree of system response severity being equal the system loading scenario can be deduced from another scenario from Table 5-11:

Woody material system loading severity – high ($\hat{q}_{1,2}^{1,3}$), woody material entrapment propensity – high ($\hat{q}_{2,2}^{1,3}$), blockage ratio – medium ($\hat{q}_{3,2}^{1,2}$), system change propensity – high ($\hat{q}_{4,2}^{1,3}$), and system response severity – high ($\hat{q}_{5,2}^{2,3}$).

The additive consistency value for this scenario is given by

$$\begin{aligned} \tilde{C}^*(S_{243,2}) &= \tilde{C}(\hat{q}_{1,2}^{1,3}, \hat{q}_{2,2}^{1,3}) \oplus \tilde{C}(\hat{q}_{2,2}^{1,3}, \hat{q}_{3,2}^{1,3}) \oplus \tilde{C}(\hat{q}_{3,2}^{1,2}, \hat{q}_{4,2}^{1,3}) \oplus \tilde{C}(\hat{q}_{4,2}^{1,3}, \hat{q}_{5,2}^{2,3}) \oplus \tilde{C}(\hat{q}_{1,2}^{1,3}, \hat{q}_{3,2}^{1,2}) \oplus \tilde{C}(\hat{q}_{1,2}^{1,3}, \hat{q}_{4,2}^{1,3}) \oplus \tilde{C}(\hat{q}_{1,2}^{1,3}, \hat{q}_{5,2}^{2,3}) \oplus \\ &\tilde{C}(\hat{q}_{2,2}^{1,3}, \hat{q}_{4,2}^{1,3}) \oplus \tilde{C}(\hat{q}_{2,2}^{1,3}, \hat{q}_{5,2}^{2,3}) \oplus \tilde{C}(\hat{q}_{3,2}^{1,2}, \hat{q}_{5,2}^{2,3}) = \tilde{H} \oplus \tilde{P} \oplus \tilde{P} \oplus \tilde{H} \oplus \tilde{P} \oplus \tilde{H} \oplus \tilde{P} \oplus \tilde{H} \oplus \tilde{H} \oplus \tilde{P} = (10.0, 16.3, 21.3, 30.0)^e \end{aligned}$$

The results obtained in terms of the scenario information systems of the two shells have considerable implications for natural hazard risk management in general and for risk due to woody material transport in particular. Problem solving strategies aiming at minimising the system response severity – SRS – can be directly deduced from the scenario information systems. In the specific case under investigation partial risk mitigation strategies, which only take into consideration exclusively a strong reduction of woody material system loading severity turn out to be less promising, because small amounts of woody material are judged to be sufficient to clog the

available flow section and to produce severe consequences. Instead, interpreting Table 5-12 in terms of a proposed strategy to mitigate system severity induced by woody material transport, woody material system loading severity should be reduced ($\widehat{q}_{1,2}^{1,3} \rightarrow \widehat{q}_{1,2}^{1,2}$) and in parallel, the reliability ($\widehat{q}_{4,2}^{1,3} \rightarrow \widehat{q}_{4,2}^{1,1}$) and functionality of the critical stream configuration ($\widehat{q}_{3,2}^{1,3} \rightarrow \widehat{q}_{3,2}^{1,1} \wedge \widehat{q}_{2,2}^{1,3} \rightarrow \widehat{q}_{2,2}^{1,1}$) should be enhanced. Such an approach mirrors the idea of integral risk management that a combination of mitigation measures often turns out to be more effective in hazard and risk reduction than only one single countermeasure (e.g., Holub and Fuchs 2008). Moreover, by implementing systematic redundancies in both, the system loading and system response shell, enhanced system resilience is achieved.

5.5 Conclusion

Current methods of risk analyses for natural hazards are from an engineering point of view based on quantitative methods of impact assessment to a given environmental setting, and require the assessment of processes as well as values exposed. With respect to torrent processes, these quantitative methods include usually process-based numerical analysis, which necessitates precise data on input parameters. Therefore, some limitations occur by applying such approaches. Above all, since complex flow mechanisms which are important for small-scale analyses such as woody material transport dynamics at critical stream configurations, cannot satisfyingly be mirrored. Moreover, the missing connectivity between causes and effects, such as precipitation input, liquid and solid discharge and woody material transport rates as output, results in simplifications and does neither represent flow mechanisms nor deposition characteristics sufficiently detailed. In particular morphological changes that induce hazard processes are of virtual importance for a reliable assessment of hazard paths and thus system configuration. As a result, system response mechanisms are only partly understood so far, leading to uncertainties in protection system functionality and mitigation efficacy.

In order to overcome these shortcomings, a scenario shell structure was proposed taking into account causes (system loading shell) and effects (system response shell) within a torrent system. By applying Formative Scenario Analysis, this shell structure was used to derive qualitative and quantitative (expert and local, respectively) knowledge that can be integrated into scenario definition within the framework of natural hazard risk management. From a conceptual point of view, the extension of Formative Scenario Analysis by introducing elements of fuzzy modelling resulted in an enhancement

- (1) of the representation of impacts by an impact matrix through fuzzy intervals, resulting in an integration of the broad expert knowledge spectrum;
- (2) in characterisation of the impacts by relevant key variables influencing the processes studied;
- (3) in modelling of importance and uncertainties assessed by the expert team;
- (4) in modelling of conjoined consistency values for pairs of different key variables impact levels;
- (5) in selecting the most consistent scenarios with respect to efficient mitigation strategies.

By Rough Set Data theory it was possible to organise the knowledge content in scenario information systems for each shell. Hence, the robustness of the hazard assessment procedure was increased by using such an approach, and the management of hydrological hazards was supplemented by an integration of expert knowledge into the framework of calculation. With respect to basic and operational principles (Shepard 2005), formative analysis can provide crucial insights into the entire process of hazard assessment and mapping. Consequently, consistent assumptions either concerning system loading or system response mechanisms will be integrated into the decision process, and bounding uncertainties can be considered where possible. Thereby, the presented method has to be used complementary to hydrological and hydraulic simulation models in order to produce consistent, intelligible and retraceable results. As a result, available resources can be utilised more efficiently to meet the requirements of integral risk management strategies.

It is of fundamental importance to capture at least qualitatively the different aspects of multi-hazard situations and nonlinearity in cause-effect relationships in order to design resilient protection systems by minimising conceptual susceptibilities and by providing robustness over the entire life cycle of a protection system. The case study performed in this work had proven that a small set of consistent and reliable exploratory scenarios is suitable to identify effects given a specific set of causes, if the overall objective is to obtain a broad spectrum of possible system responses.

One of the challenges of integral risk management is to be prepared for unexpected system behaviour. If weak signals of such unexpected system behaviour are not discerned and represented by deterministic models, and probabilistic models neglect important impact factors, the possibility-based approach of Formative Scenario Analysis provides clear problem-solving advantages. A further development step will foster towards a widening of possible applications of Formative Scenario Analyses to sets of cases with a high degree of similarity, e.g. similar protection system configurations in different torrent basins or similar depositional zone characteristics of different

alluvial fans. These issues can be addressed introducing the fuzzy logic paradigm, without any loss of significance and rigor. The flexibility of the proposed knowledge modelling and integration framework seems to be particularly suitable for providing in-depth insights into coping strategies emerging from interdisciplinary expert workshops and participatory planning processes.

Consequently, if risk management processes were adjusted to these findings, risk communication could be enhanced, and awareness-building of the public will be increased. In particular concerning the European Flood Risk Directive, but also with respect to the overall aim of building hazard-resilient communities, future studies might include the applicability of Formative Scenario Analysis and its extension by fuzzy modelling within flood risk management planning.

5.6 References

Autonome Provinz Bozen-Südtirol, 2008. Informationssystem zu hydrogeologischen Risiken. Methodischer Endbericht. Bozen: Autonome Provinz Bozen-Südtirol.

Berger, E., Grisotto, S., Hübl, J., Kienholz, H., Kollarits, S., Leber, D., Loipersberger, A., Marchi, L., Mazzorana, B., Moser, M., Nössing, T., Riedler, S., Scheidl, C., Schmid, F., Schnetzer, I., Siegel, H. and Volk, G., 2007. DIS-ALP. Disaster information system of alpine regions. Final report. unpublished.

Bezzola, G. and Hegg, C., 2007. Ereignisanalyse Hochwasser 2005, Teil 1 – Prozesse, Schäden und erste Einordnung. Bern und Birmensdorf: Bundesamt für Umwelt BAFU, Eidgenössische Forschungsanstalt WSL.

Brown, J., Heuvelink, G. and Refsgaard, J., 2005. An integrated framework for assessing and recording uncertainties about environmental data. *Water Science and Technology* 52 (6), 153-160.

Diehl, T., 1997. Potential drift accumulation at bridges. Washington, U.S. Department of Transportation, Federal Highway Administration Research and Development, Turner-Fairbank Highway Research Center.

Fuchs, S., Keiler, M., Zischg, A. and Bründl, M., 2005. The long-term development of avalanche risk in settlements considering the temporal variability of damage potential. *Natural Hazards and Earth System Sciences* 5 (6), 893-901.

Fuchs, S. and McAlpin, M., 2005. The net benefit of public expenditures on avalanche defence structures in the municipality of Davos, Switzerland. *Natural Hazards and Earth System Sciences* 5 (3), 319-330.

- Fuchs, S. and Keiler, M., 2006. Natural hazard risk depending on the variability of damage potential. *WIT Transactions on Ecology and the Environment* 91, 13-22.
- Fuchs, S., Thöni, M., McAlpin, M. C., Gruber, U. and Bründl, M., 2007. Avalanche hazard mitigation strategies assessed by cost effectiveness analyses and cost benefit analyses – Evidence from Davos, Switzerland. *Natural Hazards* 41 (1), 113-129.
- Fuchs, S., Kaitna, R., Scheidl, C. and Hübl, J., 2008. The application of the risk concept to debris flow hazards. *Geomechanics and Tunnelling* 1 (2), 120-129.
- Fuchs, S., 2009. Susceptibility versus resilience to mountain hazards in Austria – Paradigms of vulnerability revisited. *Natural Hazards and Earth System Sciences* 9 (2), 337-352.
- Funtowicz, S. and Ravetz, J., 1994. Uncertainty, complexity and post-normal science. *Environmental Toxicology and Chemistry* 13 (12), 1881-1885.
- Girod, B. and Mieg, H., 2008. Wissenschaftliche und politische Gründe für den Wandel der IPCC-Szenarien. *Gaia* 17 (3), 302-311.
- Greco, S., Matarazzo, B. and Slowinski, R., 2001. Rough sets theory for multicriteria decision making. *European Journal of Operational Research* 129 (1), 1-47.
- Holub, M., and Fuchs, S., 2008. Benefits of local structural protection to mitigate torrent-related hazards. *WIT Transactions on Information and Communication Technologies* 39, 401-411.
- Houghton, J., Yihui, D. and Griggs, D., 2001. *Climate Change 2001, The Scientific Basis: Contribution of Working Group I to the Third Assessment Report of the Intergovernmental Panel on Climate Change*. Cambridge: Cambridge University Press.
- Kahn, H. and Wiener, J., 1967. *The year 2000: A framework for speculation on the next thirty-three years*. New York: Macmillan Publishing Company.
- Keiler, M., Sailer, R., Jörg, P., Weber, C., Fuchs, S., Zischg, A. and Sauer Moser, S., 2006. Avalanche risk assessment – A multi-temporal approach, results from Galtür, Austria. *Natural Hazards and Earth System Sciences* 6 (4), 637-651.
- Kolkman, M., Kok, M. and van der Veen, A., 2005. Mental model mapping as a new tool to analyse the use of information in decision-making in integrated water management. *Physics and Chemistry of the Earth* 30 (4-5), 317-332.
- Kosko, B., 1992. *Neural networks and fuzzy systems. A dynamical approach to machine intelligence*. Englewood Cliffs: Prentice Hall.
- Kruse, R., Gebhardt, J. and Klawonn, F., 1994. *Foundations of fuzzy systems*. New York: John Wiley & Sons.

- Lange, D. and Bezzola, G., 2006. Schwemmholz: Probleme und Lösungsansätze. Mitteilungen der Versuchsanstalt für Wasserbau, Hydrologie und Glaziologie (VAW) der ETH Zürich 188. Zürich: ETH.
- Lyn, D., Cooper, T., Condon, D. and Gan, L., 2007. Factors in debris accumulation at bridge piers. Washington, U.S. Department of Transportation, Federal Highway Administration Research and Development, Turner-Fairbank Highway Research Center.
- Mahmoud, M., Liu, Y., Hartmann, H., Stewart, S., Wagener, T., Semmens, D., Stewart, R., Gupta, H., Dominguez, D., Dominguez, F., Hulse, D., Letcher, R., Rashleigh, B., Smith, C., Streetm, R., Ticehurst, J., Twery, M., van Delden, H., Waldick, R., White, D., and Winter, L., 2009. A formal framework for scenario development in support of environmental decision-making. *Environmental Modelling and Software* 27 (7), 798-808.
- Mazzorana, B., Hübl, J. and Fuchs, S., 2009. Improving risk assessment by defining consistent and reliable system scenarios. *Natural Hazards and Earth System Sciences* 9 (1), 145-159.
- Mazzorana, B., Hübl, J., Zischg, A. and Largiader, A., in press. Modelling woody material transport and deposition in alpine rivers. *Natural Hazards*.
- Merz, B., Kreibich, H. and Apel, H., 2008. Flood risk analysis: Uncertainties and validation. *Österreichische Wasser- und Abfallwirtschaft* 60 (5-6), 89-94.
- Montgomery, D. and Piégay, H., 2003. Wood in rivers: interactions with channel morphology and processes. *Geomorphology* 51 (1-3), 1-5.
- Mouton, A., De Baets, B. and Goethals, P., 2009. Knowledge-based versus data-driven habitat suitability models for river management. *Environmental Modelling and Software* 24 (8), 982-993.
- O'Brien, F. and Dyson, R., 2007. Supporting strategy: Frameworks, methods and models. Chichester: Wiley.
- Olson, D. and Delen, D., 2008. Advanced data mining techniques. Berlin: Springer.
- Paté-Cornell, E., 1996. Uncertainty in risk analysis: Six levels of treatment. *Reliability Engineering and System Safety* 54 (2-3), 95-111.
- Pawlak, Z., (1997) Rough set approach to knowledge-based decision support. *European Journal of Operational Research* 99 (1), 48-57.
- PLANAT, 2004. Strategie Naturgefahren Schweiz. Synthesebericht in Erfüllung des Auftrages des Bundesrates vom 20. August 2003. Biel: Bundesamt für Wasser und Geologie.
- Refsgaard, J., van der Sluijs, J., Højberg, A. and Vanrolleghem, P., 2007. Uncertainty in the environmental modelling process – A framework and guidance. *Environmental Modelling and Software* 22 (11), 1543-1556.

- Renn, O., 2008a. Concepts of risk: An interdisciplinary review. Part 1: Disciplinary risk concepts. *Gaia* 17 (1), 50-66.
- Renn, O., 2008b. Concepts of risk: An interdisciplinary review. Part 2: Integrative approaches. *Gaia* 17 (2), 196-204.
- Rommelfanger, H. and Eickemeier, S., 2001. *Entscheidungstheorie: Klassische Konzepte und Fuzzy-Erweiterungen*. Heidelberg: Springer.
- Rutkowski, L., 2008. *Computational intelligence: Methods and techniques*. Berlin: Springer.
- Scholz, R. and Tietje, O., 2002. *Embedded case study methods*. London: Sage.
- Shepard, R., 2005. *Quantifying environmental impact assessments using fuzzy logic*. New York: Springer.
- Solomon, S., Qin, D., Manning, M., Chen, Z., Marquis, M., Averyt, K., Tignor, M. and Miller, H., 2007. *Climate change 2007. The scientific basis: Contribution of Working Group I to the Fourth Assessment Report of the Intergovernmental Panel on Climate Change*. Cambridge: Cambridge University Press.
- Stötter, J. and Fuchs, S., 2006. Umgang mit Naturgefahren – Status quo und zukünftige Anforderungen. In: Fuchs, S., Khakzadeh, L. and Weber, K., (Eds.), *Recht im Naturgefahrenmanagement*. Innsbruck: Studienverlag, 19-34.
- Tan, R., 2005. Rule-based life cycle impact assessment using modified rough set induction methodology. *Environmental Modelling and Software* 29 (5), 509-513.
- Tietje, O., 2005. Identification of a small reliable and efficient set of consistent scenarios. *European Journal of Operational Research* 167 (2), 418-432.
- USACE (2008). *River analysis system HEC-RAS*. US Army Corps of Engineers, Hydrologic Engineering Center.
- van der Heijden, K., 2005. *Scenarios: The art of strategic conversation*. Chichester: Wiley.
- Varnes, D., 1984. *Landslide hazard zonation*. Paris: UNESCO.
- Vester, F., 1988. The bio-cybernetic approach as a basis for planning our environment. *Systemic Practice and Action Research* 1 (4), 10-16.
- Weck-Hannemann, H., 2006. Efficiency of protection measures. In: Ammann, W., Dannenmann, S. and Vulliet, L., (Eds.), *Risk21 – Coping with risks due to natural hazards in the 21st century*. London: Taylor & Francis, 147-154.
- Wiek, A. and Binder, C., 2005. Solution spaces for decision-making – a sustainability assessment tool for city-regions. *Environmental Impact Assessment Review* 25 (6), 589-608.

6. SYNOPSIS

*There are essentially four kinds of risk:
The risk one must accept. The risk one can afford to take.
The risk one cannot afford to take. The risk one cannot afford not to take.
Peter F. Drucker.*

In the previous sections the following four tasks were set: (1) the modelling of woody material recruitment and entrainment as well as transport processes in Alpine torrents and rivers on a hazard index level (Petraschek and Kienholz, 2003); (2) the detection of possible hazard process patterns at critical stream configurations (e.g. bridges); (3) the application of a scenario analysis based approach (FSA – Formative Scenario Analysis) for woody material transport processes to complement currently applied hazard and risk assessment procedures; (4) the integration of additional knowledge by using an extended FSA based approach aiming at an enhanced knowledge processing; this innovative concept of knowledge integration led to a rigorous scenario analysis framework as well as to a comprehensive scenario information system definition. The resulting coherent list of objectives has been derived by taking a knowledge management perspective; thus, the needs of public authorities dealing with natural hazard risks in general, and with woody material transport hazards in particular, were mirrored (Berger et al., 2007; Staffler et al., 2008). Several case studies have been conducted to test the applicability of the developed methods and to disclose the intricacy of woody material transport induced hazards in mountain streams.

During the set of analyses, the main challenge was not to lose sight of the essential but to take both a scientific view and the view of a later practical application and operational implementation of the results. Considering on the one hand the immature stage of research in the specific field of woody material dynamics in alpine streams and on the other hand the demands by public authorities for reliable risk mitigation principles, a balanced research strategy was adopted.

Acknowledging the importance and recognising the need of comprehensive flume experiments to assess woody material entrainment, transport and deposition processes on a detailed scale of analysis, the main goals of this thesis were to contribute from a conceptual point of view:

- (1) The first step consisted of highlighting those Alpine catchments which are particularly susceptible to woody material transport hazards. Subsequently, a ranking of the catchments was carried out on the basis of reliable prioritisation criteria and hazard indicators, followed

by a substantiation of the hazard indications provided on regional scale of analysis, resulting in the assessment on a hazard index level.

- (2) In order to identify possible risk mitigation concepts, woody material transport induced hazard processes patterns need to be modelled. However, modelling hazard processes involving woody material transport on a detailed scale is complex task. Although promising mathematical models with the capability to simulate moving objects in a three dimensional flow field exist (Wei, 2005; Wei, 2006), their applicability performance to real-world woody material transport processes in mountain streams have not sufficiently been studied so far. Therefore, a two-dimensional flow-path tracking simulation was developed and applied to simulate woody material transport processes.
- (3) Since the results of this simulation were based on a less-detailed scale, additional information on scenario development was necessary to describe process patterns at critical configurations. Therefore, expert knowledge was integrated in order to provide enhanced information on possible scenarios as a prerequisite for a reliable delineation of hazard areas. It was proven that suitable knowledge integration frameworks support both a structured elicitation and a cost-effective processing of the expert knowledge.

In the following section, the essential research strategies are revisited and essential results are summarized.

As outlined in **Chapter 2** a procedure to enable the detection of hazards related to woody material transport was developed. A woody material transport indicator – WM – was proposed to estimate the relative availability of recruited woody material and the relative propensity for entrainment and delivery of woody material under given transport conditions. The computing procedure set up accounted for the entire process chain ranging from woody material recruitment on hill slopes and in-stream recruitment within the wetted perimeter to entrainment and transport of the recruited woody material. The hazard process oriented view taken required a functional classification of woody material dynamics, i.e., of the woody material recruitment areas according either to the activity/intensity of the recruitment processes or to the activity/intensity of the torrential processes (Table 6-1 and Figure 6-1).

Type of recruitment area	Description
SIZ – areas (stream influence zone)	The extent of these areas is determined by the wetted perimeter corresponding to the peak discharge of the considered extreme event.
AWB – areas (active wood buffer)	These active recruitment areas border the SIZ-areas. Toppling trees can directly reach the stream and considerably influence geomorphic processes.
RWB – areas (recharging wood buffer)	This forested strip is directly connected to the outside of the AWB. Toppling trees destabilize other trees from the AWB-areas.
PRP – areas (preferential recruitment paths)	These are mainly steep gullies in forested areas well connected with the main channel. In these preferential paths transportation of woody material is possible even if the width of the AWB and RWB is exceeded.
PCA – areas (preferential contributing areas)	These are areas of potential shallow landslides in forested areas close to the stream channel.

Table 6-1: Classification of woody material recruitment areas.

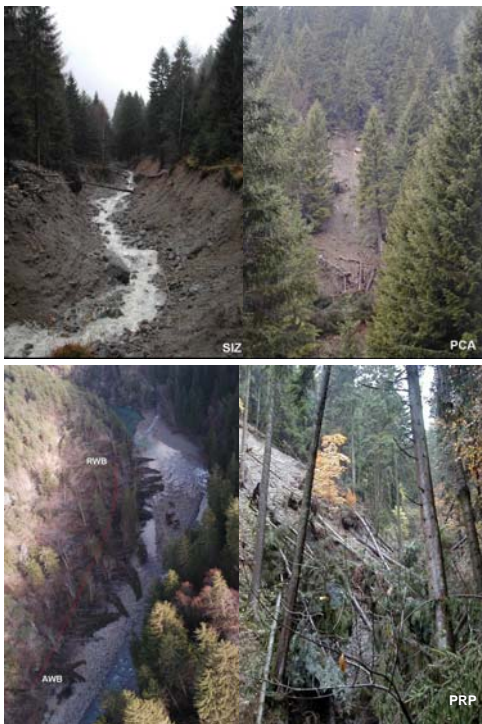


Figure 6-1: Examples of classified woody material recruitment areas

The flowchart presented in Figure 6-2 outlines the necessary steps for the determination of the relative propensity of mountain streams to the entrainment and delivery of recruited woody material on the basis of empirical indicators.

Step 1: Identification and spatial delimitation of the woody material recruitment areas

- a) Calculation of the width of the active wood buffer (**AWB**) and the recharging wood buffer (**RWB**)
- b) Identification of the preferential recruitment paths (**PRP**)
- c) Identification of the preferential contributing areas (**PCA**)
- d) Determination of the particularly active recruitment areas (**PARA**) as:
 $PARA = PRP \cup PCA$
- e) Identification of the torrent influence zones (**SIZ**)

Step 2: Calculation of the woody material recruitment indicator

$$RA_{hs,i} = a \cdot (AWB_{left,i} + AWB_{right,i}) + b \cdot (RWB_{left,i} + RWB_{right,i}) + c \cdot (PARA_{left,i} + PARA_{right,i})$$

$RA_{hs,i}$...recruitment areas on hill slopes connected to the i^{th} stretch of the stream
a, b and c are empirical constants

$$RA_{instream,i} = d \cdot (SIZ_i)$$

$RA_{instream,i}$...in-stream recruitment areas of the i^{th} stretch of the stream

d is an empirical constant

$$RA_{tot,i} = RA_{hs,i} + RA_{instream,i}$$

$RA_{tot,i}$...total recruitment areas connected to the i^{th} stretch of the stream.

Step 3: Calculation of the woody material entrainment and transport indicator – WM indicator

a) WM indicator for the bedload transport case:

$$WM = Q_{tot,bedload} \cdot \frac{1}{A_{tot}} \cdot \sum_{i=1}^k (l_{Q,i} \cdot RA_{tot,i})$$

b) WM indicator for the debris flow case:

$$WM = Q_{tot,df} \cdot \frac{1}{A_{tot}} \cdot \sum_{i=1}^k (l_{Q,i} \cdot RA_{tot,i})$$

k ...number of control points, $i=1, \dots, k$

A_{tot} ...catchment area

WM ...hazard potential indicator for wood material delivery

$Q_{tot,df}$ $Q_{tot,bedload}$...design event peak discharges for debris flow and bedload transport

Figure 6-2: Flow chart for the calculation of the woody material recruitment and transport indicator WM

The calculation of the WM indicator was performed on a GIS basis for all stream catchments within the Autonomous Province of Bolzano that were susceptible to debris flows and sediment transport

related phenomena. The classified stream catchments according to their WM indicator values are shown in Figure 6-3.

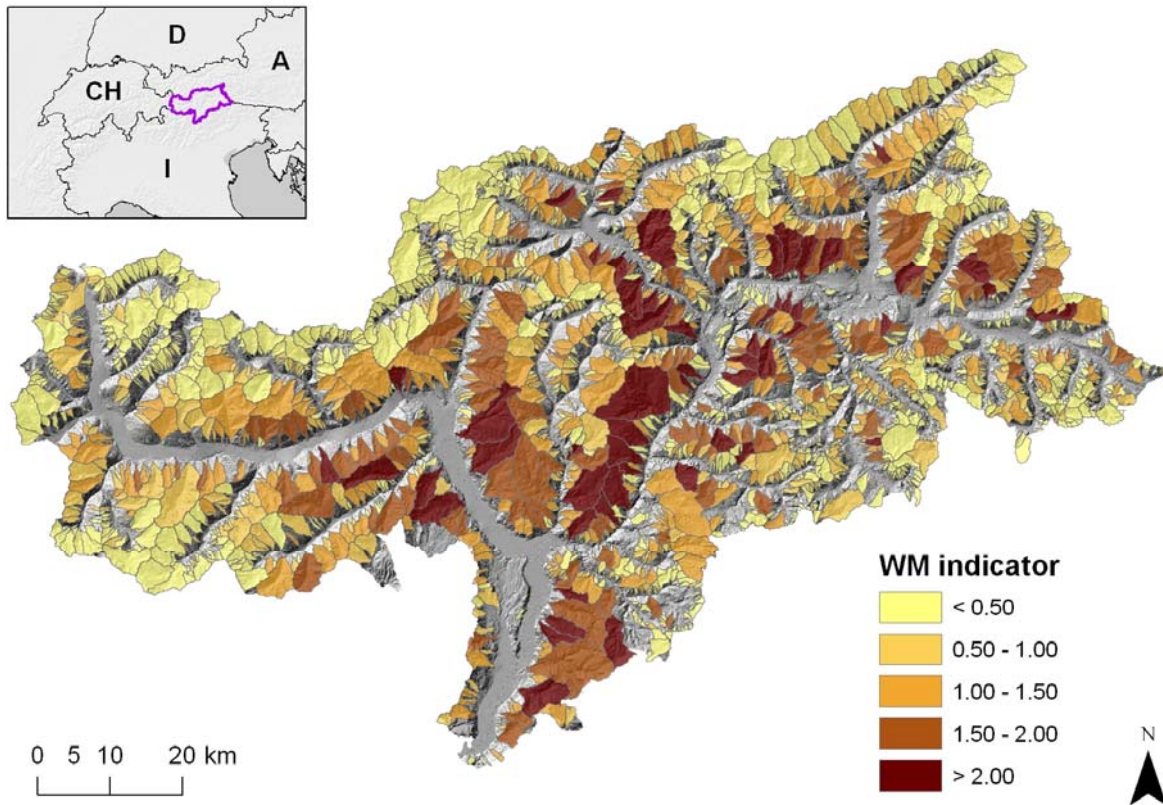


Figure 6-3: Classification of the stream catchments by the woody material recruitment and transport indicator WM. Legend classification in equal intervals.

The results derived from the application of the WM indicator were verified qualitatively and semi-quantitatively by using approximately 1,800 images taken in the Autonomous Province of Bolzano which showed evidence for woody material recruitment, transport and deposition phenomena. The validation procedure resulted in a significant correspondence of the calculated WM indicator values with the analysed photographs. The generated hazard index maps supported a comprehensive risk management approach:

- (1) During the early stage of hazard zone planning these hazard index maps contribute to rationalise and adjust the level of detail required for a complete hazard assessment.
- (2) During the conceptual planning of risk mitigation strategies the knowledge of possible hazard scenarios involving woody material dynamics provide the basis for a comprehensive system analysis. Reliable indicators about possible woody material transport related hazard processes occurring at critical configurations support the practitioner to develop a successful risk mitigation strategy.

- (3) The conceptual framework the modelling approach was based upon might be used as a reference for a structured documentation of extreme torrential events including aspects related to woody material recruitment, entrainment and transport.

From a development perspective further improvements of the presented approach might include either the introduction of a connectivity based probabilistic approach for assessing recruitment or the consideration of a 2D hydrodynamic computational scheme for the evaluation of entrainment and transport.

In **Chapter 3** the research focus was shifted to the evaluation of woody material transport and deposition in alpine rivers, a topic for which considerable gaps had been proven during recent flash flood events in Switzerland and western Austria in 2005 by the research community as well as from the practitioners side. In order to overcome specific shortcomings of the currently used hazard mapping procedures, a procedure was designed allowing for: (1) the estimation of woody material recruitment from wood covered river banks and floodplains; (2) the evaluation of woody material entrainment; (3) the calculation of transport and deposition pathways in alpine rivers; (4) the identification of hazard process patterns at critical configurations. In a successive step the developed procedure has been applied in a case study. Figure 6-4 summarises the modelling steps for the evaluation of hazards induced by woody material dynamics in alpine rivers.

Step 1: Assessment of the recruited woody material volume

- a) *from hill slopes (compare chapter 2 and Figure 7-2 for details)*
- b) *from tributaries:*
 - b.1) *through event documentation or*
 - b.2) *through empirical formulas (Rickenmann, 1997)*
 - b.3) *through survey procedures (Rimböck, 2003)*
- c) *within the flooded area with an ad hoc developed procedure based on:*
 - c.1) *hydrodynamic impact*
 - c.2) *resistance of the vegetation structure*
 - c.3) *frequency of exposure)*

Step 2: Woody material transport dynamics

- a) *Calculation of the woody material transport inhibition parameter*
- b) *Calculation of the woody material transport pathways*

Step 3: Calculation of the hazard impacts at critical stream configurations

- a) *Detection of obstacles as potential wood entrapment locations*
- b) *Simulation of the relevant entrapment mechanisms*

Figure 6-4: Flow chart of the modelling steps for the evaluation of woody material transport hazard dynamics in alpine rivers

The main results of the woody material transport simulations on a cell-by-cell basis carried out for the case study on the Passer/Passirio river are presented in Figure 6-5.

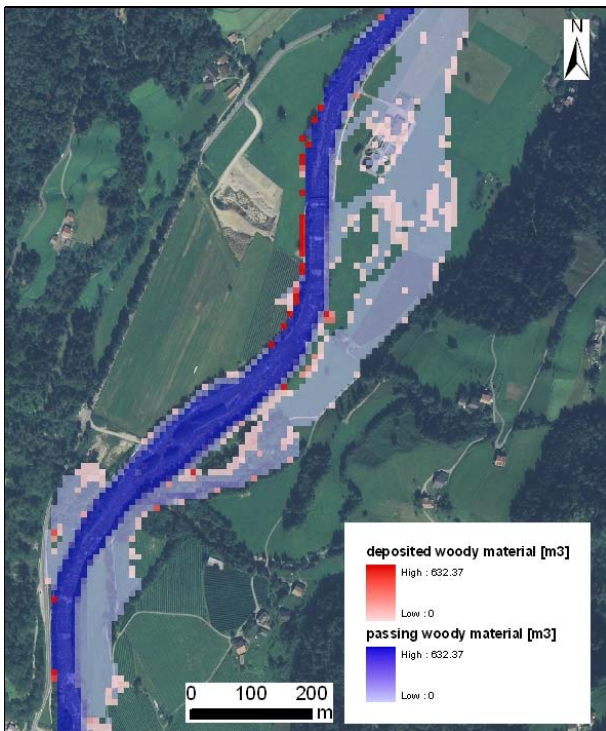


Figure 6-5: Woody material transport simulation results for a section of the Passer/Passirio river, Italy

The results suggest an increased concentration of woody material transport close to the centre streamline. Additionally, the potential deposition areas of woody material are provided; deposition primarily takes place in flooded areas with low flow depths or low flow velocities outside of the river channel. Within the river channel, deposition of woody material is modelled at the waterside slopes, at the waterside of river bends and at calm loops. The modelled woody material deposition areas correspond accurately to the potential deposition areas mapped during a field campaign. The maximum of transported woody material was calculated as 632 m^3 in the last flow cell. This value indicates the maximum amount of transported woody material during a flood event with a reoccurrence period of 1 in 300 years at the outflow cell of the studied river reach.

In addition to the cell-by-cell modelling approach, an object-oriented modelling approach was developed. This approach considered the instationary flow dynamics and its effect on woody material transport in a simplified way. In Figure 6-6 the computed woody material deposition at a critical configuration are shown.

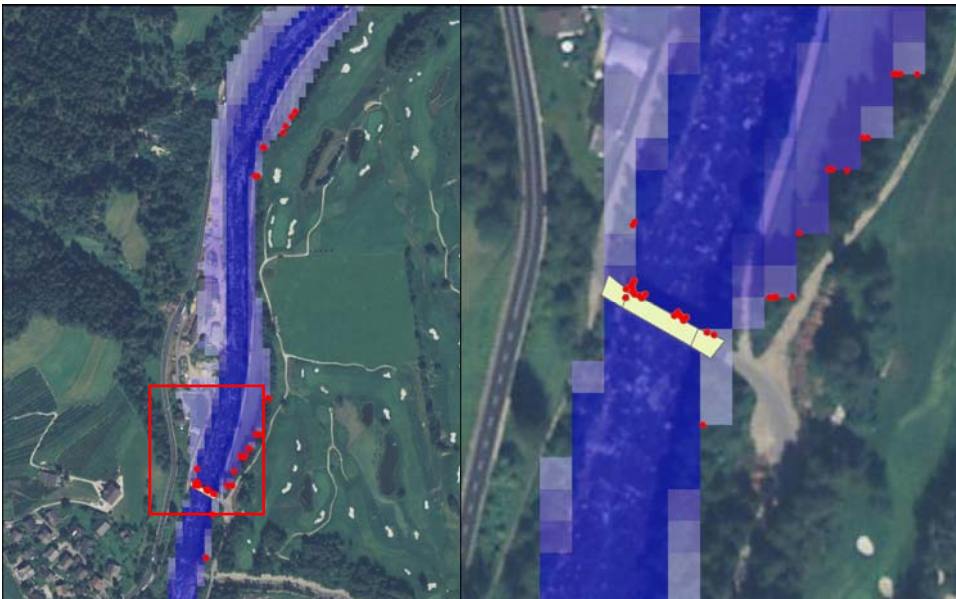


Figure 6-6: Entrapment at a critical configuration. The graphic at the right side shows the entrapped driftwood on a higher resolution.

By the application of the developed method, valuable insights were provided regarding woody material recruitment processes and the propensity for entrainment and transport at critical configurations during extreme flood events. The main pathways of the woody material in the river channel were traced and subsequently the potential depositional areas were identified. The procedure was able to provide the order of dimension of the woody material volume expected to pass through bridges during a flood event. Such knowledge is necessary for a reliable scenario definition during hazard assessment, in particular with respect to a possible log jam formation, clogging or a similar obstruction phenomenon. Consequently, the transparency of hazard mapping procedure and the quality of the results will be increased and the supervision of the entire hazard mapping procedure by the respective public authorities will be facilitated. The outcomes might also be used in order to support the definition of policies in riparian forest management and to define particular measures such as thinning and other forest management actions.

In **Chapter 4** Formative Scenario Analysis was introduced in the field of natural hazard research to supplement conventional risk assessment. The applicability of this technique was shown by two case studies, both of them addressing the description of complex systems behaviour due to (1) sediment transport and (2) woody material transport dynamics. It was shown that Formative Scenario Analysis supported the integration of quantitative and qualitative knowledge, and contributed to the optimisation of the delineation of hazard areas. Furthermore, the particular effects of changing channel morphology and associated woody material transport phenomena were found

to amplify process intensities considerably (e.g., Diehl, 1997; Lyn et al., 2007). In Figure 6-7 the applied workflow through the nine steps of Formative Scenario Analysis is presented.

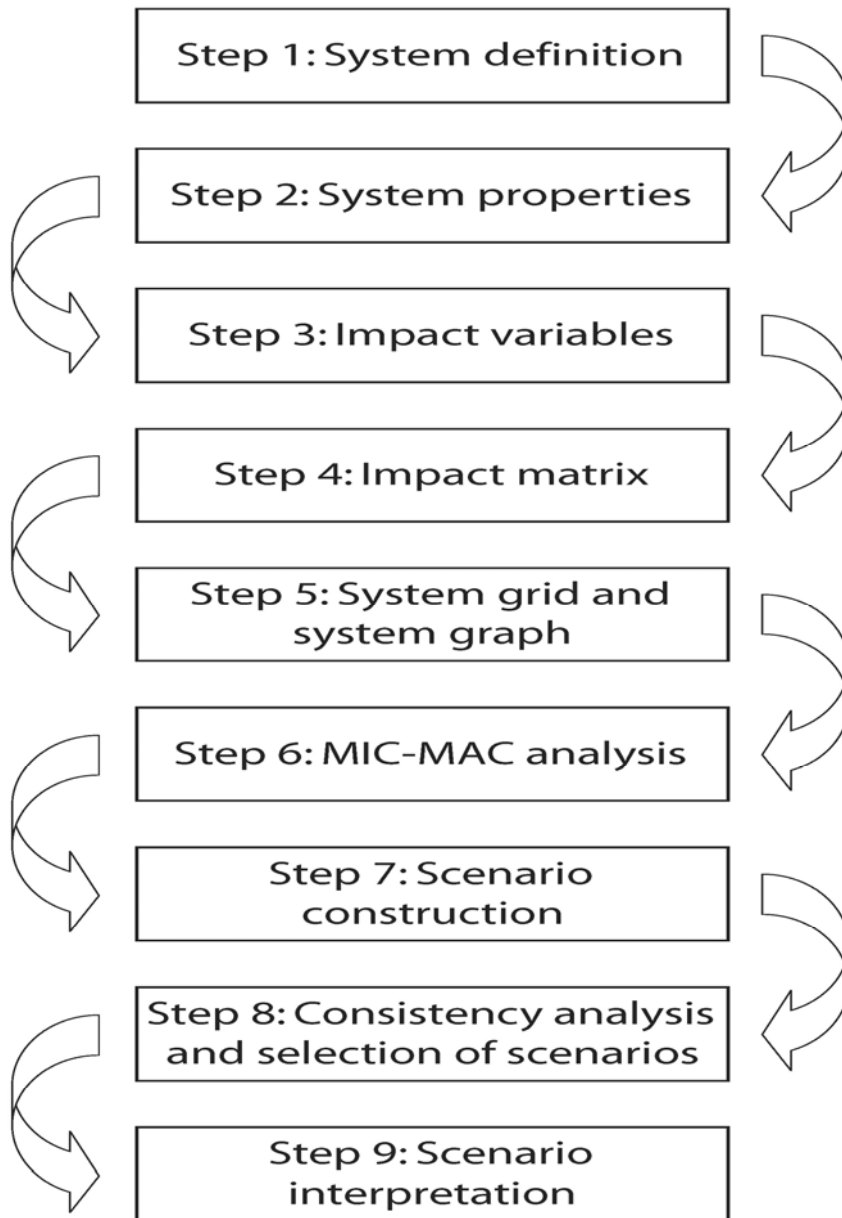


Figure 6-7: The nine steps of Formative Scenario Analysis.

In this synopsis the method and results of the case study on the analysis of woody material transport induced hazard scenarios at hydraulic weak points is briefly summarised. The study team, after having pre-selected a set of possible impact factors or key variables (see Figure 6-8) performed an analysis of the degree of uncertainty and importance for each key variable and subsequently selected the core set of key variables controlling the system behaviour. An additional key variable, named entrapment propensity (CWP) was included in the final set of variables.

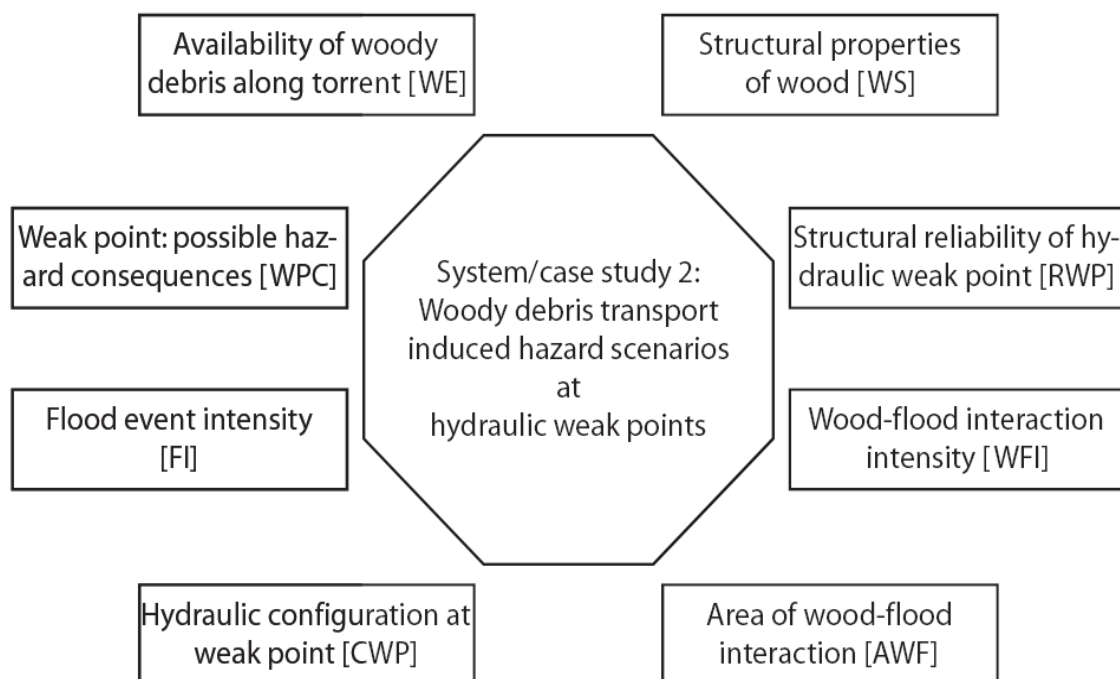


Figure 6-8. Pre-selection of possible impact factors or key variables

	WFI	CWP	WS	RWP	WPC	Activity	Impact strength	Mean activity	4.4
WFI	0	1	1	1	2	5	1.25		
CWP	2	0	0	2	2	6	1.50		
WS	1	0	0	1	2	4	4.00		
RWP	0	1	0	0	2	3	0.60		
WPC	1	2	0	1	0	4	0.50		
Passivity	4	4	1	5	8				
Involvement	20	24	4	15	32				
Mean passivity									
4.4									

Table 6-2. Impact Matrix: Woody material transport induced hazard scenarios at hydraulic weak points

Based on the results of an impact analysis (impact matrix) the influence by each of the selected key variables was clarified (compare the system grid in Figure 6-9).

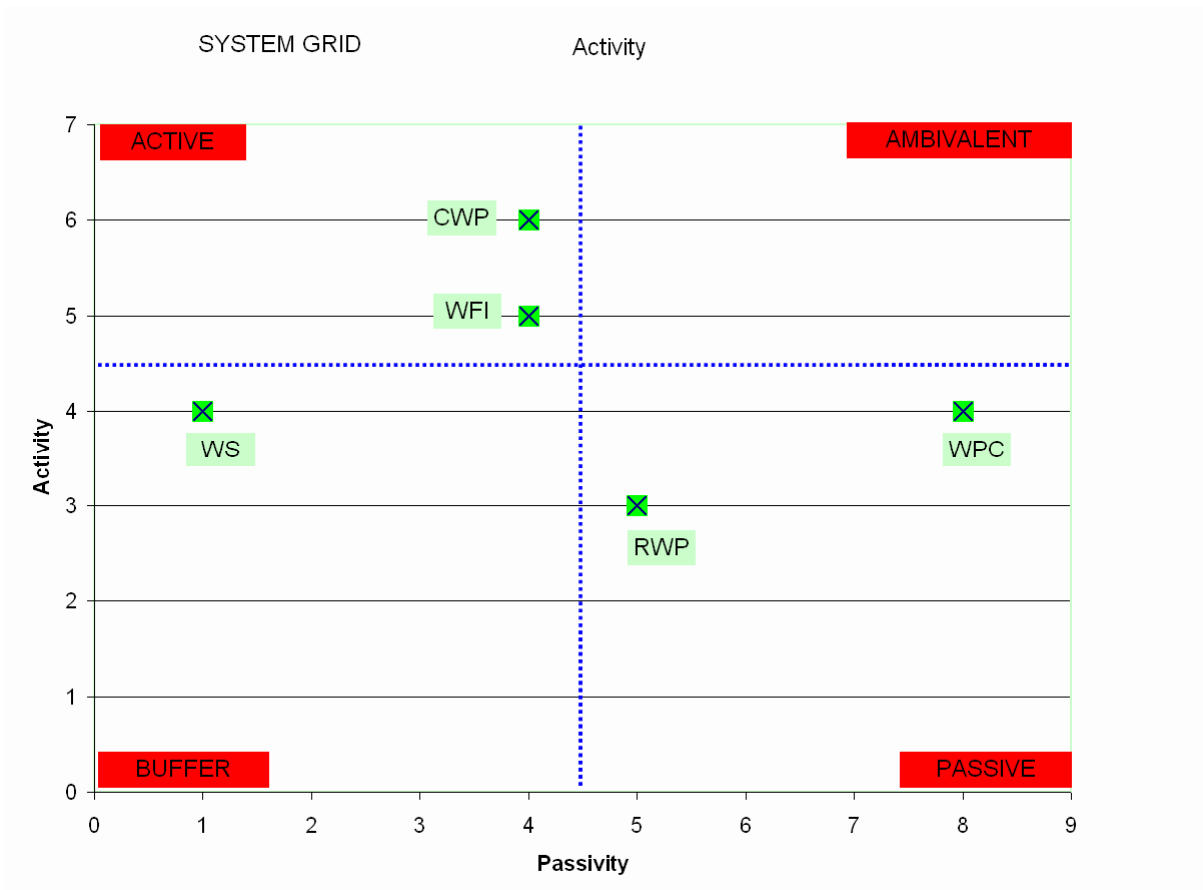


Figure 6-9. System grid of the activity and passivity scores

After having fixed the impact levels for each key variable the study team performed a consistency analysis which led to the identification of a small set of consistent and relevant systems scenarios (compare Table 6-3) through a comprehensive selection procedure. The most consistent scenarios are highlighted in light green.

Entrapment propensity – CWP →	Likely	likely	Unlikely	Unlikely			
Wood-flood interaction – WFI →	Intense	Light	Intense	Light			
	1	2	3	4	Wood structure – WS	Structural reliability – RWP	WPC
1	16	13	10	11	Long pieces	High reliability	Catastrophic effect – ↑↑↑
2	21	17	15	15	Long pieces	High reliability	Hazard increase – ↑
3	14	15	14	19	Long pieces	High reliability	No variation – →
4	19	12	11	8	Long pieces	Low reliability	Catastrophic effect – ↑↑↑
5	25	17	17	13	Long pieces	Low reliability	Hazard increase – ↑
6	14	11	12	13	Long pieces	Low reliability	No variation – →
7	10	11	8	13	Short pieces	High reliability	Catastrophic effect – ↑↑↑
8	14	14	12	16	Short pieces	High reliability	Hazard increase – ↑
9	10	15	14	23	Short pieces	High reliability	No variation – →
10	15	12	11	12	Short pieces	Low reliability	Catastrophic effect – ↑↑↑
11	20	16	16	16	Short pieces	Low reliability	Hazard increase – ↑
12	12	13	14	19	Short pieces	Low reliability	No variation – →

Table 6-3. Set of all scenarios (step 7 of FSA) and identification of the set of most consistent scenarios (step 8, highlighted): Woody material transport induced hazard scenarios at hydraulic weak points

By adopting the Formative Scenario Analysis framework the study team analysed relevant issues in hazard analysis essential for a comprehensive risk assessment procedure. The expert knowledge available in the different domains was successfully integrated by interaction and collaboration of

the study team through a guided scenario building and a rigorous scenario selection procedure. Throughout the entire process of hazard assessment and mapping the identification of consistent assumptions either concerning system loading or system response mechanisms provided crucial insights into the systems behaviour. It had been shown that possible case developments can be described with a particular focus on nonlinear cause-effect chains (transported woody debris vs. entrapment propensity at hydraulic weak point locations).

In **Chapter 5** the procedure of Formative Scenario Analysis was extended based on the results of Chapter 4. The model being set up was implemented, based on the case study on selected woody material transport induced hazard scenarios at hydraulic weak points. Within the framework of risk assessment a scenario shell structure was proposed taking into account causes (system loading shell) and effects (system response shell). By applying Formative Scenario Analysis, this shell structure was used to derive qualitative and quantitative (expert and local, respectively) knowledge that can be integrated into scenario definition within the framework of natural hazard risk management.

By the application of the Formative Scenario Analysis procedure it was possible (1) to assess and validate the expert knowledge contained in the mental system map (Figure 6-10) and (2) to specify and weight the relevant system components in the system loading and system response shell.

twelve system loading scenarios and nine system response scenarios, respectively, as shown in Tables 6-4 and 6-5 in terms of a Scenario Information System.

NR	RPH - recruitment propensity from hill slopes				IRP- In-stream recruitment propensity			WTC- Woody material transport cost (transportability) to reach the critical configuration			PWD- potential woody material distribution at the considered configuration			WSL- Woody material system loading severity
	$q_{1,1}^{1,1}$	$q_{1,1}^{1,2}$	$q_{1,1}^{1,3}$	$q_{1,1}^{1,4}$	$q_{2,1}^{1,2}$	$q_{2,1}^{1,2}$	$q_{2,1}^{1,3}$	$q_{3,1}^{1,1}$	$q_{3,1}^{1,2}$	$q_{3,1}^{1,3}$	$q_{4,1}^{1,1}$	$q_{4,1}^{1,2}$	$q_{4,1}^{1,3}$	$q_{5,1}^{2,1} \vee q_{5,1}^{2,2} \vee q_{5,1}^{2,3}$
1	1	0	0	0	1	0	0	1	0	0	1	0	0	1
2	1	0	0	0	1	0	0	1	0	0	0	1	0	1
3	1	0	0	0	1	0	0	0	1	0	1	0	0	2
4	0	1	0	0	1	0	0	1	0	0	1	0	0	1
5	0	1	0	0	1	0	0	0	1	0	1	0	0	1
6	1	0	0	0	0	1	0	1	0	0	1	0	0	1
7	0	0	0	1	0	1	0	0	0	1	0	0	1	3
8	0	0	1	0	0	0	1	0	1	0	0	0	1	3
9	0	0	1	0	0	0	1	0	0	1	0	0	1	3
10	0	0	0	1	0	0	1	0	1	0	0	0	1	3
11	0	0	0	1	0	0	1	0	0	1	0	1	0	3
12	0	0	0	1	0	0	1	0	0	1	0	0	1	3

Table 6-4: Scenario information system SIS_k for the system loading scenario shell represented as a decision table

NR	WSL - Woody material system loading severity			WEP - Woody material entrapment propensity			BR - Blockage ratio			SCP - System change propensity			SRS - System response severity
	$q_{1,2}^{1,1}$	$q_{1,2}^{1,2}$	$q_{1,2}^{1,3}$	$q_{2,2}^{1,1}$	$q_{2,2}^{1,2}$	$q_{2,2}^{1,3}$	$q_{3,2}^{1,1}$	$q_{3,2}^{1,2}$	$q_{3,2}^{1,3}$	$q_{4,2}^{1,1}$	$q_{4,2}^{1,2}$	$q_{4,2}^{1,3}$	$q_{5,2}^{2,1} \vee q_{5,2}^{2,2} \vee q_{5,2}^{2,3}$
1	1	0	0	1	0	0	1	0	0	1	0	0	1
2	1	0	0	1	0	0	0	1	0	1	0	0	1
3	1	0	0	1	0	0	1	0	0	0	1	0	1
4	0	1	0	1	0	0	1	0	0	1	0	0	1
5	0	1	0	0	1	0	0	1	0	0	1	0	2
6	0	0	1	0	1	0	0	1	0	0	1	0	2
7	0	1	0	0	0	1	0	0	1	0	0	1	3
8	0	0	1	0	0	1	0	1	0	0	0	1	3
9	0	0	1	0	0	1	0	0	1	0	0	1	3

Table 6-5: Scenario information system SIS_k for the system response scenario shell represented as a decision table.

A relevant system loading scenario written out in full length reads as follows (cf. Table 6-4):

Recruitment propensity from hill slopes – very high ($\hat{q}_{1,1}^{1,4}$), in-stream recruitment propensity – medium ($\hat{q}_{2,1}^{1,3}$), woody material transport costs – low ($\hat{q}_{3,1}^{1,3}$), potential woody material transport distribution extremely unfavourable ($\hat{q}_{4,1}^{1,3}$), and woody material system loading severity – high ($\hat{q}_{5,1}^{2,3}$).

Analogously a relevant system response scenario could be read as (cf. Table 6-5):

Woody material system loading severity – high ($\hat{q}_{1,2}^{1,3}$), woody material entrapment propensity – high ($\hat{q}_{2,2}^{1,3}$), blockage ratio – medium ($\hat{q}_{3,2}^{1,2}$), system change propensity – high ($\hat{q}_{4,2}^{1,3}$), and system response severity – high ($\hat{q}_{5,2}^{2,3}$).

Problem solving strategies aiming at minimising risk (decreasing of the parameter SRS) can directly be gathered from the Scenario Information Systems (Tables 6-4 and 6-5) and thus, incomplete problem solutions of questionable effectiveness (regularly being state of the art in practice so far) can be avoided. Taking as an example the sole reduction of recruitable woody material would not result in an effective risk reduction since only the system loading severity is temporarily reduced. Conversely mixed risk reduction strategies aiming also at enhancing the flow capacity and avoiding log jam formations at critical configurations might be more successful.

From a conceptual point of view, the application of the extended Formative Scenario Analysis results in the following problem solving advantages:

- (1) Enhanced possibilities to represent the diverse impacts on the system behaviour;
- (2) agile and simultaneously structured knowledge integration;
- (3) consideration of the uncertainties intrinsically tied to hazard assessment; and
- (4) strict traceability, reproducibility and validity check of the deduced system scenarios.

The main contribution of this dissertation to integral risk management is foremost the provision of a broad spectrum of developed methods, procedures and simulation models to methodically structure, to rationally prioritize and to comprehensively analyse the problems to be solved. In doing so, the essential requisites for conceiving sustainable risk reduction strategies are given.

Starting with the analysis of the diverse hazard processes (e.g. debris flows, landslides) the methods developed and the insights gained in this thesis can be applied to enhance the explanatory power (validity) of the hazard assessments. Furthermore these methods enhance the analysis of the different components of natural hazard risk (e.g. vulnerability, as a hazard dependent, spatially and

temporally variable determinant factor). In addition, the introduced methods support the conceptual planning and the efficient implementation of risk reduction strategies from a sustainability perspective. The tipping points in the risk genesis process can be identified and the spectrum of risk reduction measures can be tuned accordingly.

References

- Autonome Provinz Bozen-Südtirol, 2008. Informationssystem zu hydrogeologischen Risiken. Methodischer Endbericht. Bozen: Autonome Provinz Bozen-Südtirol.
- Berger, E., Grisotto, S., Hübl, J., Kienholz, H., Kollarits, S., Leber, D., Loipersberger, A., Marchi, L., Mazzorana, B., Moser, M., Nössing, T., Riedler, S., Scheidl, C., Schmid, F., Schnetzer, I., Siegel, H. and Volk, G., 2007. DIS-ALP. Disaster information system of alpine regions. Final report. unpublished.
- Diehl, T., 1997. Potential drift accumulation at bridges. Washington, U.S. Department of Transportation, Federal Highway Administration Research and Development, Turner-Fairbank Highway Research Center.
- Holub, M., and Fuchs, S., 2008. Benefits of local structural protection to mitigate torrent-related hazards. WIT Transactions on Information and Communication Technologies 39, 401-411.
- Lyn, D., Cooper, T., Condon, D. and Gan, L., 2007. Factors in debris accumulation at bridge piers. Washington, U.S. Department of Transportation, Federal Highway Administration Research and Development, Turner-Fairbank Highway Research Center.
- Petraschek, A., Kienholz, H., 2003. Hazard assessment and mapping of mountain risks in Switzerland. In: Rickenmann, D. und Chen, C. L. (ed) Debris-flow hazard mitigation: mechanics, prediction and assessment. Millpress, Rotterdam.
- Rickenmann, D., 1997. Schwemmholz und Hochwasser. Wasser, Energie, Luft. Schweizer Wasserwirtschaftsverband, Baden. 89. Jahrgang, 5/6, pp 115-119.
- Rimböck, A., Strobl, T., 2002. Loads on rope net constructions for woody debris entrapment in torrents. International Congress „Interpraevent 2002 in the Pacific Rim“, Matsumoto, Japan; Congress publication, volume 2, pp 797-807.
- Shepard, R., 2005. Quantifying environmental impact assessments using fuzzy logic. New York: Springer.

Staffler, H.; Pollinger, R.; Zischg, A.; Mani, P., 2008. Spatial variability and potential impacts of climate change on flood and debris flow hazard zone mapping and implications for risk management, *Natural Hazards and Earth System Sciences*, 8, 539-558.

Wei, G., 2005. A fixed-mesh method for general moving objects in fluid flow. *International Journal of Modern Physics*.

Wei, G., 2006. Three-Dimensional Collision Modeling for Rigid Bodies and its Coupling with Fluid Flow Computation, *Flow Science Technical Note #75*, FSI-06-TN75.

7. ZUSAMMENFASSUNG

Es gibt im Wesentlichen vier Risikoarten:

*Es gibt Risiken, die du akzeptieren musst
und es gibt Risiken, die du eingehen kannst.*

*Es gibt Risiken, die einzugehen du dir nicht leisten kannst
und es gibt Risiken, die nicht einzugehen du dir nicht leisten kannst.*

P.F. Drucker

In den vorangegangenen Abschnitten wurden folgende vier Aufgabenstellungen eingehend beleuchtet: (1) die Modellierung der Schwemmholzeintrags-, Bewegungsbeginn- und Transportprozesse in alpinen Wildbächen und Flüssen auf Gefahrenhinweisebene (Petraschek und Kienholz, 2003); (2) die Erkennung möglicher Gefahrenprozessmuster im Bereich kritischer Konfigurationen (z.B. Brücken); (3) der Einsatz eines auf Szenarioanalyse basierten Ansatzes (FSA – Formative Szenario Analyse) als Prozedur zur Gefahren- und Risikobewertung komplementär zu den gängigen Verfahren der Gefahrenbewertung für Schwemmholztransportprozesse; (4) Ausbau des Instrumentariums der Formativen Szenario Analyse unter besonderer Berücksichtigung von Wissensintegrationsaspekten. Diese kohärente Prioritätenliste spiegelt aus dem Blickwinkel des Wissensmanagements die Bedürfnisse der öffentlichen Institutionen wider, die sich mit Naturgefahren und daher auch Schwemmholztransportgefahren beschäftigen (Berger et al., 2007; Staffler et al., 2008). Mehrere Fallstudien wurden zu den einzelnen Themenblöcken durchgeführt, um die Anwendbarkeit der diversen Methoden zur Analyse der mit dem Schwemmholztransport verbundenen Gefahrenprozesse zu testen.

Den großen Rahmen im Auge zu behalten, ohne dabei wissenschaftliche Details einerseits und die Bedürfnisse der Praxis andererseits außer Acht zu lassen, war zurückblickend eine der größten Herausforderungen. Es wurde eine ausgewogene Forschungsstrategie angewandt, die auf der einen Seite den jungen Forschungsstand auf dem behandelten Gebiet und auf der anderen Seite die dringende Nachfrage seitens der öffentlichen Institutionen nach verlässlichen Gefahrenbewertungsinstrumenten berücksichtigt.

Obwohl zur vollständigen Klärung der Schwemmholz-Bewegungsbeginn-, Transport- und Ablagerungsprozesse weit reichende Laborexperimente einen wichtigen Beitrag geleistet hätten, wurde der Rahmen dieser Dissertation auf die oben genannten dringenden Erfordernisse der Praxis zugeschnitten.

Der erste Bearbeitungsschritt bestand darin, jene alpinen Einzugsgebiete zu identifizieren, die als besonders kritisch hinsichtlich der vom Schwemmholttransport ausgehenden Gefahren anzusehen waren. Der zweite Bearbeitungsschritt sah eine Gefährlichkeitsreihung der Einzugsgebiete vor, unter Zuhilfenahme verlässlicher Kriterien und Indikatoren zur Prioritätenfestlegung.

Ein darauf folgender Bearbeitungsschritt bestand darin, die auf Gefahrenhinweisebene ermittelten Gefahrenindikationen detailliert zu analysieren. Um erfolgsversprechende Risikoreduktionsstrategien konzipieren zu können, wurde zunächst ein Modellierungsansatz zur Bewertung der vom Schwemmholttransport ausgehenden Gefahrenprozesse entwickelt und in ausgewählten Testgebieten angewandt.

Die hoch aufgelöste Modellierung von Gefahrenprozessen die auf Schwemmholttransport zurückzuführen sind, ist komplex. Obwohl erfolgsversprechende mathematische Modelle zur Simulation von sich in einem dreidimensionalen Strömungsfeld bewegenden Objekten bereits existieren (Wei, 2005; Wei, 2006), ist ihre Verwendbarkeit für reale Schwemmholttransportprobleme in Gebirgsfließgewässern noch unzureichend untersucht worden. Die unter Punkt (1) und (2) angeführten Bearbeitungsschritte behandeln diese Forschungsaspekte.

Die Integration des Expertenwissens erweist sich als wesentlicher Bestandteil einer zuverlässigen Ermittlung der von derartigen Gefahren betroffenen Flächen. Zudem unterstützen Wissensintegrationsinstrumente ein strukturiertes Vorgehen bei der Expertenbefragung und bei der Bündelung des erworbenen Wissens. Die oben angeführten Punkte (3) und (4) betreffen genau diesen Forschungsaspekt.

Wie in **Kapitel 2** dargelegt, wurde eine Prozedur entwickelt, die es ermöglicht, Schwemmholttransportgefahren zu erkennen und bewerten. Es wurde ein Schwemmholttransportindikator – WM – hergeleitet, der zum einen zur Bewertung der relativen Schwemmholtverfügbarkeit und zum anderen zur Bewertung der relativen Schwemmholttransportkapazität eingesetzt werden kann.

Die hergeleitete Berechnungsprozedur berücksichtigt die gesamte Prozesskette vom Schwemmholtseintrag aus den bewaldeten Hängen in den Hochwasserbereichen (benetzter Umfang), über den Bewegungsbeginn bis hin zum Transportprozess. Aus dem Blickwinkel der Gefahrenbeurteilung wurde eine funktionale Klassifizierung der Schwemmholtseintragsflächen gemäß der Aktivität/Intensität der Eintragsprozesse und gemäß der Aktivität/Intensität der Gerinneprozesse vorgenommen (Tabelle 7-1 und Abbildung 7-1).

Eintragsflächentypisierung	Beschreibung
SIZ – Flächen (Einflussbereiche des Gerinnes)	Die Ausdehnung dieser Einflussbereiche wird aufgrund des zum Bemessungshochwasser gehörenden benetzten Umfang ermittelt
AWB – Flächen (Waldsaum – aktiver Eintrag)	Diese aktiven Eintragsflächen grenzen direkt an die SIZ – Flächen an. Fallende Bäume erreichen unmittelbar das Gerinne und beeinflussen wesentlich die Grinnemorphologie.
RWB – Flächen (Waldsaum der eine zusätzliche Schwemmhölzeintragsbelastung ausübt)	Dieser Waldsaum grenzt nach außen unmittelbar an die AWB – Flächen an. Fallende Bäume aus den RWB – Flächen destabilisieren zusätzliche Bäume in den AWB – Flächen.
PRP – Pfade (präferentielle Eintragspfade)	Diese Eintragspfade sind im Wesentlichen Runsen am Hang die eine direkte Verbindung von den bewaldeten Hängen zum Gerinne herstellen. Längs dieser präferentiellen Fließwege kann Wildholz auch aus Entfernungen, die die Breite der AWB – und RWB Flächen überschreiten, ins Gerinne gelangen.
PCA - Flächen (Flächen mit präferentiellen Eintrag)	Aus diesen bewaldeten Flächen, die in Verbindung mit dem Gerinne stehen, finden häufig Oberflächenrutschungen statt

Tabelle 7-1: Klassifizierung der Schwemmhölzeintragsflächen.

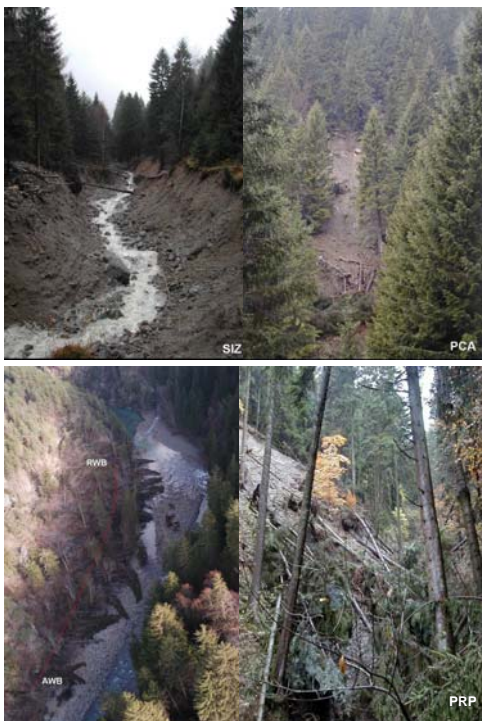


Abbildung 7-1: Beispiele klassifizierter Schwemmhölzeintragsflächen

Das in Abbildung 7-2 dargestellte Flussdiagramm fasst die wesentlichen Schritte der entwickelten Prozedur zur Ermittlung der relativen Schwemmh Holzverfügbarkeit und der Bewertung der relativen Schwemmh Holztransportkapazität zusammen.

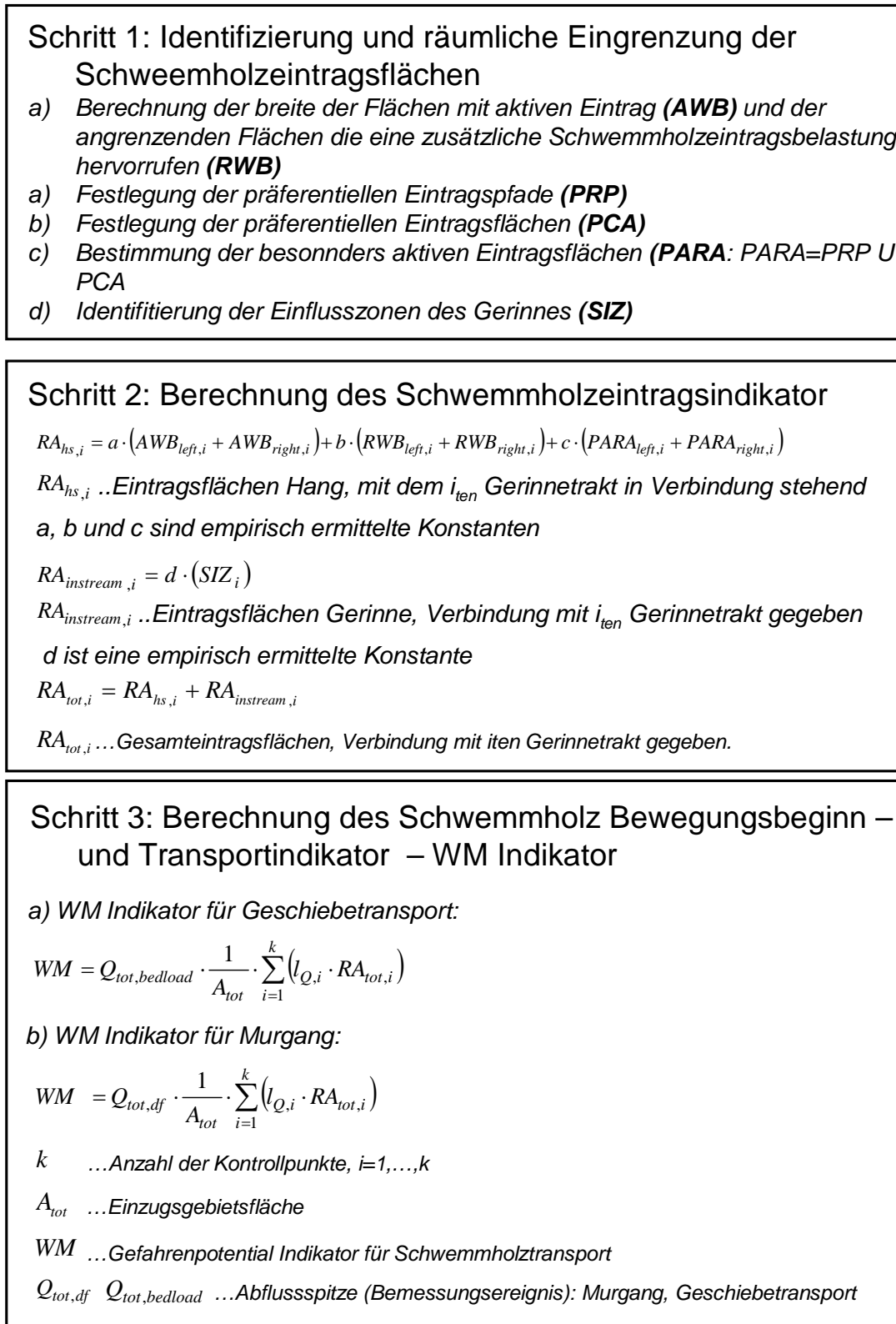


Abbildung 7-2: Flussdiagramm für die Berechnung des Gefahrenindikators – WM.

Die Berechnung des WM Indikators wurde durch eine im GIS implementierte Prozedur für alle Einzugsgebiete der Autonomen Provinz Bozen, in denen Murgang und Übersarungsprozesse stattfinden können, berechnet. Die gemäß dem WM-Indikatorwert klassifizierten Einzugsgebiete sind in Abbildung 7-3 dargestellt.

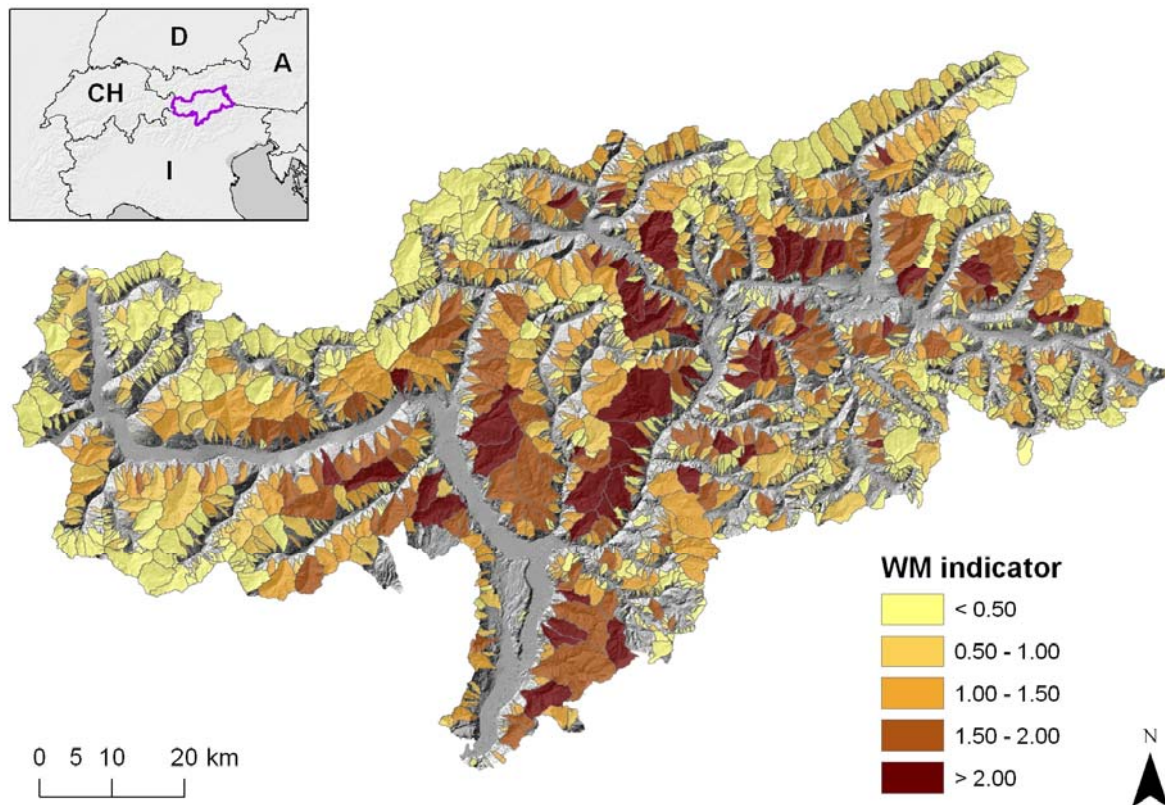


Abbildung 7-3: Klassifizierung der Einzugsgebiete gemäß dem WM-Indikator

Die Ergebnisse der Anwendung des WM-Indikators auf qualitativer und semi-quantitativer Ebene konnten anhand von 1.800 Photos verifiziert werden, die Schwemmhölzeintrags- und Transportprozesse entsprechend belegen.

Das fundierte Wissen in Form von Schwemmhölzgefahrenhinweiskarten bereichert auf mehrfache Art und Weise das Instrumentarium des nachhaltigen Risikomanagements:

- (4) Der Gefahrenzonenplanung zeitlich vorgeschaltet unterstützt dieses Gefahrenhinweisinstrument die Festlegung der erforderlichen Bearbeitungstiefe für eine vollständige Gefahrenbeurteilung.
- (5) Das Wissen über mögliche Gefahrenszenarien, bei denen der Schwemmhölztransport eine wichtige Rolle spielt, ist ein wesentlicher Bestandteil einer vollständigen Systemanalyse, die wiederum Grundvoraussetzung für die Konzeption hochwertiger Risikoreduktionsstrategien ist.

- (6) Das konzeptionelle Rahmenwerk auf das sich der vorgeschlagene Berechnungsansatz stützt, kann als Referenz herangezogen werden, wenn Extremereignisse auch aus der Sicht der Schwemmholzdynamik vollständig dokumentiert werden sollen.

Weiterentwicklungen der hier vorgestellten Methodik, sei es durch eine verbesserte Berücksichtigung der Konnektivität bei der Ermittlung des Schwemmholzeintrages oder durch die Einbindung eines 2D hydrodynamischen Berechnungsansatzes für den Schwemmholztransport, sind möglich.

In **Kapitel 3** wurde der Forschungsschwerpunkt auf die Modellierung und Evaluation der Schwemmholztransport- und Ablagerungsprozesse in Gebirgsflüssen gelegt. Es handelt sich dabei um ein Themenfeld, welches nach den Hochwasserereignissen in der Schweiz und im westlichen Teil Österreichs im Jahre 2005 evident wurde, da die Intensitäten der Schadenseinwirkung dieser Ereignisse maßgeblich durch die beträchtlichen Volumina mitgeführten Schwemmholzes erhöht wurden.

Um einige spezifische Schwächen der derzeit eingesetzten Richtlinien zur Gefahrenzonenplanung zu beheben, wurde zunächst eine Simulationsprozedur konzipiert, die (1) die Bewertung des Schwemmholzeintrages aus den vegetationsbedeckten Uferbereichen, (2) die Evaluierung des Transportbeginns, (3) die Verfolgung der Transportpfade und die Identifizierung der Ablagerungsbereiche, sowie (4) die Ermittlung des Gefahrenpotentials an kritischen Konfigurationen ermöglicht. Daraufhin wurde die Anwendbarkeit der entwickelten Prozedur anhand einer Fallstudie getestet.

Abbildung 7-4 bietet einen Überblick der Schritte zur Ermittlung der Schwemmholzgefahr in Gebirgsflüssen.

Schritt 1: Evaluierung des Schwemmholzeintrags

- a) *Vom Hang (vergleiche Kapitel 2 und Abbildung 7-2)*
- b) *Von den Zubringern*
 - b.1) *mit Hilfe der Ereignisdokumentation*
 - b.2) *durch empirische Formeln (Rickenmann, 1997)*
 - b.3) *durch Erhebungsprozeduren (Rimböck, 2003)*
- c) *In den überfluteten Bereichen durch ad hoc entwickelte Prozeduren. Folgende Parameter müssen ermittelt werden:*
 - c.1) *hydrodynamische Einwirkung*
 - c.2) *Resistenz der Vegetationsstrukturen*
 - c.3) *Frequenz und Exposition*

Schritt 2: Bewertung der Schwemmholzdynamik

- a) *Berechnung des Inhibitionsparameters für den Schwemmholztransport*
- b) *Berechnung der vom Schwemmholz zurückgelegten Transportwege*

Schritt 3: Berechnung der Gefahreneinwirkung an kritischen Gerinnekonfigurationen

- a) *Identifizierung von Objekten an denen sich das Schwemmholz ansammeln kann*
- b) *Simulation der relevanten Ablagerungs- und Ansammlungsmechanismen*

Abbildung 7-4: Ablaufschema der Modellierung der Schwemmholztransportdynamik in Gebirgsflüssen zur Ermittlung der potentiellen Gefahr

Die wichtigsten Ergebnisse der auf Raster-Ebene durchgeführten Schwemmholztransportsimulationen sind für die Fallstudie an der Passer, Italien, in Abbildung 7-5 dargestellt.

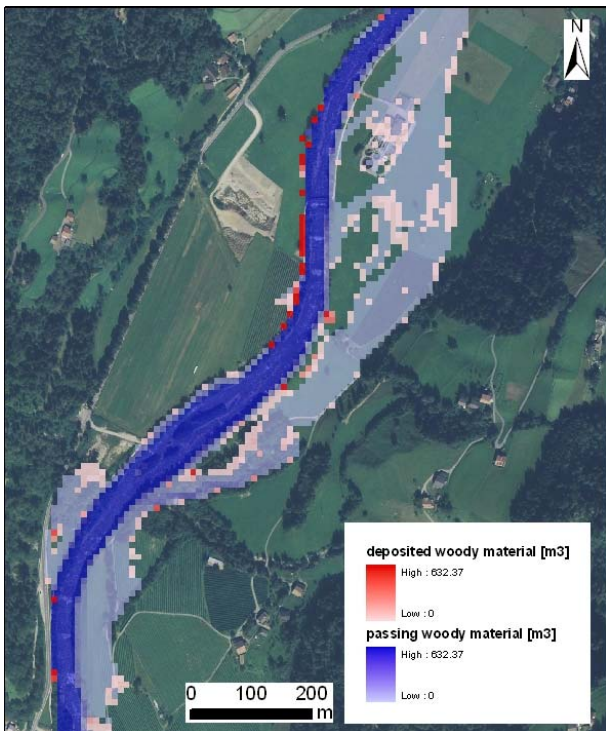


Abbildung 7-5: Ergebnisse der Schwemmholztransportsimulationen

Die Ergebnisse weisen auf einen erhöhten Schwemmholztransport im zentralen Gerinnebereich hin. Zusätzlich sind die potentiellen Ablagerungsbereiche dargestellt. Ablagerung trat erwartungsgemäß vor allem in jenen Überflutungsbereichen auf, in denen die errechneten Fliesstiefen und Geschwindigkeiten gering sind. Im Gerinnebereich konnten Schwemmholzablagerungsphänomene an den Uferböschungen, in Kurvenbereichen und im Bereich von Flussschleifen festgestellt werden. Die modellierten Schwemmholzablagerungsflächen sind in Übereinstimmung mit jenen Bereichen, in denen die Schwemmholzablagerungen im Zuge der Feldaufnahme kartiert wurden. Der berechnete Maximalwert des transportierten Schwemmholzes betrug 632 m^3 in der letzten Fliesszelle. Dieser Wert gibt das Maximalvolumen transportiertes Schwemmholzes im untersuchten Flussabschnitt während eines extremen Hochwassers mit einer Wiederkehrperiode von 300 Jahren an.

Zusätzlich zum Berechnungsansatz auf Raster-Basis wurde ein objekt-orientierter Modellierungsansatz entwickelt. Die Anwendung dieses Ansatzes ermöglichte es, in vereinfachter Form der instationären Hochwasserdynamik Rechnung zu tragen, und die Auswirkungen auf den Schwemmholztransport abzuschätzen. In Abbildung 7-6 sind die Schwemmholzablagerungen im Bereich kritischer Gerinnekonfigurationen dargestellt.

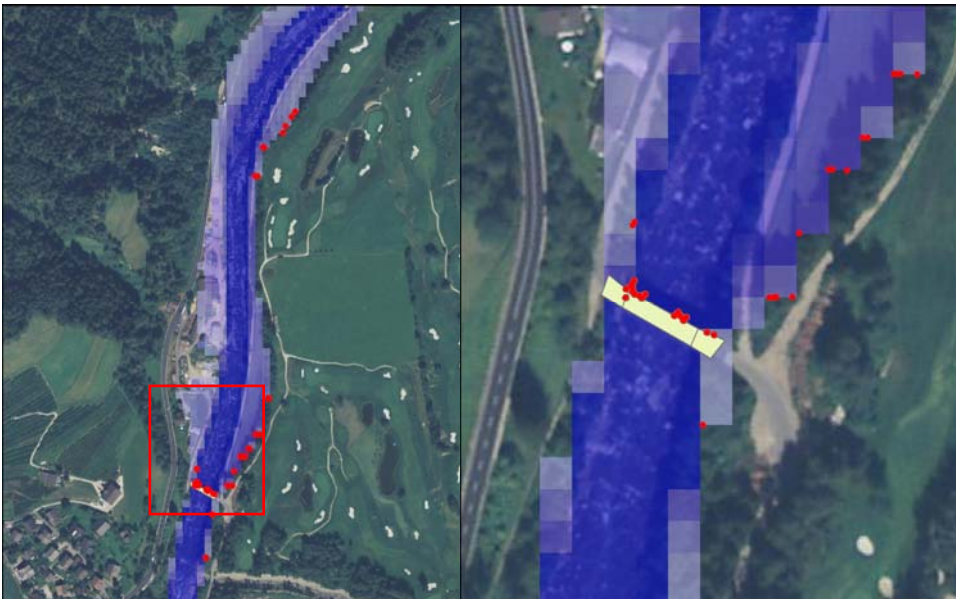


Abbildung 7-6: Schwemmholzablagerungen im Bereich kritischer Konfigurationen. Detailsicht rechts.

Durch die Anwendung der entwickelten Methode konnten wertvolle Einsichten in die Schwemmholzeintrags-, Transport- und Ablagerungsprozesse im Zusammenhang mit extremen Hochwasserereignissen gewonnen werden. Die relevanten Transportwege, die vom Schwemmholz im Gerinne zurückgelegt werden, wurden aufgezeigt und die potentiellen Ablagerungsflächen konnten lokalisiert werden. Durch die Anwendung der entwickelten Prozedur war es möglich, die Größenordnung der transportierten Schwemmholzvolumina, die im Bereich von Schwachstellen kritische Systemzustände induzieren können, abzuschätzen. Das gewonnene Wissen ist eine wesentliche Voraussetzung für die Festlegung nachvollziehbarer Naturgefahrenszenarien, besonders wenn es darauf ankommt, die Auswirkungen möglicher Verklausungen zu beschreiben. Die Aufschlüsselung der auftretenden Prozessdynamiken und das transparente Vorgehen tragen zur Qualitätssteigerung der Gefahrenbewertungen bei und ermöglichen somit eine Validierung der Gefahrenzonenpläne. Die Simulationsergebnisse können zur Planung von Risikoreduktionsstrategien herangezogen und forstliche Maßnahmen in den Schwemmholzeintragsbereichen somit gezielt geplant werden.

In **Kapitel 4** wurde die Formative Szenario-Analyse als zusätzliche Bewertungsmethode in die Praxis der Naturgefahrenforschung eingeführt. Die Anwendbarkeit der Szenariotechnik zur Beschreibung komplexen Systemverhaltens in alpinen Wildbächen und Flüssen wurde anhand von zwei Fallbeispielen getestet: (1) Fallstudie zur Feststofftransportdynamik und (2) Fallstudie zur Schwemmholztransportdynamik.

Es konnte gezeigt werden, dass die Formative Szenario-Analyse einen wesentlichen Beitrag zur Integration qualitativen und quantitativen Wissens leistet und dadurch zur Optimierung der Gefahrenzonenplanungsprozedur beitragen kann.

Das Ablaufschema der neun Schritte der Formativen Szenario Analyse ist in Abbildung 7-7 dargestellt.

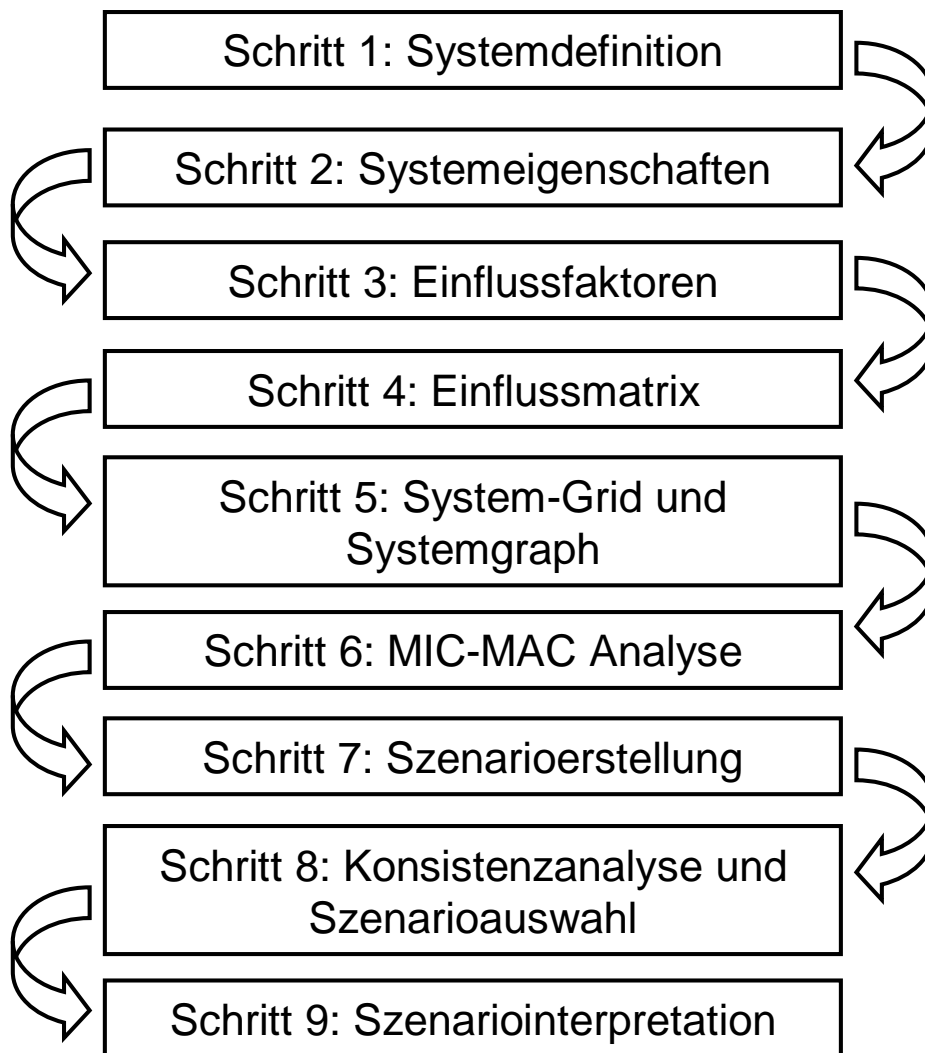


Abbildung 7-7: Die neun Schritte der Formativen Szenario-Analyse.

In dieser Synopsis wird die Fallstudie zur Schwemmhologdynamik zusammengefasst. Das Expertenteam, welches die Aufgabe hatte, die Formative Szenario-Analyse durchzuführen, identifizierte, nachdem das zu analysierende System definiert wurde, eine Liste möglicher Einflussfaktoren (vergleiche Abbildung 7-8). Für jeden dieser Einflussfaktoren wurden die Relevanz und der Unsicherheitsgrad bei der Quantifizierung bestimmt und daraufhin wurde aus der

Liste mögliche Einflussfaktoren die Einflussfaktorenmenge bestimmt, die das Systemverhalten maßgeblich beeinflusst. Ein neuer relevanter Einflussfaktor, die Verklausungsmöglichkeit (CWP), wurde hinzugenommen.

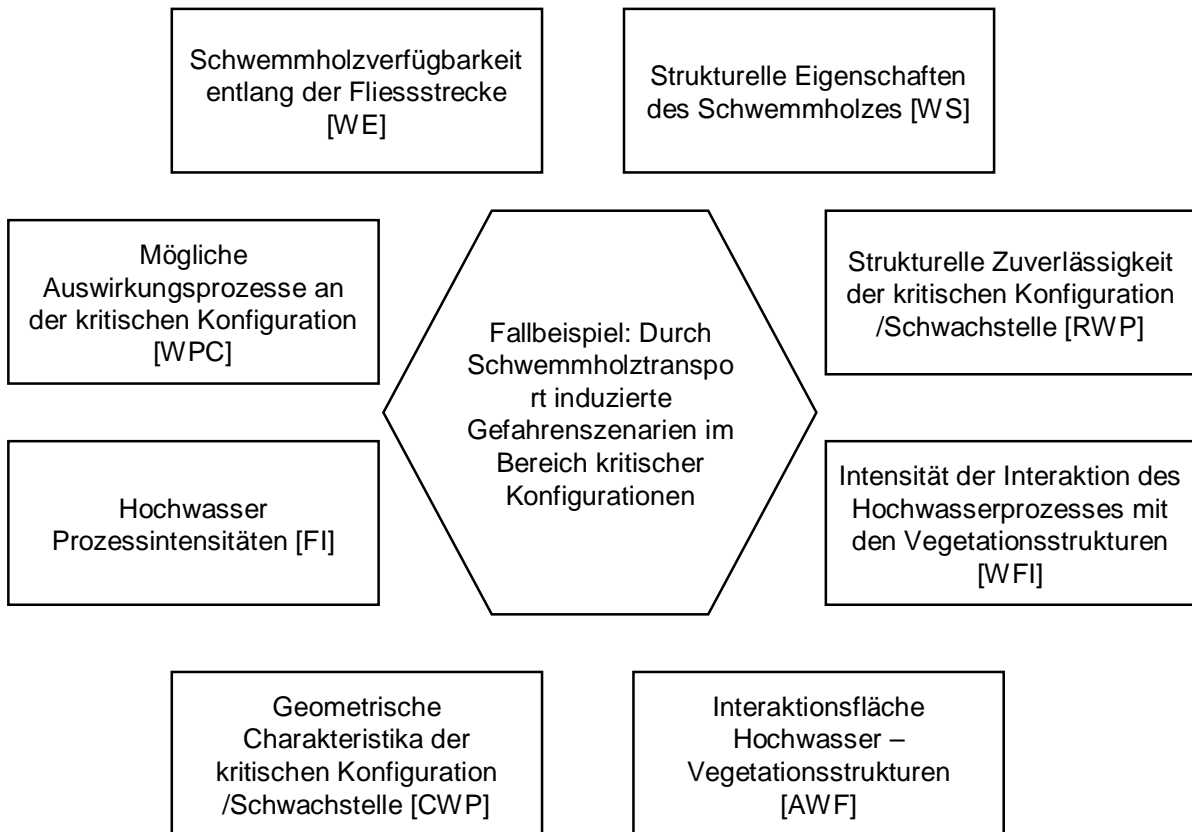


Abbildung 7-8. Vorselektion der Einflussfaktoren für das Fallbeispiel

	WFI	CWP	WS	RWP	WPC	Activity	Impact strength	Mean activity	4.4	
WFI	0	1	1	1	2	5	1.25			
CWP	2	0	0	2	2	6	1.50			
WS	1	0	0	1	2	4	4.00			
RWP	0	1	0	0	2	3	0.60			
WPC	1	2	0	1	0	4	0.50			
Passivity	4	4	1	5	8					
Involvement	20	24	4	15	32					
Mean passivity										
4.4										

Tabelle 7-2. Einflussmatrix: Schwemmholztransport Gefahrenszenarien im Bereich kritischer Konfigurationen

Aufbauend auf den Ergebnissen der durchgeführten Einflussanalyse (Einflussmatrix) wurde die Funktion eines jeden Einflussfaktors dargestellt (vergleiche das System-Grid in Abbildung 7-9).

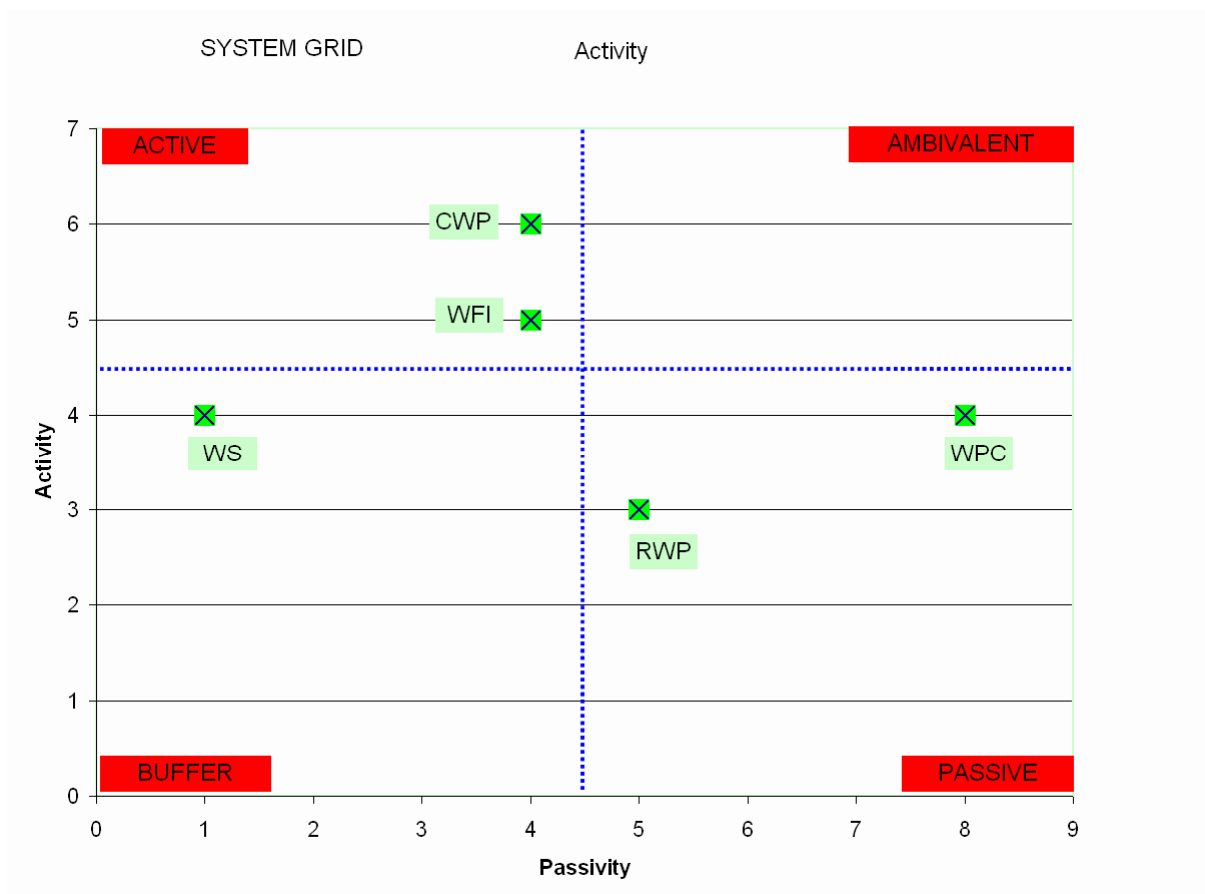


Abbildung 7-9. System-Grid: „Activity“ und „Passivity“ Bewertungen für die Einflussfaktoren.

Nachdem das Expertenteam für jeden Einflussfaktor die Einflusslevels definiert hatte, wurde eine Konsistenzanalyse durchgeführt, auf deren Grundlage durch eine Auswahlprozedur eine „kompakte“ Menge schlüssiger Systemszenarien identifiziert werden konnte (vergleiche Tabelle 7-3). Die plausibelsten Szenarien sind in Tabelle 7-3 in hellgrün hervorgehoben.

Verklaesungsmöglichkeit – CWP →	Durchaus möglich	Durchaus möglich	Eher unmöglich	Eher unmöglich			
Intensität der Interaktion Hochwasserprozesses ↔ Vegetationsstrukturen WFI →	Hohe Intensität	Geringe Intensität	Hohe Intensität	Geringe Intensität			
	1	2	3	4	Strukturelle Eigenschaften Schwemmholz – WS	Strukturelle Zuverlässigkeit – RWP	Auswirkungsprozesse an der kritischen Konfiguration -WPC
1	16	13	10	11	Grosse Stücke	Hohe Zuverlässigkeit	Katastrophische Wirkung – ↑↑↑
2	21	17	15	15	Grosse Stücke	Hohe Zuverlässigkeit	Gefahrenzunahme – ↑
3	14	15	14	19	Grosse Stücke	Hohe Zuverlässigkeit	Keine Änderung – →
4	19	12	11	8	Grosse Stücke	Niedere Zuverlässigkeit	Katastrophische Wirkung – ↑↑↑
5	25	17	17	13	Grosse Stücke	Niedere Zuverlässig- keit	Gefahrenzunahme – ↑
6	14	11	12	13	Grosse Stücke	Niedere Zuverlässigkeit	Keine Änderung – →
7	10	11	8	13	Kleine Stücke	Hohe Zuverlässigkeit	Katastrophische Wirkung – ↑↑↑
8	14	14	12	16	Kleine Stücke	Hohe Zuverlässig- keit	Gefahrenzunahme – ↑
9	10	15	14	23	Kleine Stücke	Hohe Zuverlässigkeit	Keine Änderung – →
10	15	12	11	12	Kleine Stücke	Niedere Zuverlässigkeit	Katastrophische Wirkung – ↑↑↑
11	20	16	16	16	Kleine Stücke	Niedere Zuverlässigkeit	Gefahrenzunahme – ↑
12	12	13	14	19	Kleine Stücke	Niedere Zuverlässigkeit	Keine Änderung – →

Tabelle 7-3. Mögliche Szenarien (Schritt 7 der FSA) und Auswahl der plausibelsten (hell leuchtend hervorgehoben) Szenarien (Schritt 8 der FSA) für das untersuchte Fallbeispiel

Das vorhandene Expertenwissen in den verschiedenen Fachbereichen konnte durch den Einsatz der Formativen Szenario-Analyse in gebündelter Form (Szenarien) dargestellt werden. Mögliche nicht-lineare Systementwicklungen und Ursache-Wirkungsprozessketten konnten identifiziert werden. So sind ausgehend von verschiedenen Systembelastungszuständen verschiedene Systemreaktionen möglich. Das plausibelste Szenario kann wie folgt in Worte gefasst werden (vgl. Tabelle 7-3):

Bei hohen Einwirkungsintensitäten des Hochwasserprozesses auf die Vegetation, und gleichzeitigem Vorhandensein von Schwemmholz, bei welchem die Stücke großer Dimension vorherrschen, sowie bei gegebener Verklausungsmöglichkeit, muss im vorliegenden Fall, falls die strukturelle Zuverlässigkeit der untersuchten Schwachstelle (z.B. Brücke) fraglich ist, mit erhöhter Schwemmholzgefahr gerechnet werden.

Die in **Kapitel 5** erarbeiteten Inhalte und Konzepte stellen eine Erweiterung der theoretischen Aspekte und der praktischen Anwendbarkeit der in Kapitel 4 eingeführten Methode dar. Diese Erweiterung wurde anhand eines Fallbeispiels zur Erstellung von Gefahrenszenarien, die auf den Schwemmholztransport zurückzuführen sind, getestet.

Zunächst wurde eine spezifische „Szenario-Hüllenstruktur“ (*shell structure*) entwickelt, um eine erweiterte Bandbreite an Problemstellungen der Risikoermittlung mit einer robusten Methodik behandeln zu können. Zur Darstellung des Zusammenspiels der Systembelastungsfaktoren wurde die Systembelastungshülle definiert, und in Analogie dazu wurde zur Darstellung des sich ergebenden Wirkungsgefüges die Systemreaktionshülle eingeführt.

Durch die Anwendung der Formativen Szenario-Analyse und unter Berücksichtigung der vorgeschlagenen Hüllenstruktur konnten folgende Wissensintegrationsziele ermittelt werden: (1) Integration und Überprüfung des Expertenwissens anhand einer zuvor definierten „mentalen Systemkarte“ (*mental map*, Abbildung 7-10), und (2) Spezifizierung und Gewichtung der relevanten Einflussfaktoren der Systembelastungs- und Systemreaktionshülle.

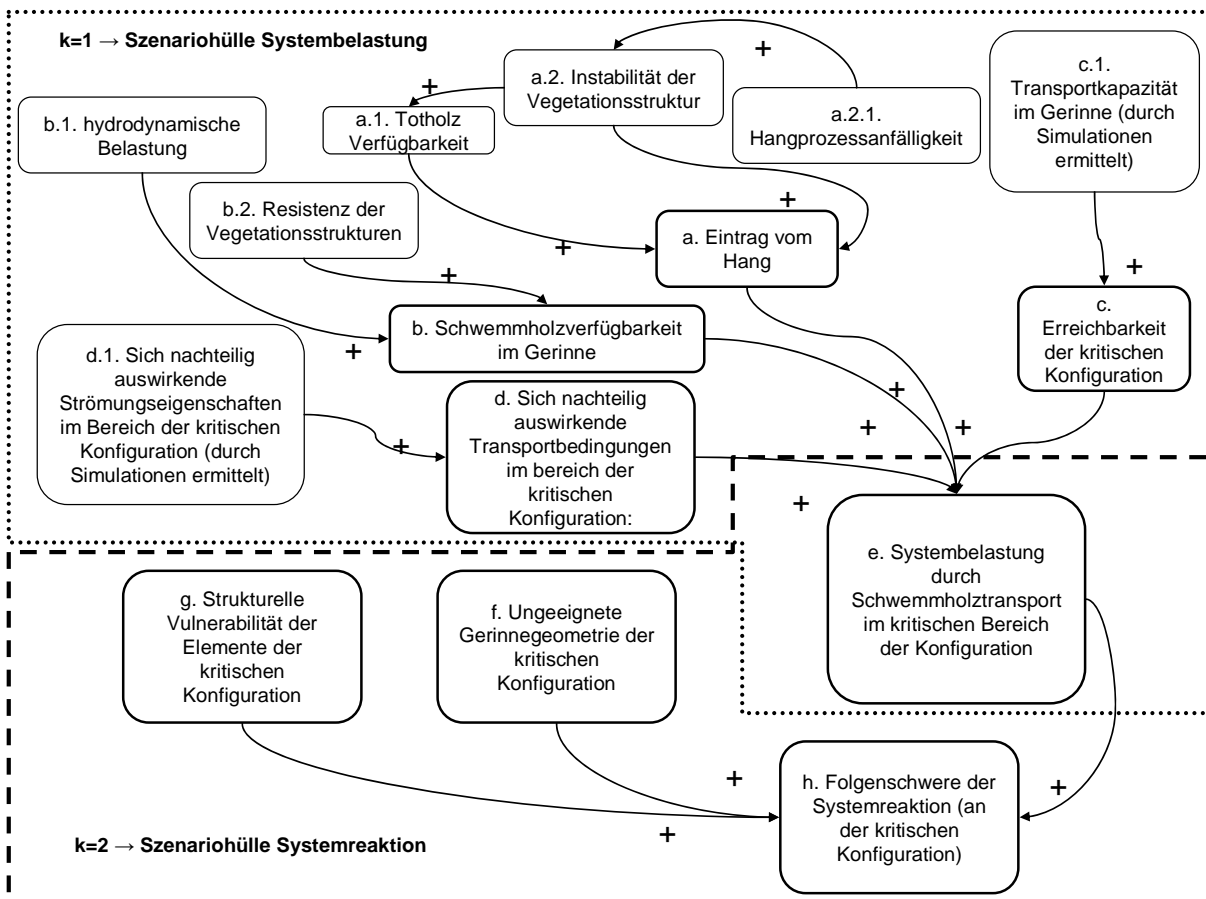


Abbildung 7-10. Mentale Systemkarte: Schwemmh Holztransportgefahren.

Der nächste Schritt bestand darin, die relevanten Einflussfaktoren für das System zu identifizieren und in unmittelbarer Folge durch „Aktivitäts- und Passivitätskennzahlen“ (*activity and passivity ratings*) zu bewerten. In der erweiterten Formativen Szenario-Analyse wurden die Bewertungen mittels Fuzzykennzahlen (z.B. Fuzzy-Intervalle) durchgeführt. Das Expertenteam hatte somit ein flexibles Bewertungsinstrument in der Hand, mit dessen Hilfe einige wesentlichen Aspekte der problem-inhärenten Komplexität erfasst werden konnten. Nachdem in nächsten Schritt die Einflusslevels für jeden Einflussfaktor definiert und beschrieben wurden (vergleiche Tabelle 5-6 in Kapitel 5), wurden sukzessive die plausibelsten Systembelastungs- und Systemreaktionsszenarien ermittelt. Die technischen Details dieser analytischen Schritte sind ausführlich in Kapitel 5 dokumentiert.

Das Ergebnis der Durchführung dieser erweiterten Formativen Szenario-Analyse waren zwölf Systembelastungsszenarien und neun dazu gekoppelte Systemreaktionsszenarien, die als Szenario-Informationssystem jeweils in den Tabellen 7-4 und 7-5 zusammengefasst sind.

NR	RPH – Wildholz Eintragsanfälligkeit am Hang				IRP– Schwemmholz- verfügbarkeit im Gerinne			WTC– Schwemmholz- transportkosten			PWD- Verteilung des transportierten Schwemmholz im Gerinne			WSL– Systembelastung durch Schwemmholz- transport
	$q_{1,1}^{1,1}$	$q_{1,1}^{1,2}$	$q_{1,1}^{1,3}$	$q_{1,1}^{1,4}$	$q_{2,1}^{1,2}$	$q_{2,1}^{1,2}$	$q_{2,1}^{1,3}$	$q_{3,1}^{1,1}$	$q_{3,1}^{1,2}$	$q_{3,1}^{1,3}$	$q_{4,1}^{1,1}$	$q_{4,1}^{1,2}$	$q_{4,1}^{1,3}$	$q_{5,1}^{2,1} \vee q_{5,1}^{2,2} \vee q_{5,1}^{2,3}$
1	1	0	0	0	1	0	0	1	0	0	1	0	0	1
2	1	0	0	0	1	0	0	1	0	0	0	1	0	1
3	1	0	0	0	1	0	0	0	1	0	1	0	0	2
4	0	1	0	0	1	0	0	1	0	0	1	0	0	1
5	0	1	0	0	1	0	0	0	1	0	1	0	0	1
6	1	0	0	0	0	1	0	1	0	0	1	0	0	1
7	0	0	0	1	0	1	0	0	0	1	0	0	1	3
8	0	0	1	0	0	0	1	0	1	0	0	0	1	3
9	0	0	1	0	0	0	1	0	0	1	0	0	1	3
10	0	0	0	1	0	0	1	0	1	0	0	0	1	3
11	0	0	0	1	0	0	1	0	0	1	0	1	0	3
12	0	0	0	1	0	0	1	0	0	1	0	0	1	3

Tabelle 7-4: Szenario Informationssystem für die „Systembelastungshülle“.

NR	WSL – Systembelastung (siehe auch Tabelle 7-4)			WEP – Verklauungs- anfälligkeit			BR – Blockage ratio			SCP – Anfälligkeit zu induzierten Systemänderungen			SRS – Folgschwere der Systemreaktion
	$q_{1,2}^{1,1}$	$q_{1,2}^{1,2}$	$q_{1,2}^{1,3}$	$q_{2,2}^{1,1}$	$q_{2,2}^{1,2}$	$q_{2,2}^{1,3}$	$q_{3,2}^{1,1}$	$q_{3,2}^{1,2}$	$q_{3,2}^{1,3}$	$q_{4,2}^{1,1}$	$q_{4,2}^{1,2}$	$q_{4,2}^{1,3}$	$q_{5,2}^{2,1} \vee q_{5,2}^{2,2} \vee q_{5,2}^{2,3}$
1	1	0	0	1	0	0	1	0	0	1	0	0	1
2	1	0	0	1	0	0	0	1	0	1	0	0	1
3	1	0	0	1	0	0	1	0	0	0	1	0	1
4	0	1	0	1	0	0	1	0	0	1	0	0	1
5	0	1	0	0	1	0	0	1	0	0	1	0	2
6	0	0	1	0	1	0	0	1	0	0	1	0	2
7	0	1	0	0	0	1	0	0	1	0	0	1	3
8	0	0	1	0	0	1	0	1	0	0	0	1	3
9	0	0	1	0	0	1	0	0	1	0	0	1	3

Tabelle 7-5: Szenario Informationssystem für die „Systemreaktionshülle“.

Ein relevantes Systembelastungsszenario sei hier als Beispiel aus Tabelle 7-4 herausgegriffen und ausformuliert:

Wildholz-Eintragsanfälligkeit am Hang – sehr hoch ($\hat{q}_{1,1}^{1,4}$), Schwemmholzverfügbarkeit im Gerinne – mittel ($\hat{q}_{2,1}^{1,3}$), “Schwemmholztransportkosten” – gering ($\hat{q}_{3,1}^{1,3}$), Verteilung des transportierten Schwemmholz im Gerinne – sehr ungünstig ($\hat{q}_{4,1}^{1,3}$), und Systembelastung durch Schwemmholztransport im kritischen Konfigurationsbereich – hoch ($\hat{q}_{5,1}^{2,3}$).

Analog dazu sei ein relevantes Systemreaktionsszenario aus Tabelle 7-5 näher betrachtet:

Systembelastung durch Schwemmholztransport im kritischen Konfigurationsbereich – hoch ($\hat{q}_{1,2}^{1,3}$), Verklausungsanfälligkeit – hoch ($\hat{q}_{2,2}^{1,3}$), *blockage ratio* – hoch ($\hat{q}_{3,2}^{1,3}$), Anfälligkeit zu induzierten Systemänderungen – hoch ($\hat{q}_{4,2}^{1,3}$), Folgeschwere der Systemreaktion – hoch ($\hat{q}_{5,2}^{2,3}$).

Problemlösungsansätze mit der Zielsetzung einer möglichst maximalen Risikoreduktion (Herabsetzung des Parameters SRS) können direkt aus den Szenario-Informationssystemen (Tabellen 7-4 und 7-5) abgeleitet werden. In Folge können einseitige Problemlösungsstrategien mit fraglicher Wirkung vermieden werden. Im konkreten Fall ist von Maßnahmen abzuraten, die alleinig auf die Herabsetzung der Systembelastung abzielen ohne parallel die Entschärfung der Schwachstellen im Gerinne anzustreben. Umgekehrt sind die Erfolgchancen gemischter Strategien bedeutend höher.

Vom konzeptionellen Standpunkt aus betrachtet bringt die Anwendung der erweiterten Formativen Szenario-Analyse zusammenfassend folgende Vorteile mit sich:

- (1) Verbesserte Darstellungsmöglichkeiten der verschiedenen Einwirkungen auf das Systemverhalten,
- (2) agile und gleichzeitig strukturierte Wissensintegration,
- (3) Berücksichtigung der mit der Gefahrenanalyse verbundenen Unsicherheiten, und
- (4) Nachvollziehbarkeit und Plausibilitätsprüfung der abgeleiteten Systemszenarien

Der konkrete Beitrag dieser Doktorarbeit zum integralen Risikomanagement ist vor allem darin zu sehen, dass die zu lösenden Probleme durch die flexible Anwendung des breiten Spektrums an entwickelten Methoden, Prozeduren und Simulationsmodellen vorerst methodisch strukturiert, dann rational priorisiert und in der jeweils erforderlichen Detailebene umfassend analysiert werden

können. Damit sind die nötigen Voraussetzungen für die Konzeption nachhaltiger Risikoreduktionsstrategien geschaffen worden.

Beginnend bei der Analyse der verschiedenen Gefahrenprozesse (z.B. Murgänge, Rutschungen) können die in dieser Doktorarbeit entwickelten Methoden und gewonnenen Erkenntnisse eingesetzt werden, um die Aussagekraft der Ergebnisse der Gefahrenanalyse zu bestärken. Darüber hinaus bieten die entwickelten Methoden zur Szenarioanalyse die Möglichkeit, effizient die verschiedenen Komponenten des naturgefahreninduzierten Risikos (z.B. die Vulnerabilität als gefahrenabhängige, sowie räumlich und zeitlich variable Bestimmungsgröße) zu untersuchen. Zusätzlich unterstützen die hier vorgestellten Methoden, falls frühzeitig genug in den Planungsprozess eingebaut, die nachhaltige Umsetzung von Risikoreduktionsstrategien. Die Schwachstellen im Risikogeneseprozess können identifiziert werden und das erforderliche Maßnahmenbündel kann gezielt auf deren Behebung ausgerichtet werden.

Literatur

Autonome Provinz Bozen-Südtirol, 2008. Informationssystem zu hydrogeologischen Risiken. Methodischer Endbericht. Bozen: Autonome Provinz Bozen-Südtirol.

Berger, E., Grisotto, S., Hübl, J., Kienholz, H., Kollarits, S., Leber, D., Loipersberger, A., Marchi, L., Mazzorana, B., Moser, M., Nössing, T., Riedler, S., Scheidl, C., Schmid, F., Schnetzer, I., Siegel, H. and Volk, G., 2007. DIS-ALP. Disaster information system of alpine regions. Final report. unpublished.

Diehl, T., 1997. Potential drift accumulation at bridges. Washington, U.S. Department of Transportation, Federal Highway Administration Research and Development, Turner-Fairbank Highway Research Center.

Holub, M., and Fuchs, S., 2008. Benefits of local structural protection to mitigate torrent-related hazards. WIT Transactions on Information and Communication Technologies 39, 401-411.

Lyn, D., Cooper, T., Condon, D. and Gan, L., 2007. Factors in debris accumulation at bridge piers. Washington, U.S. Department of Transportation, Federal Highway Administration Research and Development, Turner-Fairbank Highway Research Center.

Petraschek, A., Kienholz, H., 2003. Hazard assessment and mapping of mountain risks in Switzerland. In: Rickenmann, D. und Chen, C. L. (ed) Debris-flow hazard mitigation: mechanics, prediction and assessment. Millpress, Rotterdam.

- Rickenmann, D., 1997. Schwemmholz und Hochwasser. Wasser, Energie, Luft. Schweizer Wasserwirtschaftsverband, Baden. 89. Jahrgang, 5/6, pp 115-119.
- Rimböck, A., Strobl, T., 2002. Loads on rope net constructions for woody debris entrapment in torrents. International Congress „Interpraevent 2002 in the Pacific Rim“, Matsumoto, Japan; Congress publication, volume 2, pp 797-807.
- Shepard, R., 2005. Quantifying environmental impact assessments using fuzzy logic. New York: Springer.
- Staffler, H.; Pollinger, R.; Zischg, A.; Mani, P., 2008. Spatial variability and potential impacts of climate change on flood and debris flow hazard zone mapping and implications for risk management, Natural Hazards and Earth System Sciences, 8, 539-558.
- Wei, G., 2005. A fixed-mesh method for general moving objects in fluid flow. International Journal of Modern Physics.
- Wei, G., 2006. Three-Dimensional Collision Modeling for Rigid Bodies and its Coupling with Fluid Flow Computation, Flow Science Technical Note #75, FSI-06-TN75.

ACKNOWLEDGEMENT

Finally, I feel much obliged to all who contributed to this work, for providing an excellent research environment, many valuable discussions, technical and administrative support, collaboration and advice, providing necessary data, inspirations, thoughts, leisure, and pleasure:

Aronne Armanini, Vincenzo Casulli, Michi Chiari, Francesco Comiti, Vincenzo D'Agostino, Anna Da Sacco, Omar Formaggioni, Sven Fuchs, Willigis Gallmetzer, Helmuth Habersack, Verena Hell, Johannes Hübl, Margreth Keiler, Gernot Koboltschnig, Michele Larcher, Andri Largiader, Pierpaolo Macconi, Diego Mantovani, Nicola Marangoni, Lorenzo Marchi, Laura Martuscelli, Hildegard and Antonio Mazzorana, Luca Messina, Rudolf Pollinger, Florian Rudolf-Miklau, Christian Scheidl, Christian Scherer, Monika Stanzer, Markus Stoffel, Claudio Volcan, Andreas Zischg. Sincere thanks are given to them all.

Curriculum Vitae Bruno Mazzorana

- 1974 born on April 10, in Bolzano, Italy
- 1980 – 1985 primary School in Bolzano, Italy
- 1985 – 1988 Secondary School in Bolzano, Italy
- 1988 – 1993 Scientific Lyceum in Bolzano, Italy
- 1993 – 2000 Studies in Forestry and Environmental Sciences, University of Padua, Italy
- 2000 Diploma degree in Forestry and Environmental Sciences, University of Padua, Italy
- 2001 Internship at the Department of Hydraulic Engineering of the Autonomous Province of Bolzano
- 2001 State examination for Forest Professionals
- 2001 – 2002 Obligatory military service in Trieste and Trento, Italy
- From 2002 Forest Officer of the Autonomous Province of Bolzano, Department of Hydraulic Engineering
- 2006 – 2008 Postgraduate studies in Conflict Mediation and Peace Operators, University of Bologna, Italy.
- 2006 – 2009 Ph.D. student at the Department of Civil Engineering and Natural Hazards, Institute of Mountain Risk Engineering, University of Natural Resources and Applied Life Sciences, Vienna, Austria. Topic of thesis: “Woody debris recruitment prediction methods and transport analysis”. Advisors: Ao. Univ. Prof. Dipl.-Ing. Dr. Johannes Hübl, Institute of Mountain Risk Engineering, University of Natural Resources and Applied Life Sciences, Vienna, Austria; Univ.-Ass. Dipl.-Geogr. Dr. rer. nat. Sven Fuchs, Institute of Mountain Risk Engineering, University of Natural Resources and Applied Life Sciences, Vienna, Austria.
- 2009 Scientific Advisory Board of Interpaevent